NATIONAL ADVISORY COMMITTEE FOR AERONAUTICS

REPORT No. 364

THE PRESSURE DISTRIBUTION OVER THE WINGS AND TAIL SURFACES OF A PW-9 PURSUIT AIRPLANE IN FLIGHT

By RICHARD V. RHODE

1930

AERONAUTICAL SYMBOLS

1. FUNDAMENTAL AND DERIVED UNITS

	Symbol	Metric		English	
		Unit	Symbol	Unit	Symbol
Length	l	meter	m	foot (or mile)	ft. (or mi.)
Time	t	second	s	second (or hour)	sec. (or hr.)
Force	F	weight of one kilogram	kg	weight of one pound	lb.
Power	P	kg/m/s		horsepower	hp
Speed		km/hr	k. p. h.	mi./hr.	m. p. h.
		m/s	m. p. s.	ft./sec.	f. p. s.

2. GENERAL SYMBOLS, ETC.

W, Weight, $=mg$

g, Standard acceleration of gravity $=9.80665$ m/s^2 $=32.1740$ ft./sec.^{2}

m, Mass, $=\frac{W}{g}$

ρ, Density (mass per unit volume).

Standard density of dry air, 0.12497 (kg-m^{-4} s^2) at 15° C and 760 mm $=0.002378$ (lb.-ft.$^{-4}$ sec.^{2}).

Specific weight of "standard" air, 1.2255 kg/m^3 $=0.07651$ lb./ft.^{3}

mk^2, Moment of inertia (indicate axis of the radius of gyration, k, by proper subscript).

S, Area.

S_w, Wing area, etc.

G, Gap.

b, Span.

c, Chord length.

b/c, Aspect ratio.

f, Distance from C. G. to elevator hinge.

μ, Coefficient of viscosity.

3. AERODYNAMICAL SYMBOLS

V, True air speed.

q, Dynamic (or impact) pressure $=\frac{1}{2}\rho V^2$

L, Lift, absolute coefficient $C_L=\frac{L}{qS}$

D, Drag, absolute coefficient $C_D=\frac{D}{qS}$

C, Cross-wind force, absolute coefficient $C_C=\frac{C}{qS}$

R, Resultant force. (Note that these coefficients are twice as large as the old coefficients L_C, D_C.)

i_w, Angle of setting of wings (relative to thrust line).

i_t, Angle of stabilizer setting with reference to thrust line.

γ, Dihedral angle.

$\rho\frac{Vl}{\mu}$, Reynolds Number, where l is a linear dimension.

e. g., for a model airfoil 3 in. chord, 100 mi./hr. normal pressure, 0° C: 255,000 and at 15° C., 230,000;

or for a model of 10 cm chord 40 m/s, corresponding numbers are 299,000 and 270,000.

C_p, Center of pressure coefficient (ratio of distance of C. P. from leading edge to chord length).

β, Angle of stabilizer setting with reference to lower wing, $=(i_t-i_w)$.

α, Angle of attack.

ϵ, Angle of downwash.

REPORT No. 364

THE PRESSURE DISTRIBUTION OVER THE WINGS AND TAIL SURFACES OF A PW-9 PURSUIT AIRPLANE IN FLIGHT

By RICHARD V. RHODE
Langley Memorial Aeronautical Laboratory

8493—30——1

NATIONAL ADVISORY COMMITTEE FOR AERONAUTICS

NAVY BUILDING, WASHINGTON, D. C.

(An independent Government establishment, created by act of Congress approved March 3, 1915, for the supervision and direction of the scientific study of the problems of flight. Its membership was increased to 15 by act approved March 2, 1929 (Public, No. 908, 70th Congress). It consists of members who are appointed by the President, all of whom serve as such without compensation.)

EXECUTIVE COMMITTEE

REPORT No. 364

THE PRESSURE DISTRIBUTION OVER THE WINGS AND TAIL SURFACES OF A PW–9 PURSUIT AIRPLANE IN FLIGHT

By Richard V. Rhode

SUMMARY

The investigation reported herein was conducted at Langley Field, Va., by the National Advisory Committee for Aeronautics at the request of the Army Air Corps to determine (1) the magnitude and distribution of aerodynamic loads over the wings and tail surfaces of a pursuit-type airplane in the maneuvers likely to impose critical loads on the various subassemblies of the airplane structure, (2) to study the phenomenon of center of pressure movement and normal force coefficient variation in accelerated flight, and (3) to measure the normal accelerations at the center of gravity, wing-tip, and tail, in order to determine the nature of the inertia forces acting simultaneously with the critical aerodynamic loads.

The investigation comprised simultaneous measurements of pressure at 120 stations distributed over the right upper wing, left lower wing, right horizontal tail surfaces, and complete vertical surfaces in one installation and the same number of points distributed over those portions of the wings in the slip stream and the left horizontal tail surfaces in another installation, during a series of level flight runs, pull-ups, rolls, spins, dives, and inverted flight maneuvers. Measured also were the accelerations mentioned above, angular velocities, air speed, and control positions simultaneously with the pressures.

The results obtained throw light on a number of important questions involving structural design. Some of the more interesting results have been discussed in some detail, but in general the report is for the purpose of making this collection of airplane-load data obtained in flight available to those interested in airplane structures.

INTRODUCTION

Granting that a major factor contributing to any increase in airplane performance is a decrease in weight, it is clear that since the structural weight of an airplane constitutes 20 per cent or more of the total, any saving that can be effected in the structural parts is worth while. But to design a structure light yet safe, the engineer must have a thorough and accurate knowledge of the character of the loads that his structure must withstand. Actually, of course, the designer need not be thoroughly conversant himself with all of the factors involved in the loads that come into play in order to produce an acceptable airplane, but must only know how to apply the design rules imposed.

These rules (References 1, 2, and 3) have proven themselves satisfactory, in general, when applied to airplanes of conventional type and purpose. As applied to new airplanes of less conventional type, or to new airplanes of conventional type but considerably advanced performance, the rules are sometimes not satisfactory in all respects. This is usually not discovered, however, until a structural failure occurs. In many cases it is not discovered at all, failure having been avoided by a built-in strength in excess of that required.

It is perhaps needless to say that crashes resulting from structural failures in the air, even though relatively rare, have a particularly bad effect on the morale of flying personnel (with some notable exceptions) and on the attitude of the public toward aviation, and must be eventually eliminated if confidence in the airplane is to become deep-rooted. It is manifest, therefore, that the structural design of airplanes must be put on an indisputably sound basis. This means that design rules must be based more on known phenomena, whether discovered analytically or experimentally, and less on conjecture.

While a large number of papers have been published, both mathematical and experimental, dealing with the external loads on airplane structures, these have not been correlated to the point where a clear picture of phenomena occurring in the different conditions of flight can be obtained, if, indeed, it is possible to do so. The most extensive single experimental investigation that has been made is probably the pressure distribution tests on the *MB–3* airplane in 1923 (Reference 4). These have been criticized on the grounds that the airplane was of a very special type, and had individualities of such nature that the results were not applicable to the general problem. While some of this criticism is well founded, it is useless to expect, except to a limited degree, that complete pressure distribution investigations on any airplane will furnish data suitable for the solution of any particular problem. This is true because any airplane is necessarily individ-

ual (unless duplicated to a very fine point of perfection) and also because, which is probably more important, the labor involved in these investigations is so great that it is impossible to treat any one phase of the load problem adequately if a fairly complete picture of the whole is to be obtained.

distribution. The results are of immediate interest to those agencies responsible for structural design rulings, and even though not analyzed to any great extent should also be of value and interest to airplane designers. To expedite its presentation there has been no attempt to analyze completely any one phase

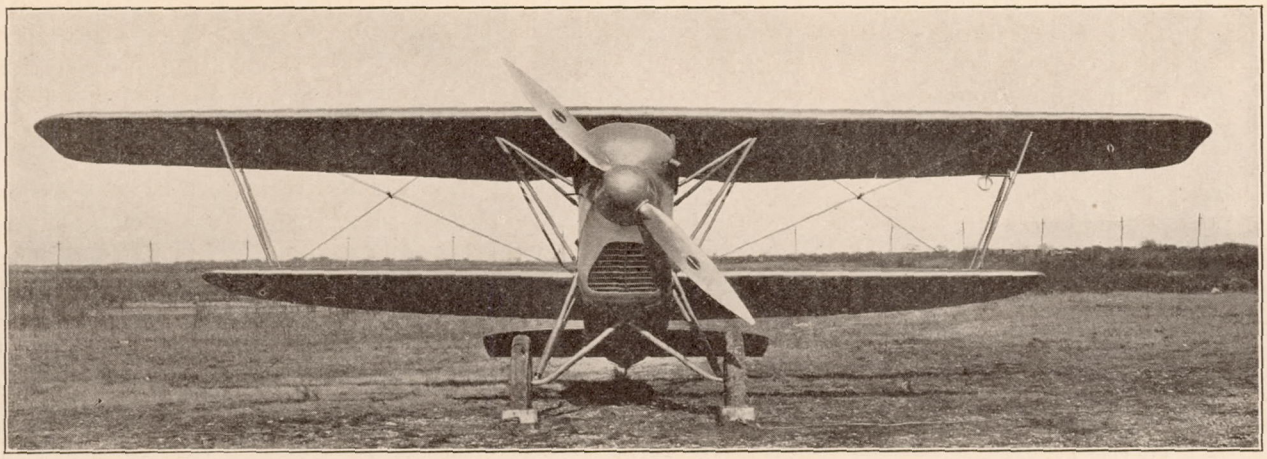

FIGURE 1.—Front view of *PW-9* airplane

Thus, the present report attempts to portray the phenomena occurring on a pursuit-type airplane in the maneuvers that it is called upon to perform, or what amounts to the same thing, in special test maneuvers outlined to impose the same conditions of load that occur at the critical times in the more familiar

of the structural phenomena that are brought to light. Instead, the present report presents the data as obtained, worked up to the stage where they can readily be used in studies of design methods, for the consideration of those concerned, and has in a few instances called to attention the more obvious points in which

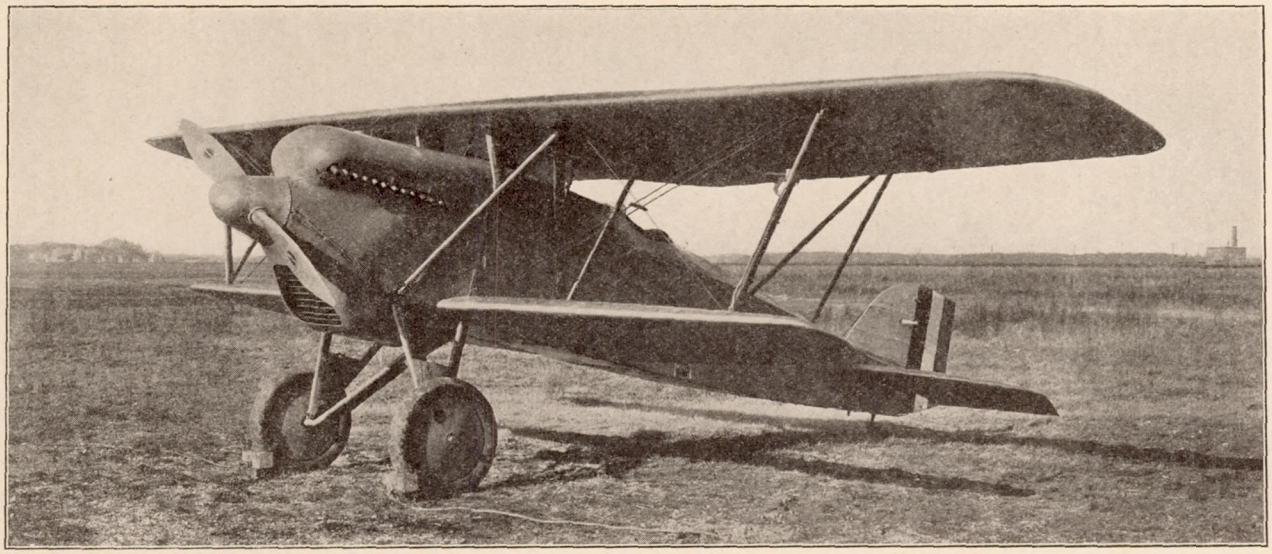

FIGURE 2.—Three-quarter front view of *PW-9* airplane

maneuvers. To this end, pressure measurements were made on the right upper wing extended to include portions affected by slip stream, fuselage, and windshield, the left lower wing, and the tail surfaces of a *Boeing PW-9* airplane, simultaneously with accelerometer readings at the center of gravity, wing tip and tail in the maneuvers above mentioned.

The data obtained represent a very extensive collection of information on structural loads and their

structural design methods now in use are open to criticism in light of these results.

The flight tests were made at the Langley Memorial Aeronautical Laboratory in 1927 and 1928, at the request of the Army Air Corps.

APPARATUS

The airplane.—The airplane used in these tests was a slightly modified *Boeing PW-9* pursuit airplane.

(Figs. 1, 2, and 3, Table I.) The military load, including the main tank, was removed and the top cowling forward of the cockpit raised slightly so that the test instruments and apparatus could be accommodated. The pressure tubes leading from the upper wing to the fuselage formed false struts which increased the drag and lowered the high speed about 6 m. p. h. On the other hand, the weight was reduced 50 pounds and the stalling speed lowered about 1 m. p. h. The pilot reported poor directional control, but the longitudinal control and aileron action were excellent. On the whole, therefore, the performance and maneuverability were not reduced sufficiently to affect the significance of the results.

The wings of the *PW–9* employ the Göttingen 436 airfoil section throughout the span. They are, however, tapered in plan form, and the upper and lower wings differ in plan form from each other (fig. 4); in addition, the upper wing is washed in at the center section. Table II gives the actual ordinates of all sections at which pressures were measured.

During the preliminary tests the airplane broke a wheel while taxying in after landing, pitched over on its back and damaged the central portion of the leading edge of the upper wing, which remained slightly deformed subsequent to repair. Outlines of some of the deformed ribs are shown in Figure 5, compared with the true sections.

A structural feature of this airplane which has a bearing on the results obtained in the tests is the lack of flying wires in the rear truss, resulting in a structure less rigid in torsion than the normal single-bay biplane structure. This allows the incidence of the cellule to vary with changing load, particularly in low angle of attack conditions of flight with the center of pressure well back.

Another characteristic of the airplane that should be mentioned is the slot-shaped gap between the wing and aileron, illustrated diagrammatically in Figure 6 and also noticeable in Figure 10. The effect of this gap will be mentioned in the discussion of results.

Pressure orifices and tubing.—Installation photographs are given in Figures 7 to 11, inclusive. The orifice and tubing installation is essentially the same as those used on previous tests, with aluminum tubes used throughout, except for short and easily replaced lengths of rubber tube at the manometer connections and between the fixed and movable surfaces. A diagram of the orifice locations is given in Figure 12, and the type of orifice used is illustrated in Figure 13.

Manometers.—The orifices were connected to two N. A. C. A. type 60 recording multiple manometers which were located just above the center of gravity in the space formerly occupied by the main gasoline tank. These manometers are the same in principle as those used in the *MB–3* and *VE–7* tests (References 4 and 5), differing mainly from them in that they accommodate 60 pressure units each instead of only 30.

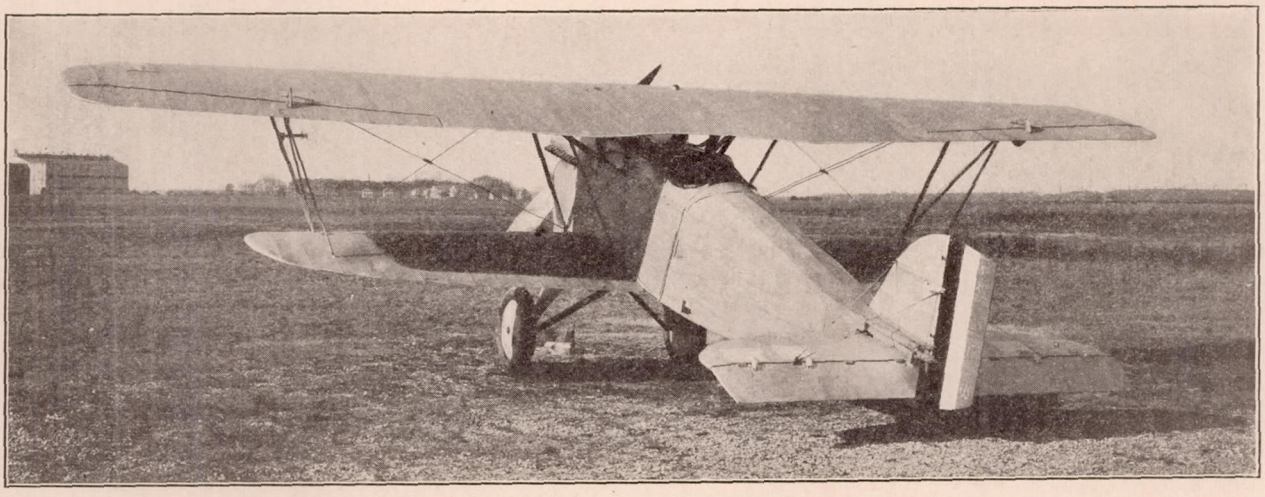

FIGURE 3.—Three-quarter rear view of *PW–9* airplane

A diagrammatic sketch of the attachment of a pair of orifices to a pressure unit or "capsule" is given in Figure 13.

Other instruments.—In addition to the manometers, the following instruments were used: N. A. C. A. recording air-speed meter (Reference 6); N. A. C. A. recording turnmeter (Reference 7); N. A. C. A. control position recorder (Reference 8); three single component accelerometers (Reference 9), located as shown in Figure 14; and a timer.

A moving-picture camera was also used to measure angle of attack as will be explained later.

METHOD

The method used in these tests does not differ in any essential feature from the methods employed in previous pressure-distribution tests. As it was desired to obtain results for all of the wing and tail surfaces simultaneously, if possible, the orifices were disposed to cover the right upper wing, left lower wing, vertical

tail surfaces, and right horizontal tail surfaces. Limitations of capacity of the apparatus that could be carried aboard the airplane prevented the investigation of the remaining surfaces simultaneously with those mentioned, but an independent set of runs was made later to investigate more thoroughly the slip stream section of both upper and lower wings and the left horizontal tail surfaces. The right upper and left lower wing arrangement (in place of the more desirable right upper and lower or left upper and lower) was imposed by the impracticability of running all of the pressure tubes into the fuselage from one side, and also because it was not desired to unbalance the airplane even slightly unless absolutely necessary.

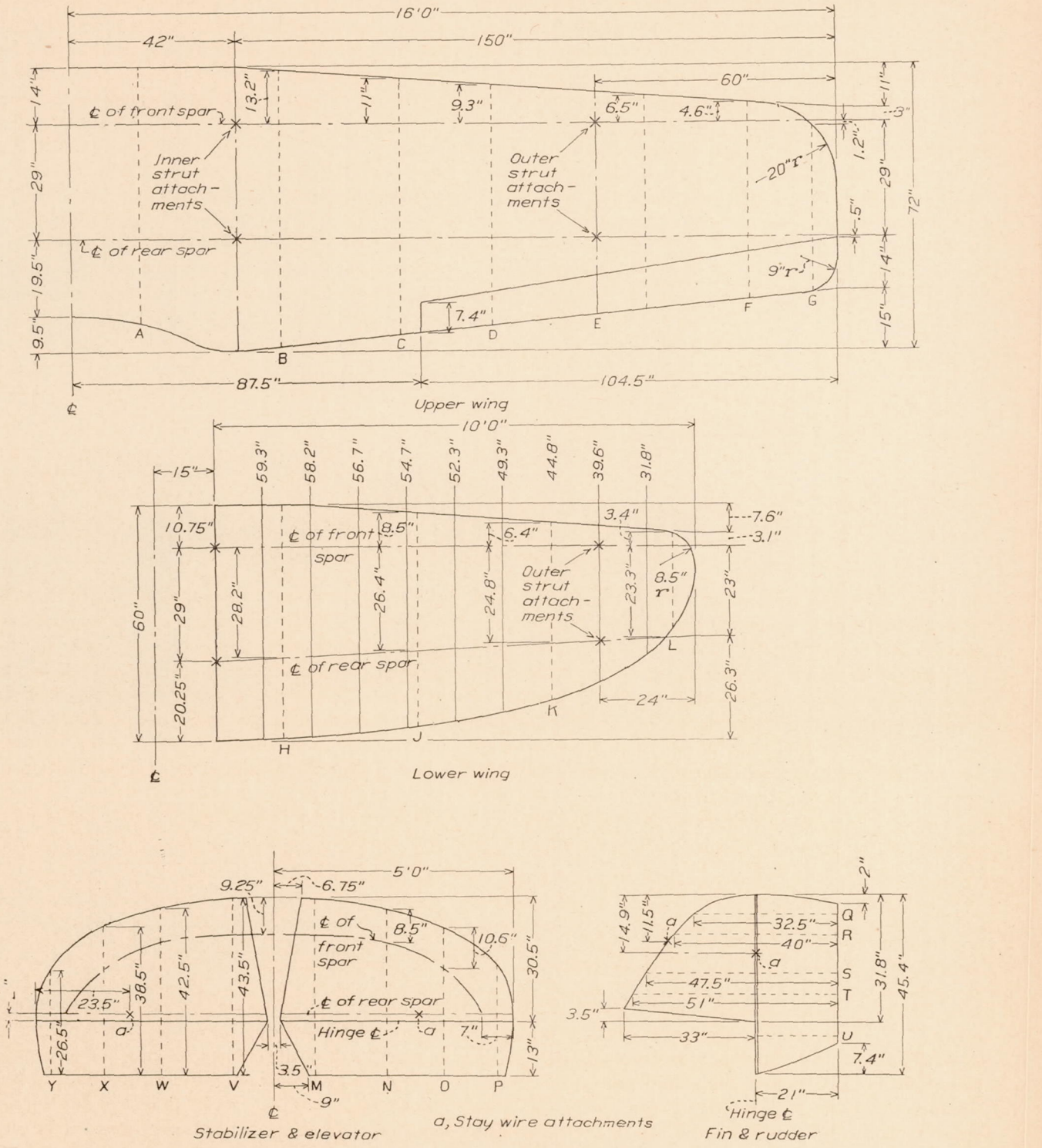

FIGURE 4.—*PW-9* wings and tail surfaces with spar locations and strut attachments

The pressure measured at each point was the algebraic sum of the pressures on the upper and lower surfaces (see fig. 13), no attempt being made to measure the pressures on these surfaces separately, except in a

few cases after the main tests had been completed. Pressure curves were mechanically integrated to obtain loads and centers of pressure. Simultaneously with the pressure measurements, records were obtained of air speed, normal acceleration at the center of gravity, left upper wing tip and tail, angular velocity in pitch or roll, depending on the maneuver being investigated, and control position. These were synchronized by means of the timer, and all of the measurements made were plotted together against time to furnish a history of each maneuver.

It will be noted, in glancing at the center of pressure data, that resultant centers of pressure are plotted in terms of per cent of "centric chord." The "centric chord" is here defined as the chord passing through the centroid of the plan form of that portion of the wing extending from the root to the tip, and it is used instead of some other arbitrary datum, because the position of the mean C. P. on the "centric chord" of tapered wings corresponds fairly closely with the mean C. P. on the constant chord of straight wings.

With respect to the maneuvers investigated, special attention was given level flight and pull-ups. A considerable number of level flight runs were made in order to furnish a basis for the study of the results obtained in accelerated flight, and also to furnish data for comparison with wind-tunnel results.

Attempts to measure angle of attack in level flight failed. First attempts were made with a pendulum inclinometer mounted in the cockpit, the pilot flying horizontally close to the ground, but with a sufficient altitude to eliminate possibilities of encountering ground effect. It was felt that level horizontal flight could be maintained accurately enough in this way to allow of the use of inclinometer readings directly as angles of attack. The method failed because the slight variations in engine speed and wind velocity caused the inclinometer to oscillate enough to make the readings quite erratic. Further attempts were made, flying as before, with a moving-picture camera mounted in the cockpit, the lens axis being normal to the XZ plane. Vertical reference lines on a row of hangars were photographed, and the angles of these lines on the picture with the frame edge were taken as angles of attack. This method showed promise, but with the hangars located on the south side of the field, as they are, it was impossible to obtain clear pictures, inasmuch as the vertical reference lines mentioned above were always in the shade. Angles as obtained were probably correct to within 1°, but this accuracy was not sufficient for the purpose for which they were desired, and all of the angle readings were thrown out. Centers of pressure, therefore, were plotted against normal force coefficient as the independent variable.

The extensive investigation of the pull-up was made for several reasons. First, it is one of the few maneuvers that can be subjected to reasonably close control, or repetition with accuracy. In other words, it is a simple maneuver requiring the pilot's attention on only the initial air speed and movement of one control surface. It is, therefore, possible to obtain a graduated series of maneuvers to allow of the study of accelerations, angular velocities, etc., as affecting the distribution of load. Also, the pull-up shows the dis-

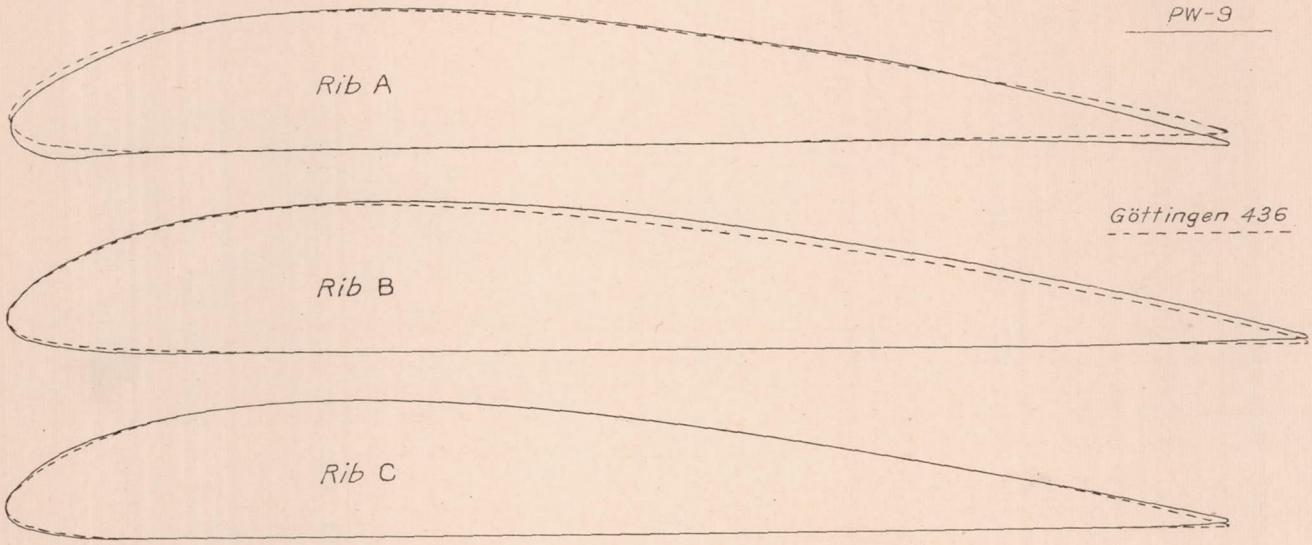

FIGURE 5.—Comparison of ribs A, B, and C with true Göttingen 436 section

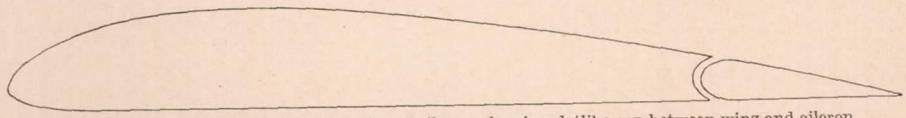

FIGURE 6.—Outline of *PW-9* wing section at aileron, showing slotlike gap between wing and aileron

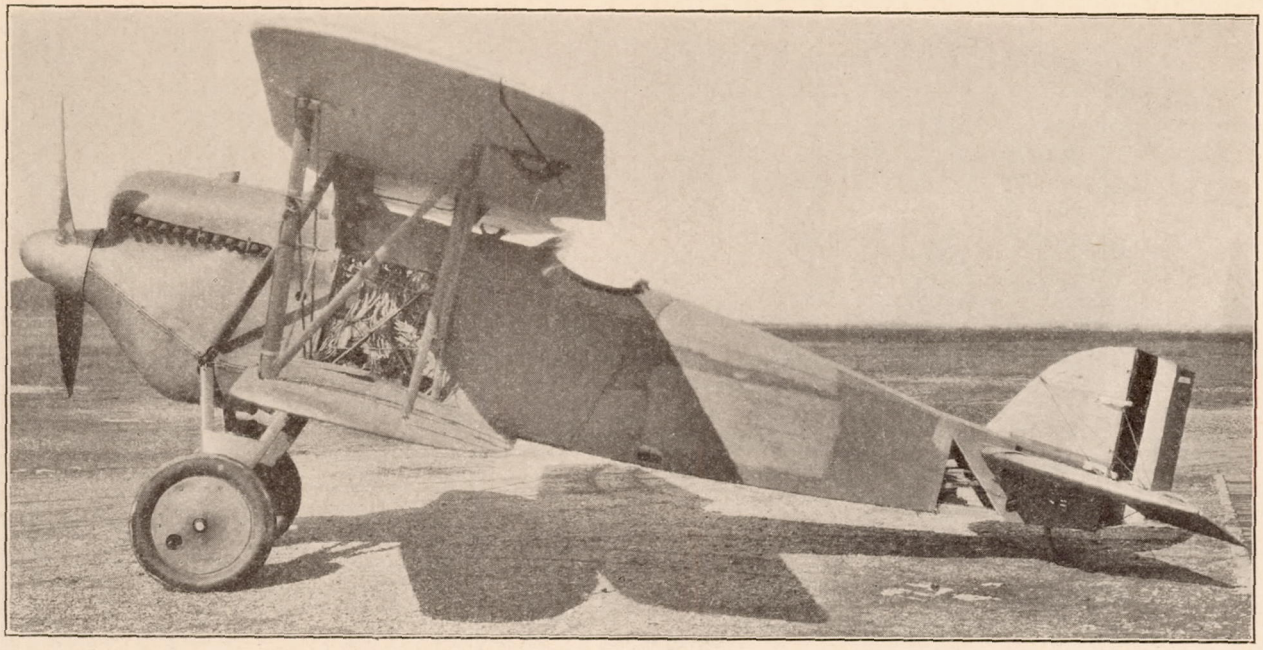

FIGURE 7.—Side view of *PW-9* airplane with instrument panels removed

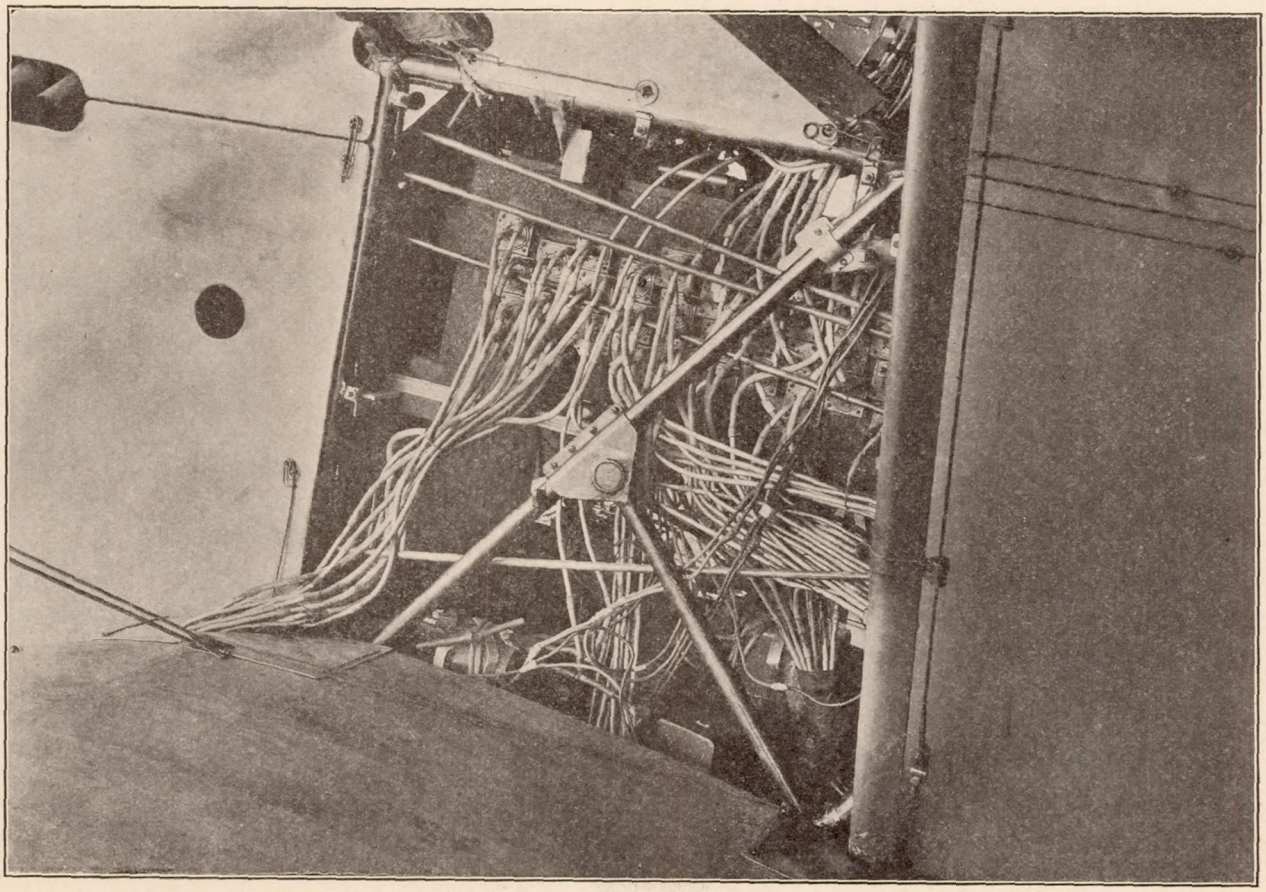

FIGURE 8.—Detail view of main instrument installation showing tube connections to manometers

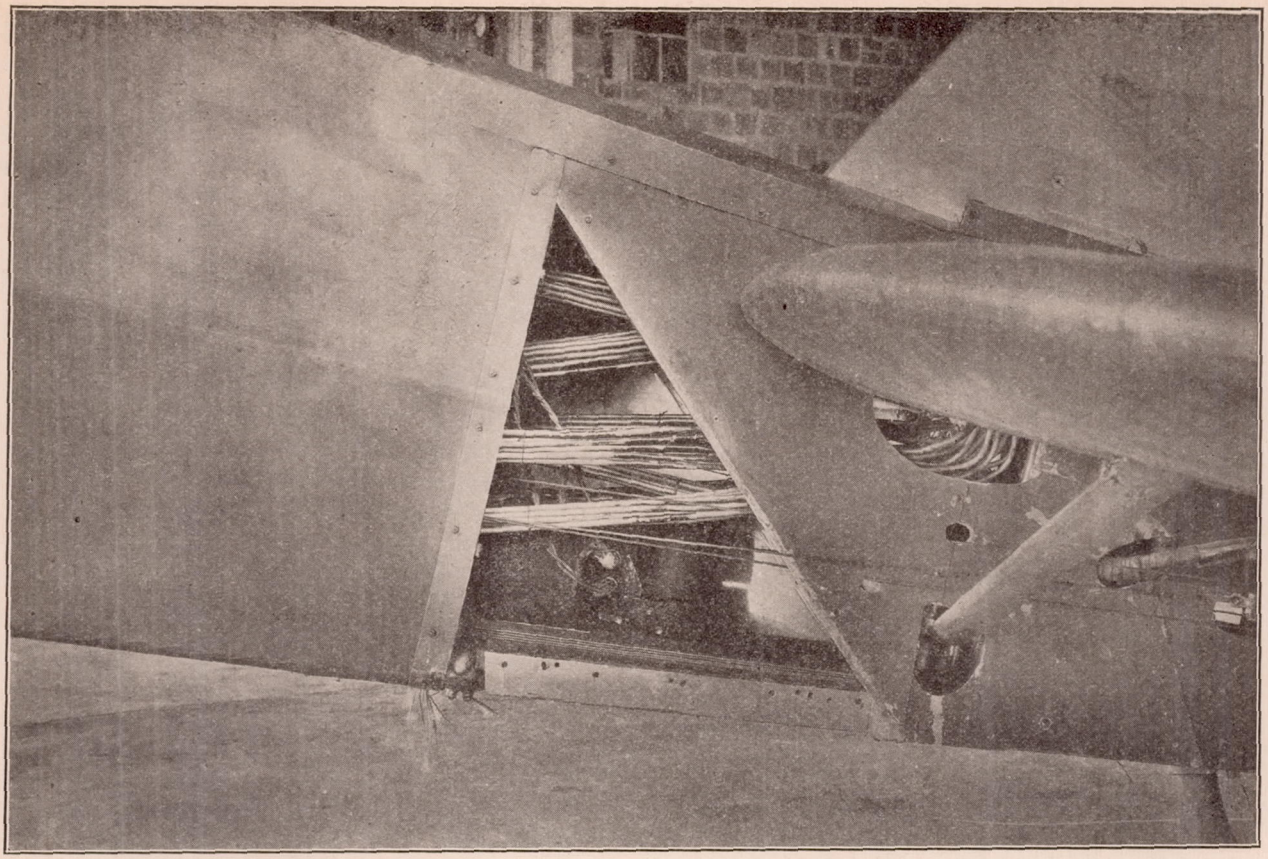

FIGURE 9.—Detail view of accelerometer installation in tail, showing also tubes from tail surfaces

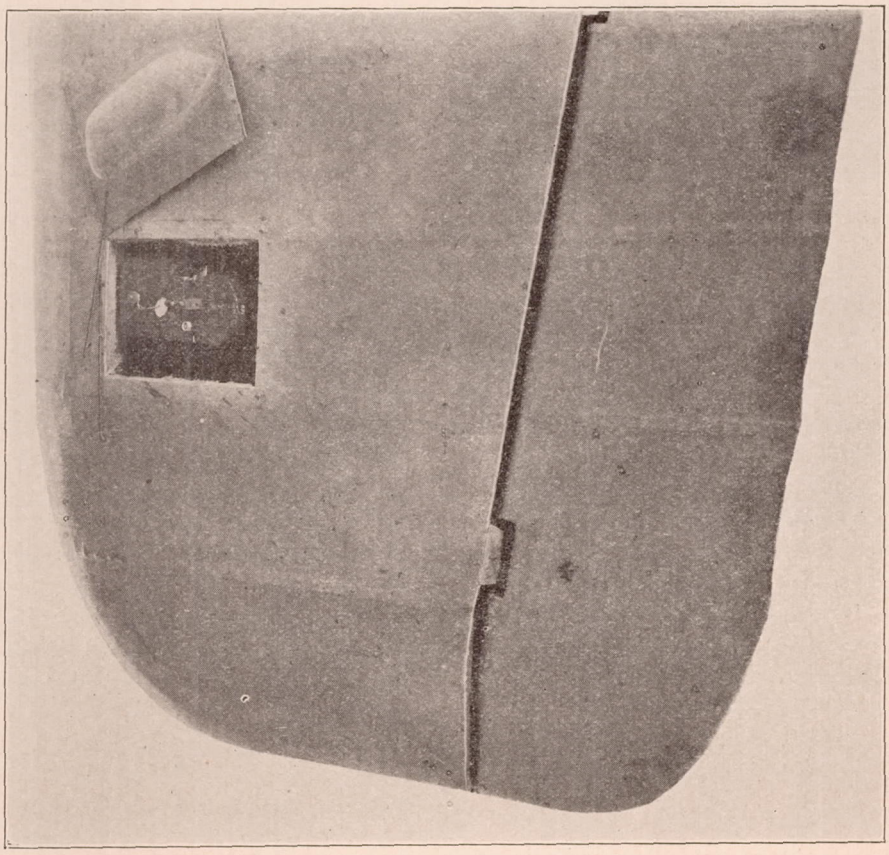

FIGURE 10.—Wing tip accelerometer installation

tribution of pressure through a large range of angle of attack and furnishes direct information on the most important loading condition, viz, high angle of attack. Third, the unusually far forward position of the center of pressure at high angles of attack in accelerated flight indicated by tests on the *VE–7* and *TS* airplanes (Reference 5), as well as the coincident high values of normal force coefficient, made it desirable to study the high angle of attack condition at some length with the hope of discovering relations which might account for the phenomena noted.

Because of the importance of accurate air-speed measurements in obtaining normal force coefficients, the air speeds as recorded from a Pitot-static head mounted on the front outer strut were carefully calibrated against those obtained from timed runs over a measured course, and also those obtained from a suspended "bomb" air-speed head. (Reference 7.) This calibration, it was found, sufficed only for level flight runs and the initial air speeds of the maneuvers. It was necessary, for the pull-ups, to measure the air speed by another method. For this purpose an air-speed head was mounted on an outrigger about 5 feet out and slightly forward of the lower wing tip in order to eliminate interference from the wings at all angles of attack encountered. Air speeds obtained from this head checked the "bomb" readings within one-fourth of 1 per cent at all angles in level flight. It was thus considered that readings obtained from this head in vertical plane maneuvers would be satisfactory, and all of the air speeds for the abrupt, power-on pull-ups were, therefore, corrected on the basis of results obtained from the outrigger head.

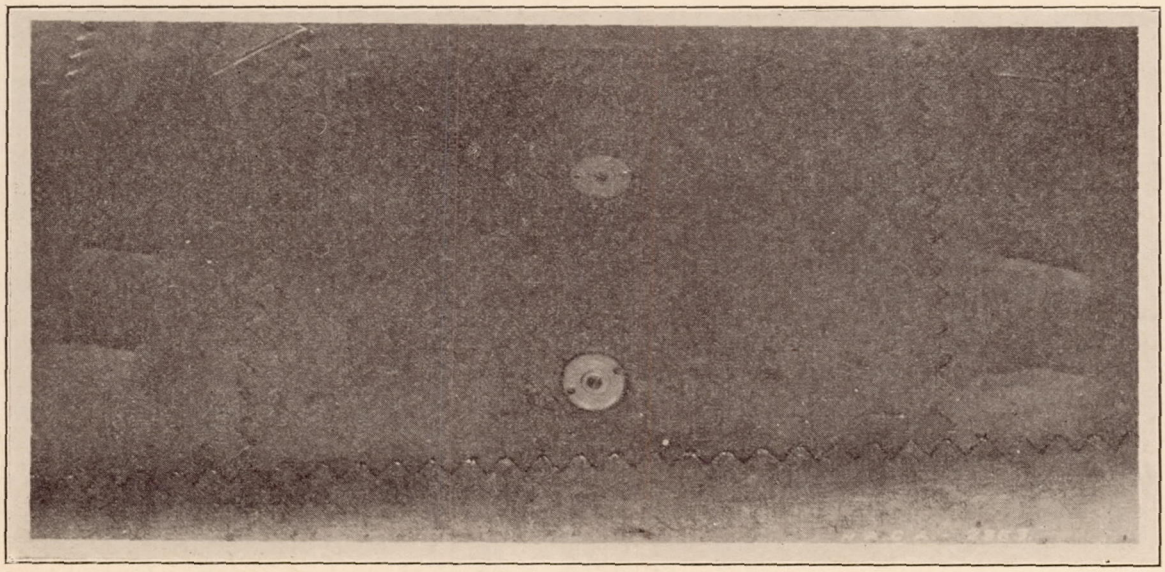

FIGURE 11.—Detail of orifice installation in wing

PRECISION

A discussion of the sources of error in pressure measurements, using the methods applied in the present tests is given in Reference 11. It was concluded there that individual pressures are correct to within ±2 per cent, while values of load are correct to within ±4 per cent. Recent investigations of the effect of temperature on the capsule calibrations indicate, however, that those figures should probably be increased by about 50 per cent for the greater part of these tests, and in some few cases should be doubled. These errors, however, have a minor effect upon the measured distribution of load, since the temperature errors are, in the main, a certain percentage for a given temperature regardless of pressure. Furthermore, most of the capsules, being identical in construction, show comparable temperature errors.

Air speeds are correct to within 3 per cent at all speeds in level flight. They are probably correct within about 4 per cent in accelerated flight, since it is believed that interference effects have been largely eliminated, although some uncertainty still exists on this point.

Individual values of rib center of pressure are correct to within about 2 per cent in the high angle of attack conditions, except in the case of rib L on the lower wing, and within an increasing error as the angle of attack decreases until, for conditions approaching zero lift, they are quite erratic and unreliable. For this reason, moments instead of centers of pressure are given for these last cases. Longitudinal centers of pressure of resultant forces are correct to within ±1 per cent at high angles of attack, while lateral centers of pressure are correct to within about 2 per cent.

Accelerations are correct to within $\pm 0.2g$ except where noted.

Control position angles are probably not correct to within less than 2 or 3 degrees, since the instrument was connected to the control levers in the cockpit, and did not measure change of angle caused by deflection of the control system under load.

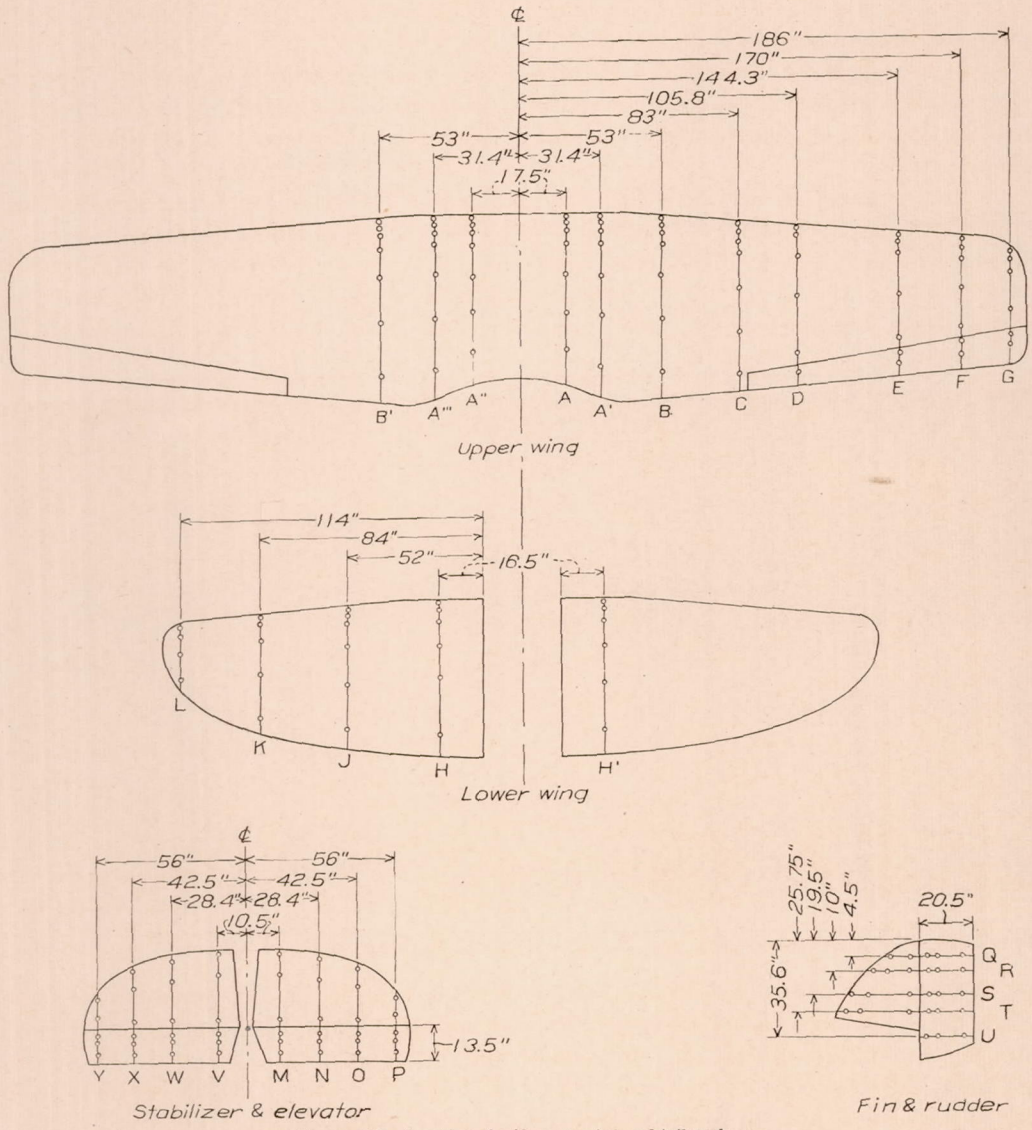

FIGURE 12.—Location of orifices on wing and tail surfaces

Location of stations

[In inches aft of leading edge]

Station	B'	A'''	A''	A	A'	B	C	D	E	F	G	H'	H	J	K	L	V M	W N	X O	Y P	Q	R	S	T	U
1	1.0	1.0	1.0	1.0	1.0	1.0	1.0	1.0	1.0	1.0	2.2	1.0	1.0	1.0	1.0	2.0	2.0	2.0	2.0	2.0	2.0	2.5	2.0	3.0	3.0
2	3.0	3.0	3.0	3.0	3.0	3.0	3.0	3.0	3.0	3.0	4.8	3.0	3.0	3.0	3.0	5.0	10.0	10.0	9.0	9.5	10.0	7.5	8.0	8.0	7.5
3	6.0	6.0	6.0	6.0	6.0	6.0	6.0	12.0	8.5	8.5	9.0	8.0	8.0	6.5	10.0	12.0	27.5	26.5	22.0	15.5	16.0	17.5	25.0	28.5	18.5
4	11.0	11.0	11.0	11.0	11.0	11.0	13.0	28.0	25.0	20.0	25.3	18.5	18.5	16.5	23.0	22.0	32.5	31.5	27.5	18.0	20.0	23.5	31.0	34.5	----
5	22.0	23.0	23.0	23.0	23.0	22.0	26.0	49.0	41.0	35.2	33.5	32.0	32.0	30.0	40.0	----	35.0	34.0	30.0	24.0	30.0	27.5	35.0	38.5	----
6	40.0	40.0	38.0	38.0	40.0	40.0	42.6	55.8	46.5	40.8	37.3	52.5	52.5	48.0	----	----	41.0	40.0	36.0	----	----	37.5	45.0	48.5	----
7	60.6	58.0	52.0	52.0	58.0	60.6	58.1	----	49.9	45.5	----	----	----	----	----	----	----	----	----	----	----	----	----	----	----
Chord	68.0	70.0	64.0	64.0	70.0	68.0	64.0	60.4	54.0	49.2	42.0	58.8	58.8	54.0	44.8	25.6	43.5	42.5	38.5	26.5	32.5	40.0	47.5	51.0	20.5

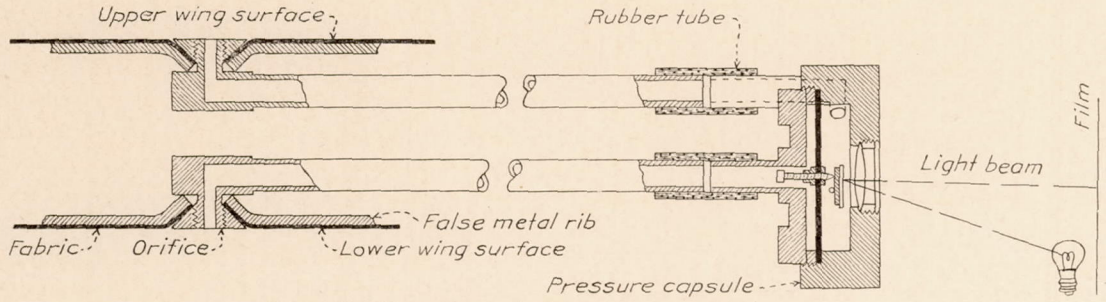

FIGURE 13.—Diagram showing type of orifice and connection to capsule

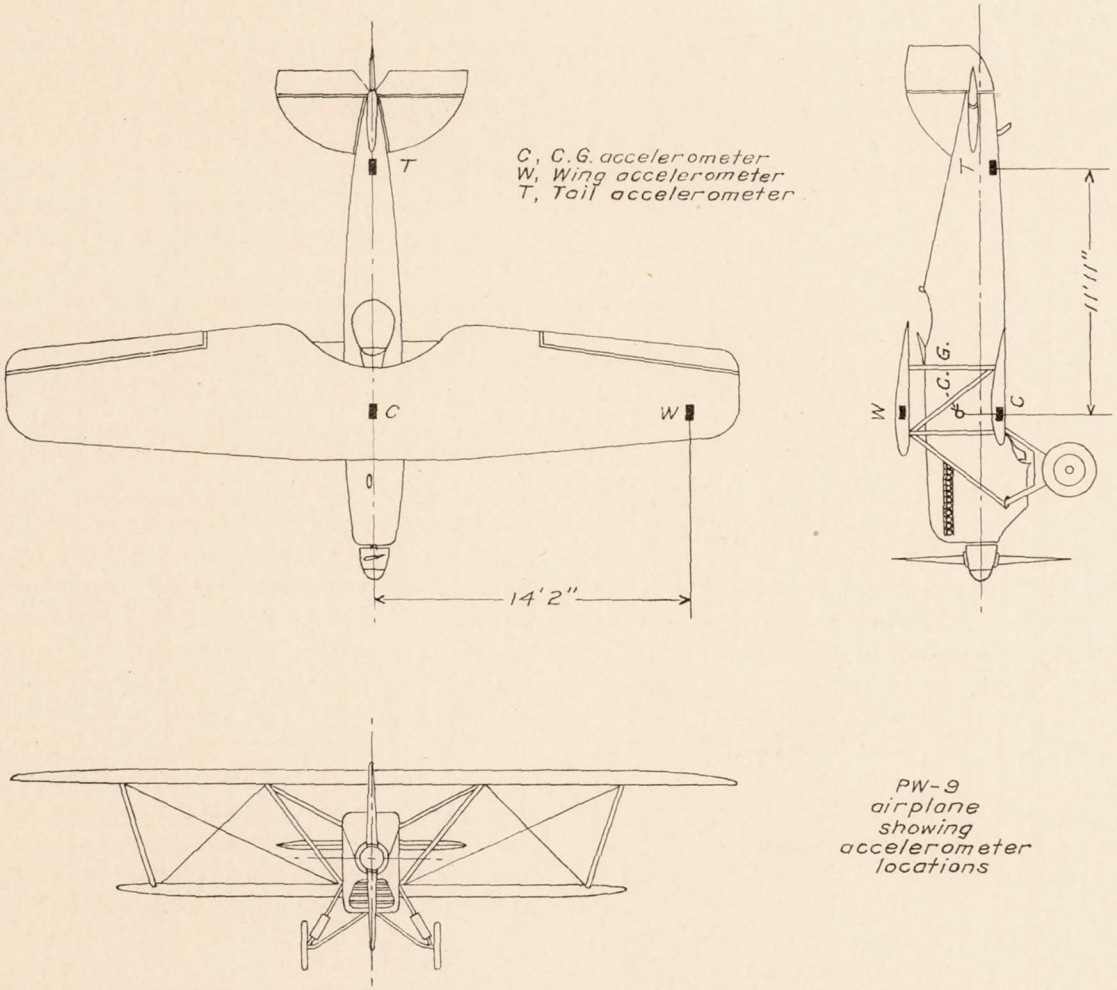

FIGURE 14.—Three-view drawing of *PW-9* airplane showing accelerometer locations

Time synchronization is correct in most cases to within about one-twentieth of a second, although in some runs, because of instrument difficulties, the synchronization is rather poor. For this reason, any calculated quantities depending on the records of two or more different instruments may be quite unreliable. This is particularly true of abrupt maneuvers in which the measured quantities vary through a wide range in less than 1 second.

PRESENTATION AND DISCUSSION OF RESULTS

The results following are presented and discussed in groups according to the maneuver under investigation, viz:

1. Level flight.
2. Pull-ups.
3. Rolls.
4. Spins.
5. Inverted flight.
6. Dives.
7. Pull out of dive.

In addition, the tail load, slip stream, and fabric pressure data are summarized and presented separately. While all of the data obtained in the tests are not given in their entirety, representative examples of the most important cases are included, and also, where it was felt they would be of interest, more complete data are given.

Level flight.—The level flight results are given in Table III and in Figures 15a to 20. Figures 15a, 15b, 15c, and 15d show the distribution of pressure in terms of q for four representative cases through the speed range or useful range of angle of attack. An inspection of these figures at once discloses several salient points, viz: 1. At low speed, or high angle of attack, the center of pressure locus is, for all practical purposes, at the same per cent of chord along the span until the tip is approached, where it bends suddenly to the rear. This is particularly true of the upper wing. With respect to the lower wing, this point is questionable since pressures at only four points were measured on rib L, and the accuracy of the pressure curve at that station is poor. 2. As the speed increases, the center of pressure moves back varying amounts at different stations along the span, the trend being farther to the rear as the tip is approached until, at high speed, the center of pressure at the tip is almost twice as far back as it is on the inner portion of the wing. 3. In practically all cases, minor peaks of pressure occur on the aileron.

This rearward trend of the center of pressure from the center line to the tip at low angles of attack is worthy of special note. Figures 17a to 18e afford a closer study of the center of pressure movement. Figures 17a and 18a show the variation of resultant center of pressure with normal force coefficient for upper and lower wings, respectively. Figures 17b to 17h and 18b to 18e give the center of pressure vs. C_N for each individual rib. As might be expected, the points for ribs in the slip stream and near the wing tips are somewhat erratic, but a sufficient number of runs were made so that fairly good curves can be drawn in every case, with the exception of rib L. The rearward trend of the center of pressure toward the tip as normal force coefficient decreases is clearly apparent from these curves, and leads to the suspicion that a considerable amount of twist (washout) exists, particularly in the upper wing. This suspicion is strengthened by subsequent data which show a rapid decrease in load along the span toward the tip at low angles of attack. It is desirable, therefore, to study the effect of twist on the load distribution at some length.

The subject is discussed very well in Reference 12, in which the author points out the importance of slight angles of twist at low angles of attack, and calls attention to the fact that the twist may be a built-in feature of the wing, geometric or aerodynamic, or it may be a torsional deflection under load. He also gives methods based on the vortex theory for calculating the load curve for wings having certain simple conditions of taper and twist, comparing the results with load curves computed on the basis of the "strip" method, and pointing out that the latter method is not sufficiently exact in some cases. The method is given more completely in Reference 13, and is extended to include any tapered wing with any character of twist.

For present purposes, it is sufficient to compare the load curve obtained in flight with load curves calculated on the basis of the strip and vortex theories. To do this, it is necessary to choose a particular condition of flight and to determine what the actual twist was in this condition. The condition chosen is high-speed level flight, since several runs are available for this condition, and hence experimental errors can be reduced by taking an average load curve. To determine the twist of the wing in this condition is not difficult. The most reasonable way would seem to be by actual measurement of the rigged incidence and adding to this the extra twist induced by the application of the load existing in the particular condition being studied. Unfortunately this method is not possible, since there is evidence that the rigged incidence changed during the course of the tests, and hence the true rigged incidence for any particular run or set of runs is not known. It is necessary, therefore, to resort to a different method. Assumptions are made as follows: 1. That the curves of C_P vs. α for individual rib sections not too near the tip and outside of the propeller influence superpose upon one another; that is, that for ribs B, C, and D for instance, the center of pressure is at the same per cent of chord at the same angle of attack. 2. That scale effect does not influence the center of pressure position except to a negligible extent. With these assumptions, probable

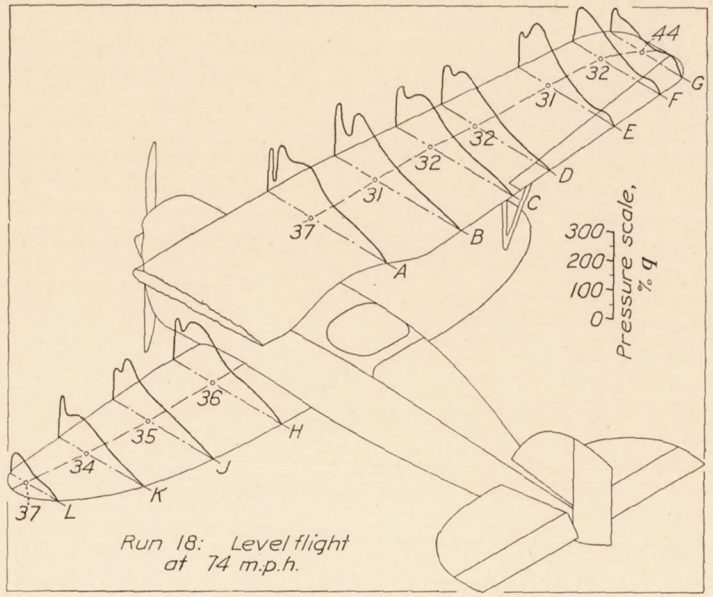

FIGURE 15a

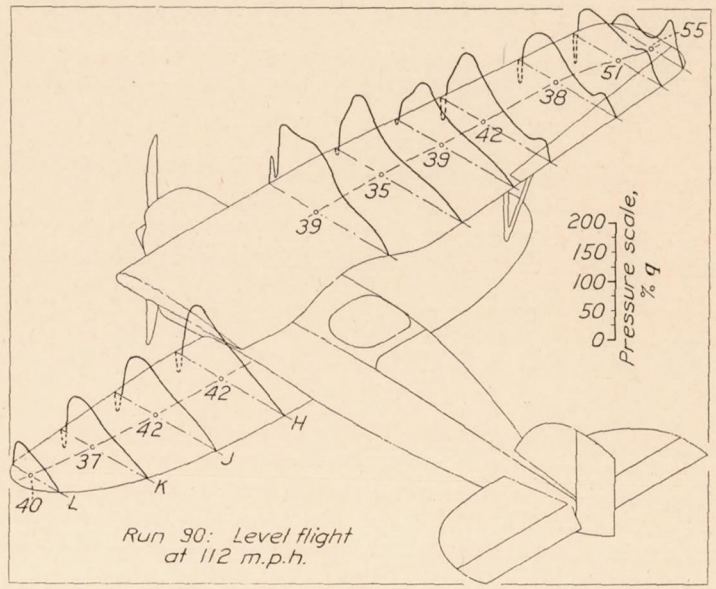

FIGURE 15b

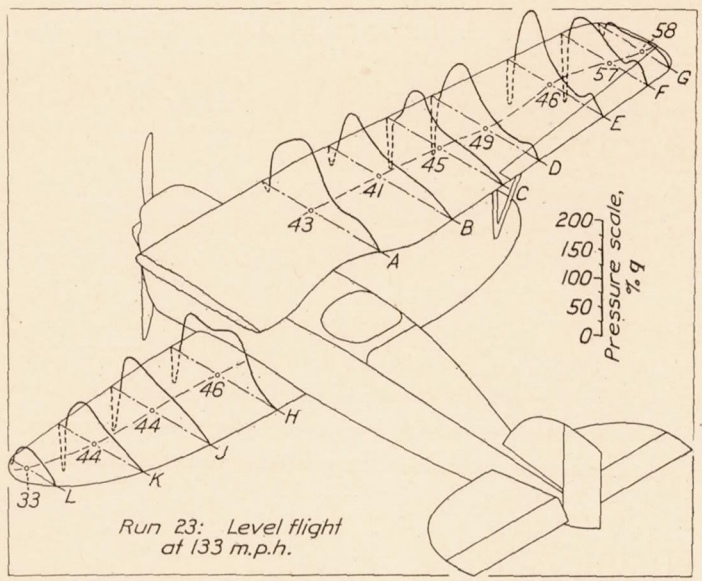

FIGURE 15c

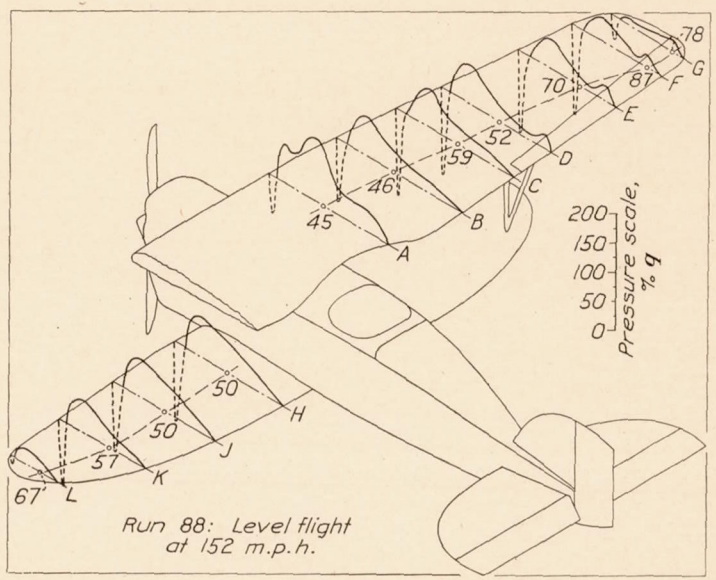

FIGURE 15d

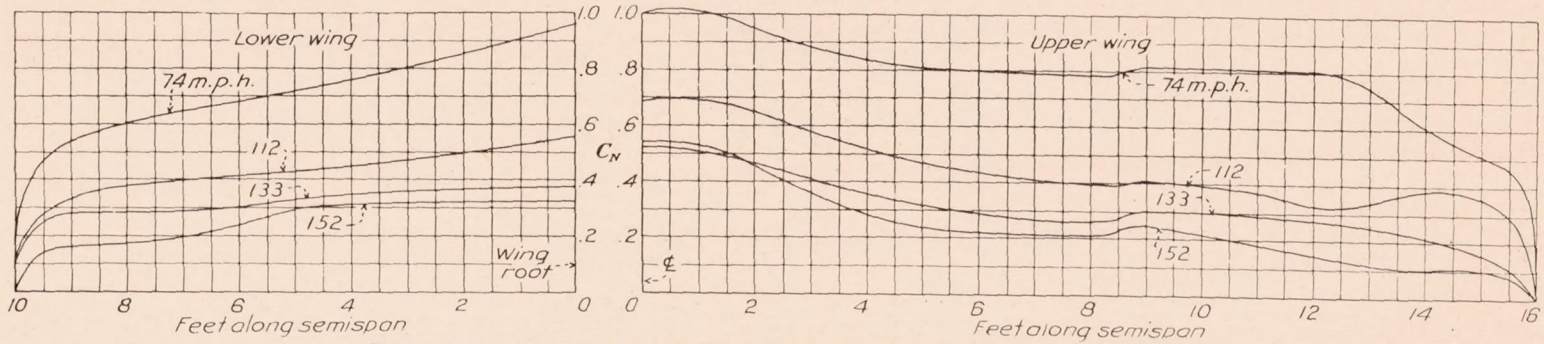

FIGURE 16.—Variation of normal force coefficient along the span in level flight through the speed range

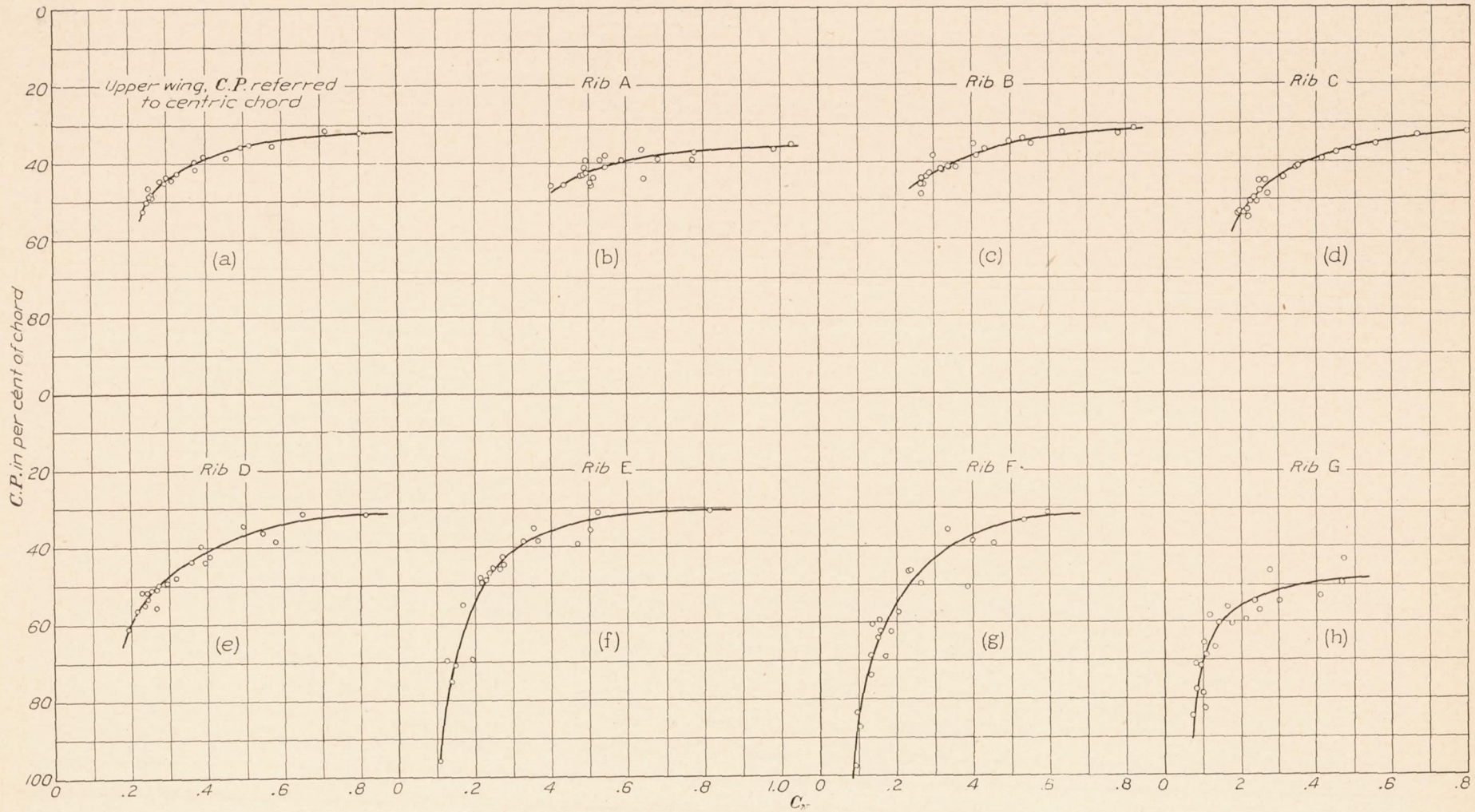

FIGURE 17.—Center of pressure in per cent of chord vs. normal force coefficient

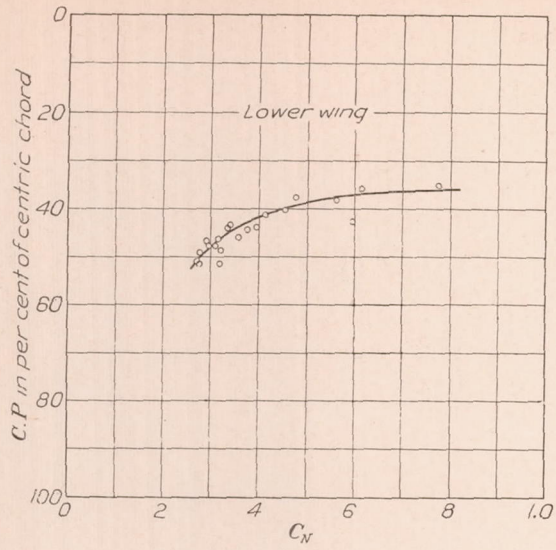

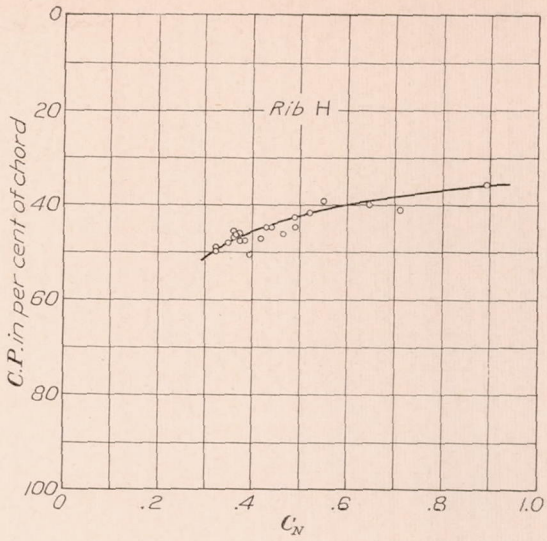

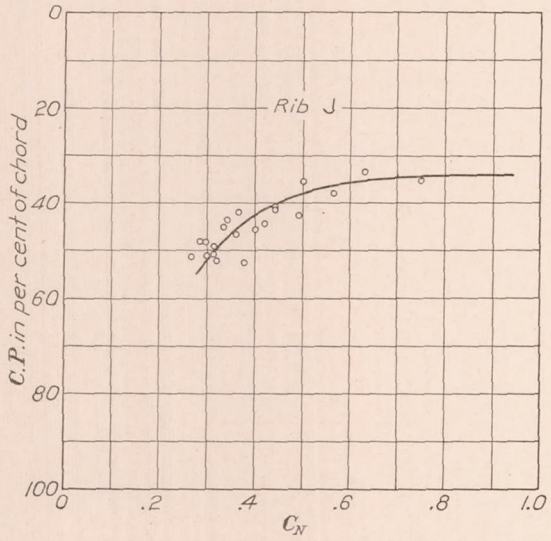

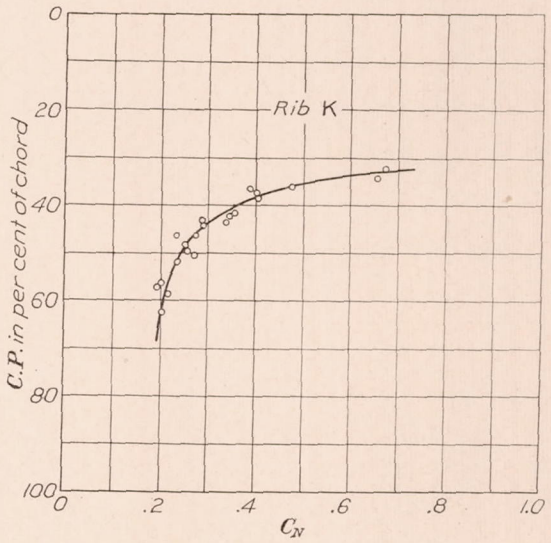

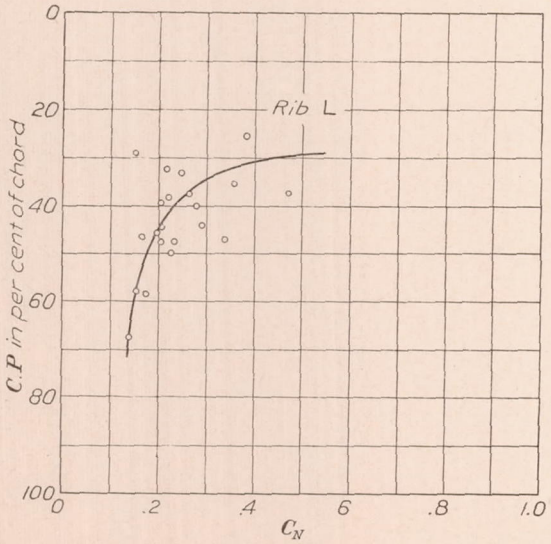

FIGURE 18.—Center of pressure in per cent of chord vs. norm force coefficient

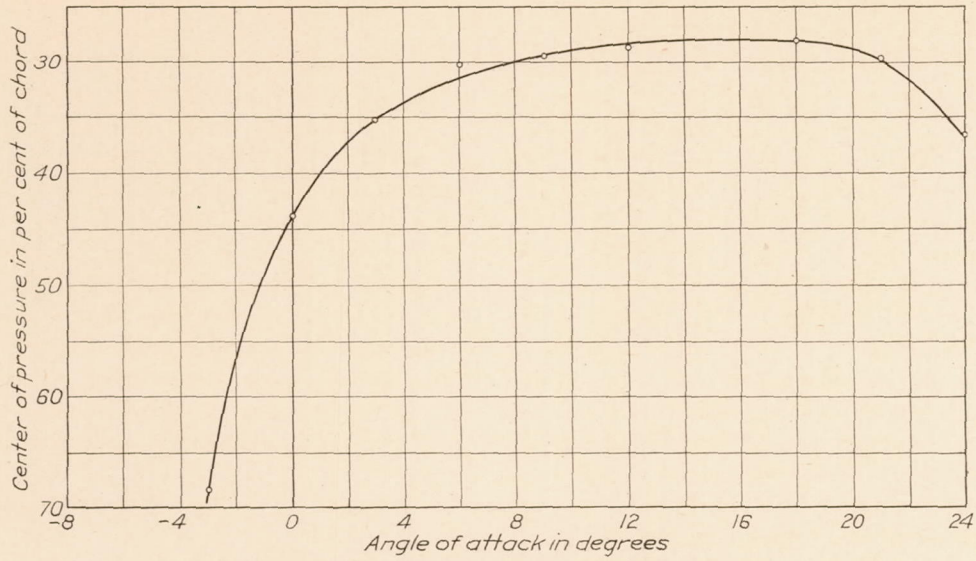

FIGURE 19.—Center of pressure vs. angle of attack for model rib C

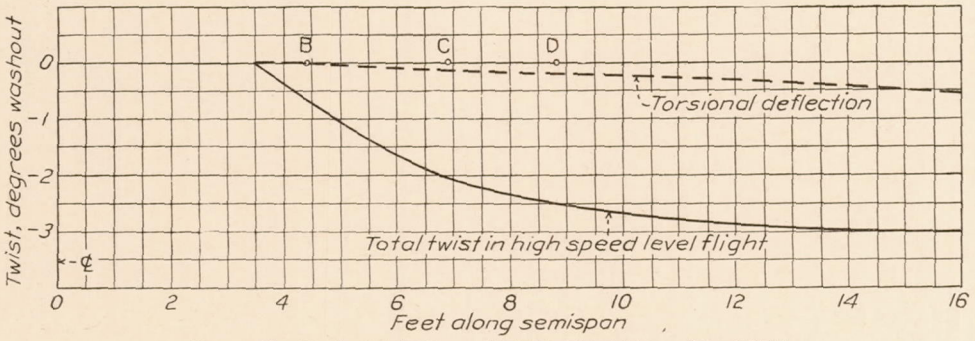

FIGURE 20.—Torsional deflection and total twist in high-speed level flight

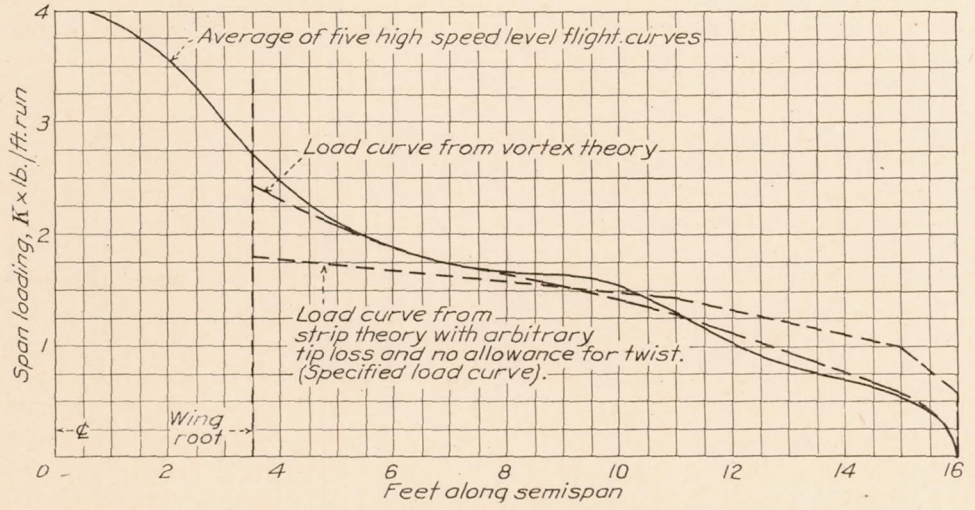

FIGURE 21.—Comparison of experimental load curve and load curves based on strip and vortex theories

values of center of pressure for ribs B, C, and D in high-speed level flight are determined from Figures 17c, 17d, and 17e. These values are referred to Figure 19, which shows the variation of C. P. with α on rib C of the *PW–9* model, and the values of angles of attack obtained therefrom. The differences in these angles are taken as the twist of the wing between the stations used. Referring to Figure 20, these differences are plotted against span, taking B as a starting point. The curve is then displaced downward until its inner end, extended, intersects the base line at 3½ feet, the point at which the wing chord is a maximum and which is subsequently to be taken as the root section for the comparison of load curves. The outer portion of the curve is extrapolated to the tip as shown. This extrapolation is not particularly hazardous, since it is based on a curve of measured rigged twist (not shown) which has a similar form, differing only in degree. Figure 20 represents then the twist of the wing in high-speed level flight, and includes both the rigged twist and torsional deflection. Using this twist and an angle of attack for the root section based on the average value of C_N at rib B and the slope of the C_N vs. α curve for a similarly located rib on the model, the span load curve is calculated on the basis of the vortex theory with the result shown in Figure 21. The agreement is quite good.

The design load curve shown for comparison is based on the strip theory without allowing for twist. It is only fair to point out here that the rigged twist on this particular wing is rather unusual, and is greater than the washout required in the design and specified by the manufacturer to compensate for propeller torque. The discrepancy between the design load curve and experimental curve is, therefore, greater than it should have been. But, further in this connection, it is necessary to mention that while the torsional deflection under the applied load in this case only amounted to one-half of a degree at the tip the applied load factor was 1, whereas the condition designed for at low angles of attack is the early stage of the pull out of a dive, in which the applied load factor may be several times unity and the torsional deflection, therefore, increased in proportion. It is manifest then that not only is the rigged incidence a matter of importance to consider in the structural design, but the torsional rigidity of the structure as well, and this latter quite apart from considerations such as wing flutter and secondary stresses. This conclusion is not new, but seems to have been overlooked in this country. In spite of the probability that stress analysts and designers will view with distaste the necessity of carrying out the additional calculations required to obtain a more exact load curve, there seems to be no simpler alternative at present. It may be remarked, however, that the solution of the load curve, once the twist is known, is neither difficult nor particularly laborious. In relatively flexible structures, however, because of the mutual relationship of twist and load, it becomes necessary to resort to trial and error, always a tedious process.

The span moment curve is readily determined on the basis of the assumption that the moment coefficient varies linearly with the lift coefficient when the moment curve for the basic airfoil section is known.

The minor peaks of load occurring on the aileron are believed to be due largely to the effect of the slot-shaped gap between the wing and the aileron, since the control position record showed that the aileron was neutral or very near neutral in all runs.

Pull-ups.—Pull-ups were made as follows:

1. Abrupt, power on, through the speed range.
2. Graduated abruptness, power on, at 70, 100, and 130 m. p. h.
3. Repetition of some of the foregoing with power off.

Figures 22a to 25f show the variation in pressure distribution throughout four abrupt pull-ups at speeds between 79 and 181 m. p. h., and Figures 26 to 29 the corresponding span load curves. In the pull-up at 79 m. p. h. the airplane was nearly stalled before the maneuver was begun, and the pressure curves for 0 time are, therefore, characteristic of the high angle of attack condition in steady flight. As the maneuver progresses, however, the angle of attack of maximum lift is reached and the mean center of pressure (see fig. 30) on the upper wing moves forward to about 26 per cent of the centric chord. It will be noted from the pressure plots for the medium and high-speed pull-ups and from the time history curves (figs. 30 to 55) that the maximum forward position of the center of pressure is the same within the experimental error in every case, the average value being about 27½ per cent. (Exceptions: Run 73 and Run 137.) This value agrees with the value found in wind-tunnel tests on the *PW–9* cellule. (Reference 14.) It does not, however, check the value found in monoplane tests, the difference being about 3½ per cent with the full-scale center of pressure farther forward. This discrepancy is ascribed to "biplane effect" or the mutual interference of the upper and lower wings.

On the lower wing the center of pressure does not move so far forward, reaching an average value of about 31 per cent. This value does not check the wind tunnel value, but comparisons are not strictly valid since the wind tunnel lower wing model was extended to the plane of symmetry, and hence has a greater span, proportionally, than the full-scale wing.

While the influence of biplane effect on the center of pressure is not an unknown phenomenon, thus far it has not been taken into account in the design rules. The importance of this phenomenon should not be overlooked. While it can be seen from Figures 56 to 59 that the distribution of load along the span on both

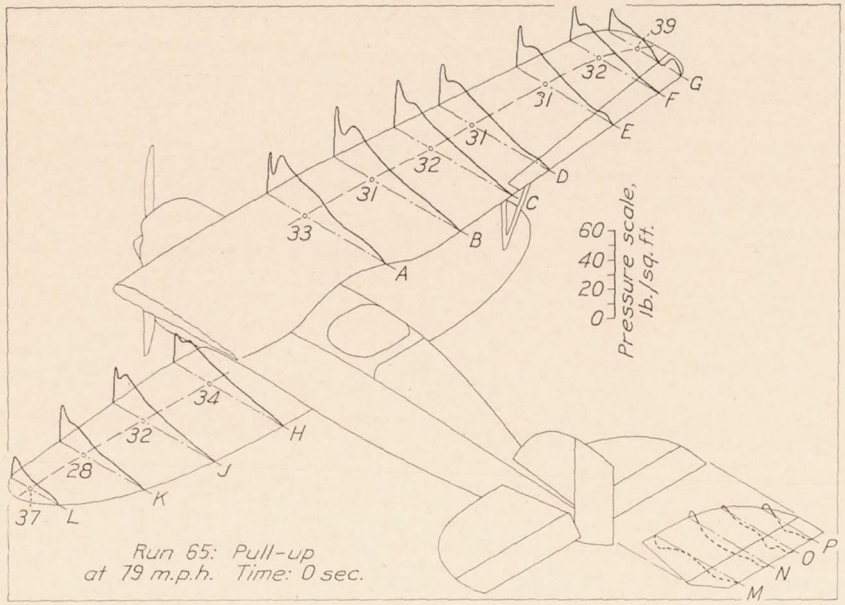

FIGURE 22a

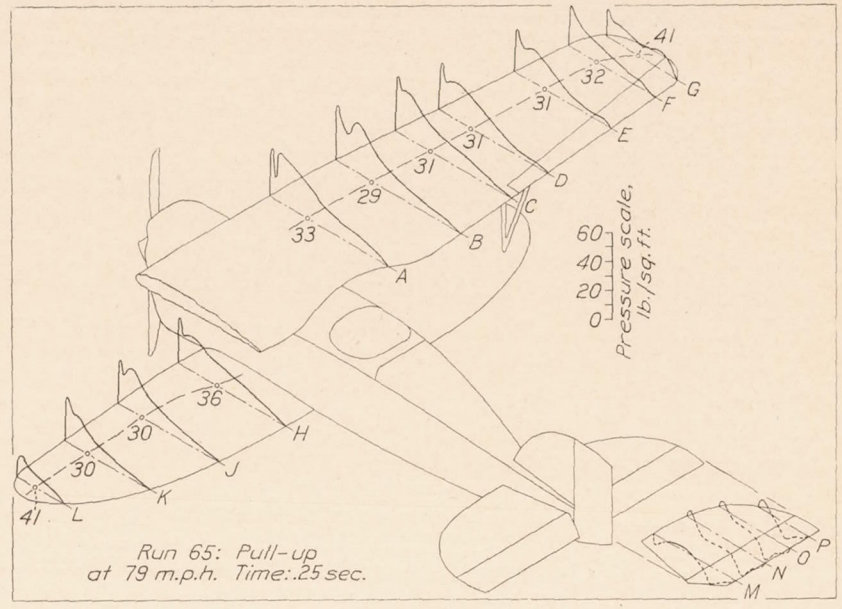

FIGURE 22b

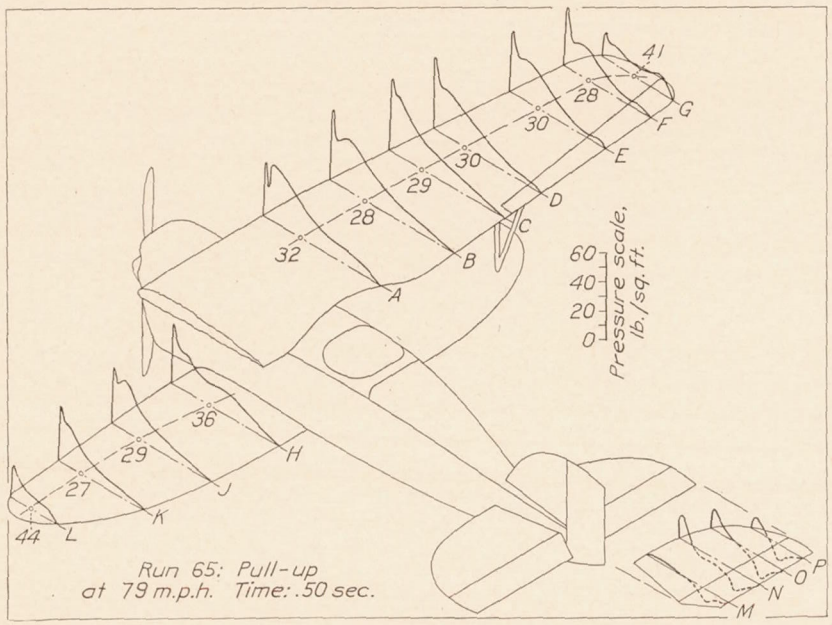

FIGURE 22c

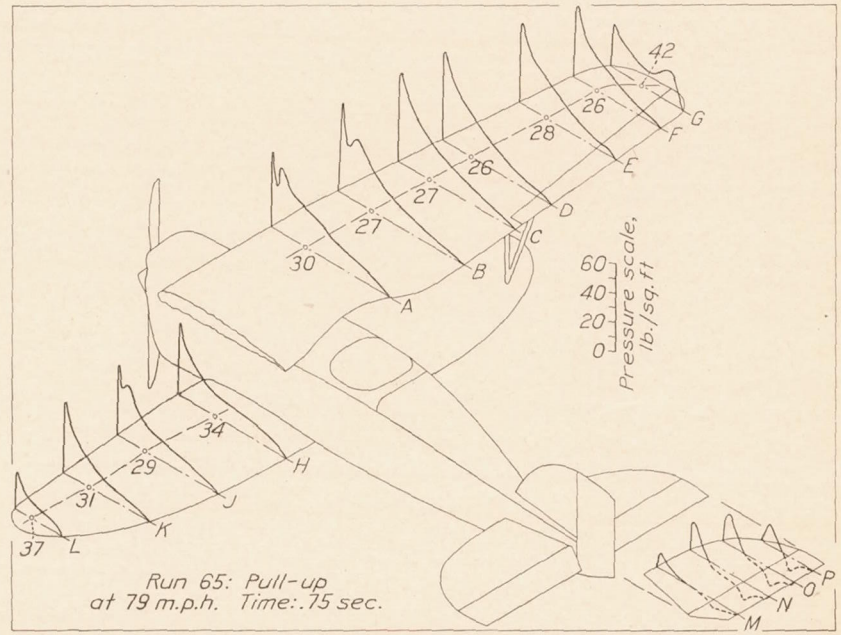

FIGURE 22d

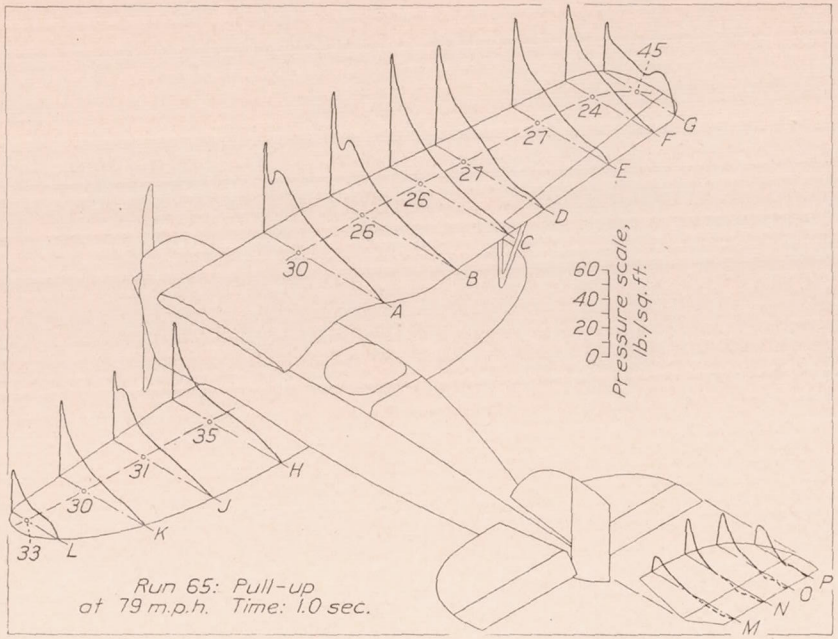

FIGURE 22e

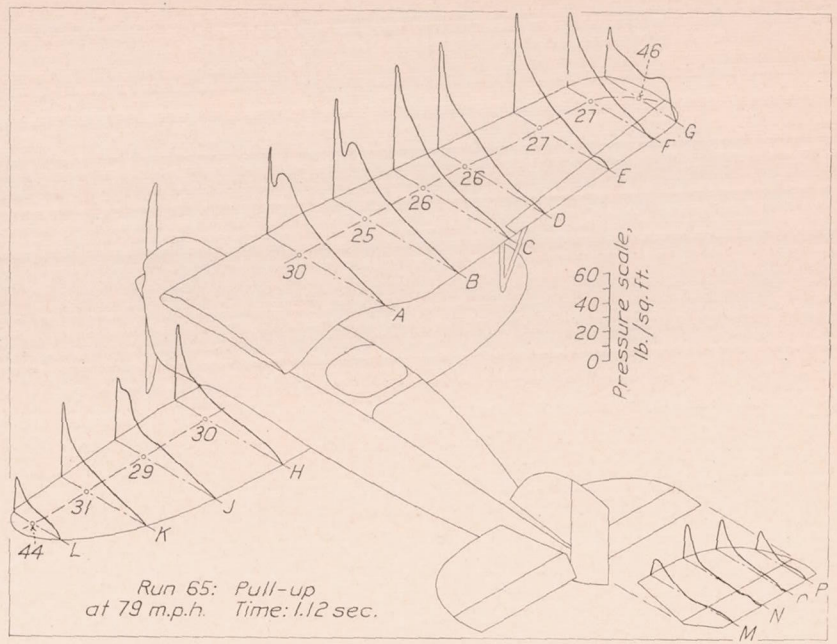

FIGURE 22f

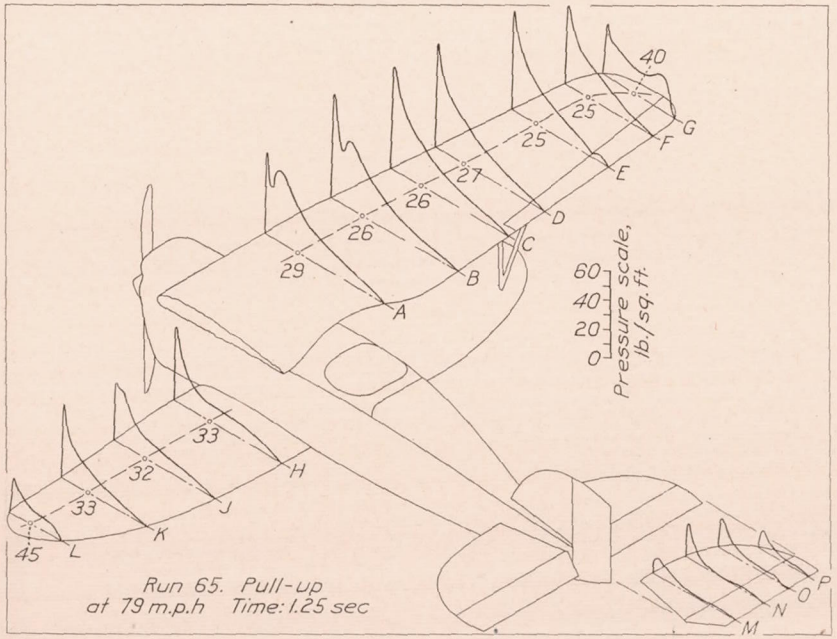

FIGURE 22g

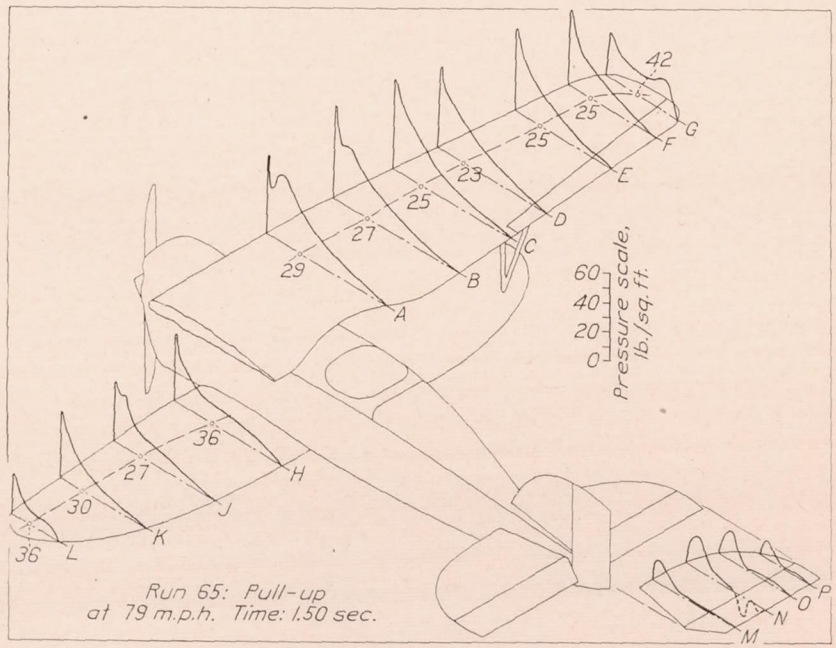

FIGURE 22h

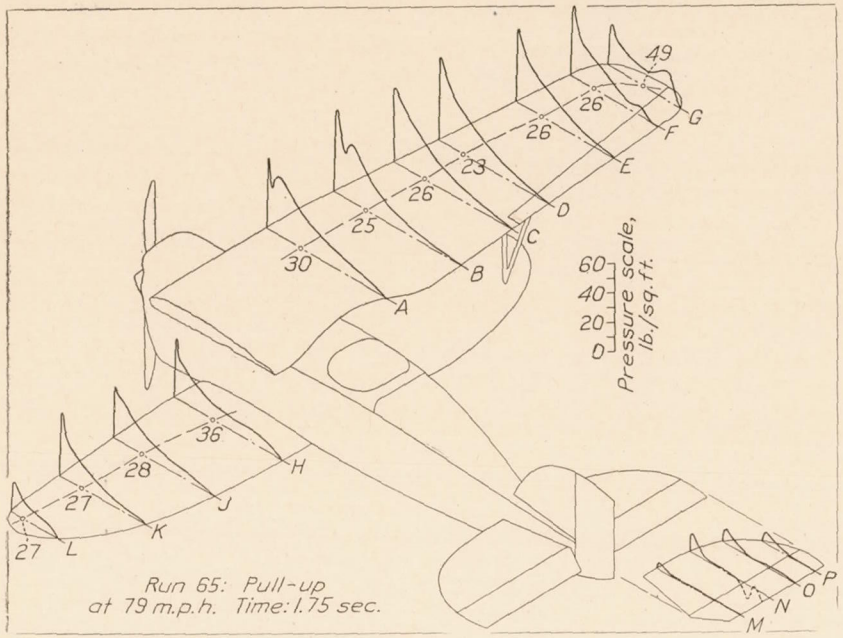

FIGURE 22i

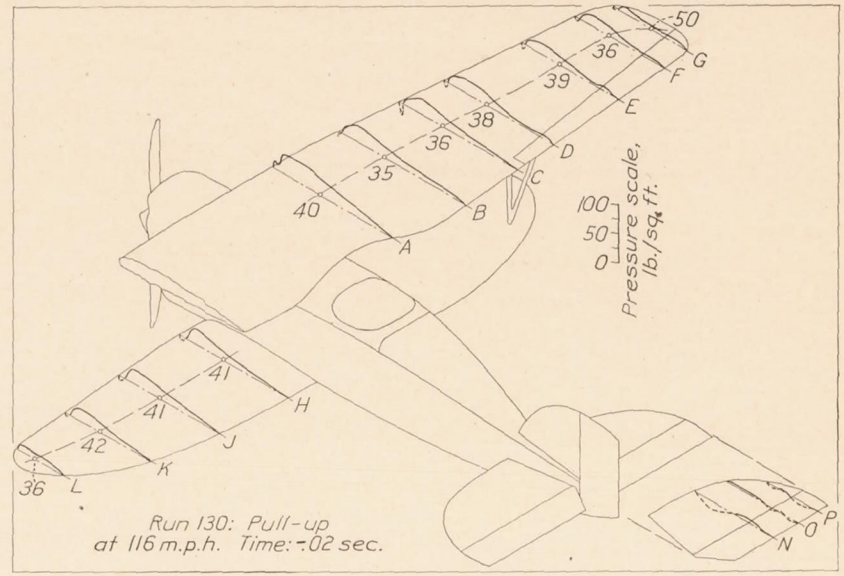

FIGURE 23a

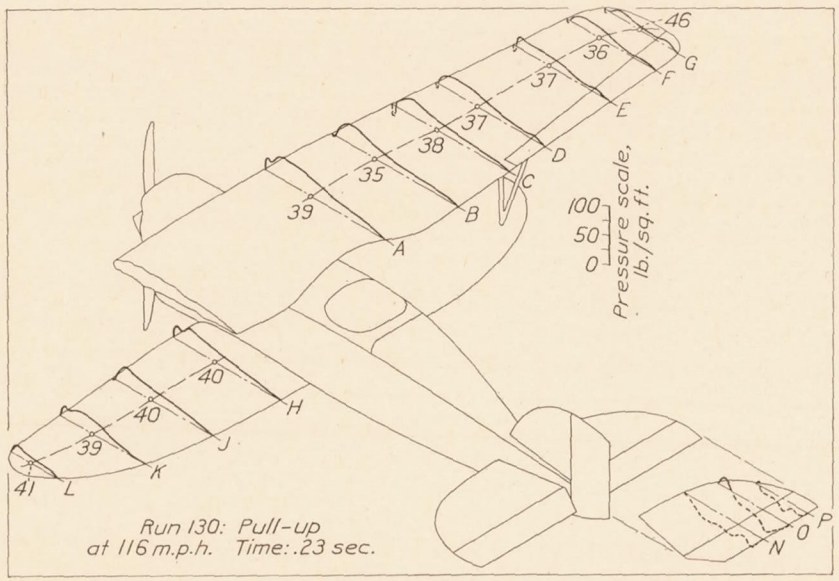

FIGURE 23b

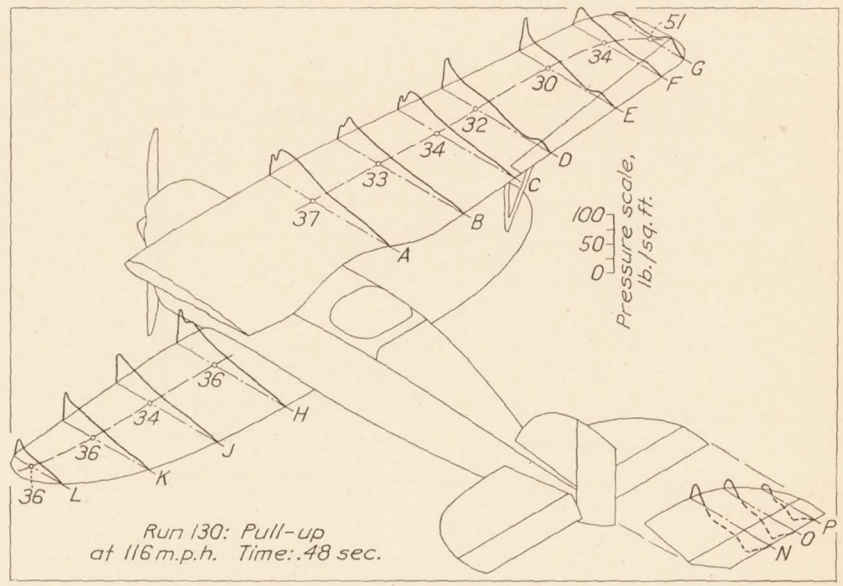

FIGURE 23c

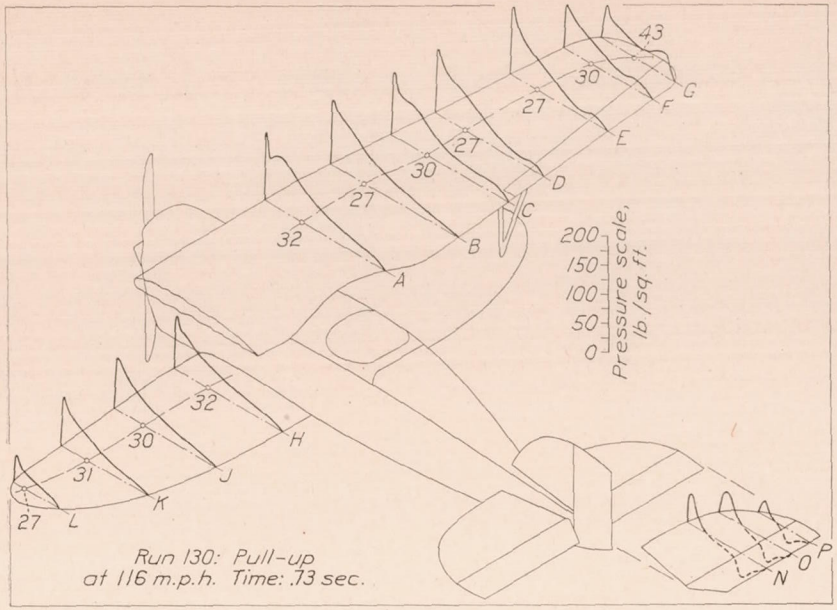

FIGURE 23d

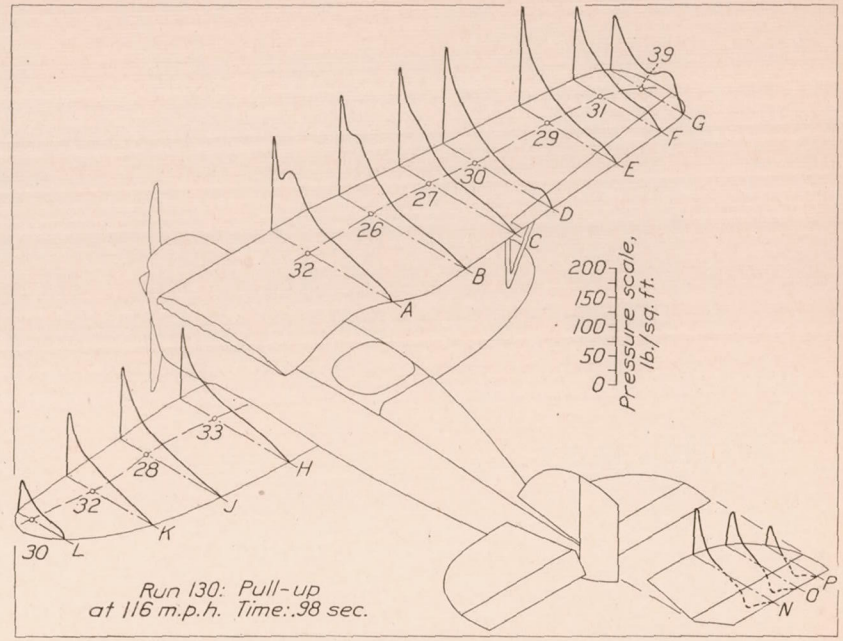

FIGURE 23e

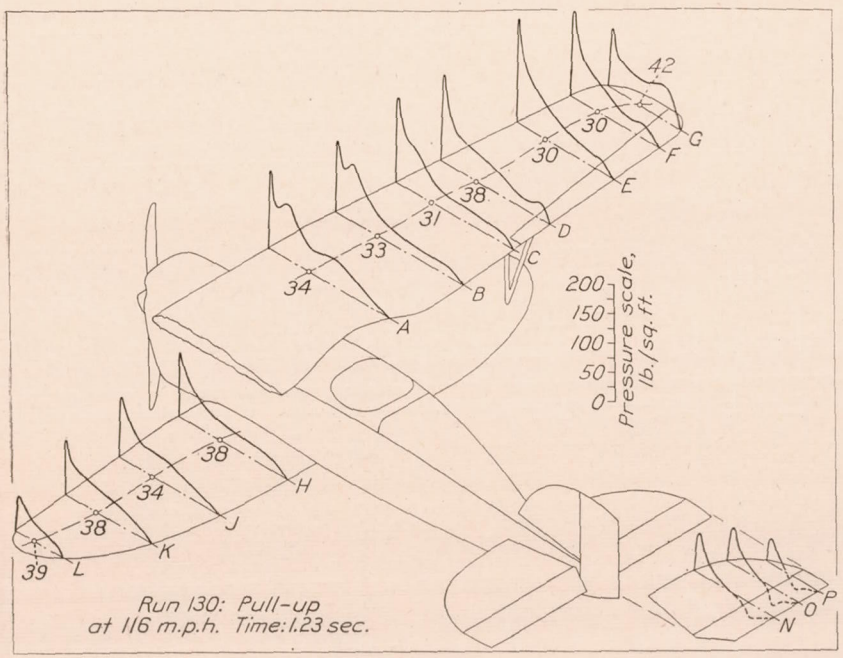

FIGURE 23f

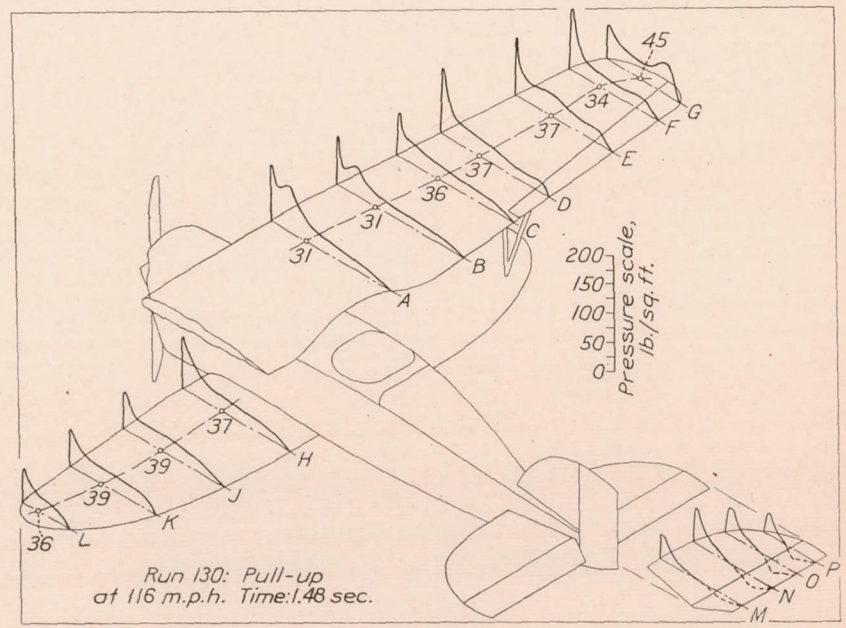

FIGURE 23g

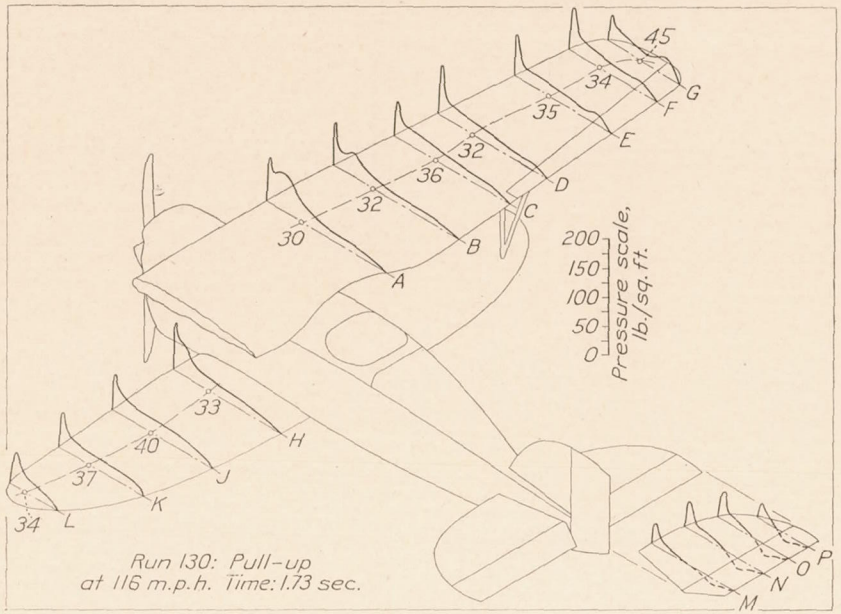

FIGURE 23h

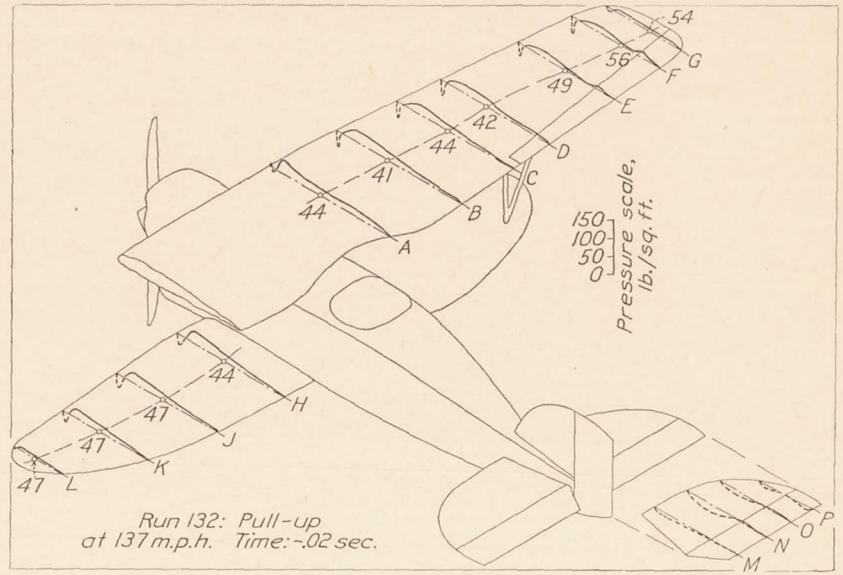

FIGURE 24a

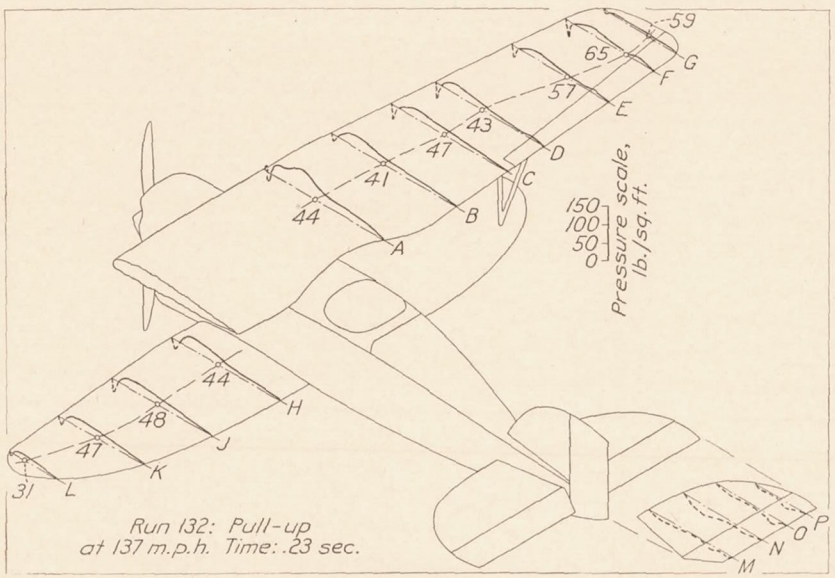

FIGURE 24b

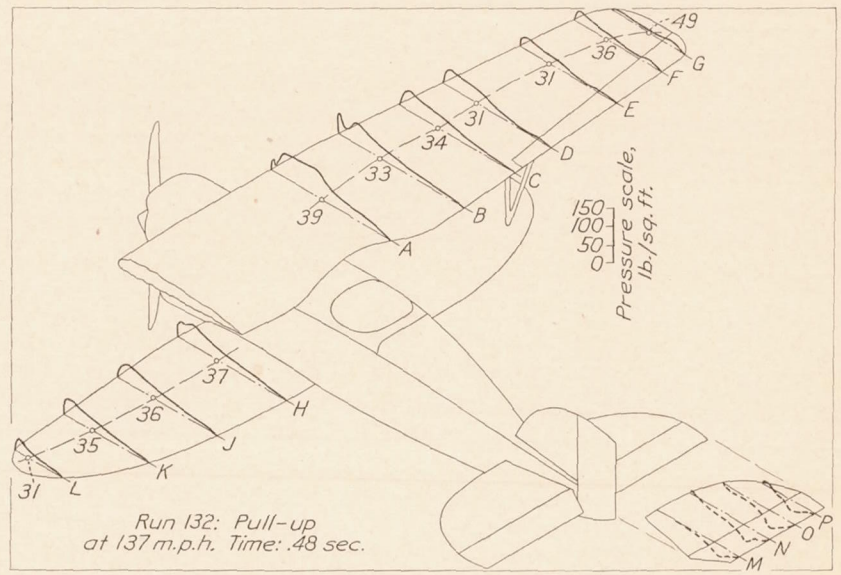

FIGURE 24c

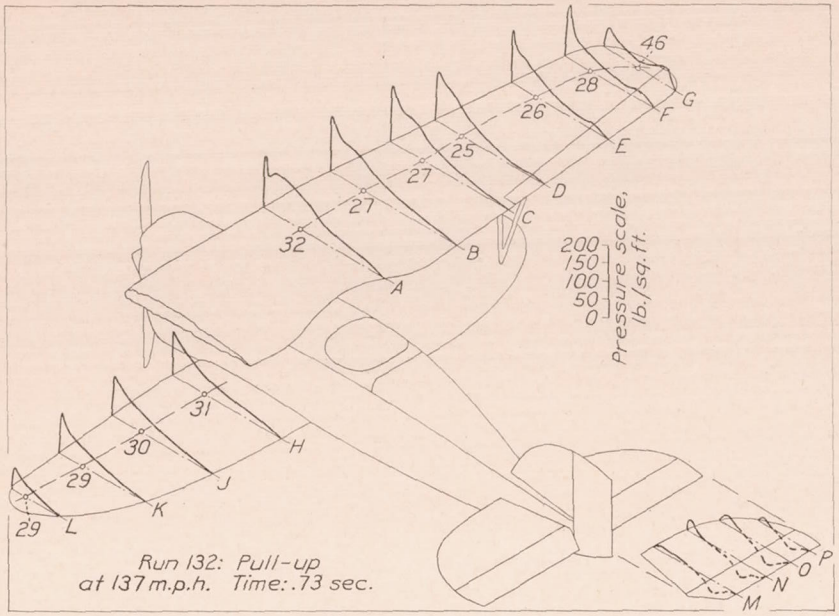

FIGURE 24d

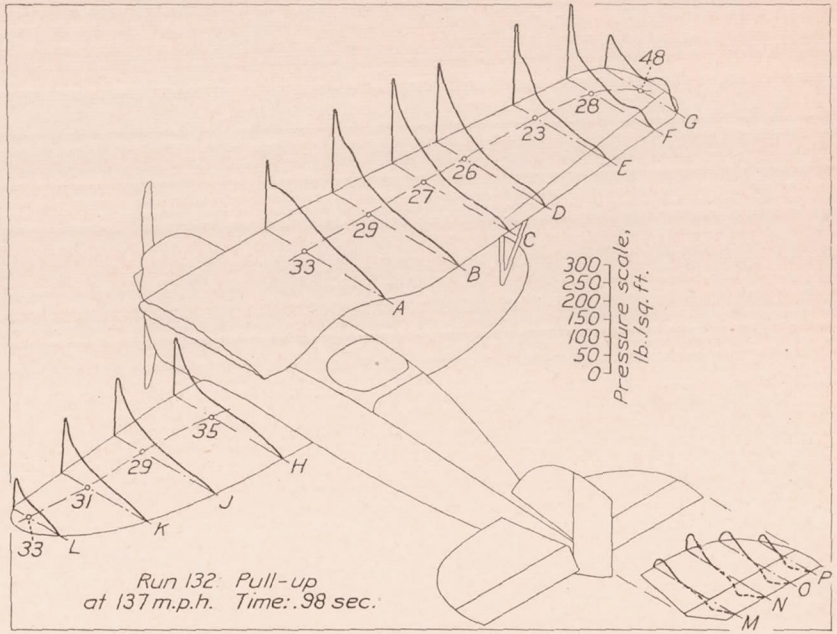

FIGURE 24e

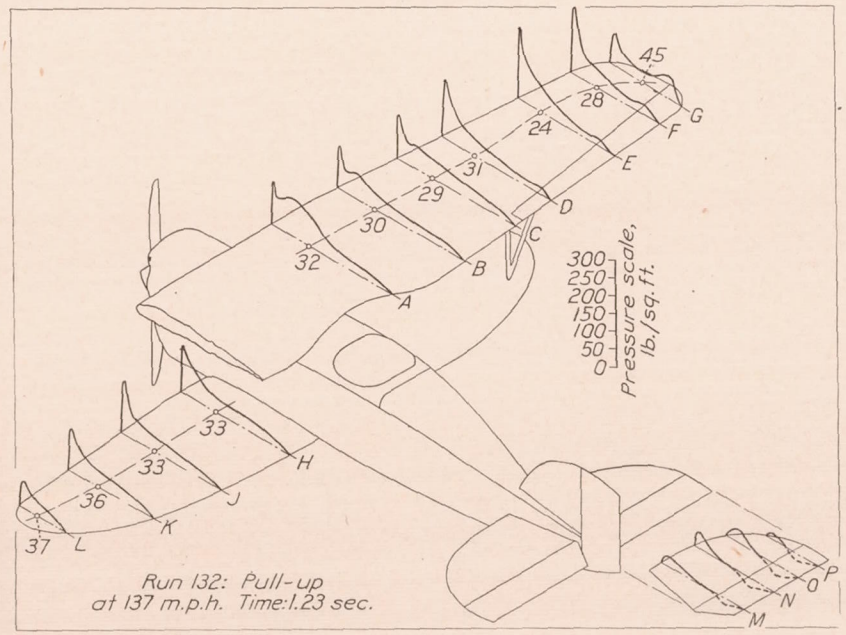

FIGURE 24f

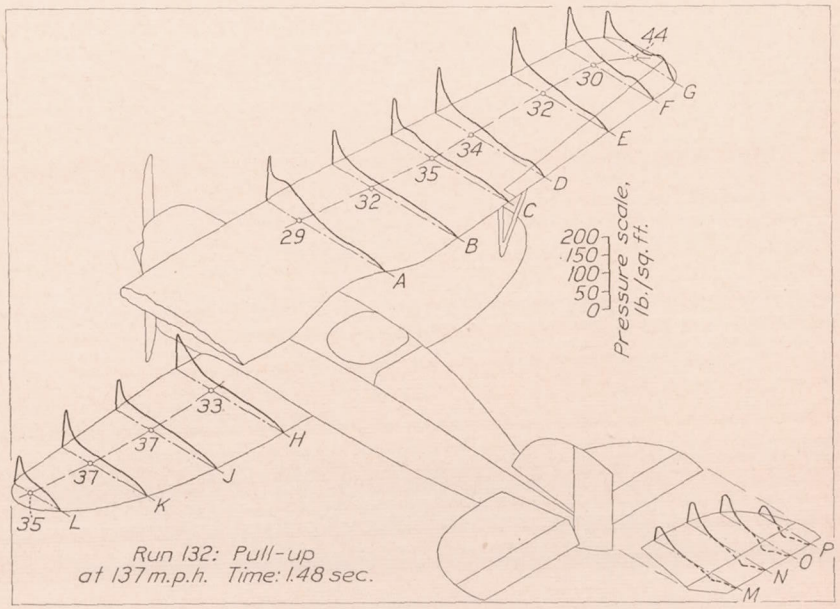

FIGURE 24g

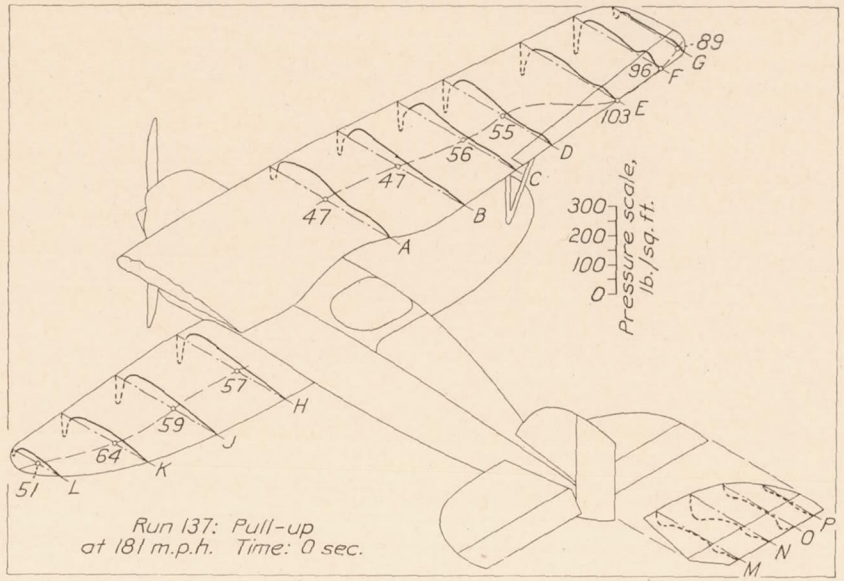

FIGURE 25a

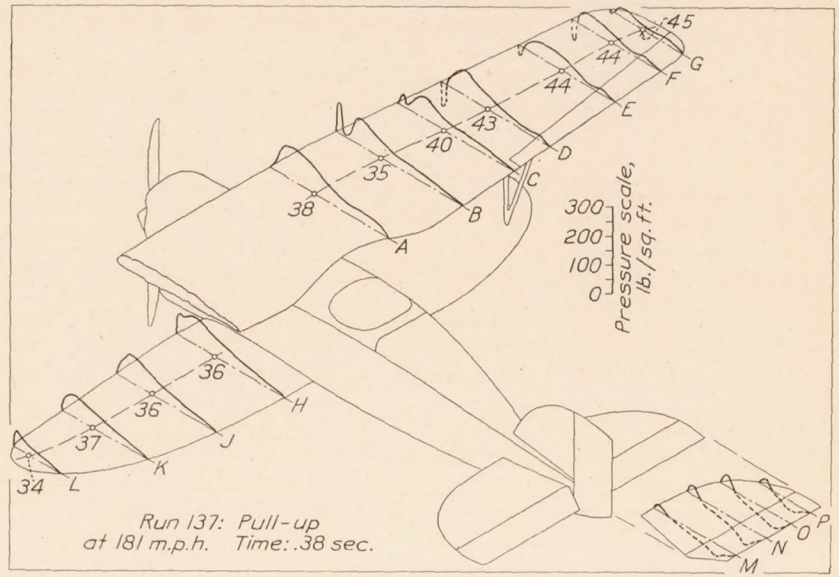

FIGURE 25b

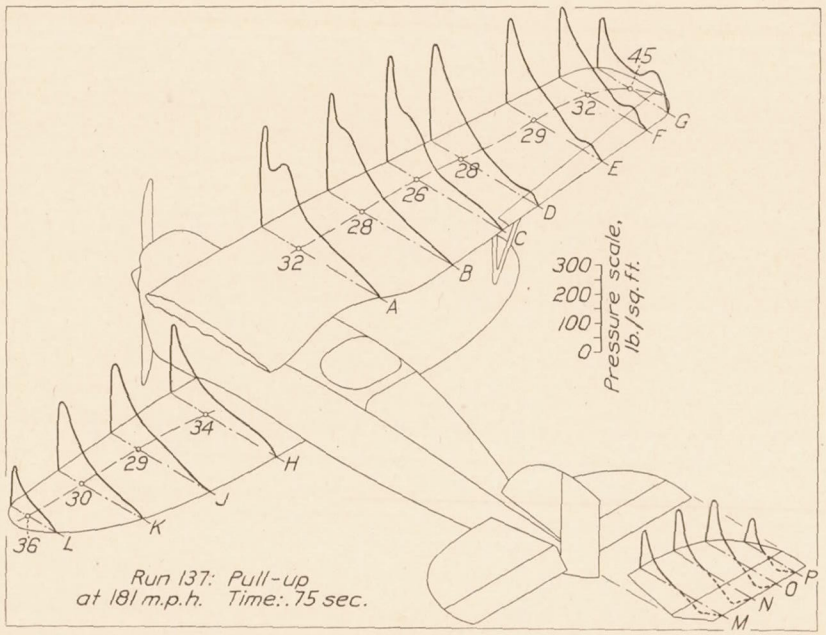

FIGURE 25c

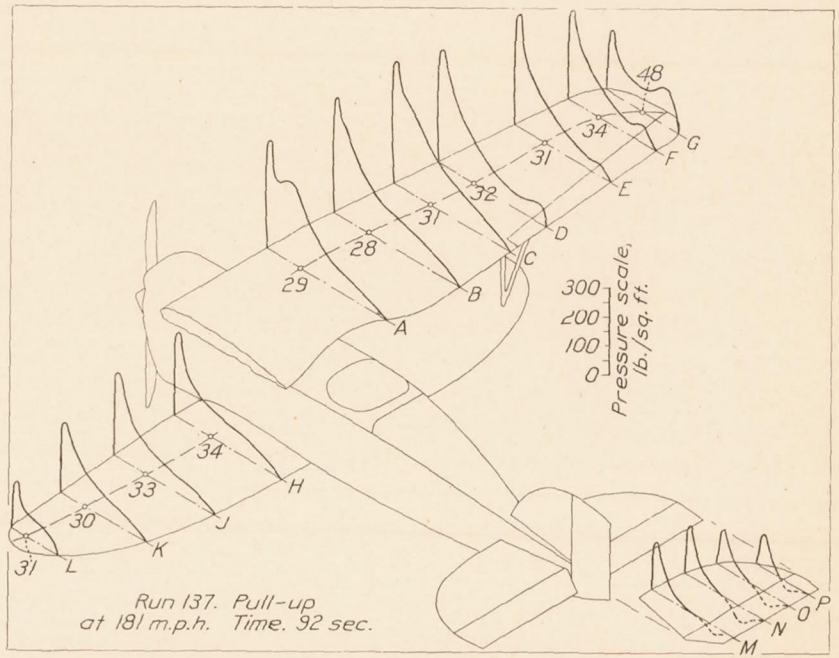

FIGURE 25d

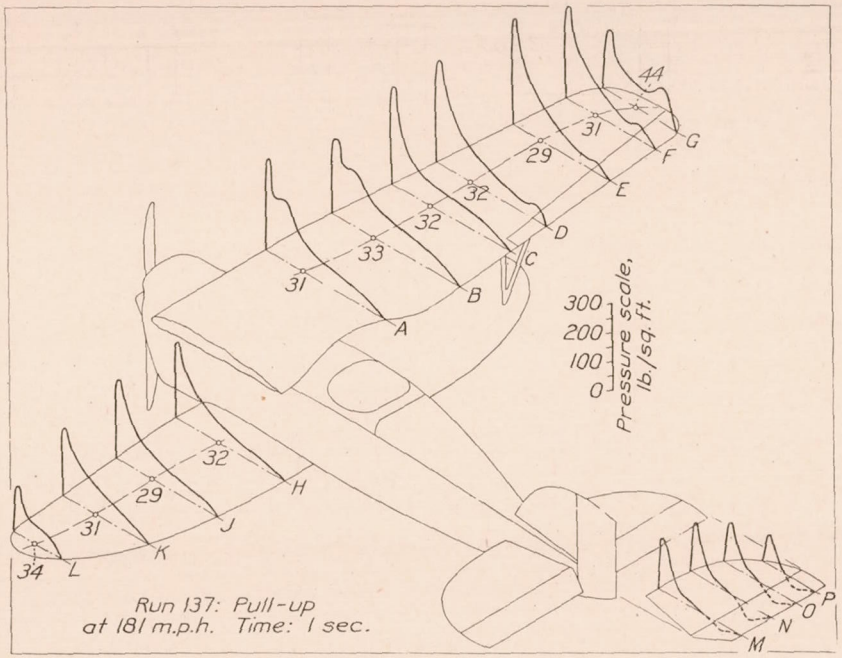

FIGURE 25e

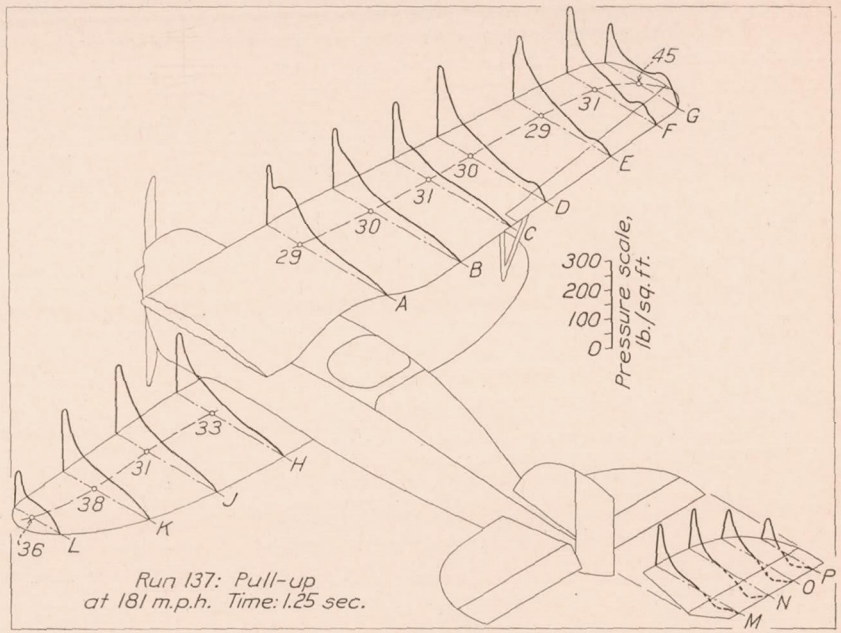

FIGURE 25f

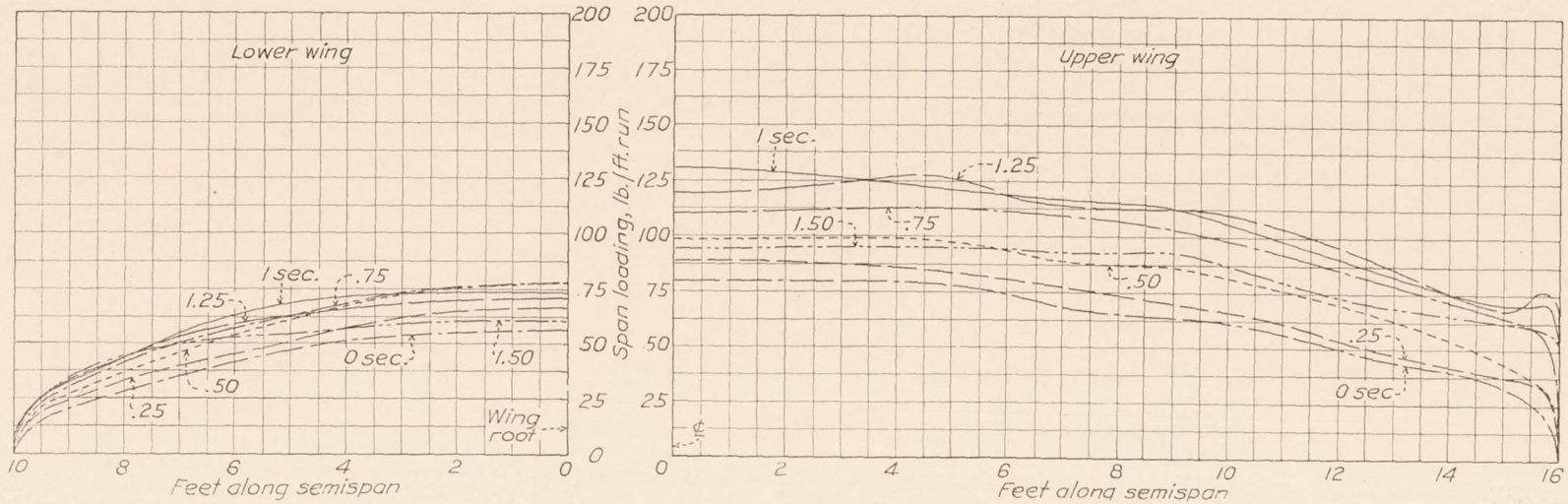

FIGURE 26.—Variation of span load distribution during a pull-up at 79 miles per hour. (Run No. 65)

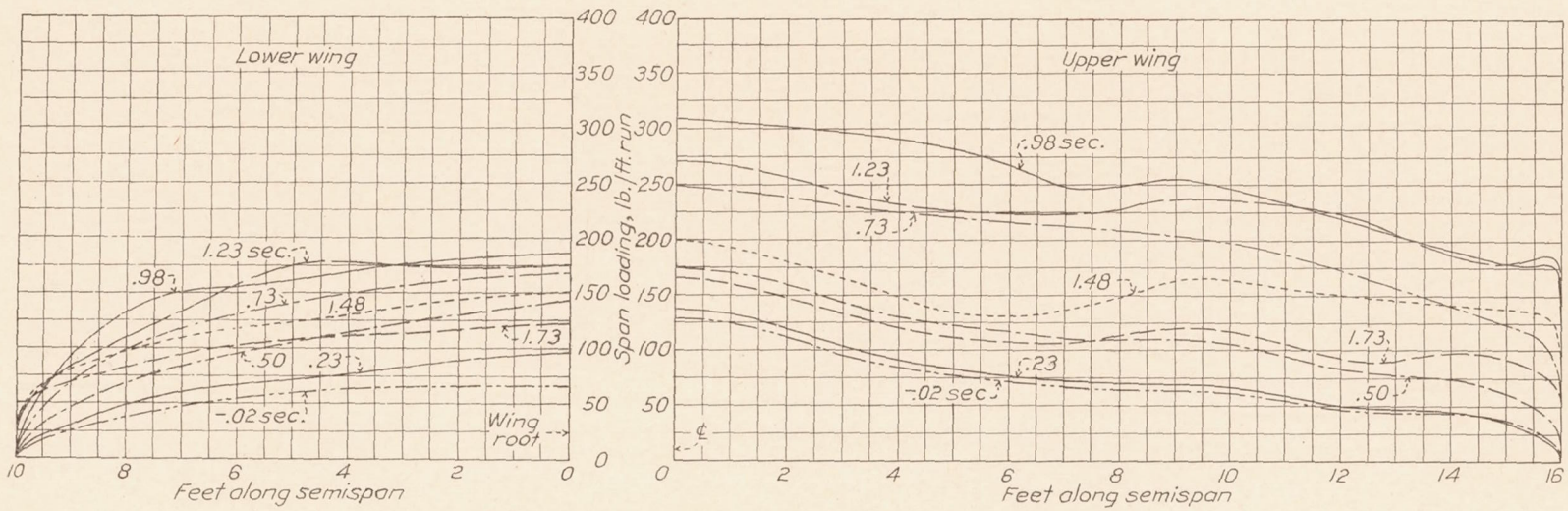

FIGURE 27.—Variation of span load distribution during a pull-up at 116 miles per hour. (Run No. 130)

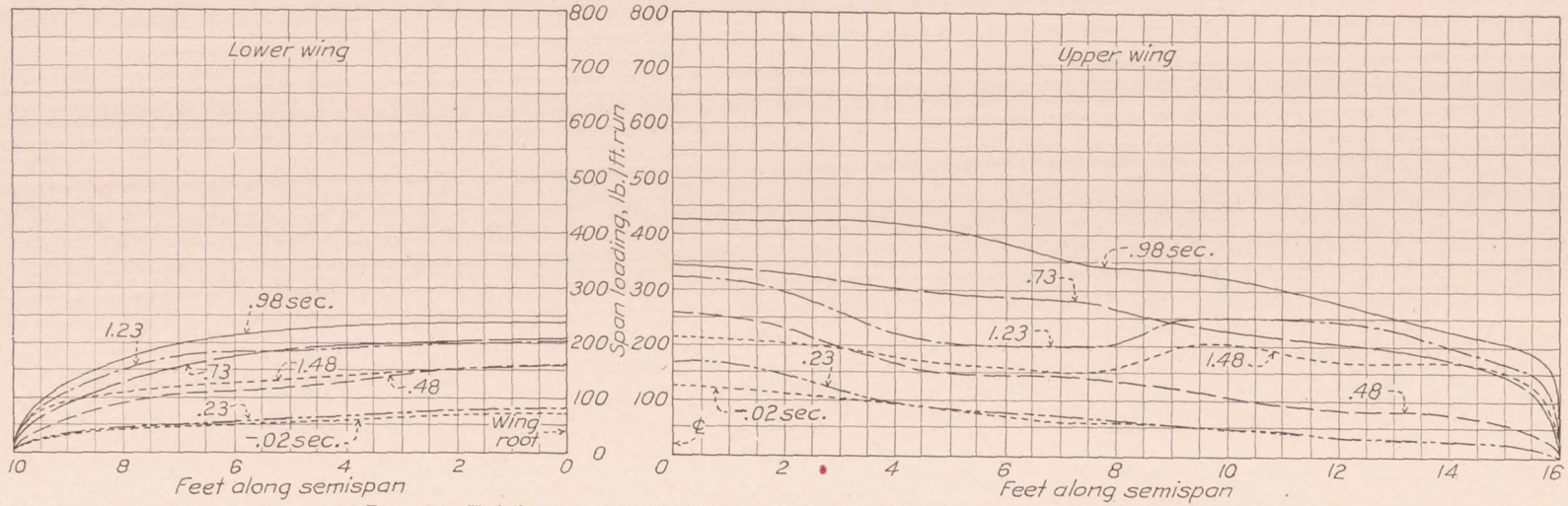

FIGURE 28.—Variation of span load distribution during a pull-up at 137 miles per hour. (Run No. 132)

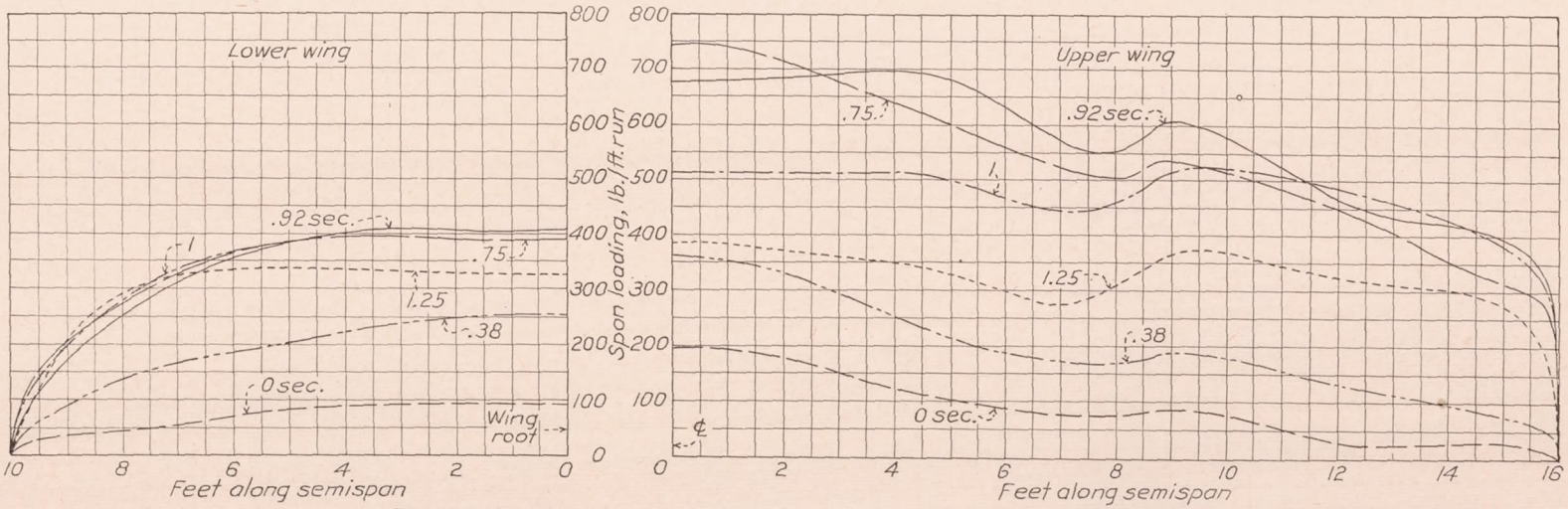

FIGURE 29.—Variation of span load distribution in a pull-up at 181 miles per hour. (Run No. 137)

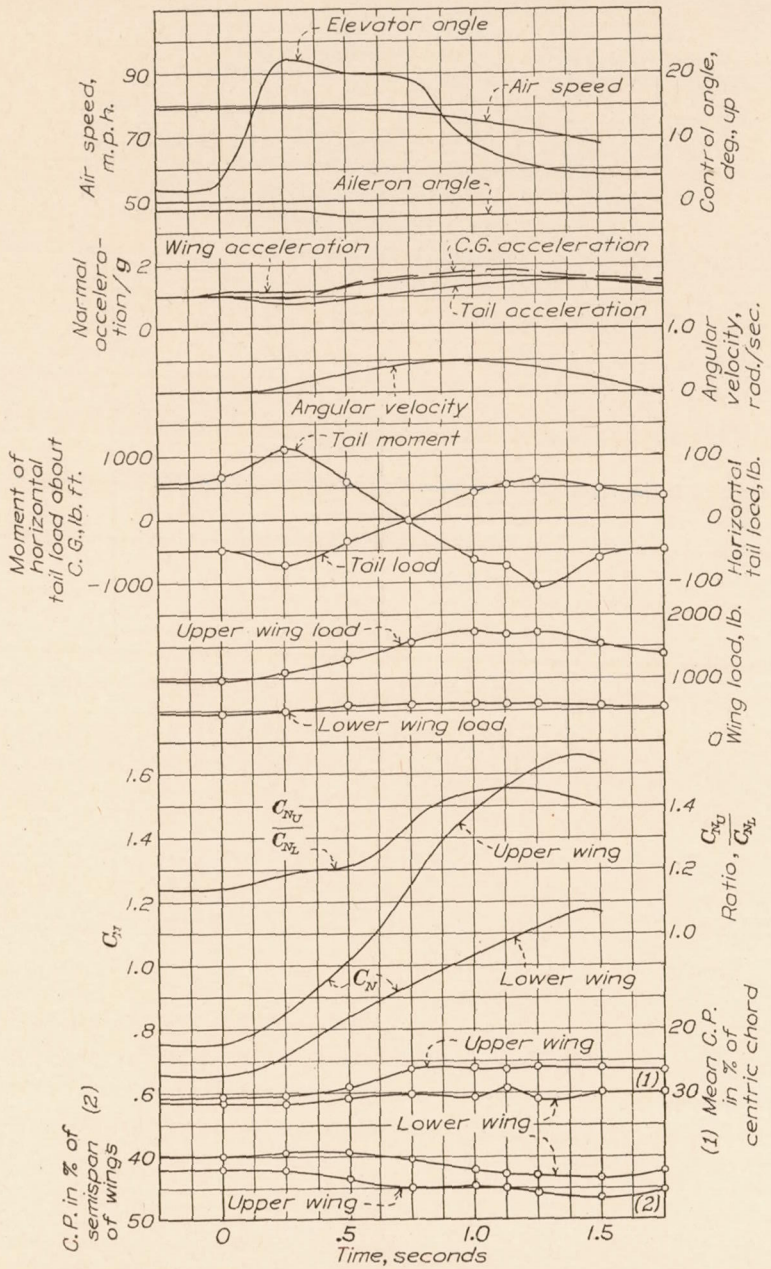

FIGURE 30.—Time history of an abrupt power-on pull-up at 79 miles per hour. (Run No. 65)

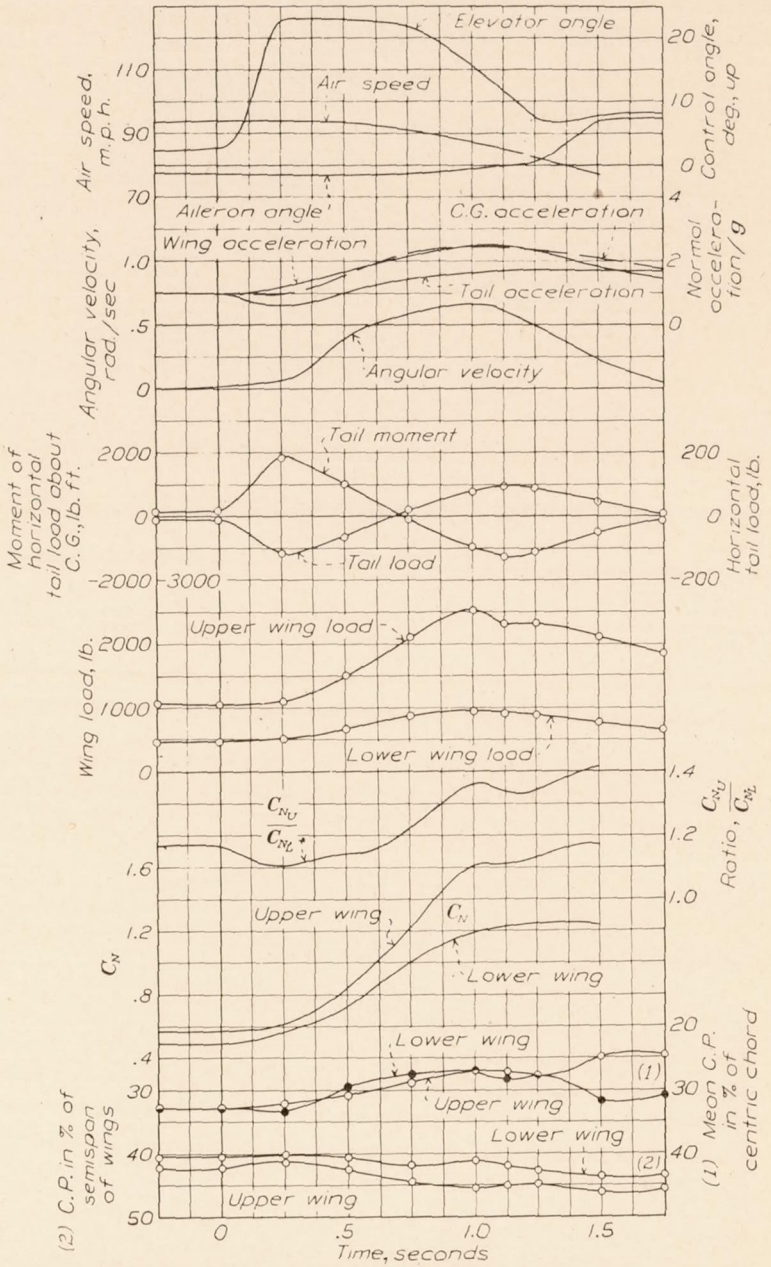

FIGURE 31.—Time history of an abrupt power-on pull-up at 94 miles per hour. (Run No. 66)

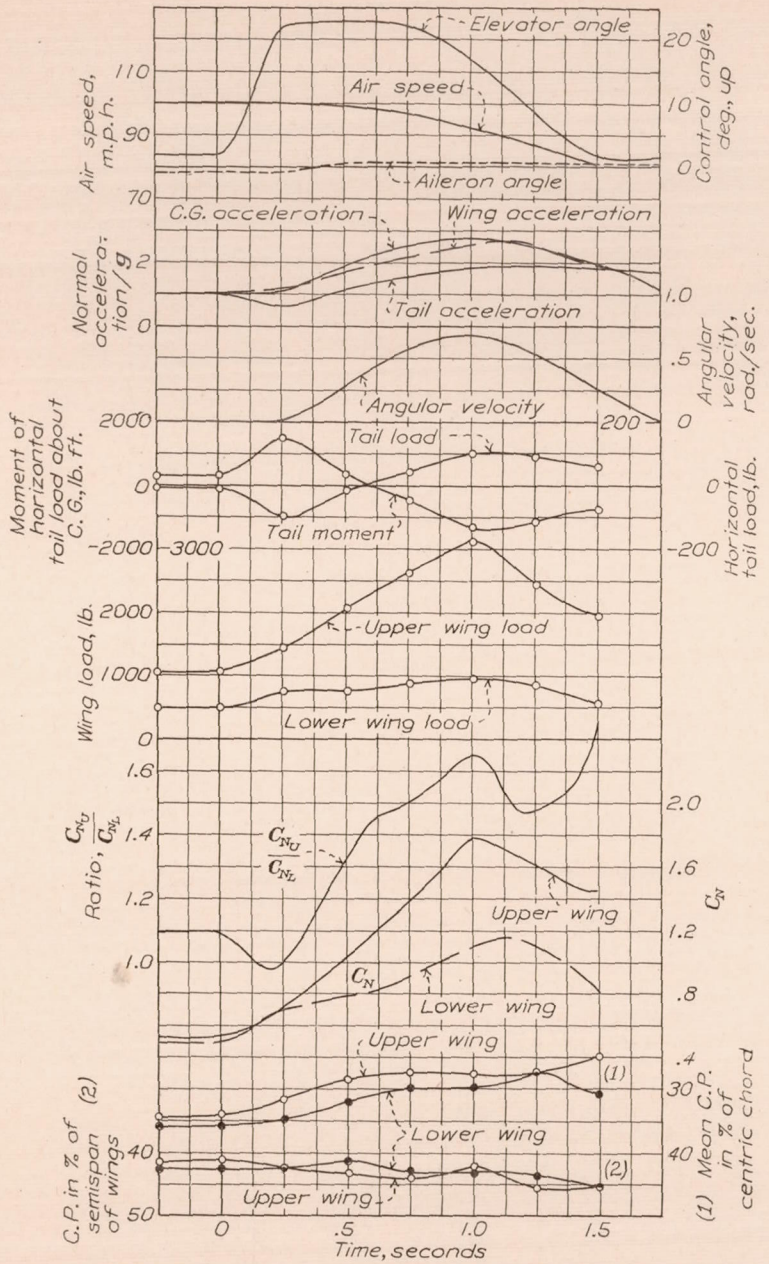

FIGURE 32.—Time history of an abrupt power-on pull-up at 100 miles per hour. (Run No. 67)

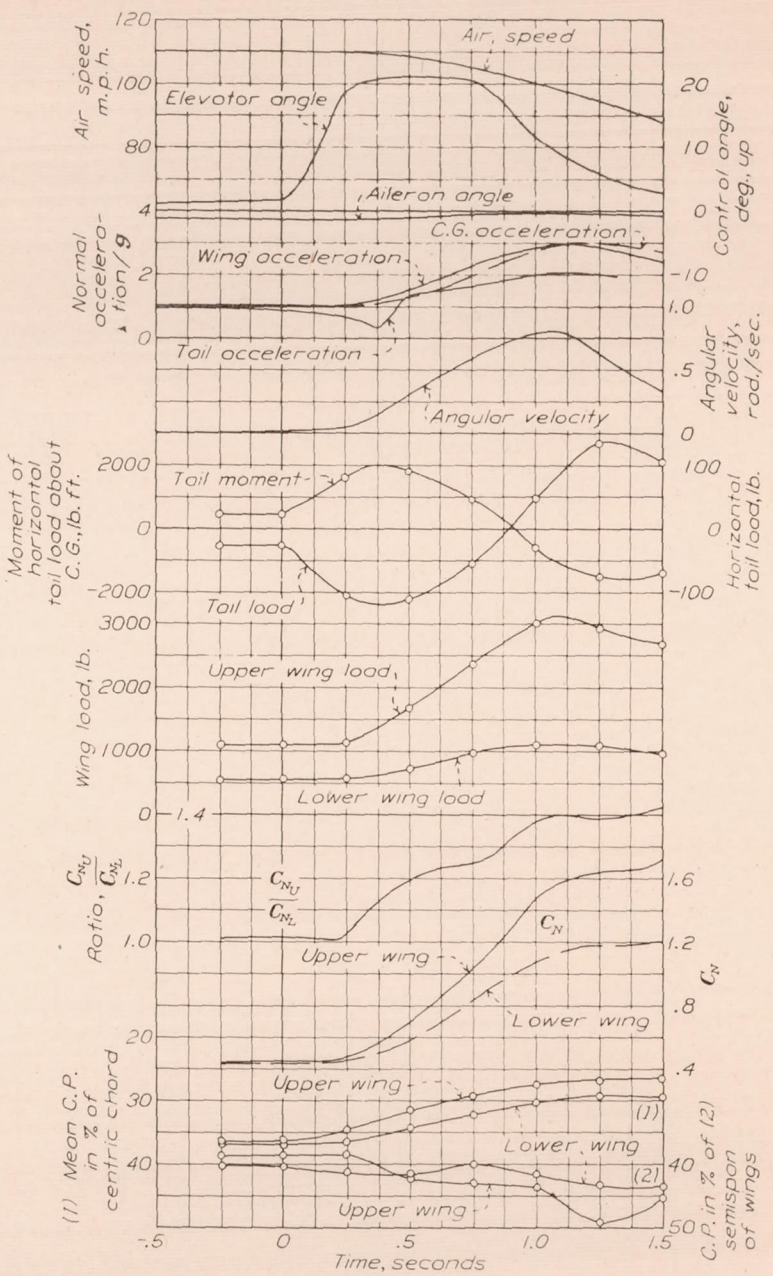

FIGURE 33.—Time history of an abrupt power-on pull-up at 110 miles per hour. (Run No. 68)

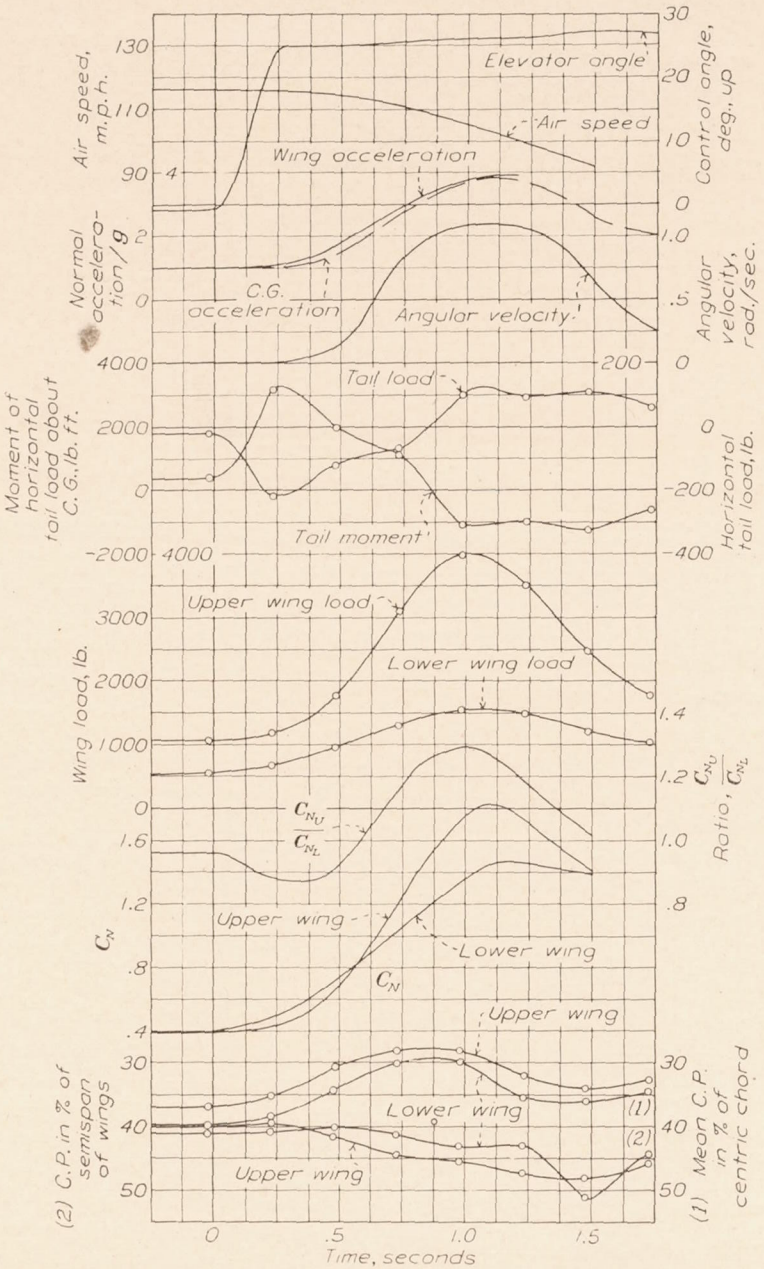

FIGURE 34.—Time history of an abrupt power-on pull-up at 116 miles per hour. (Run No. 130)

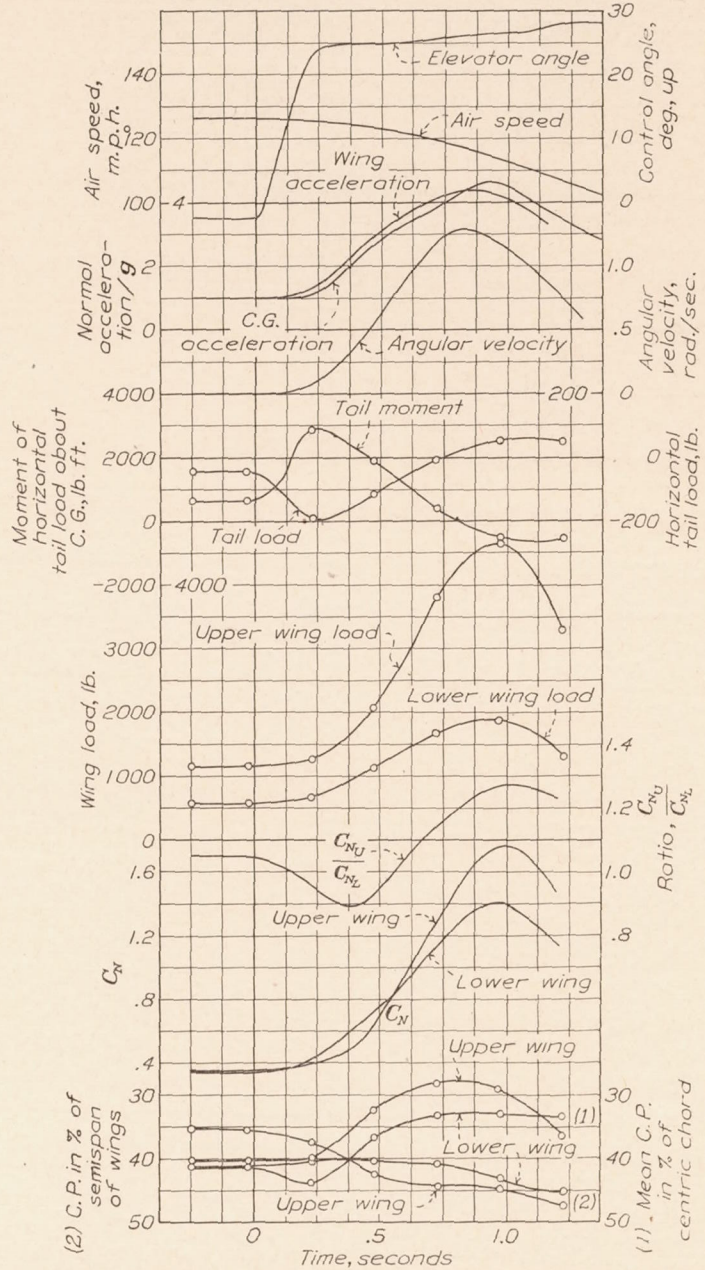

FIGURE 35.—Time history of an abrupt power-on pull-up at 126 miles per hour. (Run No. 131)

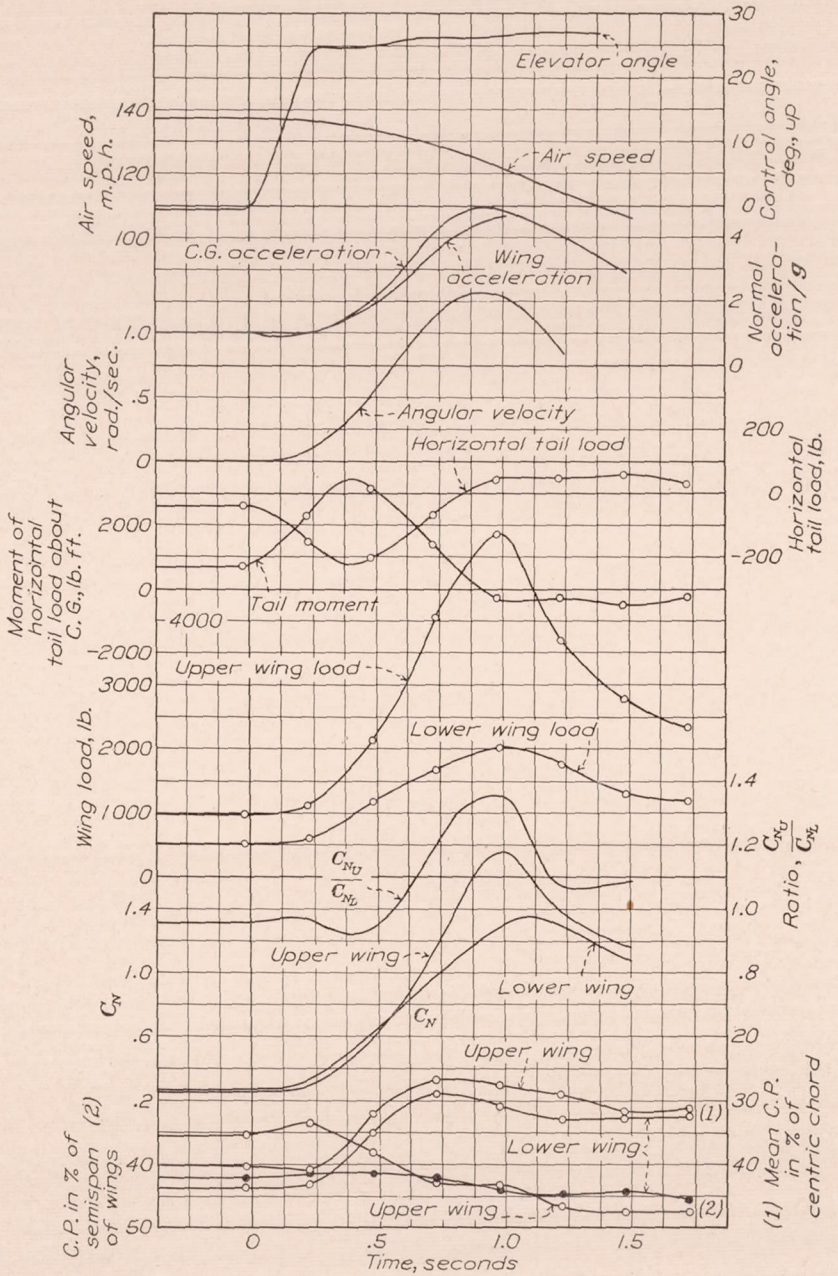

FIGURE 36.—Time history of an abrupt power-on pull-up at 137 miles per hour. (Run No. 132)

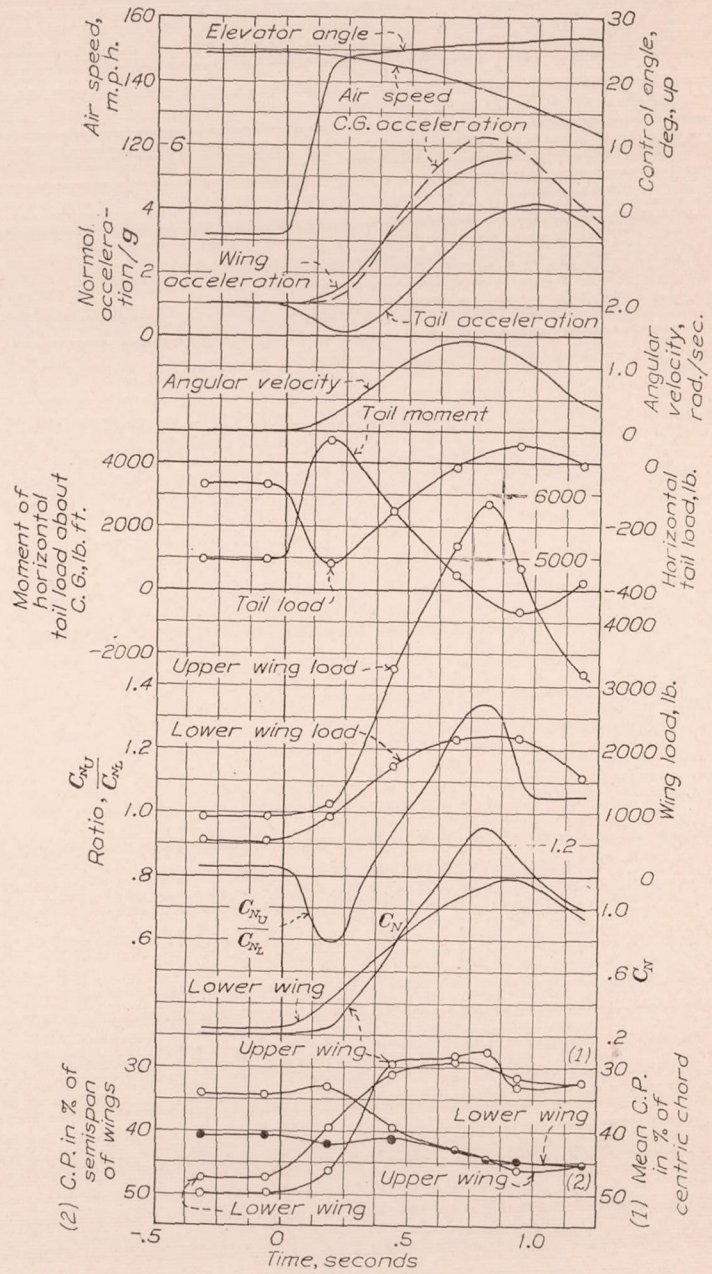

FIGURE 37.—Time history of an abrupt power-on pull-up at 149 miles per hour. (Run No. 133)

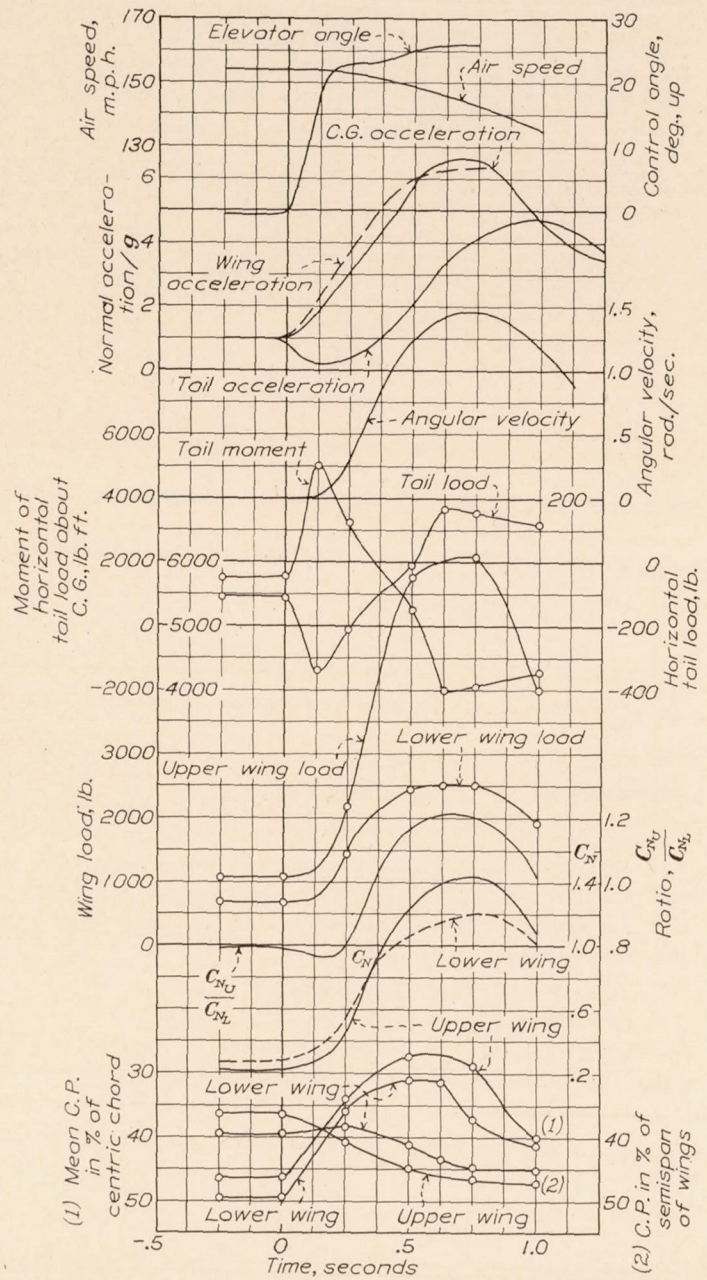

FIGURE 38.—Time history of an abrupt power-on pull-up at 154 miles per hour. (Run No. 134)

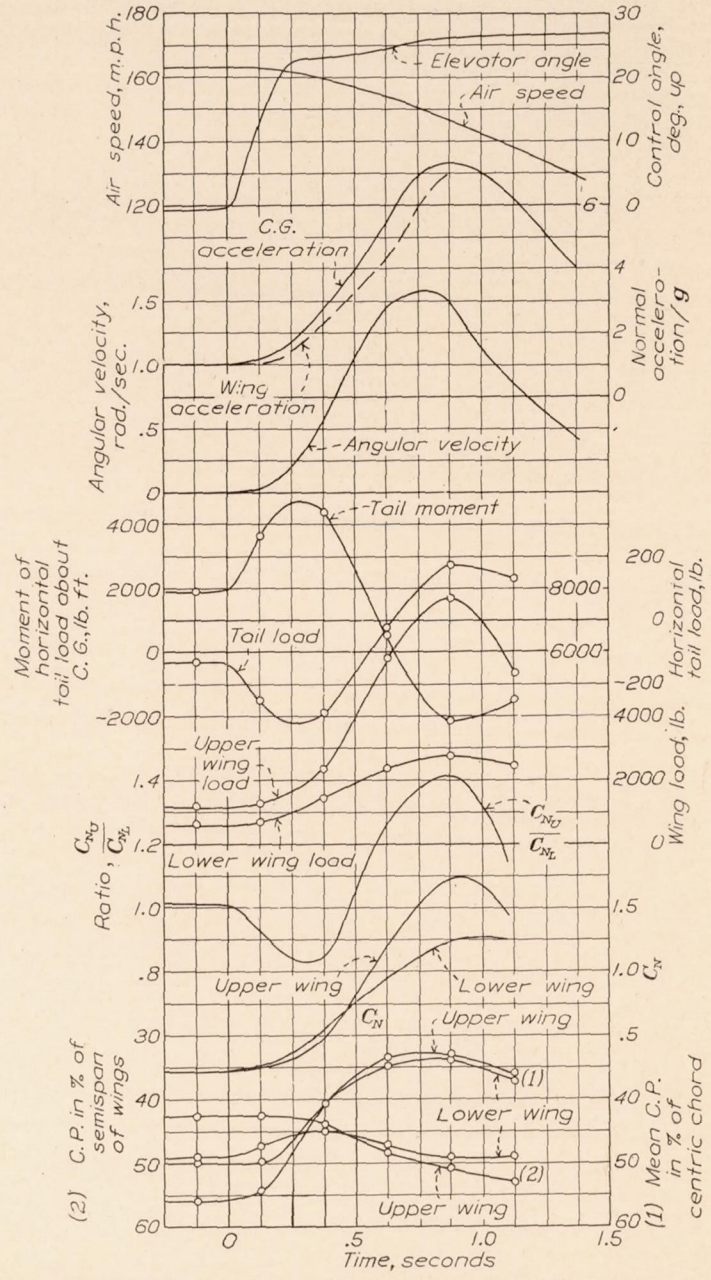

FIGURE 39.—Time history of an abrupt power-on pull-up at 163 miles per hour. (Run No. 135)

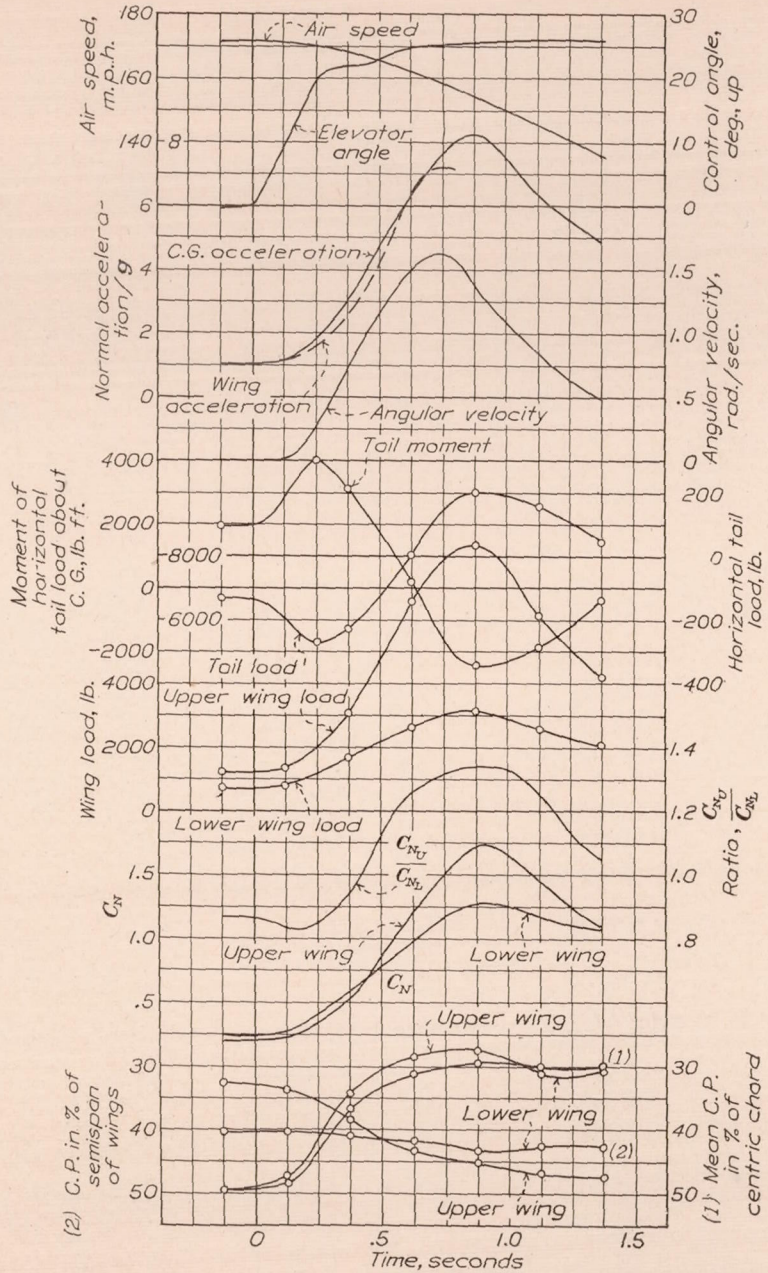

FIGURE 40.—Time history of an abrupt power-on pull-up at 172 miles per hour. (Run No. 136)

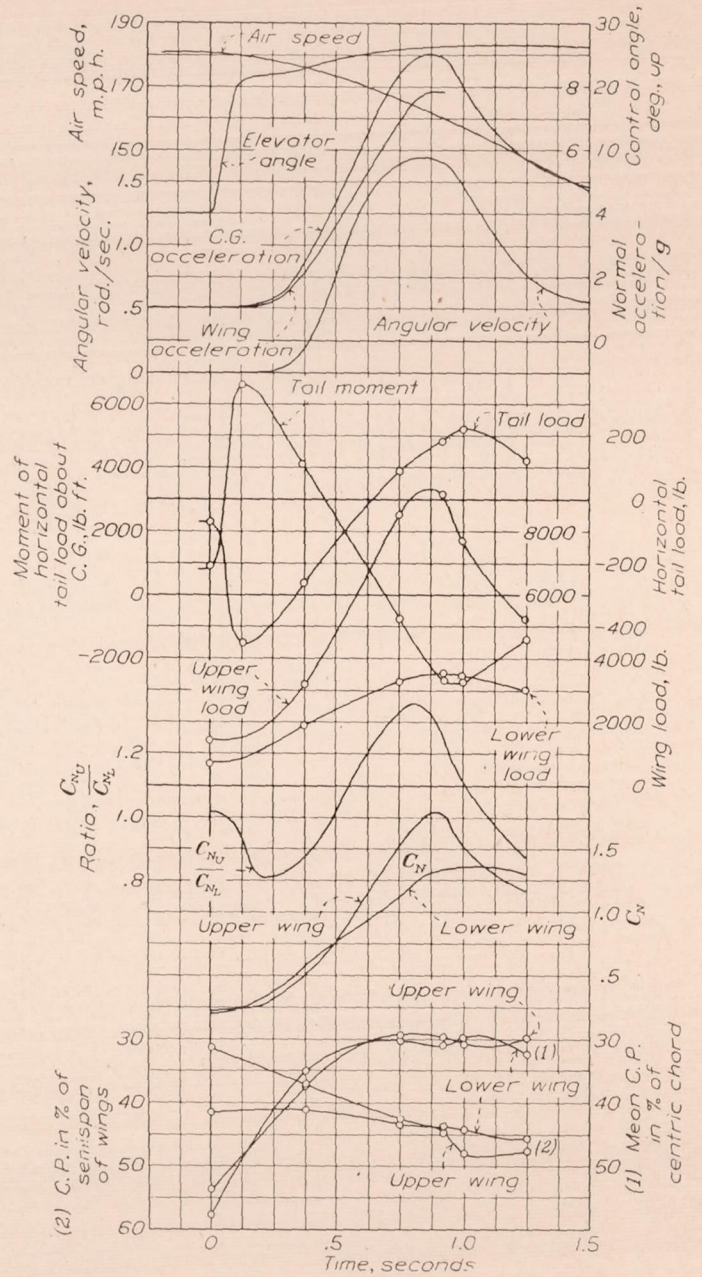

FIGURE 41.—Time history of an abrupt power-on pull-up at 181 miles per hour. (Run No. 137)

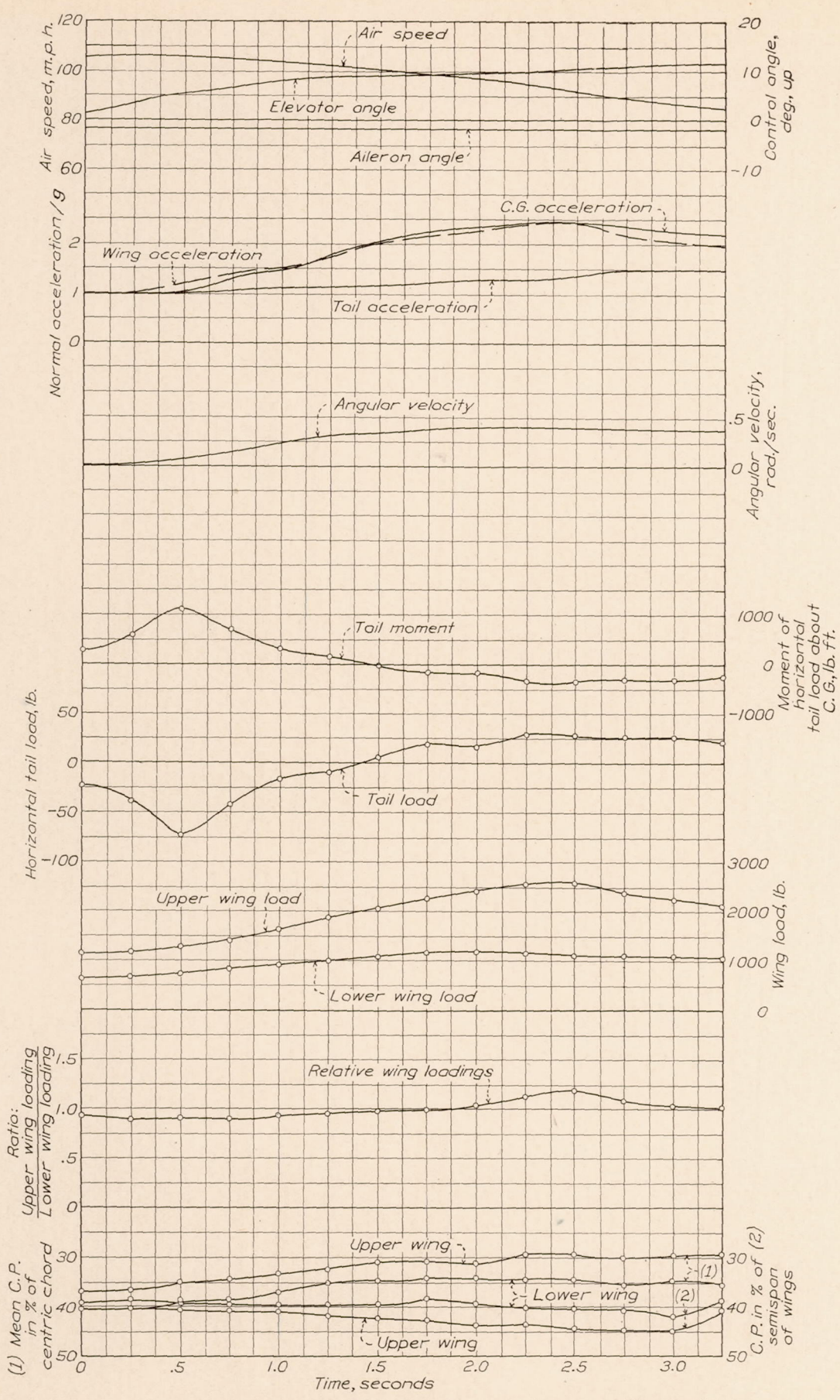

FIGURE 42.—Time history of a mild power-on pull-up at 110 miles per hour. (Run No. 73)

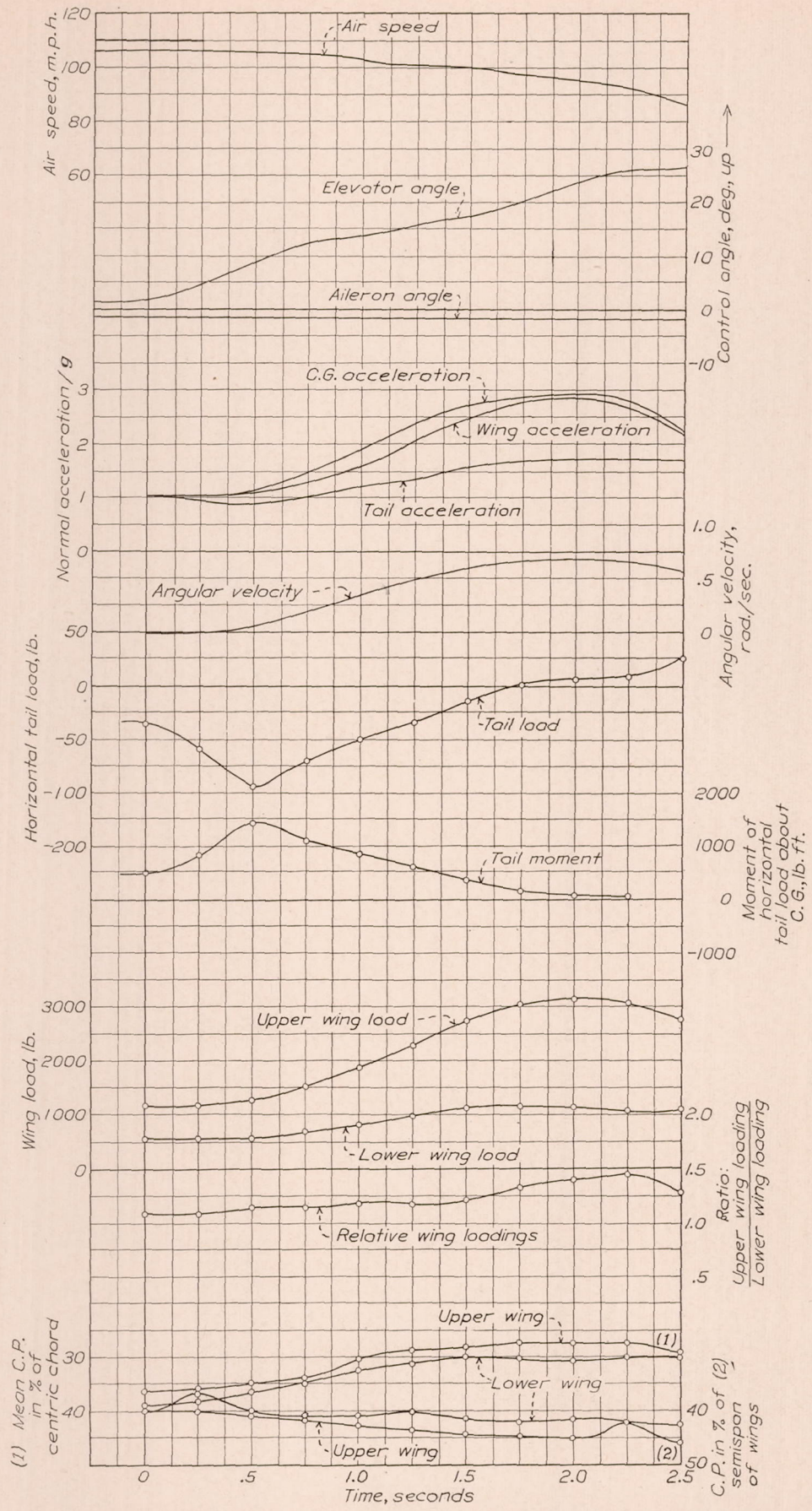

FIGURE 43.—Time history of a mild power-on pull-up at 110 miles per hour. (Run No. 75)

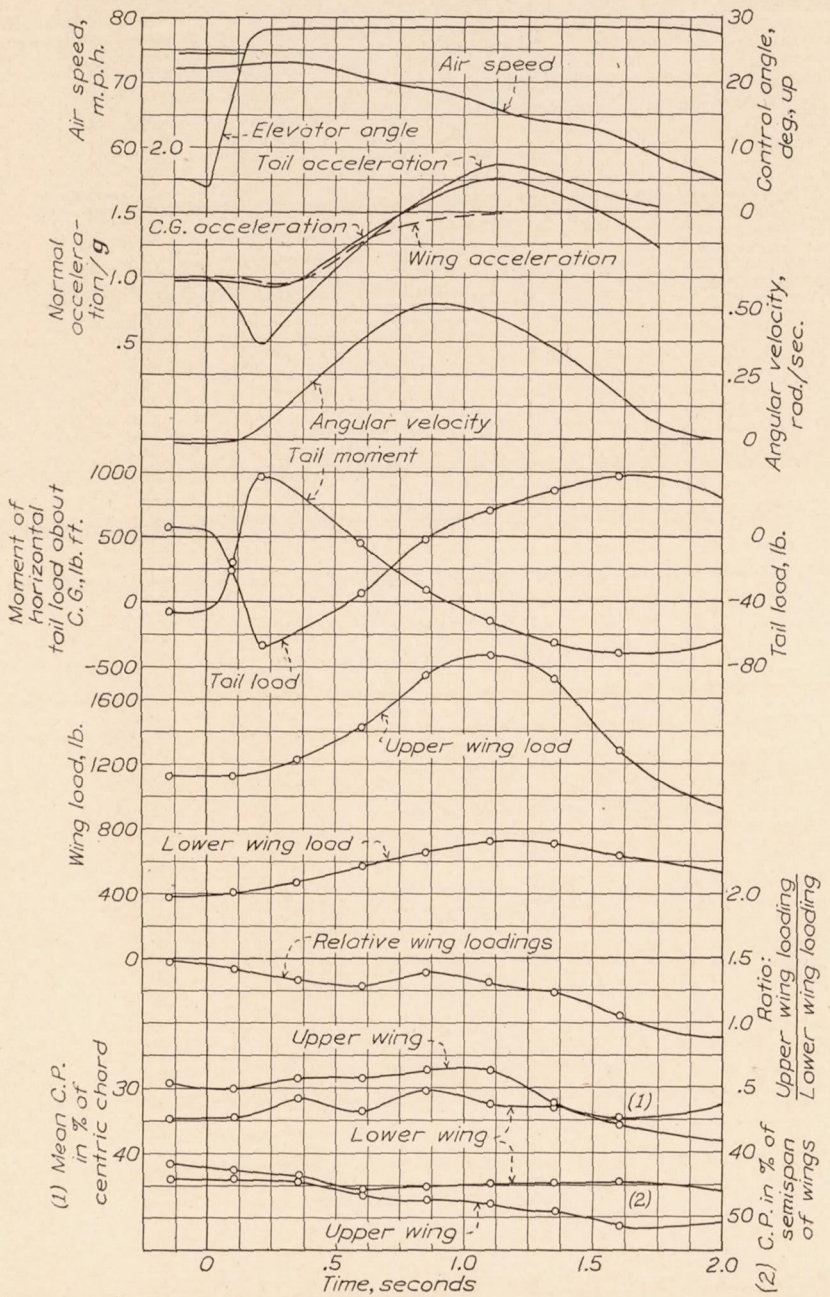

FIGURE 44.—Time history of an abrupt power-off pull-up at 79 miles per hour. (Run No. 191)

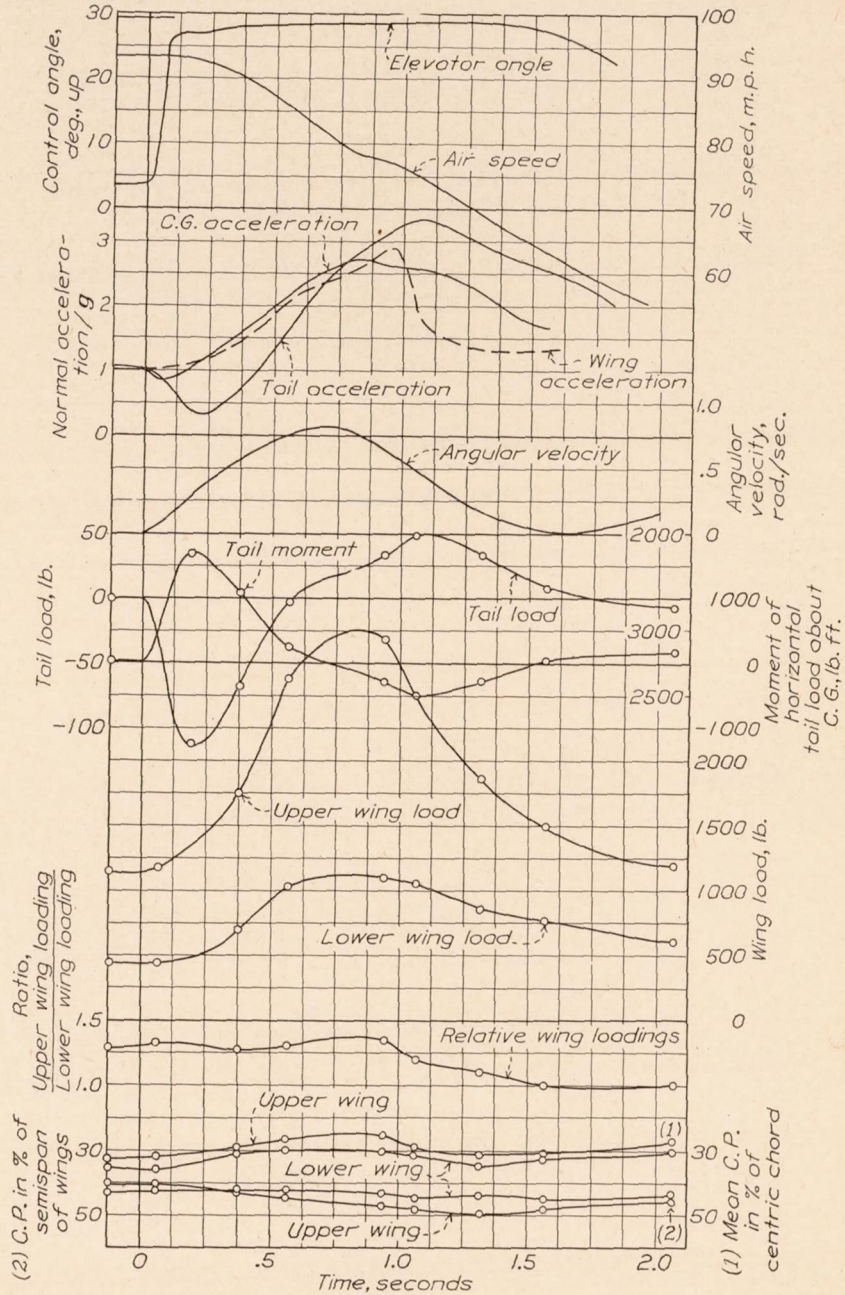

FIGURE 45.—Time history of an abrupt power-off pull-up at 99 miles per hour. (Run No. 192)

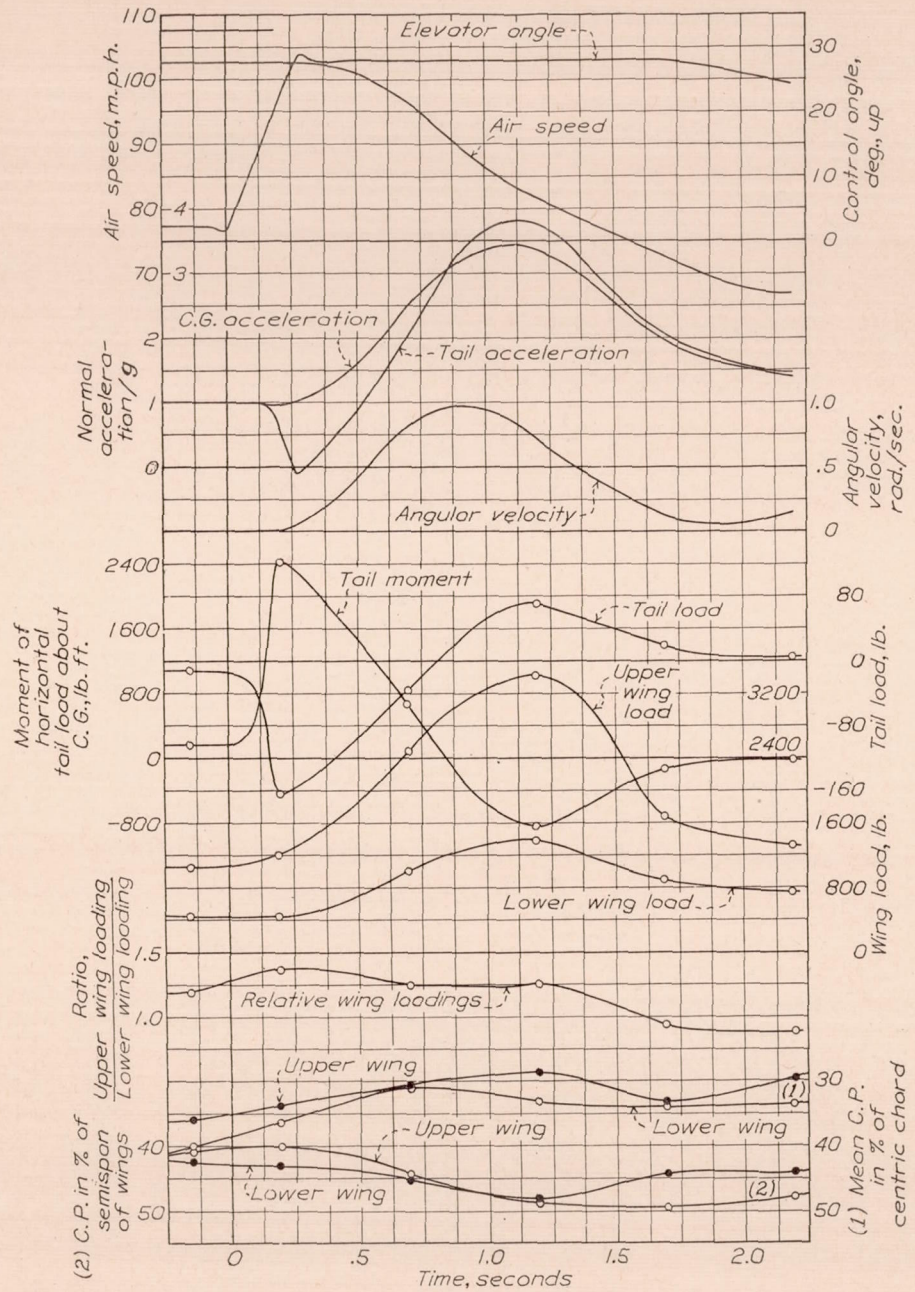

FIGURE 46.—Time history of an abrupt power-off pull-up at 108 miles per hour. (Run No. 200)

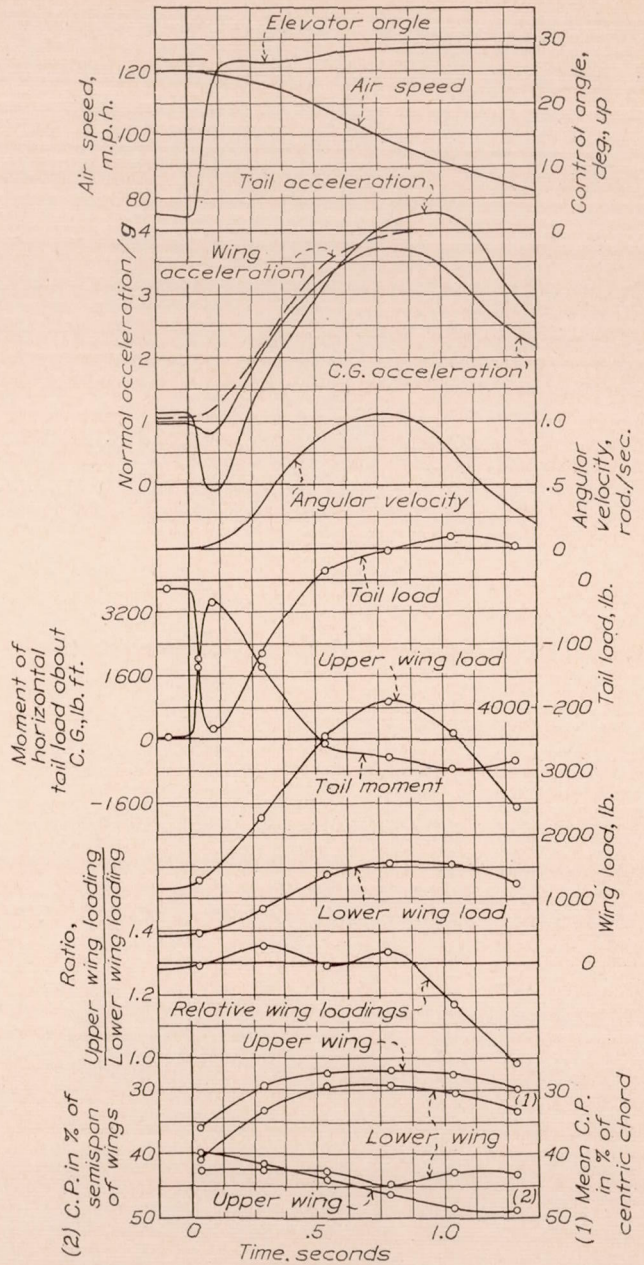

FIGURE 47.—Time history of an abrupt power-off pull-up at 124 miles per hour. (Run No. 193)

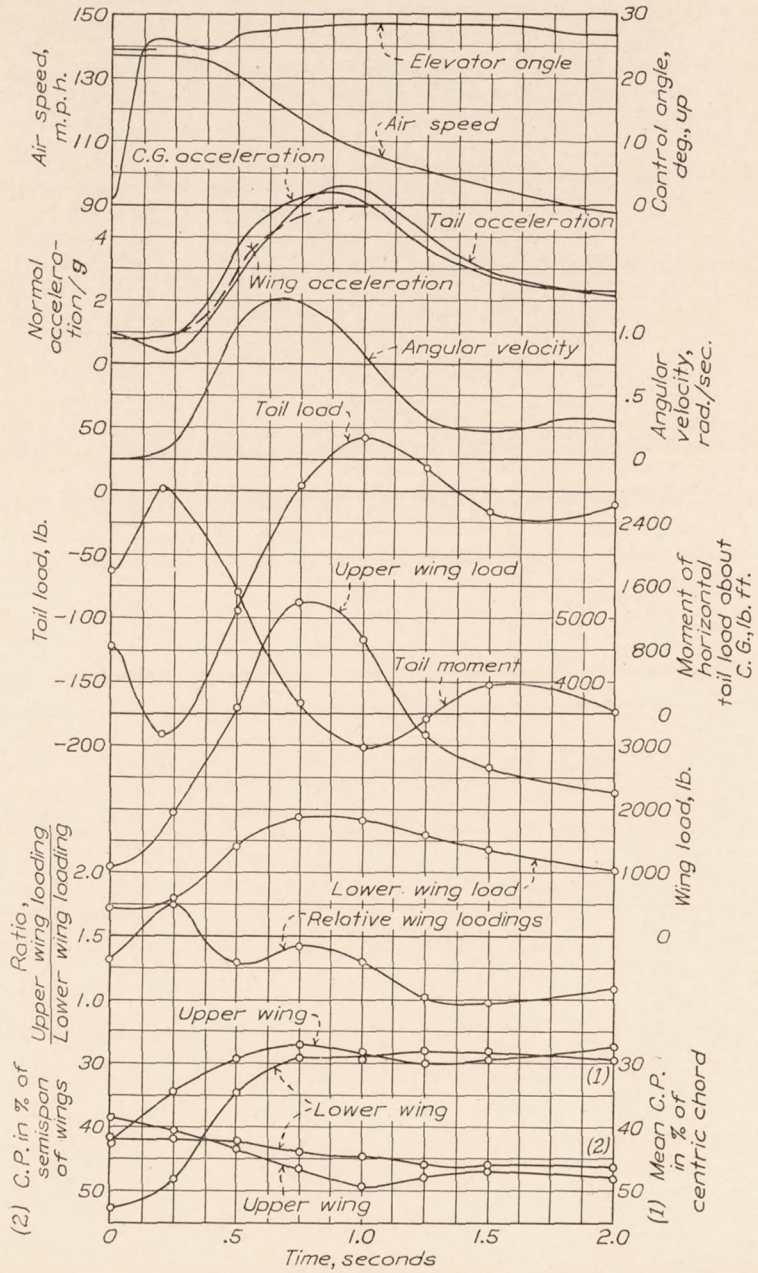

FIGURE 48.—Time history of an abrupt power-off pull-up at 139 miles per hour. (Run No. 209)

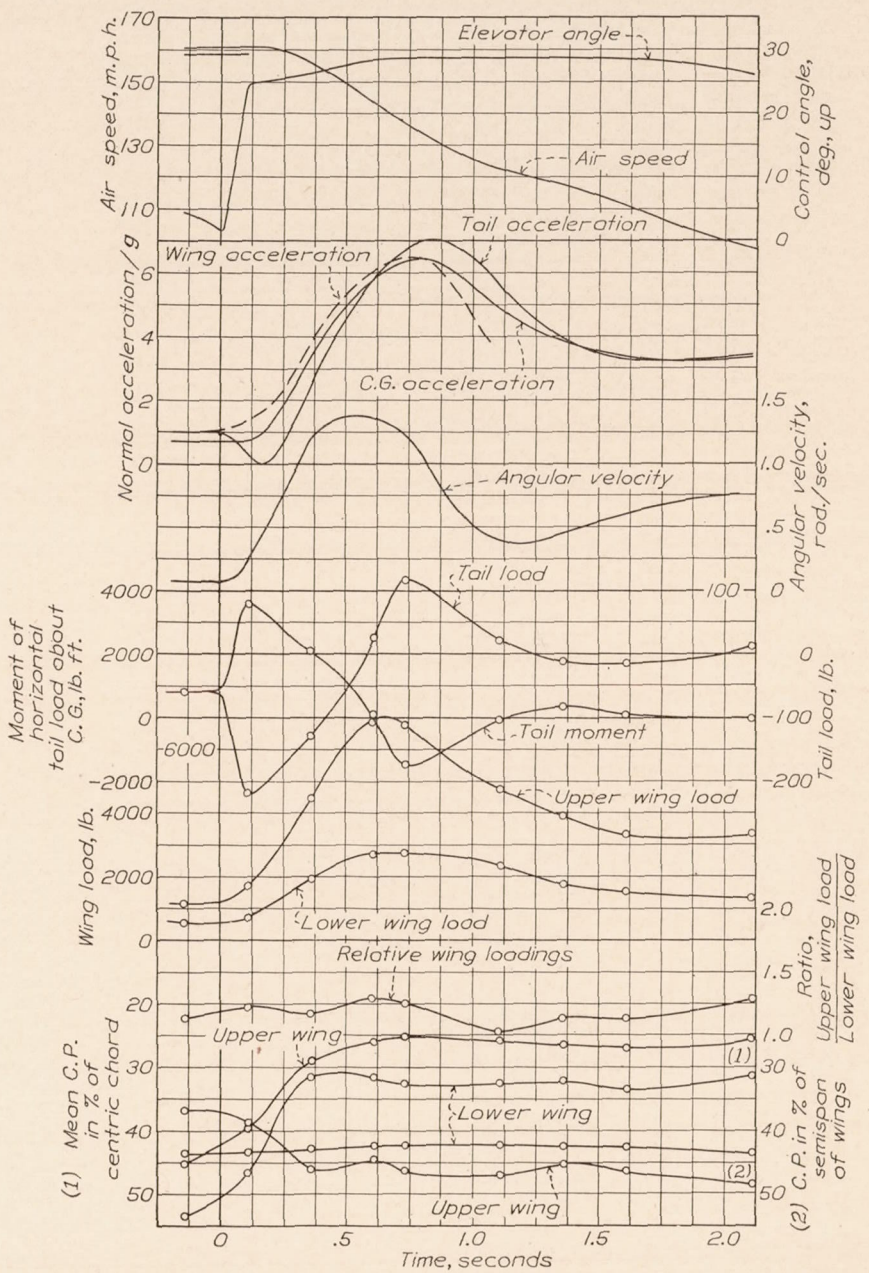

FIGURE 49.—Time history of an abrupt power-off pull-up at 159 miles per hour. (Run No. 195)

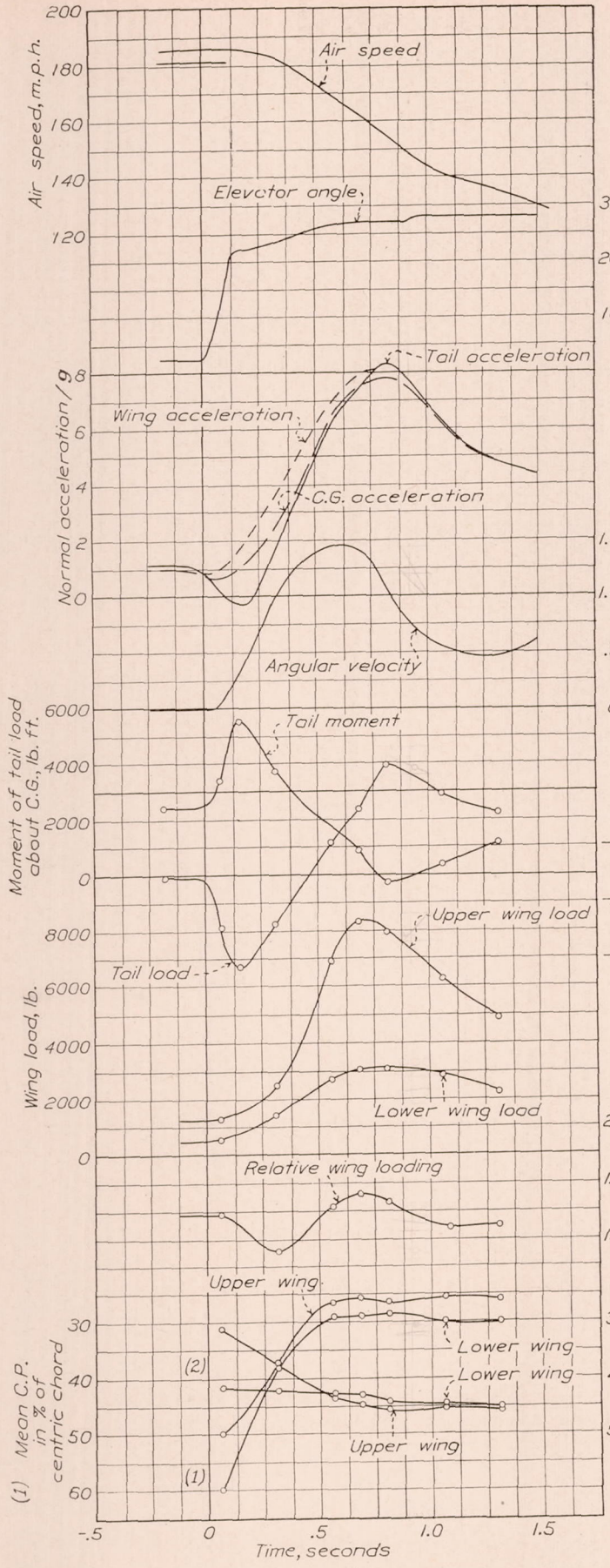

FIGURE 50.—Time history of an abrupt power-off pull-up at 181 miles per hour. (Run No. 196)

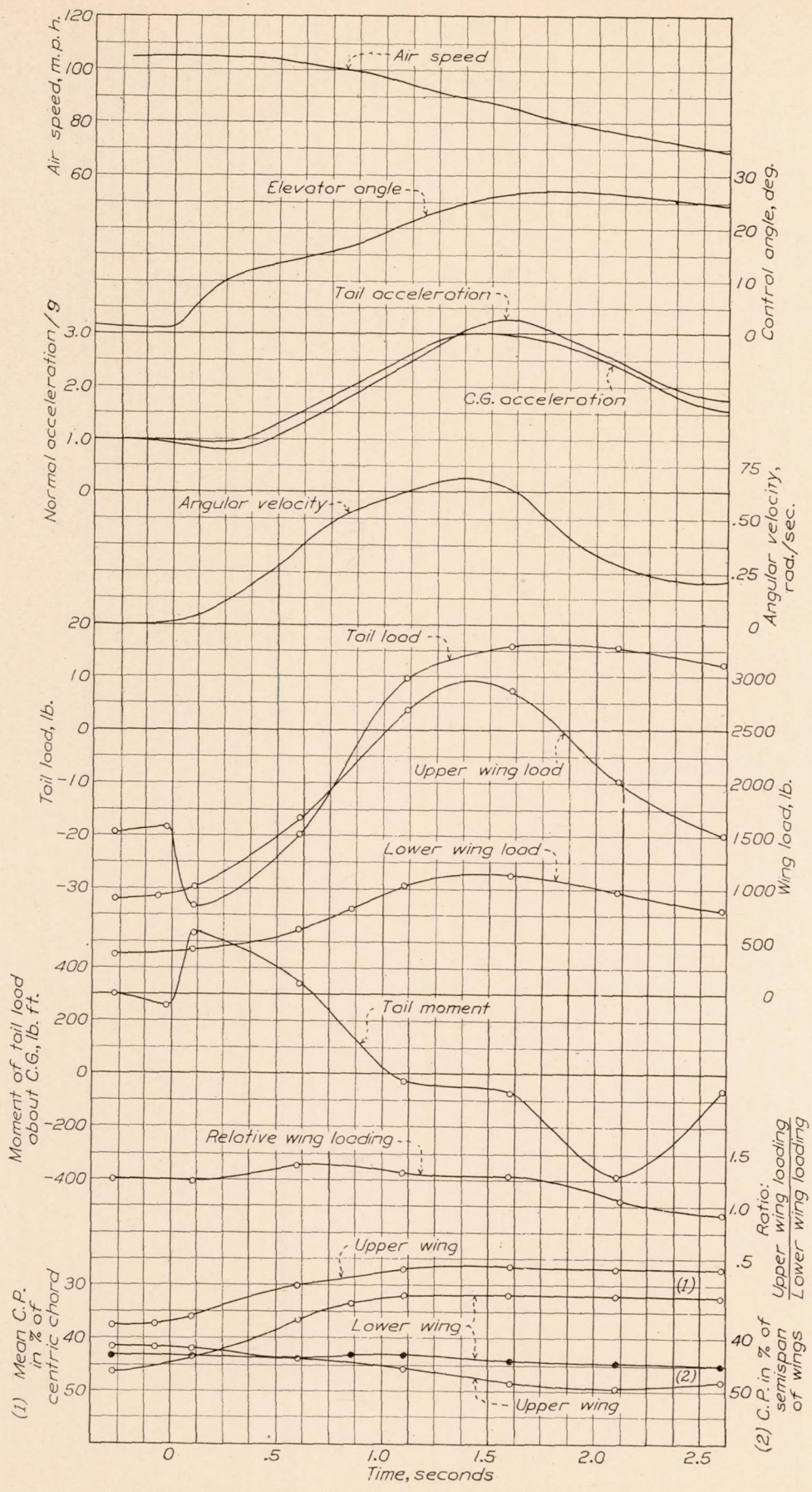

FIGURE 51.—Time history of a mild power-off pull-up at 110 miles per hour. (Run No. 197)

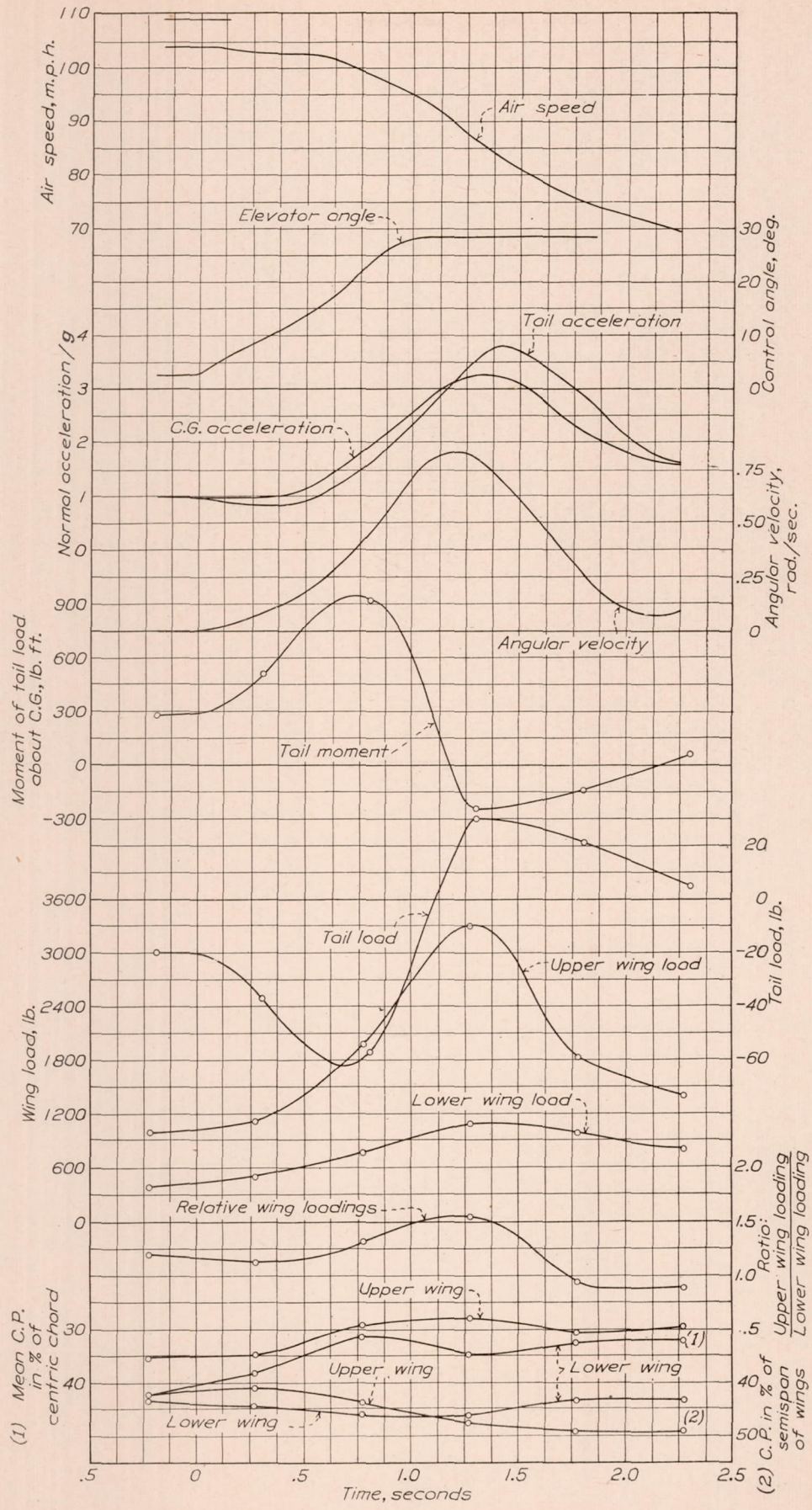

FIGURE 52.—Time history of a mild power-off pull-up at 109 miles per hour. (Run No. 198)

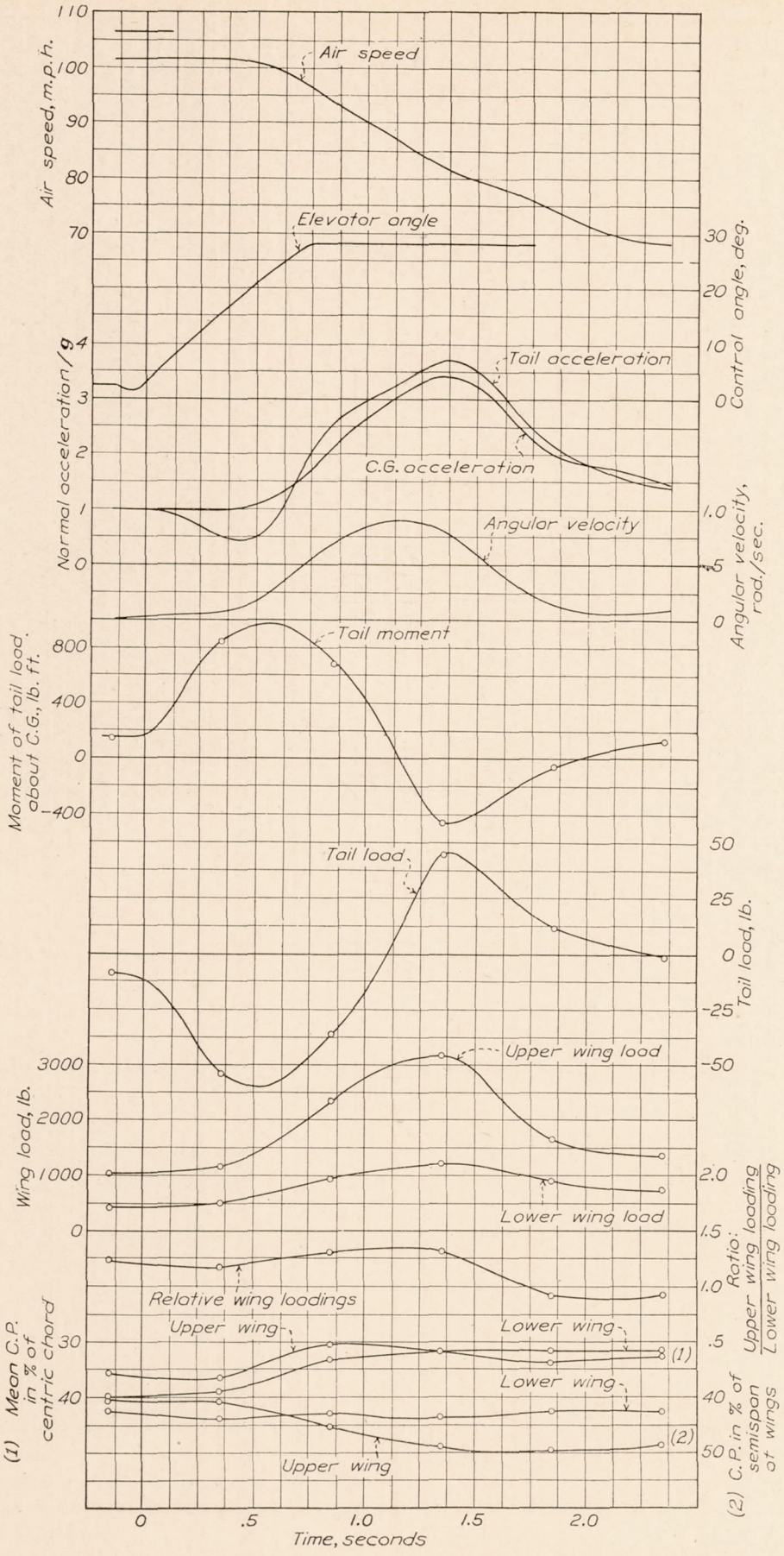

FIGURE 53.—Time history of a mild power-off pull-up at 107 miles per hour. (Run No. 199)

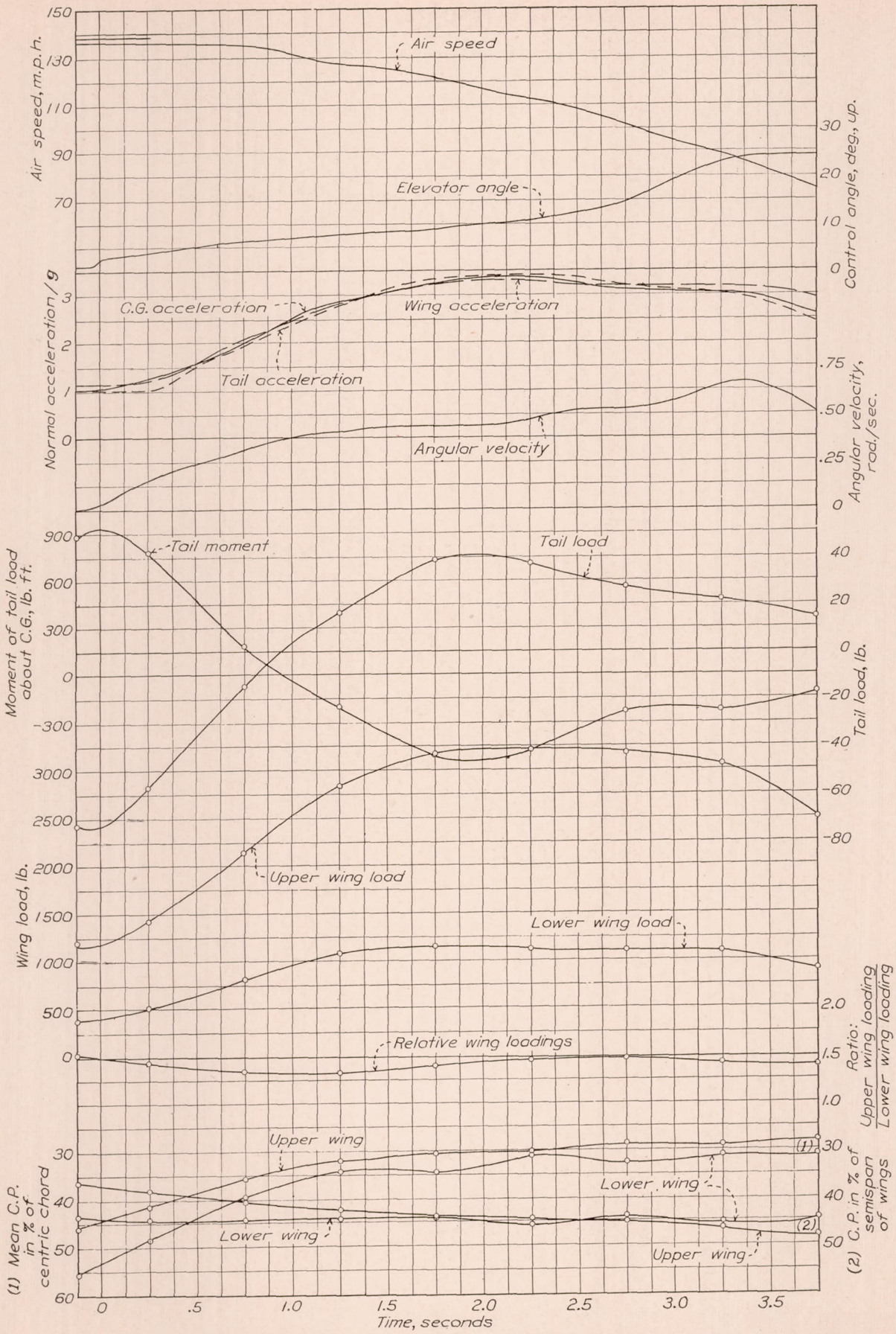

FIGURE 54.—Time history of a mild power-off pull-up at 138 miles per hour. (Run No. 207)

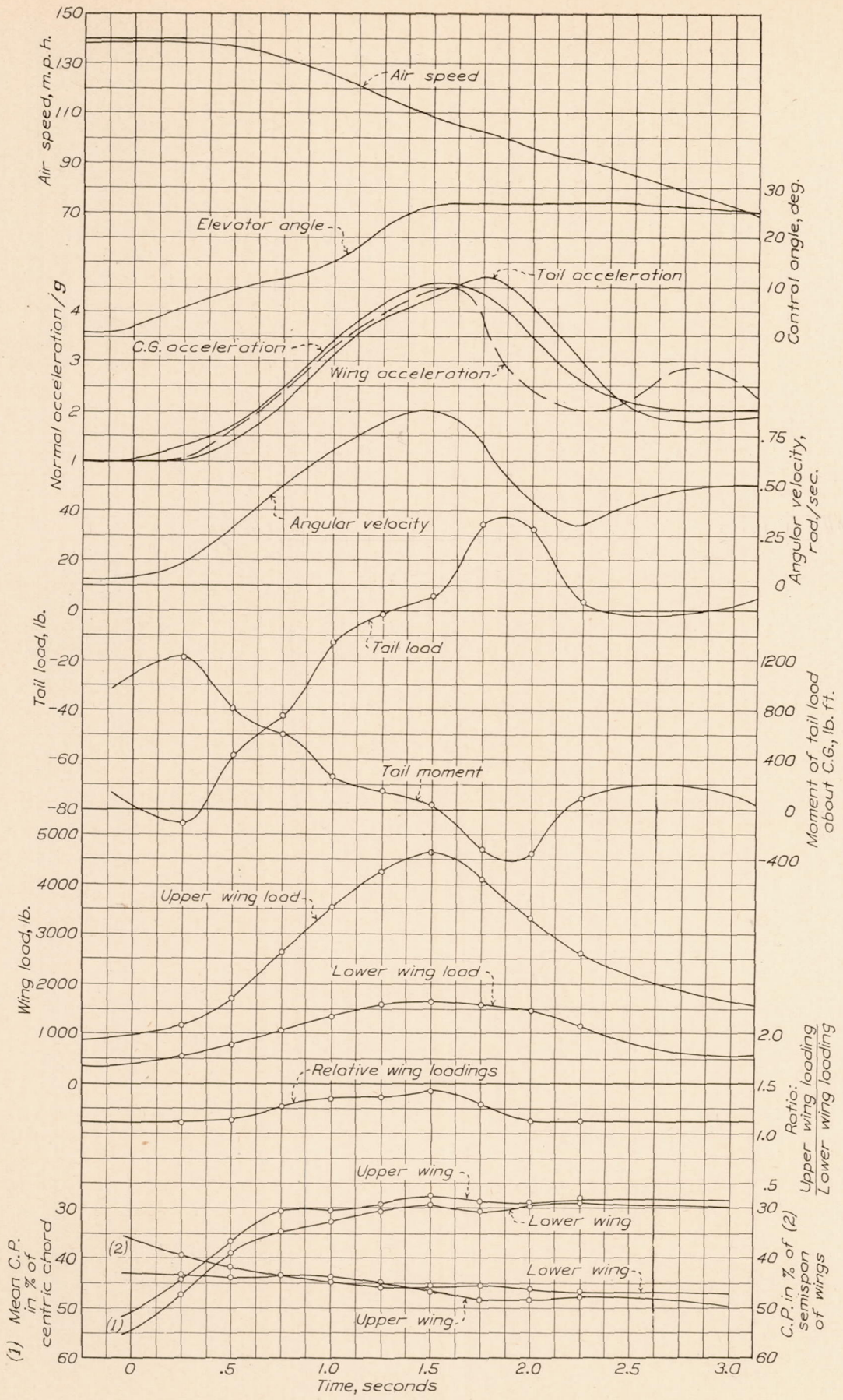

FIGURE 55.—Time history of a mild power-off pull-up at 140 miles per hour. (Run No. 208)

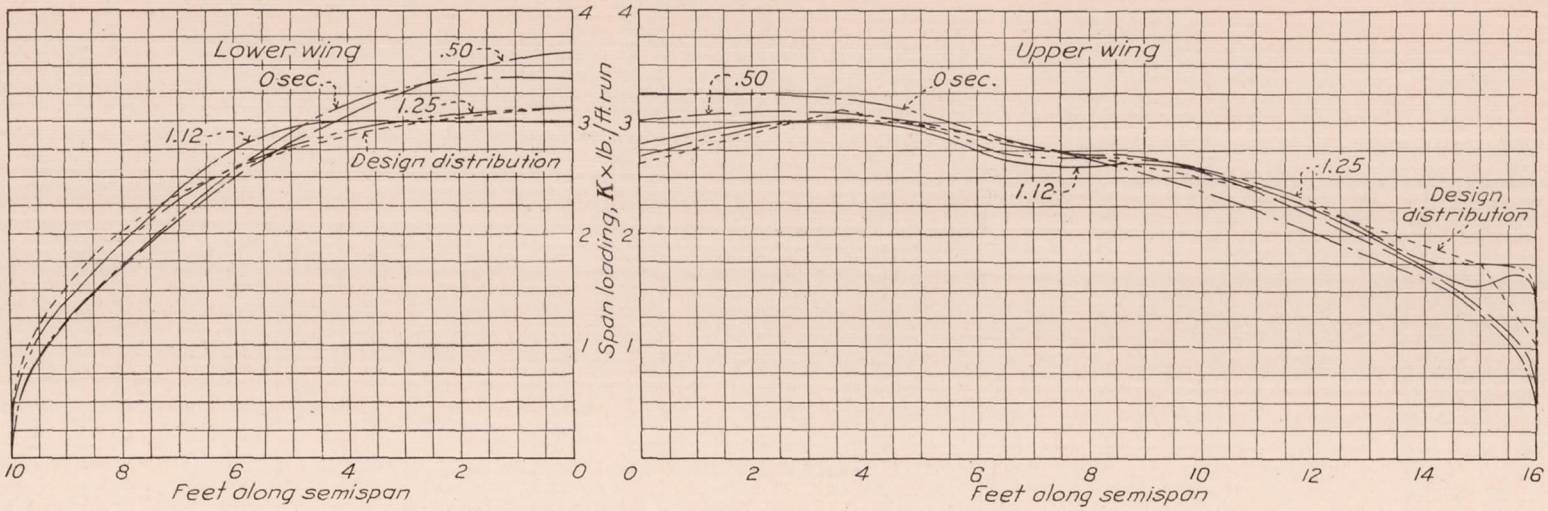

FIGURE 56.—Span load curves. Reduced to same area showing the variation in relative distribution at different stages of the maneuver. Pull-up at 79 miles per hour. (Run No. 65)

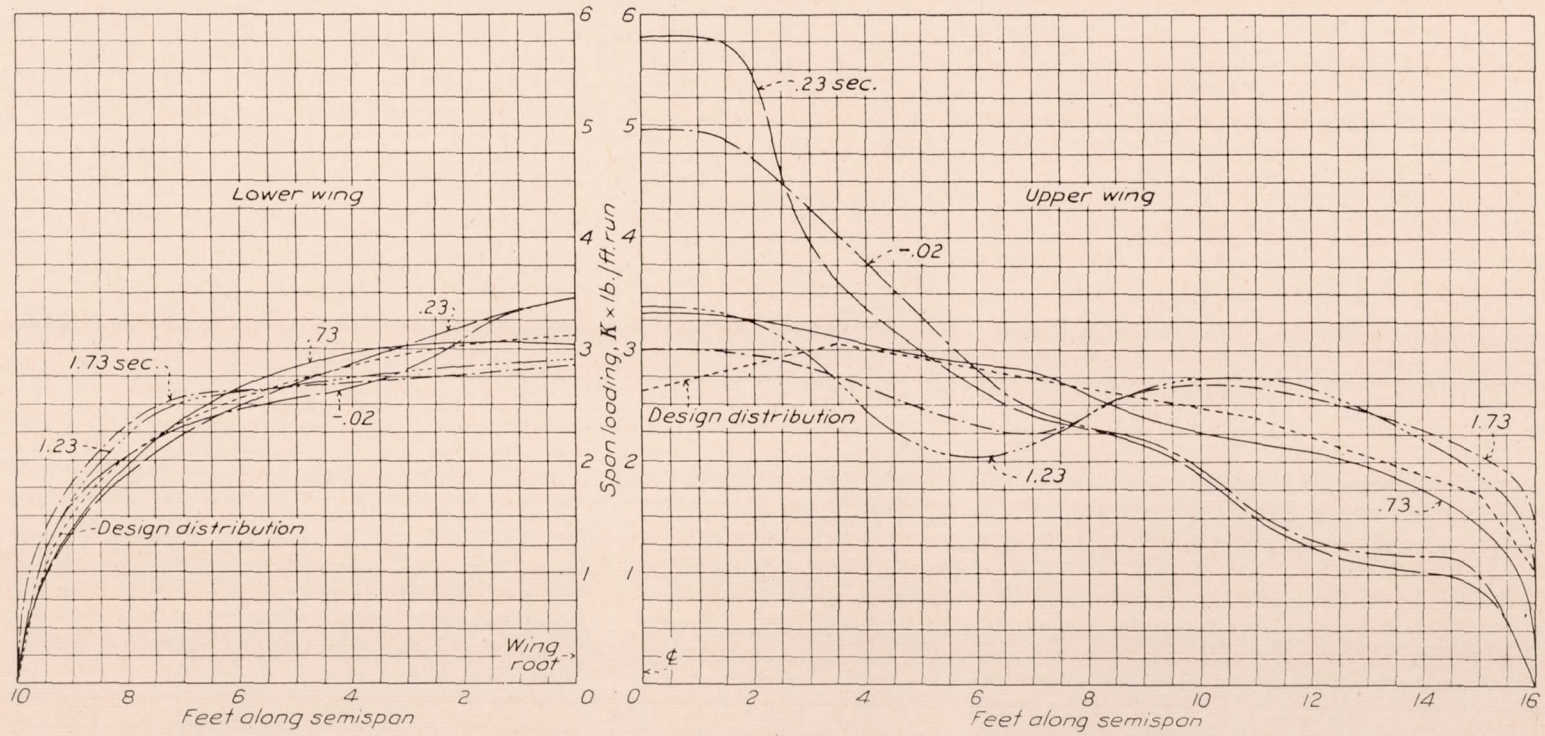

FIGURE 57.—Span load curves. Reduced to same area showing the variation in relative distribution at different stages of the maneuver. Pull-up at 137 miles per hour. (Run No. 132)

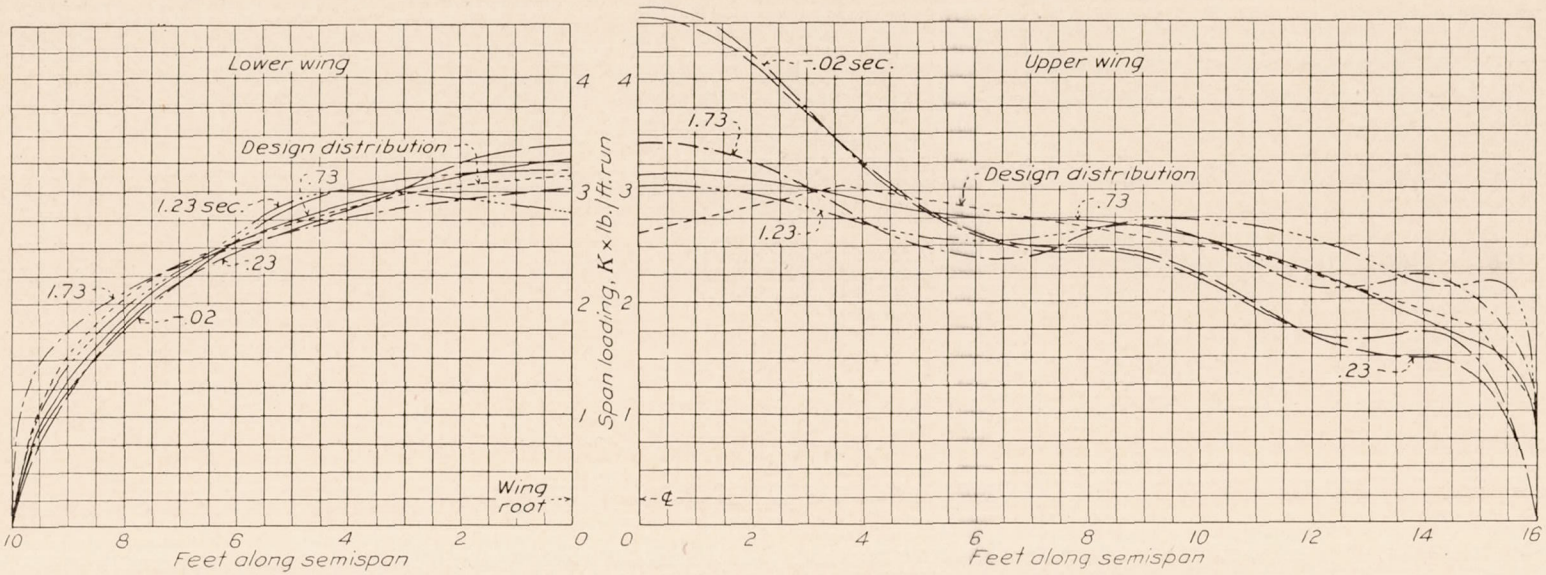

FIGURE 58.—Span load curves. Reduced to same area showing the variation in relative distribution at different stages of the maneuver. Pull-up at 116 miles per hour. (Run No. 130)

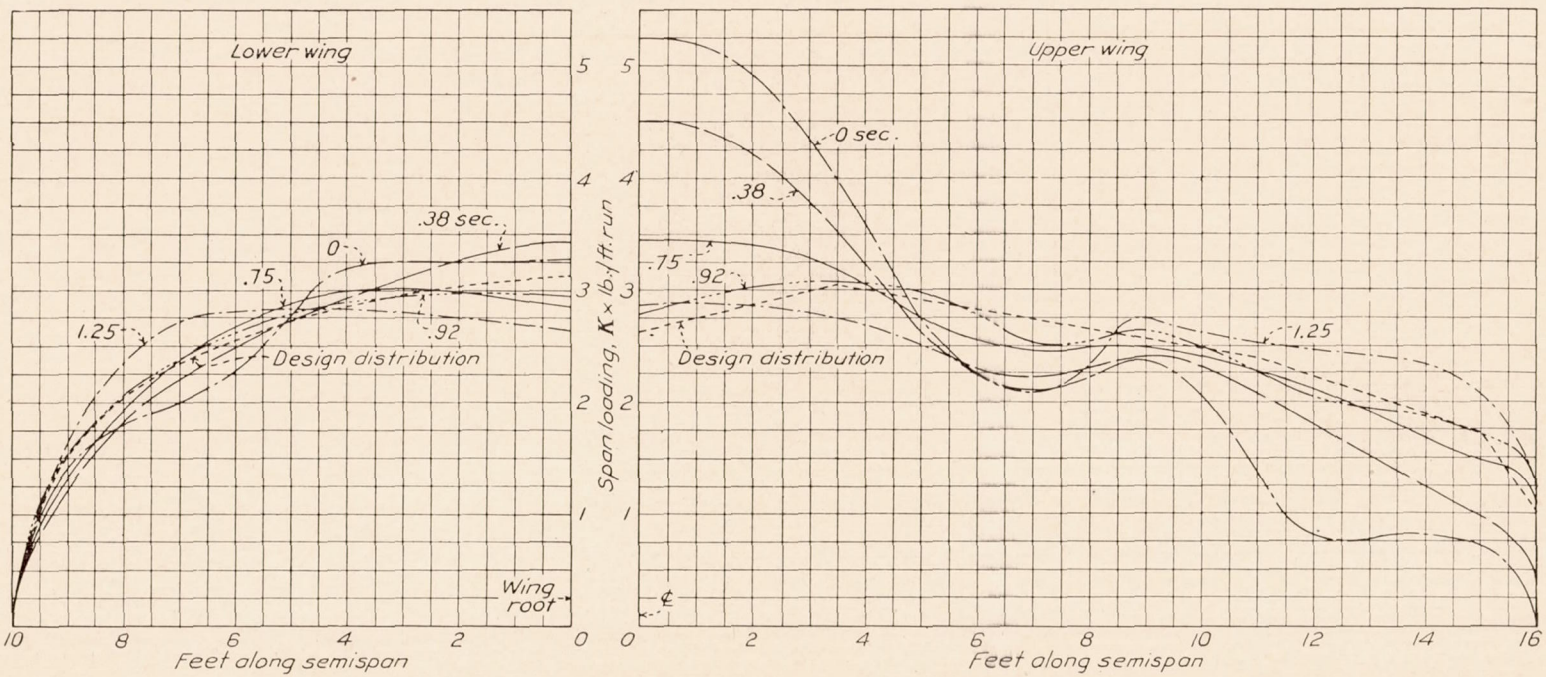

FIGURE 59.—Span load curves. Reduced to same area showing the variation in relative distribution at different stages of the maneuver. Pull-up at 181 miles per hour. (Run No. 137)

upper and lower wings at high angles of attack agrees remarkably well with the load curves derived from the design rules, still, the discrepancy between the actual center of pressure and design center of pressure (31 per cent) results in an unsafe condition for the front lift truss. Figure 60 shows the comparison between the actual gross spar load curves from Run 132, and the design load curves (dead weight not subtracted) for high angle of attack on the basis of the same load factor or total load. A small difference in relative wing load exists between flight and design rules (1.37 and 1.29, respectively, for this case) which magnifies the effect of center of pressure discrepancy on the upper wing to a slight extent. It is seen from the figure that the greater portion of the front upper spar is overloaded, but that it is underloaded at the tip. This latter condition is caused by the rearward displacement of the center of pressure at the tip sections, which is characteristic at high angles of attack. The effect of the actual load distribution on the primary bending moments is shown in Figure 61. These curves are given for illustrative purposes only, but are true comparisons on the assumption that a pin joint exists in the spar at the cabane strut attachment point, which is not actually the case. They show, however, that a considerable discrepancy exists between the bending moments actually obtained and those assumed—in this particular case, 36 per cent on the unsafe side.

In view of the importance of the high angle of attack condition in design and of the position of the center of pressure in this condition, it would seem advisable to shift the design center of pressure forward on the upper wings of biplanes by the amount indicated for the combination by wind-tunnel tests or theoretical calculations, if such are available, or if not, to shift the upper wing center of pressure forward arbitrarily by 3 to 5 per cent to be on the safe side.

It might also be advisable to increase the design bending moment of the front spar in the middle of the bay of externally braced types by an arbitrary amount to allow for the rearward displacement of the center of pressure at the tip, except in cases where the effect of tip shape is definitely known. The existing rules apply an arbitrary increase in bending moment of 30 per cent from the outer point of inflection to the tip, which takes care of possible increases in stress near the strut attachment point arising from excessive tip loads. The tip loss assumed, which is considered to be more than that actually encountered, is supposed to take care of possible excesses of stress in the bay, but is not sufficient to provide for conditions arising from displacements of the center of pressure from the assumed value. The above discussion accentuates the need for extensive research on load distribution over wing tips, which must be done before the arbitrary nature of such revisions as suggested can be eliminated.

8493—31——4

Figures 62 and 63 are presented to show the variation of spar load distribution throughout two pull-ups of different character. Both show the same general results for similar portions of the maneuver, the outstanding points being the tip peaks on the upper rear spar in the region of high angle of attack and the similarity between front and rear spar load distribution on the lower wing in all conditions.

Figures 30 to 55 represent histories of all of the pull-ups investigated for which satisfactory records were obtained. They show the relation existing between the loads acting at any instant during the maneuver. It is seen that the upper and lower wings reach maximum loads at the same time; also, that the maximum tail load is down and occurs early in the maneuver, well before the wing loads reach their maximum values. It will be noted, too, from the tail acceleration records that this down load is not accompanied by an appreciable weight or inertia load, since the acceleration at the time is approximately zero. This suggests that a critical loading condition for the fuselage is the pure maximum down load on the tail, which agrees with the present design rules.

Referring to the abrupt power on pull-ups in the high angle of attack condition, the acceleration at the tail remains at a fairly constant ratio to the acceleration at the center of gravity, and is of the order of one-half of the latter value (considering $1g$ the datum). It would follow from this that the present rules are in error in assuming the high angle of attack condition to be equivalent to a static condition with the basic load multiplied by an appropriate load factor, and that they should take account of the fact that in this condition there is, in most cases, an angular acceleration about the pitching axis which results in a varying inertia load along the fuselage. This inertia load, of course, depends on the moment of inertia of the airplane and the effectiveness of the controls, and differs with different airplanes. In any case, however, the condition would be such that the inertia load forward would be greater than anywhere else. This points to the conclusion that the present rule gives design loads for the engine mount and forward portion of the fuselage that are too small, and hence may prove unsafe.

Referring now to the histories of the power-off pull-ups, the above discussion does not apply. The tail accelerations now are about the same as the center of gravity accelerations and usually a little higher. In short, the conditions in the power-off pull-ups are in fair agreement with the conditions assumed in the design rules; the conclusion is therefore drawn that two possible critical conditions exist for the fuselage at high incidence, one corresponding to power on and the other to power off.

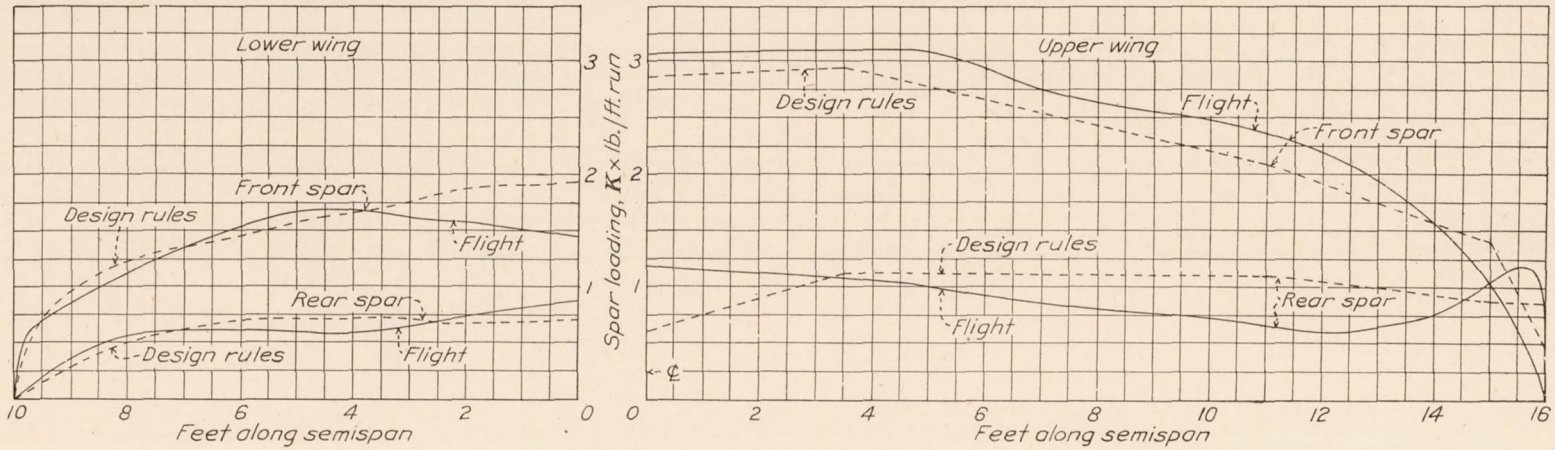

FIGURE 60.—Comparison of high angle of attack, spar loads from flight tests (run No. 132) and design rules

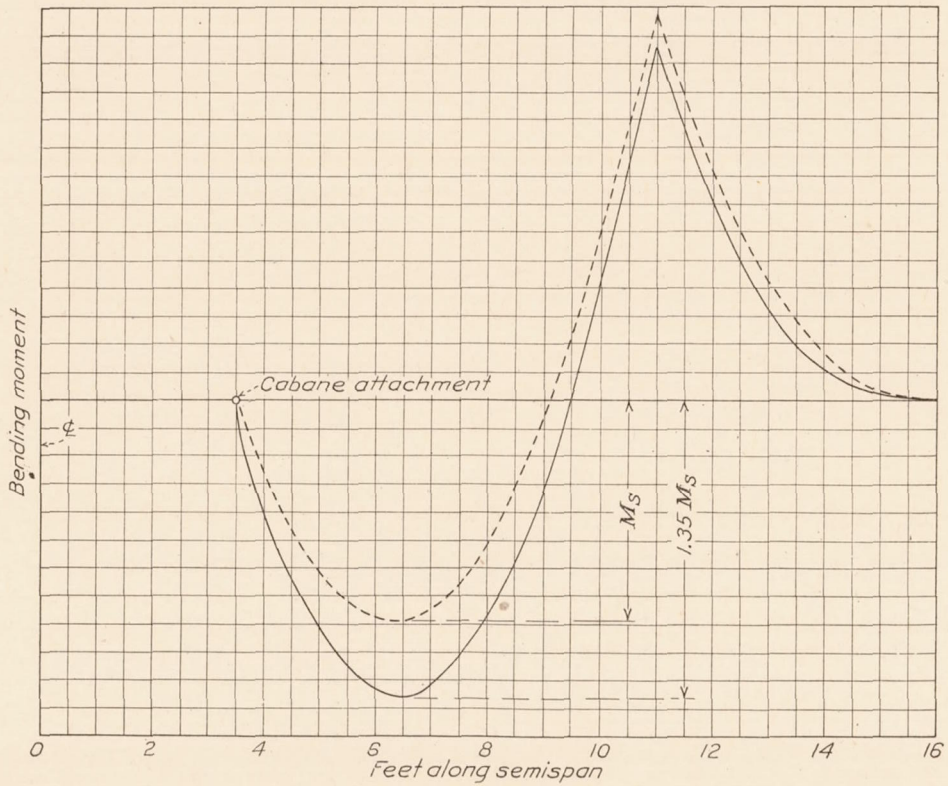

FIGURE 61.—Comparison of front spar bending moments from flight tests (run No. 132) and specification. (Pin joint assumed at cabane attachment)

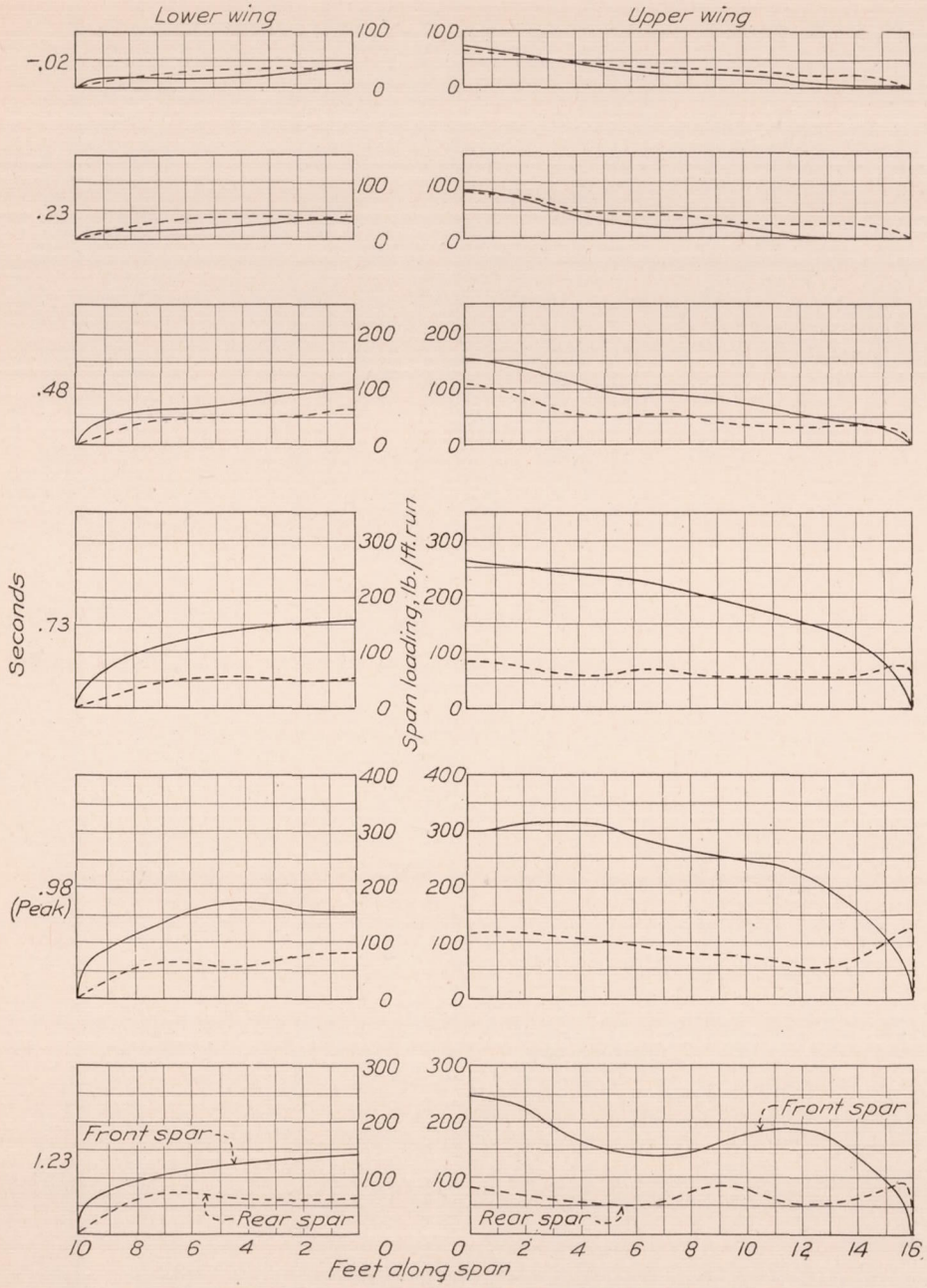

FIGURE 62.—Time history of spar loads in a pull-up at 137 miles per hour. (Run No. 132)

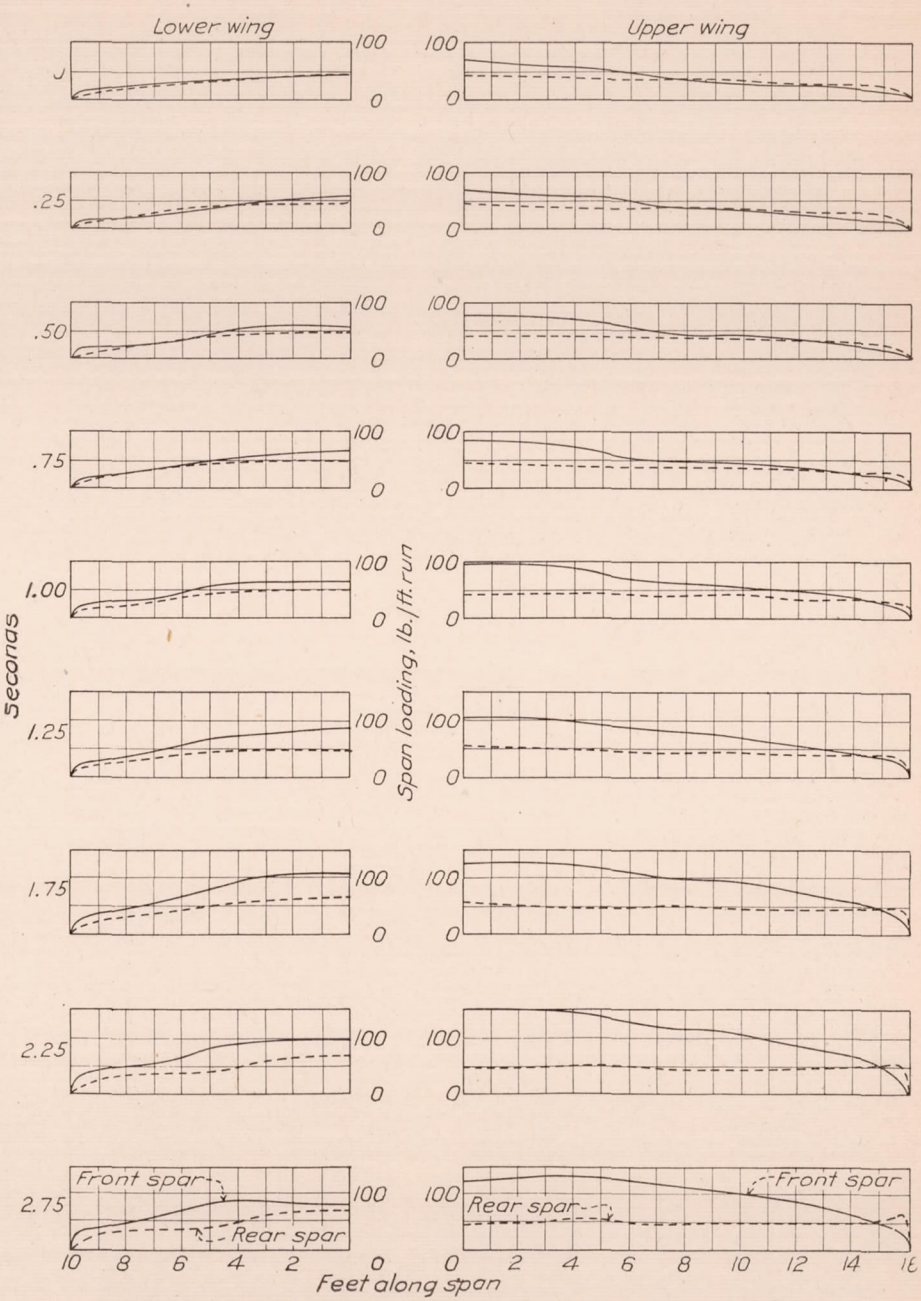

FIGURE 63.—Time history of spar loads in a pull-up at 110 miles per hour. (Run No. 73)

A point of considerable interest is disclosed by the results of the power on pull-ups. It has been mentioned previously in this report that one reason for investigating the pull-up at such length was to determine the effect of the pitching motion on the center of pressure position in the high angle of attack condition, and also on the maximum normal force coefficient. It has been shown that the maximum forward position of the center of pressure is the same within the experimental error, regardless of the character of the pull-up. It can, therefore, be concluded that pitching does not affect the C. P. in the high angle of attack condition, at least for the airfoil section and cell used here. The maximum normal force coefficients are erratic; that is, for different runs the values of normal force coefficient are not the same, and seem to bear no clear relationship with any other variable. This is believed to be due to the lack of accurate synchronization between the air-speed record and pressure records. In general, however, the values are greater than would be expected. The upper wing C_N from the model data (Reference 14), corrected for scale effect reaches a maximum value of about 1.43. The full-scale results show some maximum values as high as 1.8, with the average maximum about 1.66. In only one case is the maximum C_N less than 1.43. This would indicate strongly that the normal force coefficient of an airfoil with a positive pitching motion attains a higher value than a similar airfoil under steady conditions. This indication is further substantiated by Figure 64. It will be noted that the accelerations in the power on pull-ups lie close to the theoretical curve. Now, since the theoretical curve is based on the assumptions that the airplane is pulled up with no loss in air speed, and that $C_{N\ maximum}$ for the pitching airfoil is the same as that for steady flight at stalling speed, in view of the fact that the air speed actually does fall off an appreciable amount by the time the peak load in a pull-up is reached, it can only be concluded that the close agreement between the experimental points and the theoretical curve is due to an unusually high maximum normal force coefficient occurring in the maneuver. This close agreement, therefore, could only be expected to occur for certain conditions in which the decrease in air speed just offsets the increase in normal force coefficient. In these tests the conditions are met in abrupt power-on pull-ups started from horizontal flight. In the power-off pull-ups the air speed falls off more rapidly, and as a result the measured accelerations in general come below the theoretical curve. It might be expected from this that in abrupt pull-ups made from steep dives in which the weight component still acts forward at the peak load, the air speed would not fall off so rapidly, and as a result accelerations in excess of the theoretical would be experienced. While none of the present data show this to be so, it has been demonstrated in maneuverability tests on both an *F6C–3* and an *F6C–4* airplane (results not yet published) that this condition actually occurs.

These high normal force coefficients can probably be accounted for on the basis of the known phenomenon of vortex or eddy formation. An important consideration in these formations over a wing beginning to stall is that time is required for the back flow in the boundary layer to reach the stage where the first vortex can be formed. In the pitching wing, therefore, the flow does not instantly break down when the steady flight angle of maximum lift is reached, but continues in force for a short time while the wing rotates beyond this angle, with the result that the lift continues to build up to an abnormal value. Whatever the cause, the result is interesting and important, as it can very conceivably have some effect on high angle of attack load factors, and also on the relative distribution of load between upper and lower wings of a biplane.

With respect to this latter point it would seem reasonable to expect that the lower wing normal force coefficient at peak total load in a pull-up would be nearly equal to its steady flight value, since the effect of the upper wing in the latter case is to delay the breakdown in flow over the lower wing, and hence the explanation given for the upper wing does not apply, at least for the peak total load condition. Furthermore, the slope of the lower wing C_N curve is progressively decreasing with increasing angle of attack (Reference 14), and at the time of maximum load on the upper wing has a fairly small value. This is borne out by the relatively flat lower wing load curve in the present data.

The above assumption is substantiated by the facts, the model lower wing C_N at the angle of attack of maximum upper wing load being 1.18 (corrected for scale effect), whereas the average of the maximum full scale lower wing normal force coefficients from the power on pull-ups is 1.23, a good agreement. If the hypothesis concerning the high upper wing normal force coefficients is correct, the foregoing lower wing values can be made to agree still better by taking the model C_N at a higher angle of attack.

The effect of the phenomenon discussed in the above two paragraphs on the relative wing-load ratio would be, then, to increase the ratio for the pitching high angle of attack condition. Comparison of this ratio from the model data and from the full scale pull-up data shows this to be true, the former value at maximum upper wing load being 1.16, whereas the latter value (average of all power-on pull-ups) is 1.35. The ratio of these two values, since the lower wing normal force coefficients are essentially the same, is then practically equal to the ratio of the steady flight upper wing maximum normal force coefficient to the pitching upper wing maximum normal force coefficient.

In all pull-ups, the acceleration at the wing tip is of approximately the same magnitude as the acceleration at the center of gravity, differences being ac-

counted for as follows: in the early stages of the maneuver, the flexibility and lightness of the wing structure allow the wing tip to accelerate more rapidly than the fuselage; in later stages of the maneuver, slight rolling motion is undoubtedly the cause.

A phenomenon evidenced on the original records, but not given in the histories, shows the existence of a high-frequency vibration of large amplitude at the wing tip occurring in each case at the instant of maximum load and continuing until the end of the record. (Fig. 65.) Whether this oscillation is caused by the sudden breakdown of air flow on the wing tip, by the abrupt change of inertia load, or is associated with the more or less well-known phenomenon of wing flutter, can only be surmised. Vibration tests conducted on the airplane showed the natural frequency of the wing structure as a whole to be: (*a*) From 8.7 to 10 oscillations per second in bending, the differences being caused by the addition of various weights up to 22 pounds at the accelerometer location; (*b*) 8.5 oscillations per second in torsion. For the upper tip alone, a rigid support being provided at the strut attachment, the frequencies were taken from 10 to 14 in bending with weights added as before, and 12.5 in torsion. In the bending tests, the higher frequencies correspond to the condition of no extra weight, which is the condition occurring in flight.

It was difficult to determine frequency of oscillation from the wing accelerometer records because of the superposition of several waves of different frequencies and amplitudes, but in general the frequency of the principal oscillations was of the order of from 10 to 17. Strangely enough, the higher frequencies occurred in the slower power-off maneuvers, thus precluding the possibility that engine vibration was responsible.

Rolls.—Figures 66a to 67i show the distribution of load throughout a right and a left barrel roll. The initial stages of the maneuver up to the peak load are identical with the pull-up, except that the loads build up on the rudder in addition. Beyond the peak load, autorotation starts and is evidenced in the right roll by the shapes of the pressure curves on the right upper wing which are characteristic at angles of attack above the stall. (See Reference 14.) The left. lower wing in the right roll does not stall, the condition being similar to that at high angles near maximum lift In the left roll, the right upper wing is not stalled, but is near or at maximum lift, while the left lower wing shows evidence of being stalled very slightly. The horizontal tail surfaces show dissymmetry of load. In the left roll, the distribution of pressure on the right side is very similar throughout to the pressure distribution in a pull-up, but in the right roll the down load on the elevator is replaced by an up load in the latter stage of the maneuver. This dissymmetry is probably caused by the influence of the fuselage.

Span load curves for the two rolls are given in Figures 68 and 69, and time histories in Figures 70 and 71.

Figure 72 is a span load and inertia load diagram combined from corresponding points in the right and left rolls at the condition of maximum dissymmetry of load on the upper wing. This point occurs at 1 second. It will be noted from Figures 66 and 67 that the two maneuvers are closely similar, viz, the control action is practically the same, and the maximum accelerations at the C. G. are practically equal and occur at the same time relative to the start of the maneuver. Figure 72 is corrected for the difference in total load in the two maneuvers.

The outstanding points in connection with the unsymmetrical condition are: 1. The maximum dissymmetry of load on the upper wing occurs shortly after the maximum total load, and the total load in the unsymmetrical condition is not much less than this maximum. 2. The dissymmetry on the lower wings is of such a nature as to oppose the rolling moment due to the upper wing. The first point is of particular interest in that it shows that the unsymmetrical cabane load condition should be analyzed with an average load factor equal to the high incidence load factor. This, of course, applies only if the arbitrary nature of the existing rules is eliminated, and they are reformulated to include the effect of varying inertia load across the span and the true effect of the lower wing. The second point is of considerable interest also, although in the light of the delayed stall of lower wings of a biplane indicated by model tests, the result is not particularly surprising. (Reference 14.) The results indicate that at the point of maximum upper wing rolling moment, the angle of attack of the stalled side of the cellule is not beyond the stalling angle of the lower wing on that side. This would explain the counter-rolling moment of the lower wing.

The inertia load along the span varies as shown in the figure. The slope of the line is calculated from the angular acceleration of the airplane (5 radians per second per second) as determined from the slope of the angular velocity record for the right roll. The wing tip acceleration for the right roll checks this slope very closely, although the wing tip acceleration for the left roll does not.

It may be of interest to note that the angular acceleration as calculated from the known rolling moments and moment of inertia of the airplane checks the value from the angular velocity recorder and accelerometer fairly closely. This can only be done, however, if the total wing rolling moment, as determined from Figure 72, be assumed as that for the right roll. The reason for this is that the angular velocities in right and left rolls are not the same on account of propeller torque and because the load on the stalled wing in a roll is quite sensitive to changes in rolling velocity, whereas

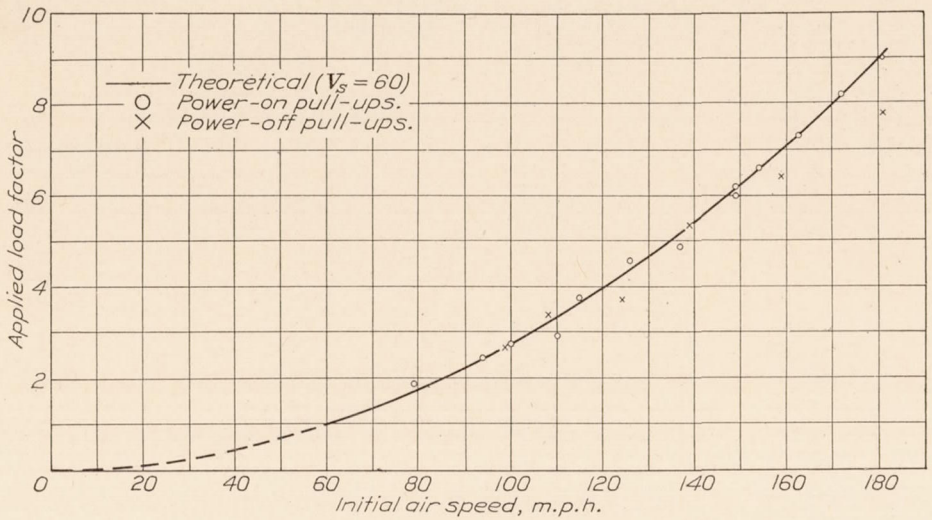

FIGURE 64.—Theoretical and experimental applied load factors in abrupt pull-ups from level flight

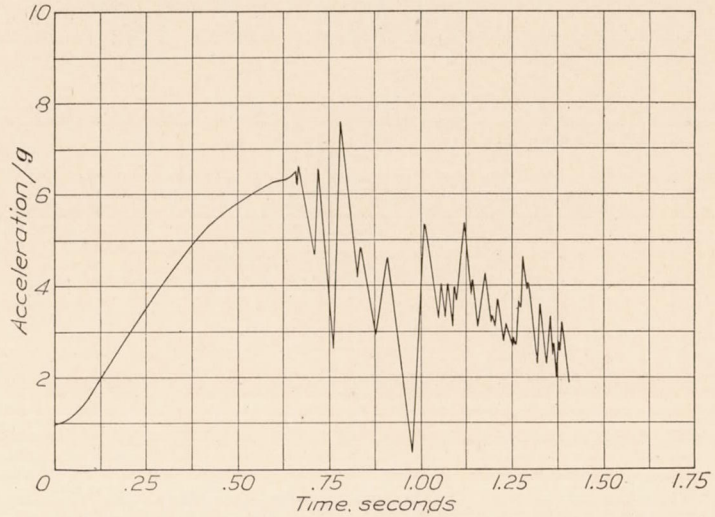

FIGURE 65.—Reproduction of wing-tip accelerometer record (run No. 134), showing character of vibration after peak load

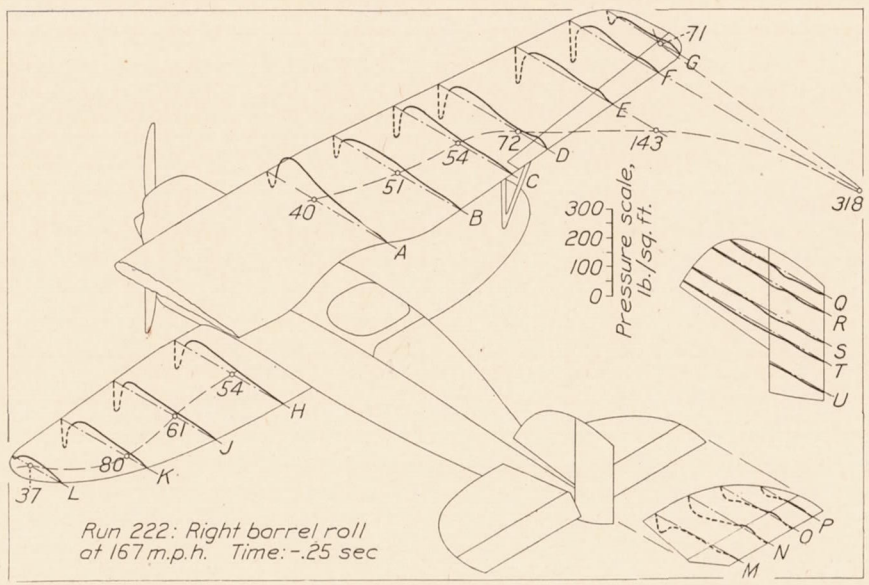

FIGURE 66a

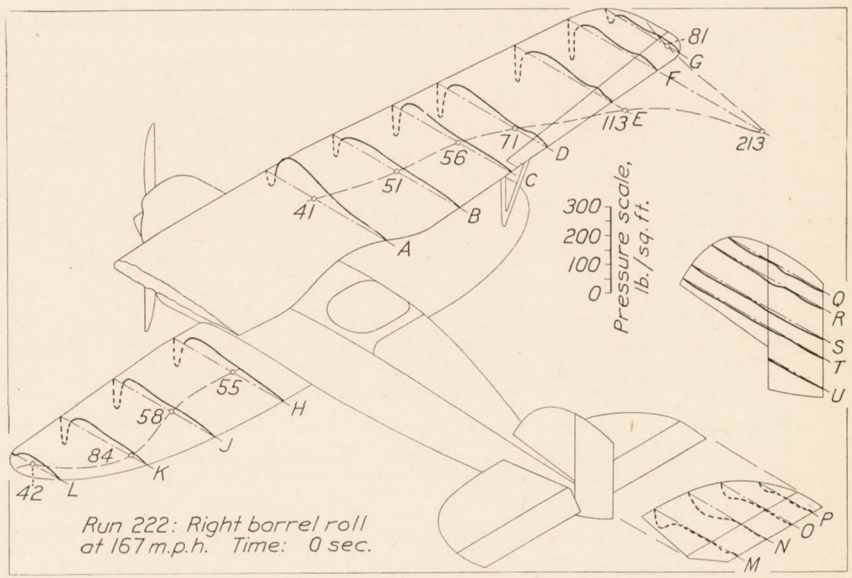

FIGURE 66b

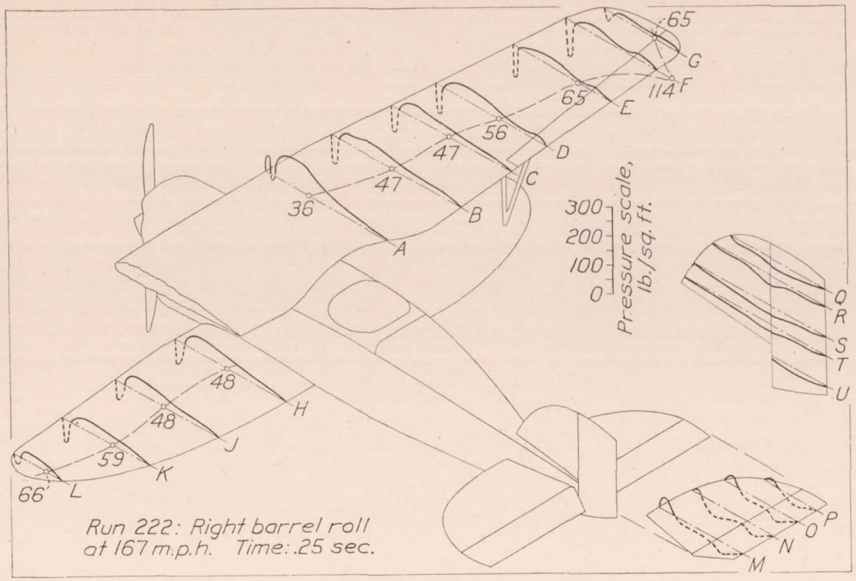

FIGURE 66c

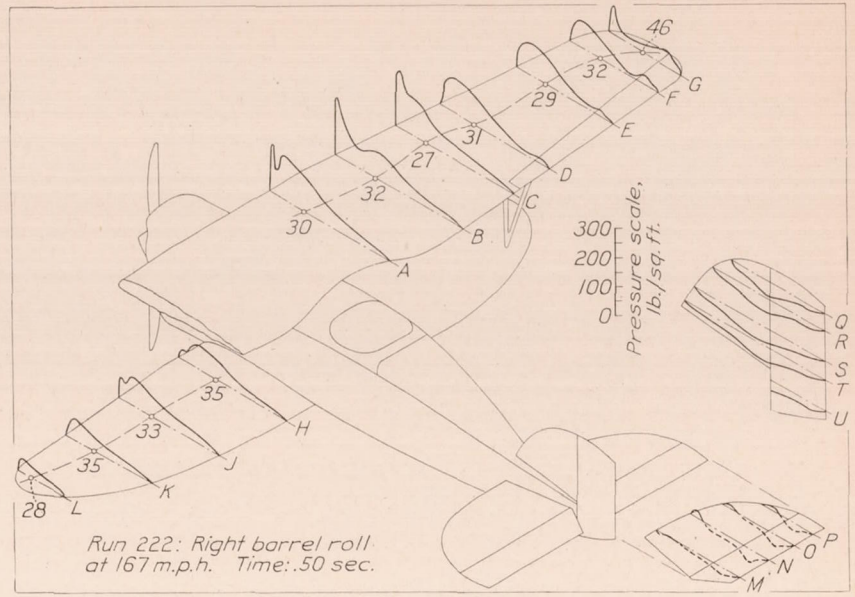

FIGURE 66d

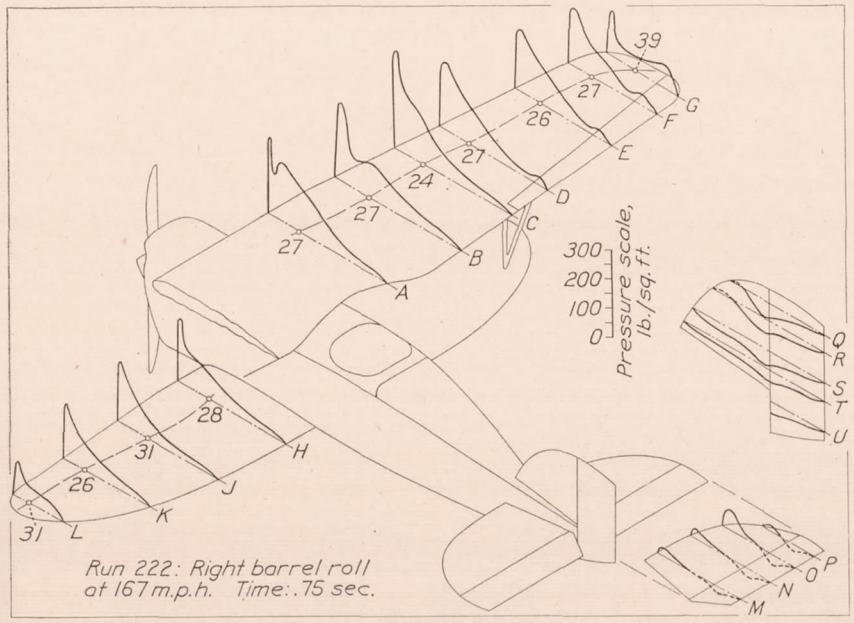

FIGURE 66e

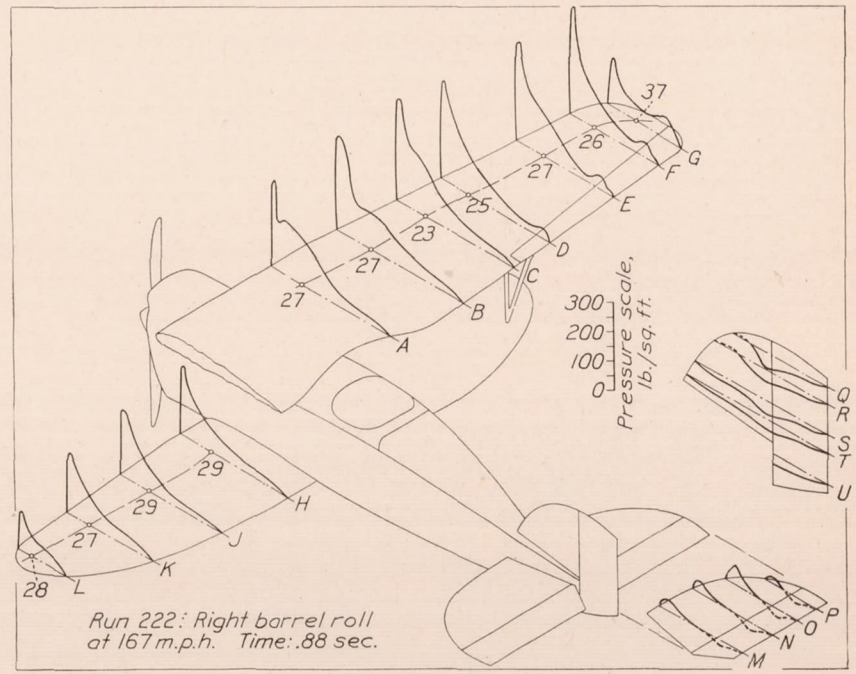

FIGURE 66f

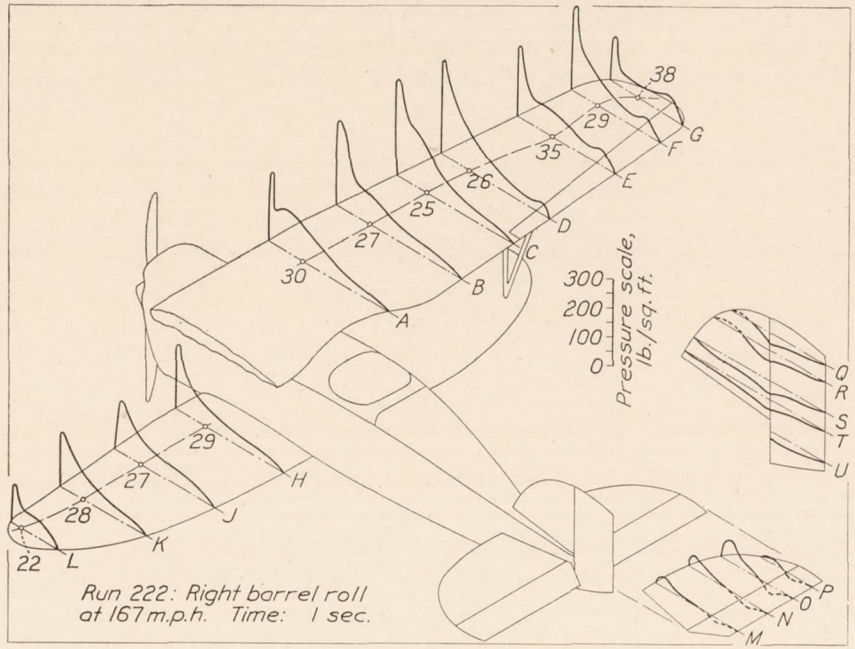

FIGURE 66g

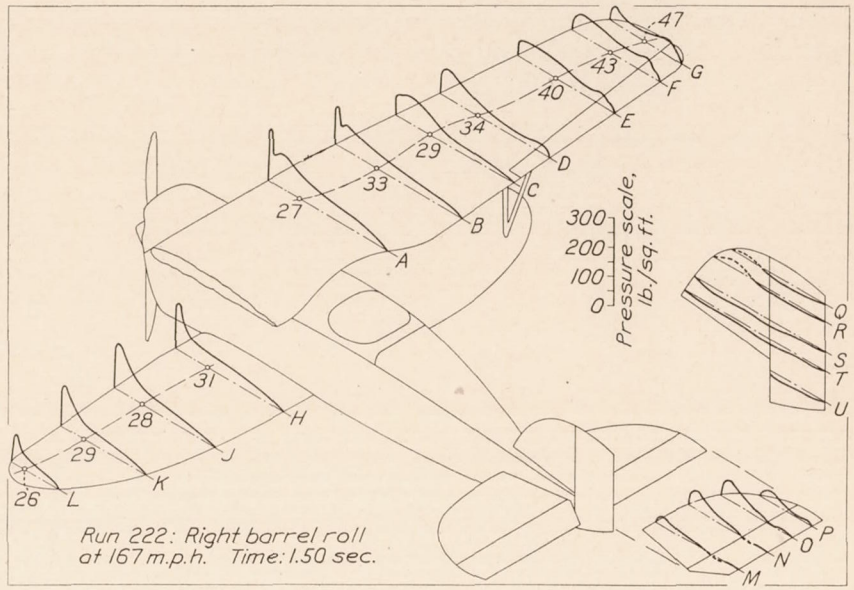

FIGURE 66h

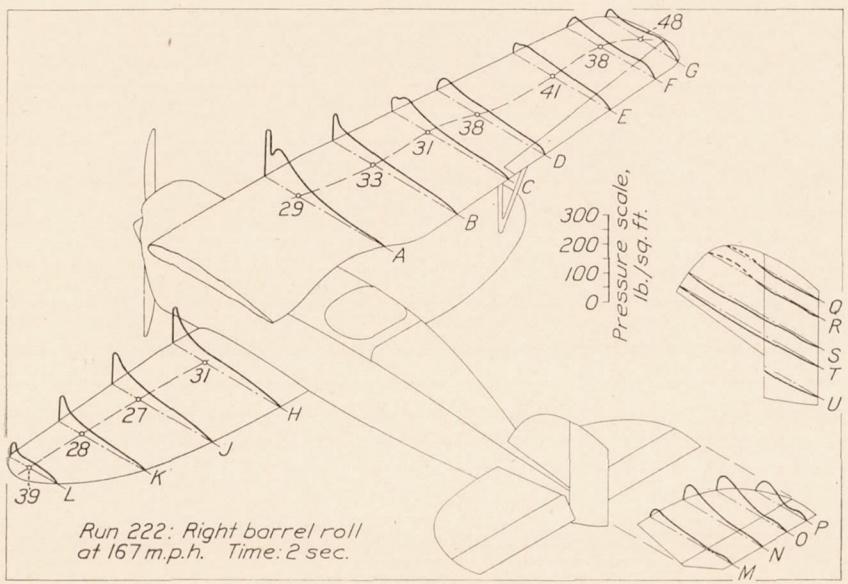

FIGURE 66i

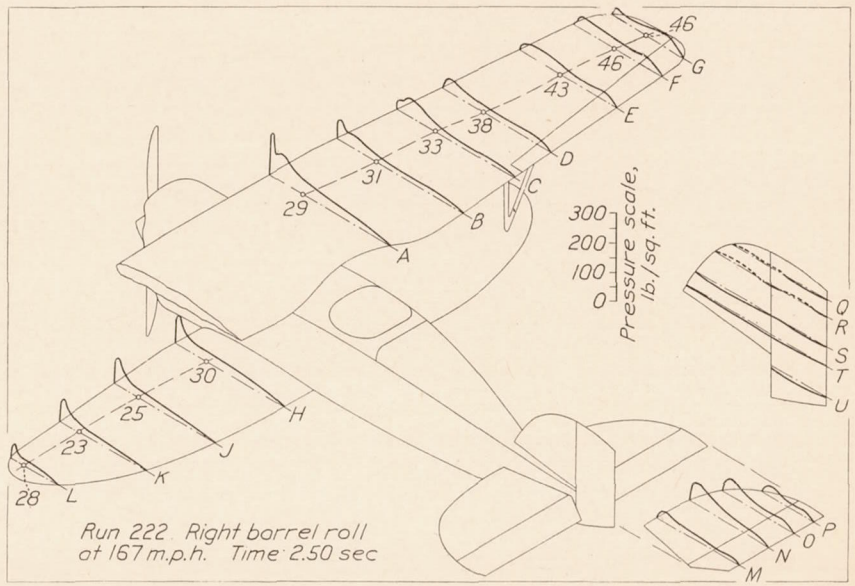

FIGURE 66j

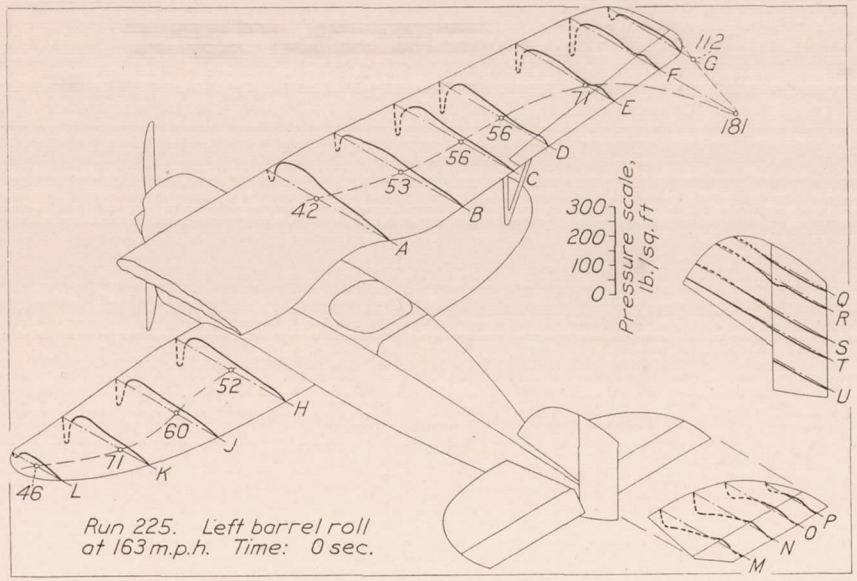

FIGURE 67a

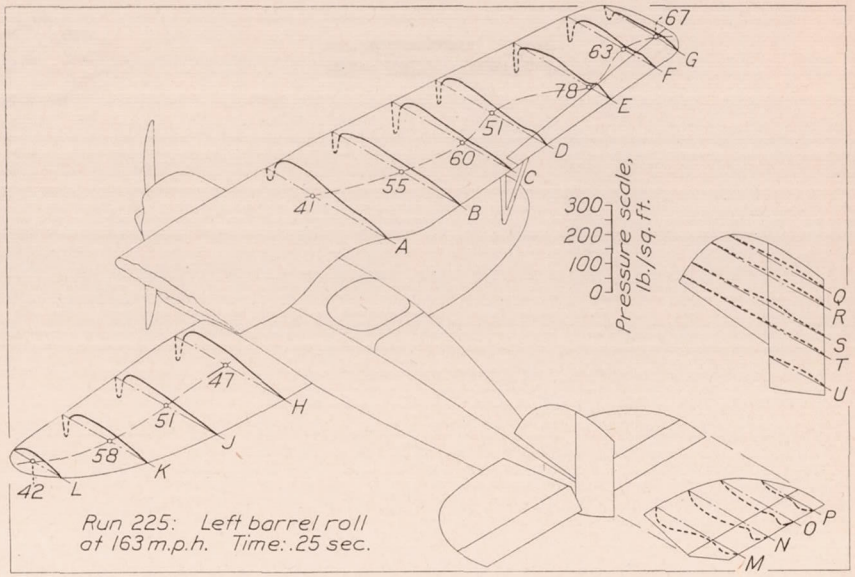

FIGURE 67b

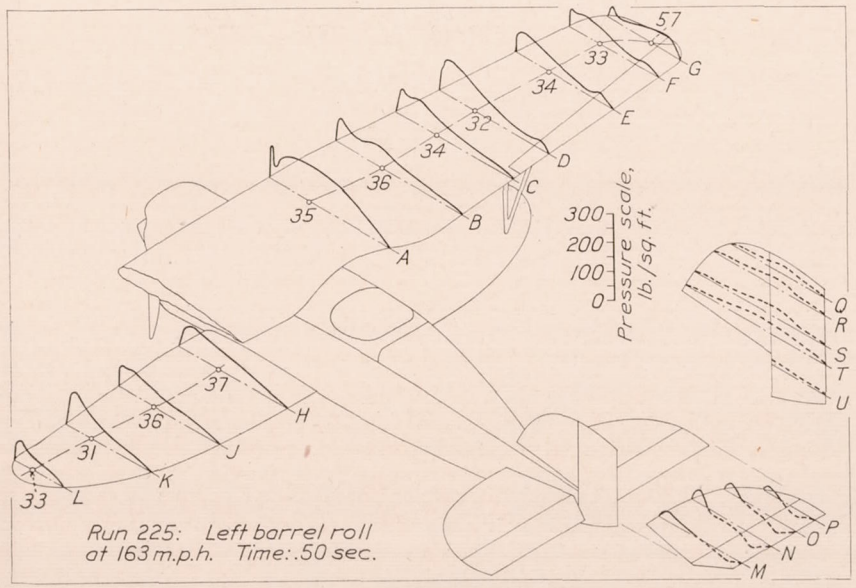

FIGURE 67c

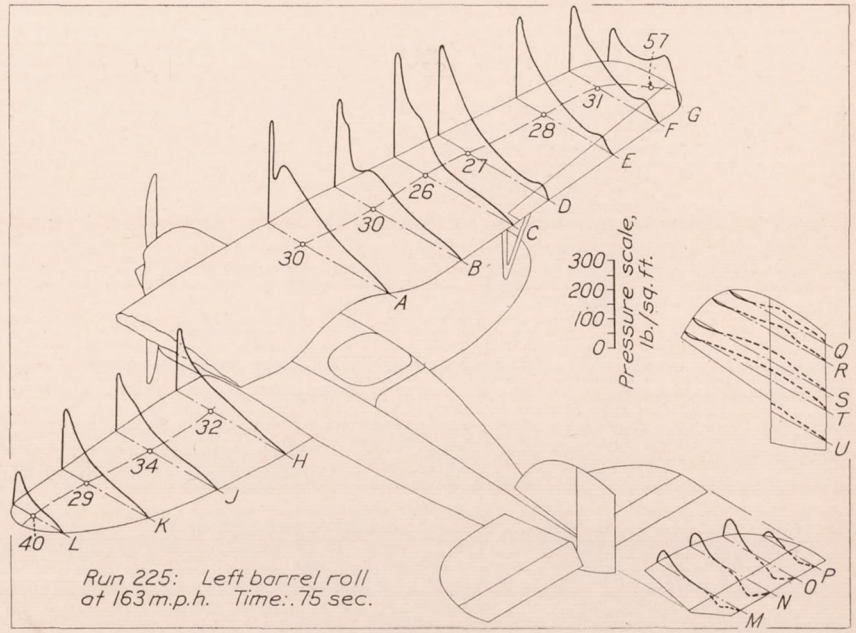

FIGURE 67d

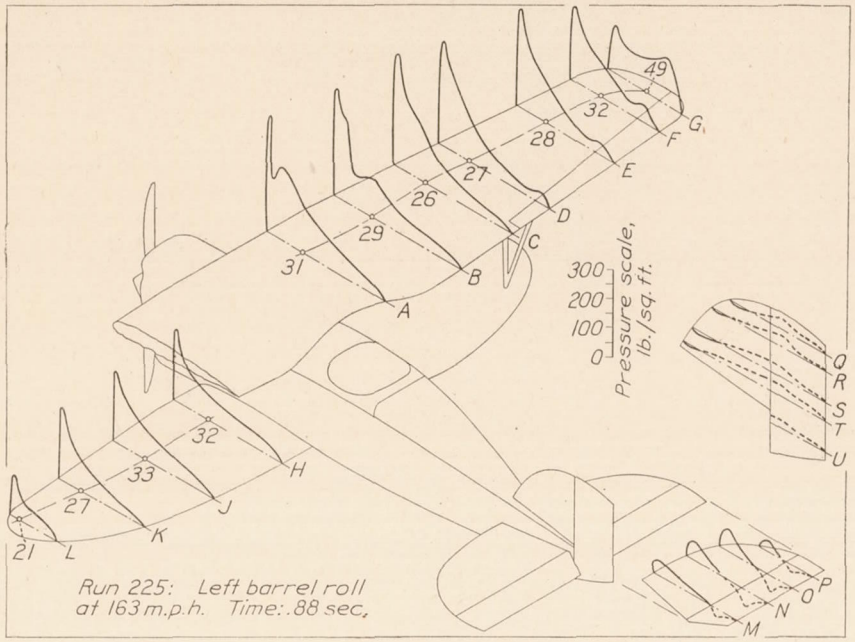

FIGURE 67e

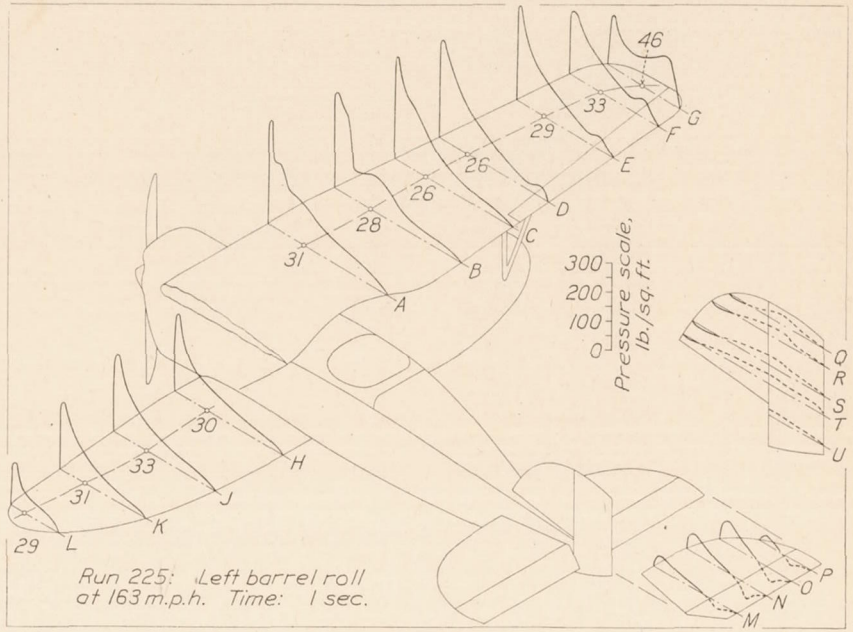

FIGURE 67f

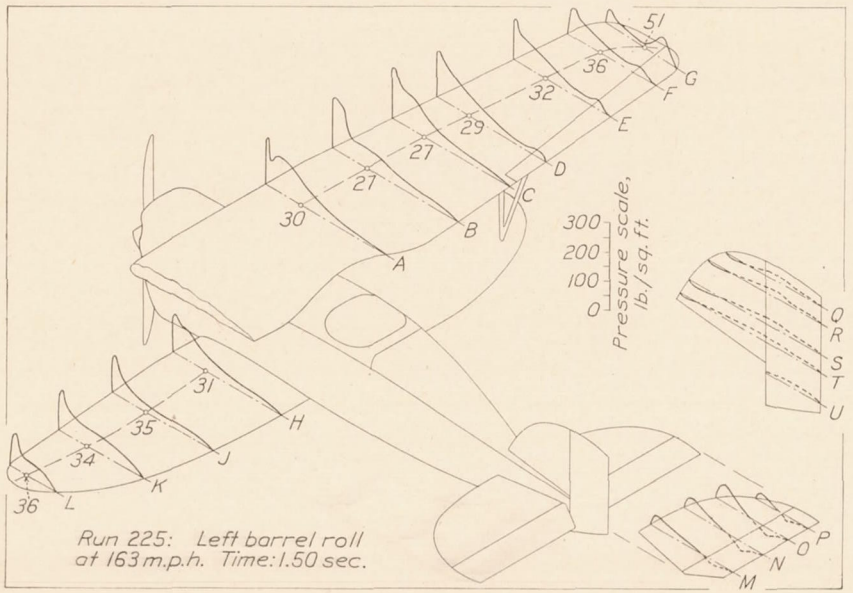

FIGURE 67g

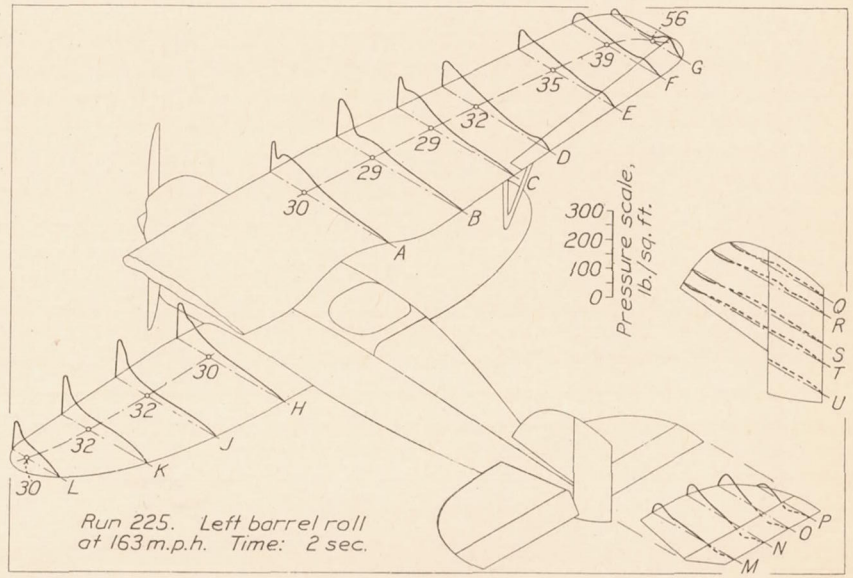

FIGURE 67h

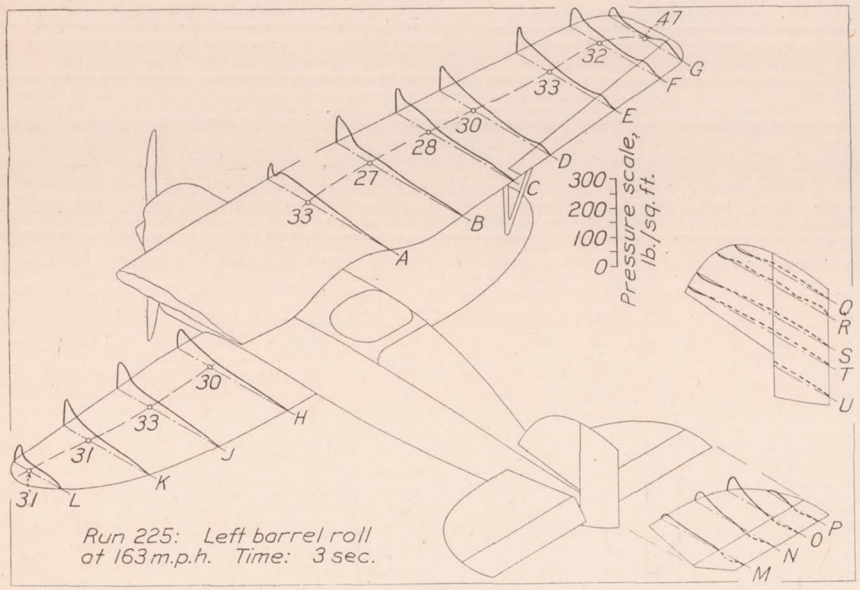

FIGURE 67i

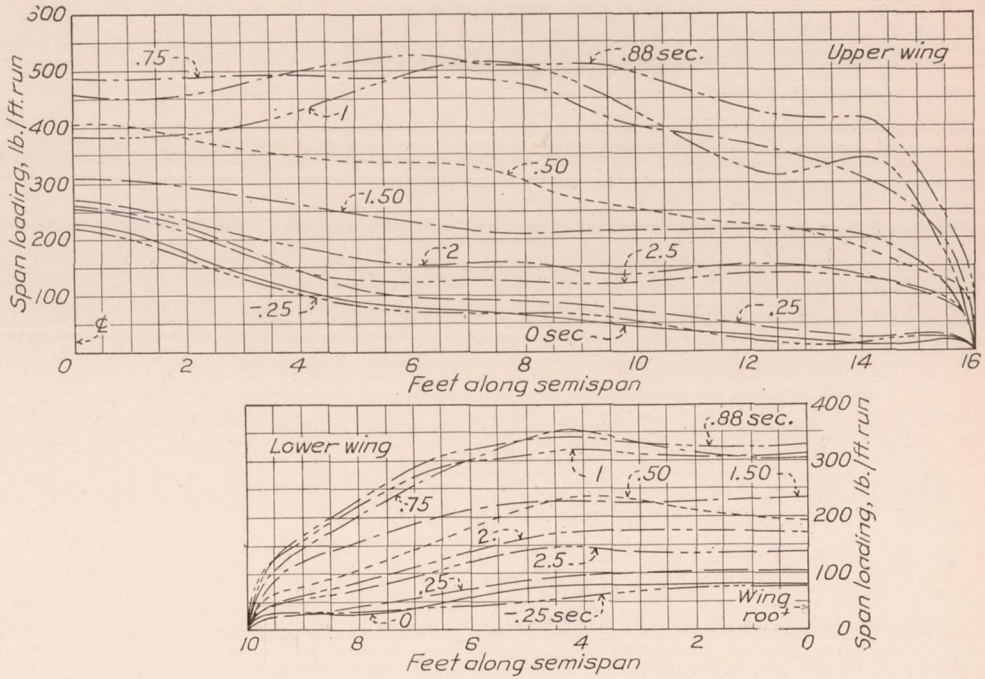

FIGURE 68.—Variation of span load distribution in a right barrel roll at 167 miles per hour. (Run No. 222)

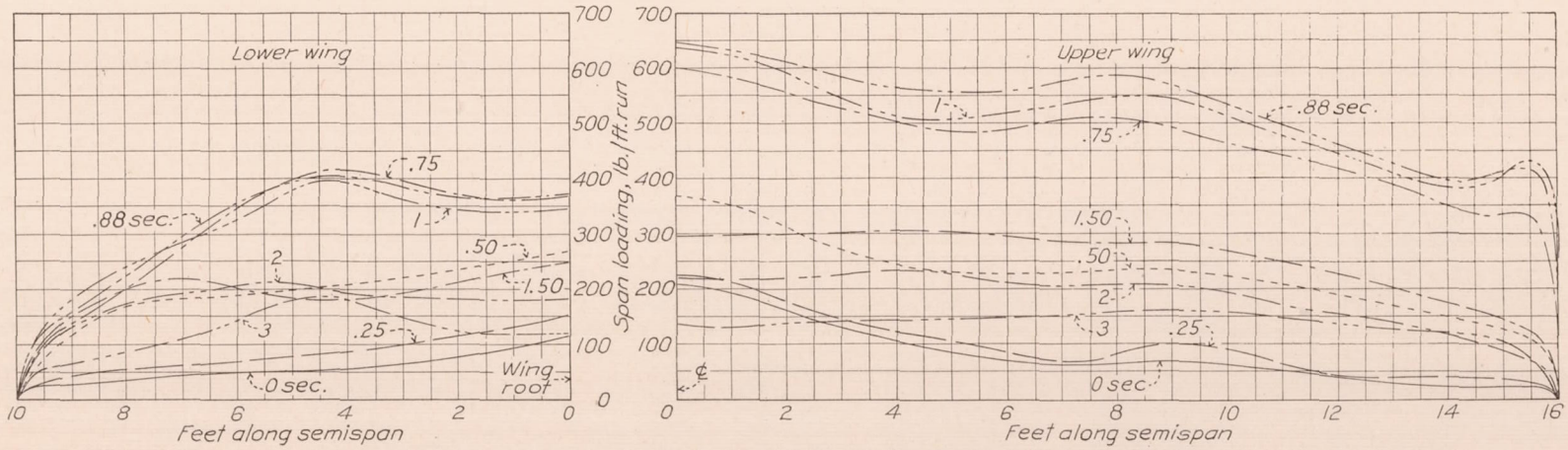

FIGURE 69.—Variation of span load distribution in a left barrel roll at 163 miles per hour. (Run No. 225)

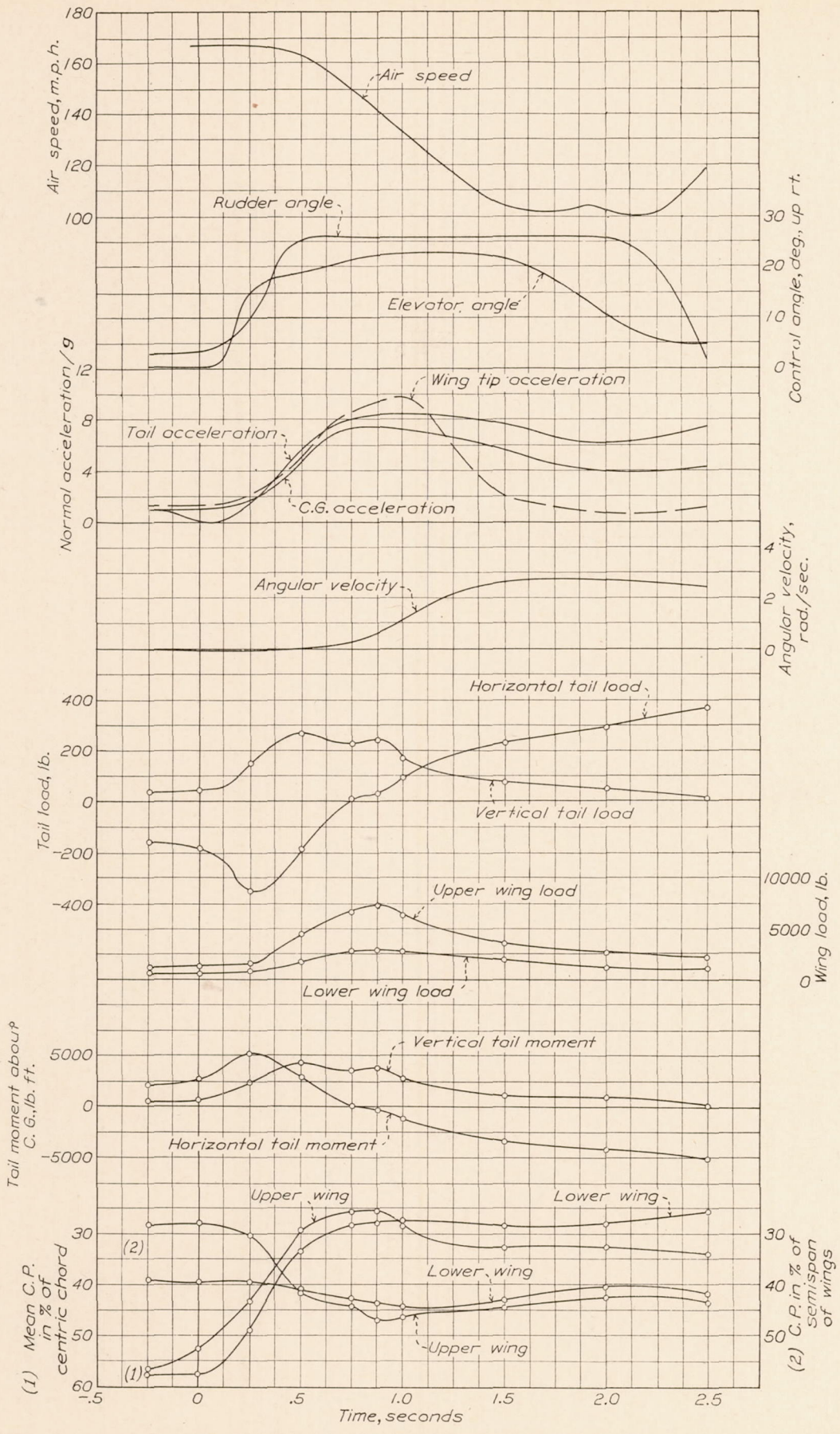

FIGURE 70.—Time history of a right barrel roll at 167 miles per hour. (Run No. 222)

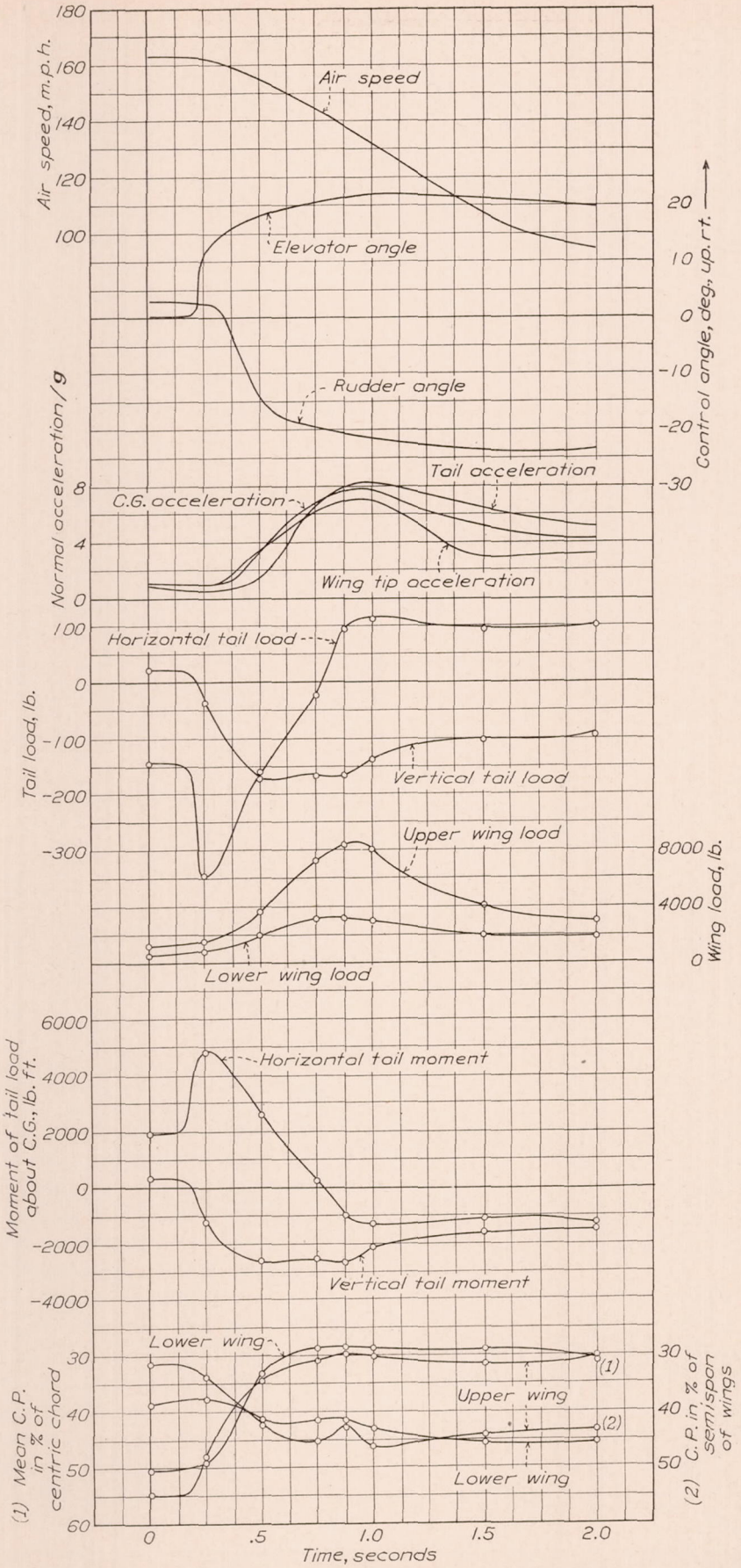

FIGURE 71.—Time history of a left barrel roll at 163 miles per hour. (Run No. 225)

the load on the unstalled wing is not. Therefore, if the right roll is chosen, we have the actual measured value of the load on the stalled or right upper wing, whereas if the left roll were chosen we should have to assume that the load on the right or stalled wing in the right roll was the same as the load on the left wing in a left roll, which would be a rather hazardous assumption. Assuming, therefore, that the wing-rolling moments given in Figure 72 represent fairly well the true wing-rolling moment in a right roll, it is only necessary to subtract the opposing torque of the propeller (in this case approximately 900 pound-feet, based on a knowledge of the propeller and engine characteristics and the conditions at which they are operating) to obtain the total moment causing angular acceleration. This value is: 9,600 − 900, or 8,700 pound-feet.

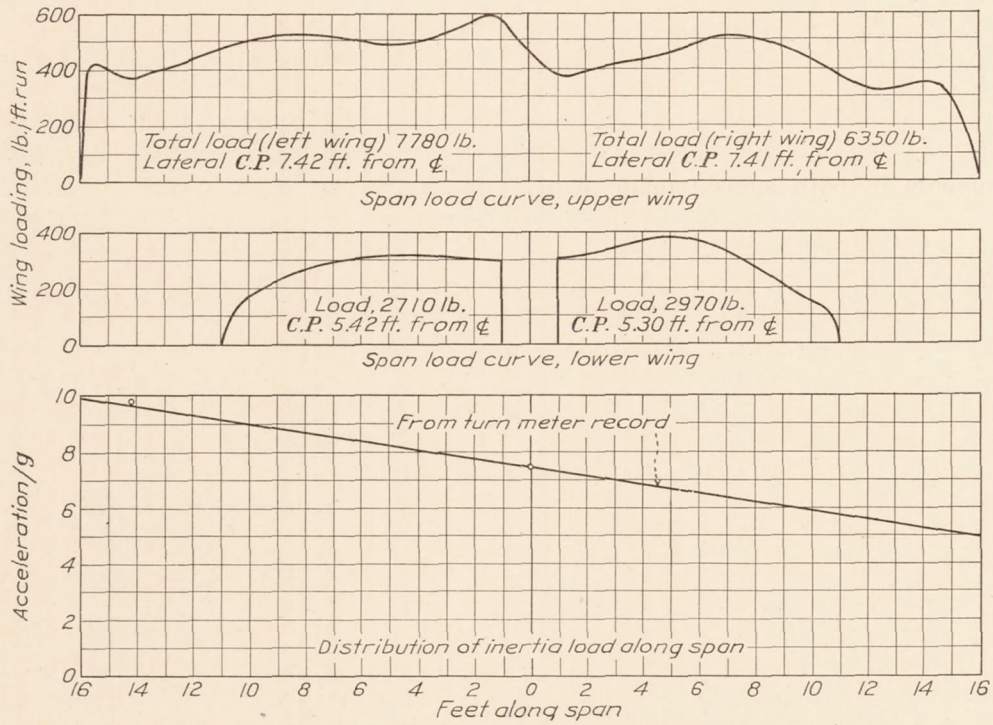

FIGURE 72.—Span load curves from right and left rolls combined to show worst unsymmetrical condition

α, therefore, is $\frac{M}{I}$

or

$$\frac{8{,}700}{1{,}697} = 5.13 \text{ radians per second per second.}$$

Time histories of right and left rolls at slower speeds are given in Figures 73 and 74. These runs do not fit together as well as the higher speed rolls, but it is apparent from a study of the time histories that the time of maximum dissymmetry occurs relatively late in the maneuver with the total load from 80 to 90 per cent of its maximum.

Spins.—Loads in the spins are relatively small and uninteresting from the structural point of view, but they assume a major importance in the study of the phenomenon of autorotation. Figures 75a to 75q and 76a to 76p show the distribution of pressure for a right and a left spin. In the right spin throughout, the left lower wing remains essentially unstalled, but at an angle very close to that of maximum lift, while the right upper wing begins to show evidences of becoming stalled at the tip at 2 seconds, and thereafter the stall progresses from the tip toward the center until at 2½ seconds the entire wing is stalled to the plane of symmetry. This condition continues, with the load becoming smaller, to 4 seconds, where the loads start to build up rapidly and the stall appears to become more pronounced; that is, the center of pressure locus moves back, indicating an increase in angle of attack. The whole motion appears to be unsteady up until the records were discontinued, although it is quite possible that a steady condition would have been reached had the spin been continued longer. Loads on the horizontal tail surfaces remain characteristic of high angles of attack with the elevator well up until about 5 seconds, when the load builds up in the positive direction, the pressure distribution becomes more irregular, and the elevator load changes from negative to positive. These changes occur without movement of the elevator and indicate a change in air-flow conditions, probably caused by the change in direction induced by the increased angular velocity. It is interesting to note from the time history (fig. 79) of this maneuver in conjunction with the pressure distribution curves that the horizontal tail moment changes early from positive to negative and continues to build up in the negative or

diving sense to a considerable value, while the airplane is still settling into a stronger spin. Even the load on the elevator changes in direction from down to up with the angular displacement remaining constant at about 24° up.

In the left spin (figs. 76, 78, and 80) the right upper wing remains unstalled throughout, but the left lower wing appears to be stalled from the beginning of the record and continues so until the end of the record, the stall becoming more pronounced as the spin continues. The motion, as in the right spin, is unsteady. As in the right spin, also, the horizontal tail load increases upward and the tail moment continues to build up in the diving sense, while the elevator remains well up. The distribution of pressure, however, is more regular than in the right spin, undoubtedly because the right side is now advancing into the wind with the fuselage and vertical tail surfaces behind it exerting little disturbing influence. It will be noticed, too, that the horizontal tail moment in the left spin does not reach as high a value as in the right spin. Vertical tail moments in both spins remain nearly constant and at about the same value in both.

It may be remarked here that this particular airplane was easily controlled in the right spin, but came out of the left spin with considerable difficulty.

Inverted flight.—Attempts were made to obtain records in the inverted flight condition without much success, as the pilot found it difficult to maintain the condition. The inverted attitude was reached by means of a half loop, but could not be held, the airplane losing altitude and having a strong tendency to nose down and continue the loop. Figure 81 shows the distribution of pressure in the inverted condition. It will be noted that the center of pressure locus is rather far forward, indicating that the angle of attack has not reached the angle of maximum negative lift. Span-load curves are given in Figure 82.

Dives.—A representative dive is illustrated in Figures 83 to 86. Leading-edge pressures reach an exceedingly high value, as noted from Figure 83 and Table III. The span-load curves (fig. 84) show the effect of the twist of the upper wing, the load inboard being positive with the tip operating below zero lift. A curve showing the variation of moment about the leading edge along the span is given in Figure 85. The spar-load curves given in Figure 86 show the effect of the washed-in central portion of the wing very clearly and also, to some extent, the effect of the washout, the front spar load increasing toward the tip with the rear spar load decreasing.

Normally in a dive, as in the case reported here, zero lift is not reached, although it could be attained if the airplane were nosed over sufficiently. This condition, however, is an uncomfortable one for the pilot, the sensation being that the airplane is slightly over on its back, which it really would be in a majority of cases. Zero lift can be attained, however, with the nose of the airplane only slightly below the horizontal in a sudden push into a dive. Pressure distribution for this case is given in Figure 87; it is similar to that in the dive, but with the negative areas at the leading edge in greater proportion. The pressures, however, are much less because of the lower speed. Span-loading curves in Figure 88 show that a considerable portion of the upper wing is at negative lift, while loads on the central portion are positive, and that the lower wing load is positive throughout the span. Spar-load curves are given in Figure 89. The effect of the twisted upper wing is apparent in these curves, the down load increasing on the front spar toward the tip and the up load on the rear spar decreasing. The condition would be much more severe in the case of a fast dive at zero lift, since the twisting moment would increase as the square of the speed, and hence the deformation would increase, resulting in a greater proportion of load on the outboard portion of the front spar. It is conceivable that the outboard rear spar load might reduce to zero, the entire load being carried on the front spar, in which case a form of partial inverted flight condition would exist that would probably be critical for the landing wires and the leading edge of the wing.

Pull out of dive.—An interesting, though isolated, case of a low incidence loading condition occurs in the pull out of the dive, Run 226. In connection with this condition it should be said that the pull out was normally executed; that is, it was made cautiously with due regard to the speed at which the airplane was traveling, and that it in nowise represents a special test condition. The point chosen in working the records was the point of maximum acceleration (3.6g), which occurred early in the pull out and which was felt would probably represent the most severe rear spar-loading condition that could be found without working up a large number of points. Figures 90 and 91 represent the distribution of load for this case. The condition is seen to be characterized by moderately high load with the center of pressure fairly well back and span load tapering off rapidly toward the tip. The spar loads given in Figure 92 show the effect of these characteristics. Spar loads derived from the specified low angle of attack loading condition are given for comparison, although the total loads for the two cases are not the same. The total load for the observed results is the true total for this case corresponding to an applied load factor of 3.6, whereas the derived curves are based on a load factor of 3.25 which is the low angle of attack load factor divided by the intended factor of safety of 2. It can be seen that the upper rear spar load is well within the design load, and although the front spar load is in excess of the specified load for low angle of attack, the condition is not critical for the member. On the lower wing, however, both spars are overloaded, the front one again being

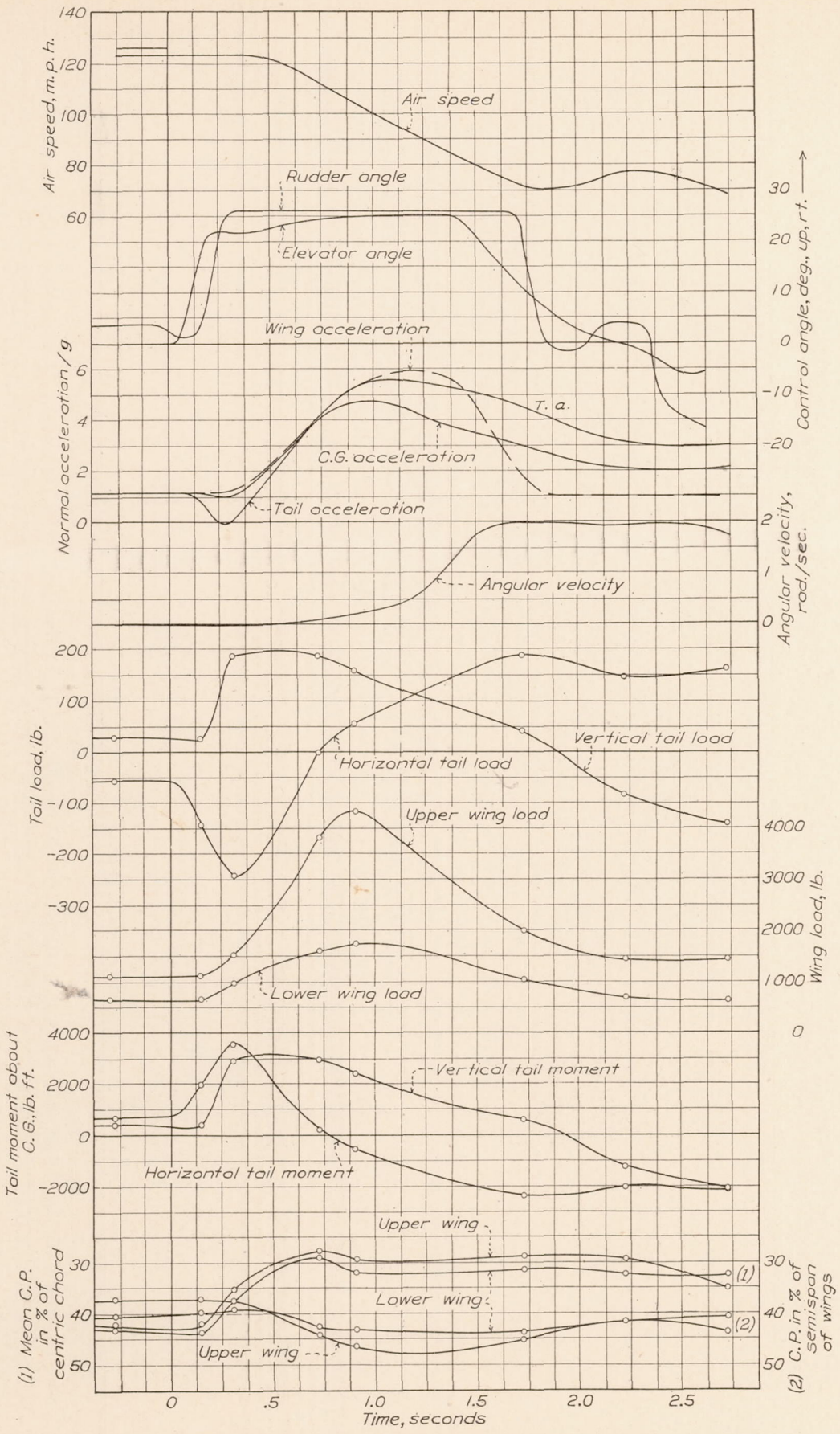

FIGURE 73.—Time history of a right barrel roll at 126 miles per hour. (Run No. 220)

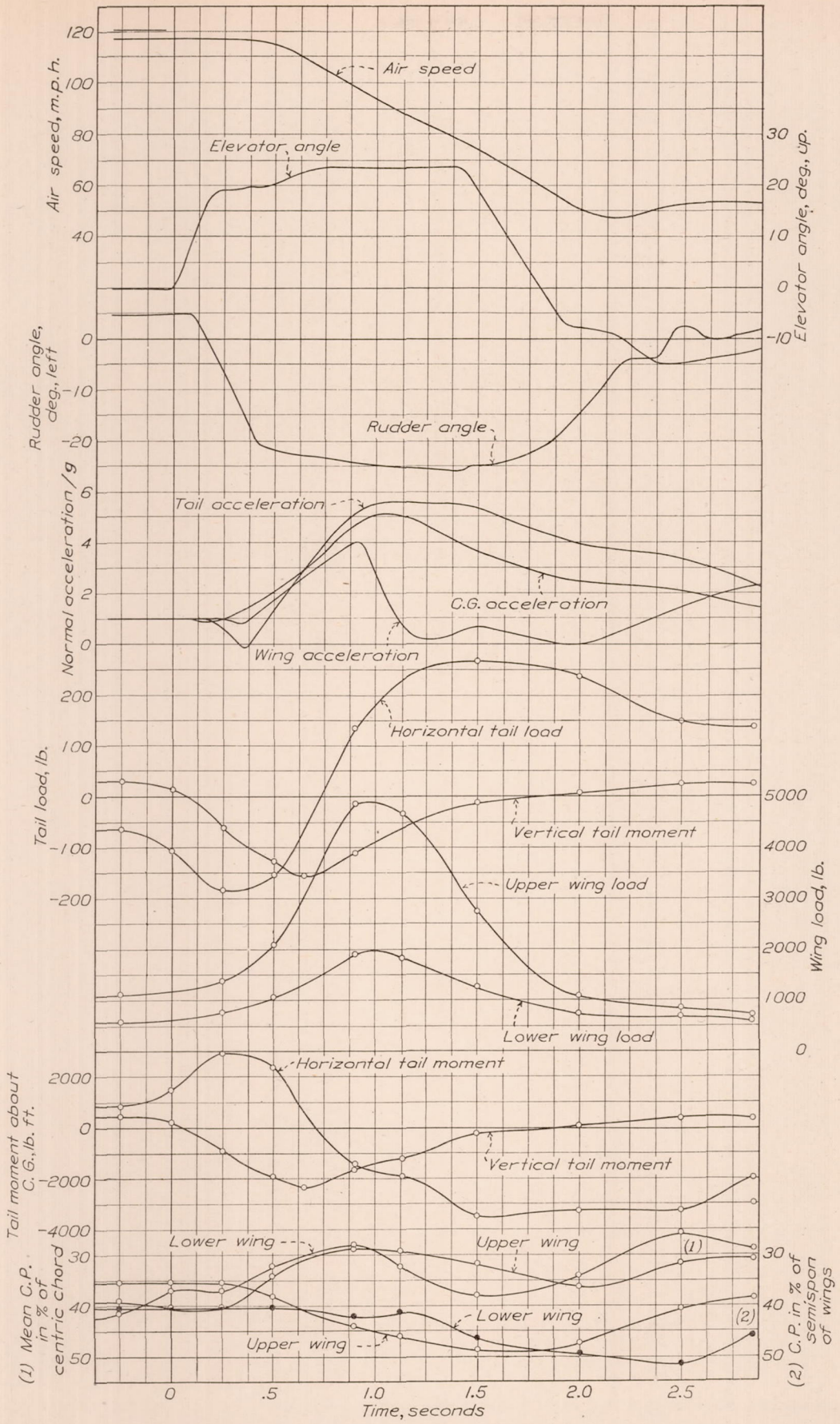

FIGURE 74.—Time history of a left barrel roll at 120.5 miles per hour. (Run No. 223)

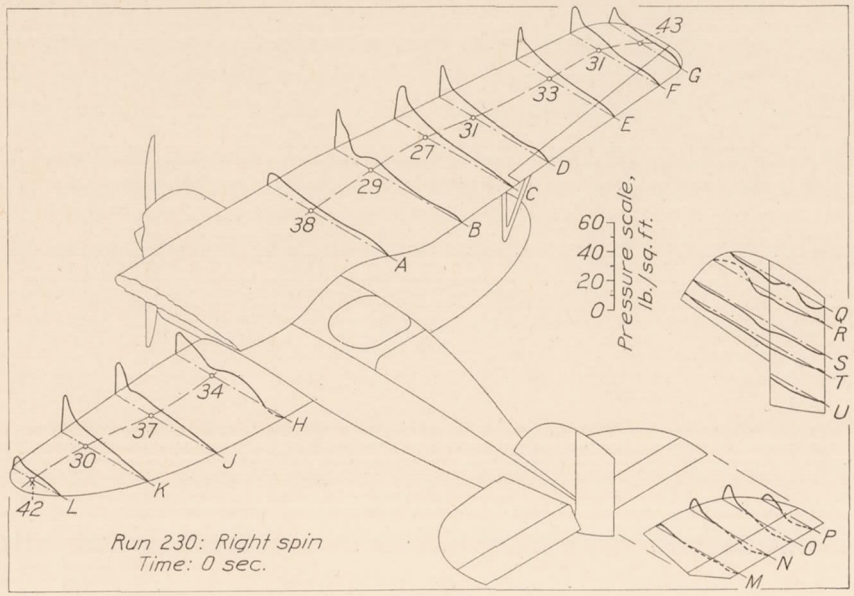

FIGURE 75a

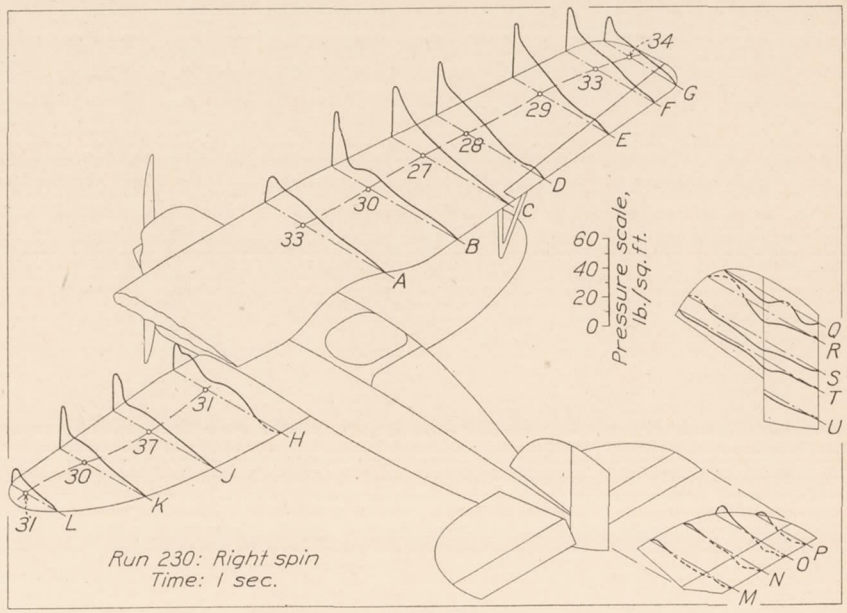

FIGURE 75b

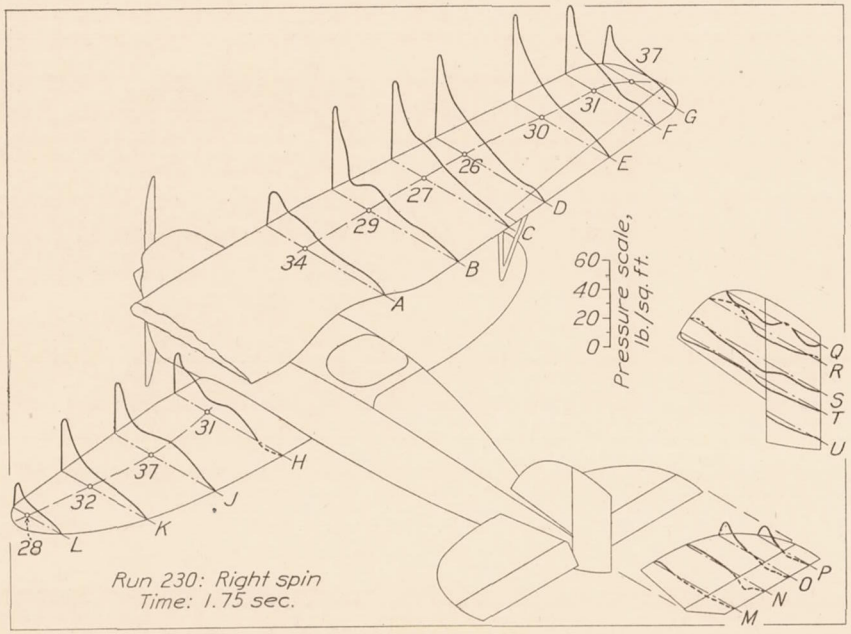

FIGURE 75c

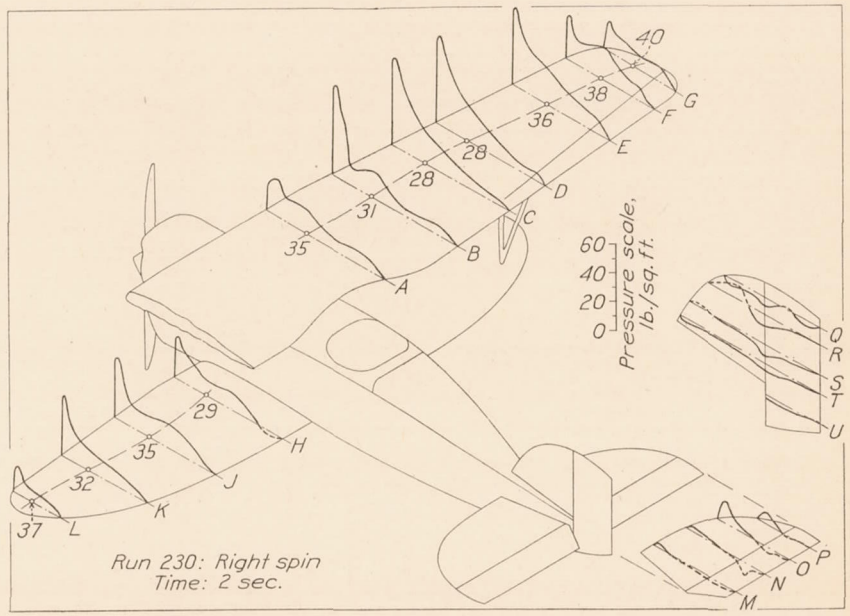

FIGURE 75d

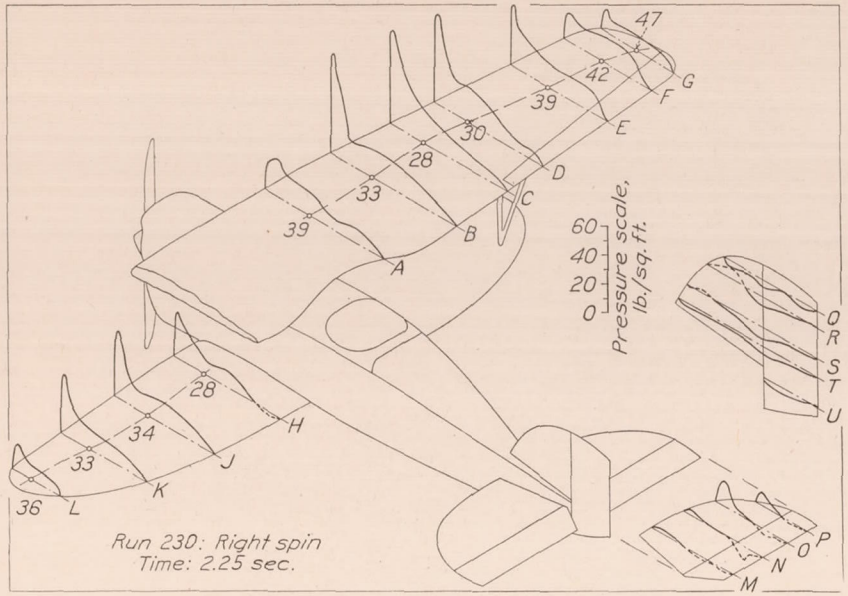

FIGURE 75e

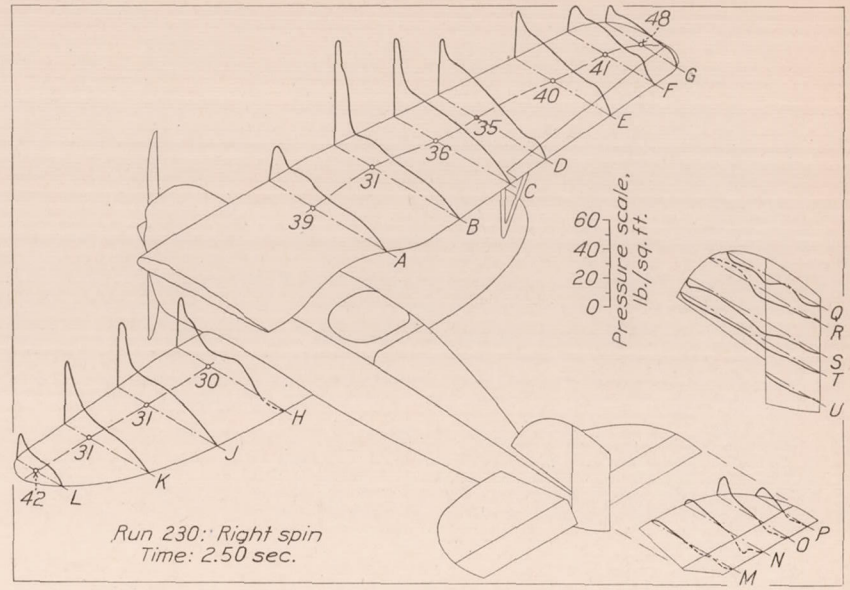

FIGURE 75f

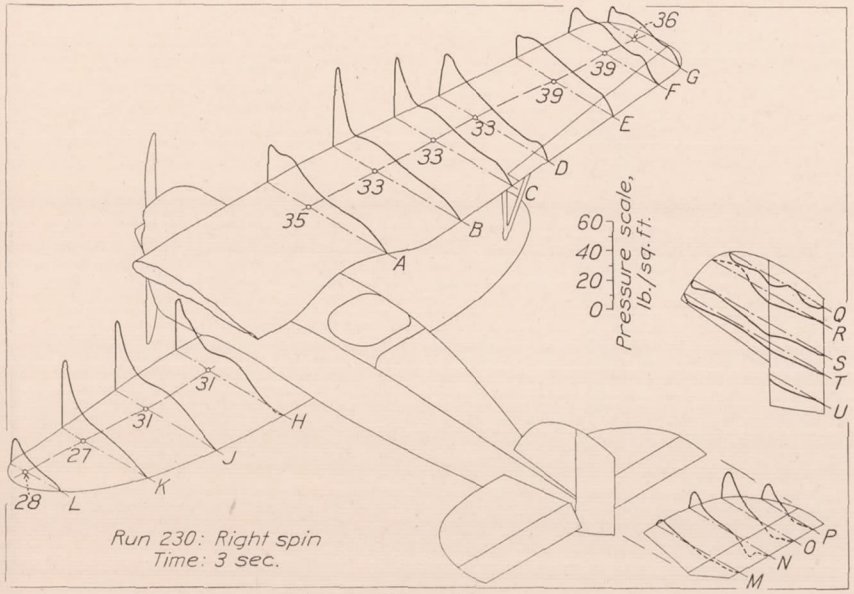

FIGURE 75g

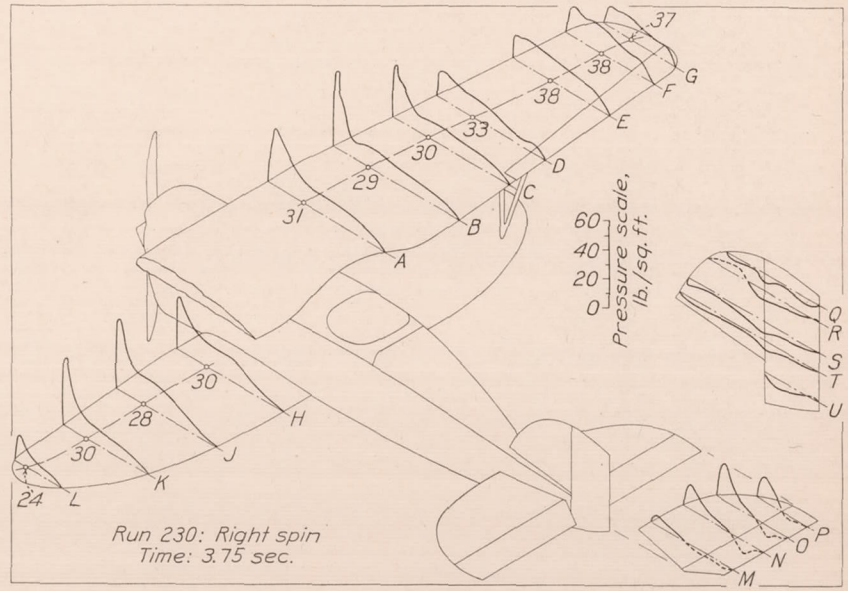

FIGURE 75h

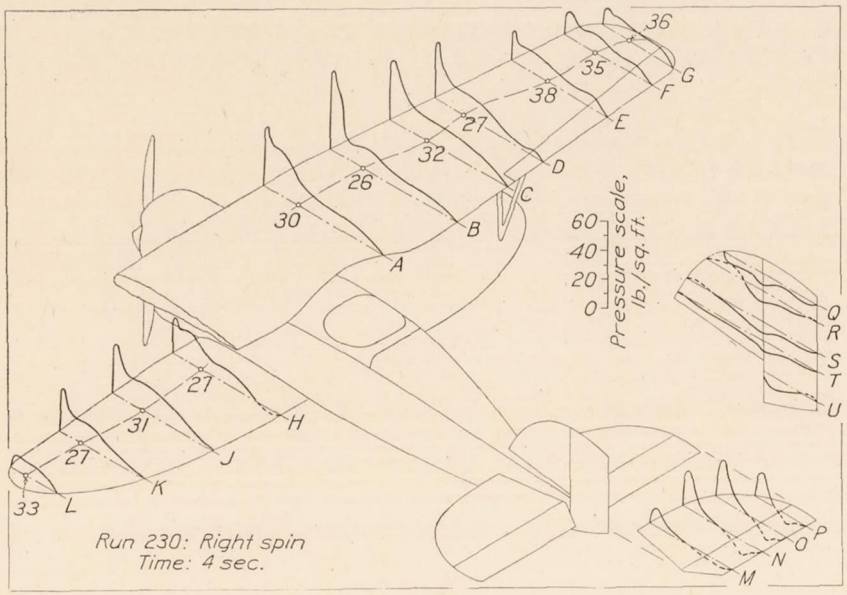

FIGURE 75i

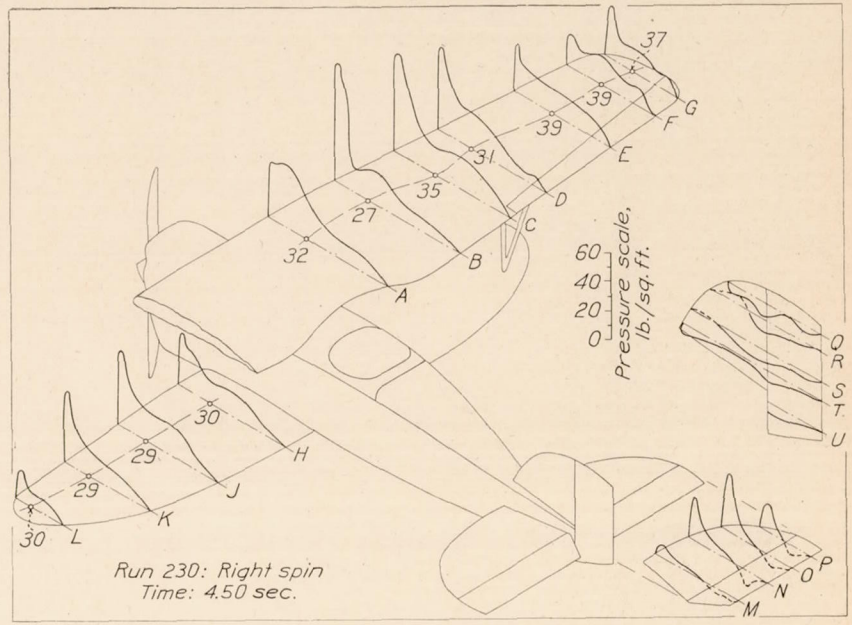

FIGURE 75j

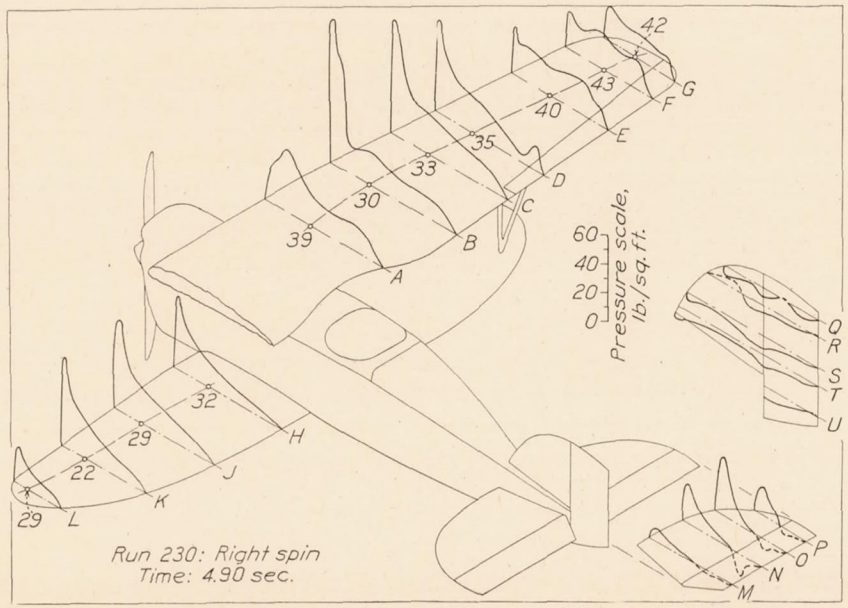

FIGURE 75k

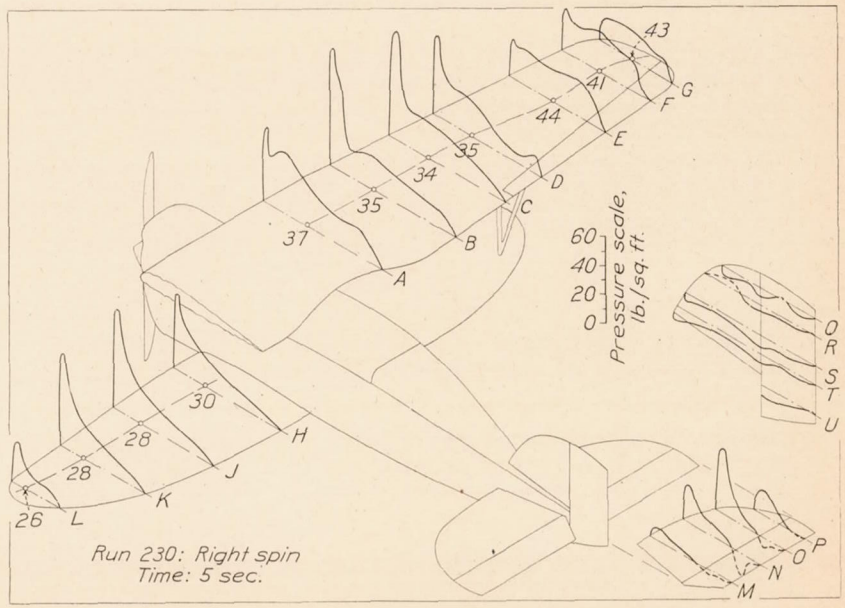

FIGURE 75l

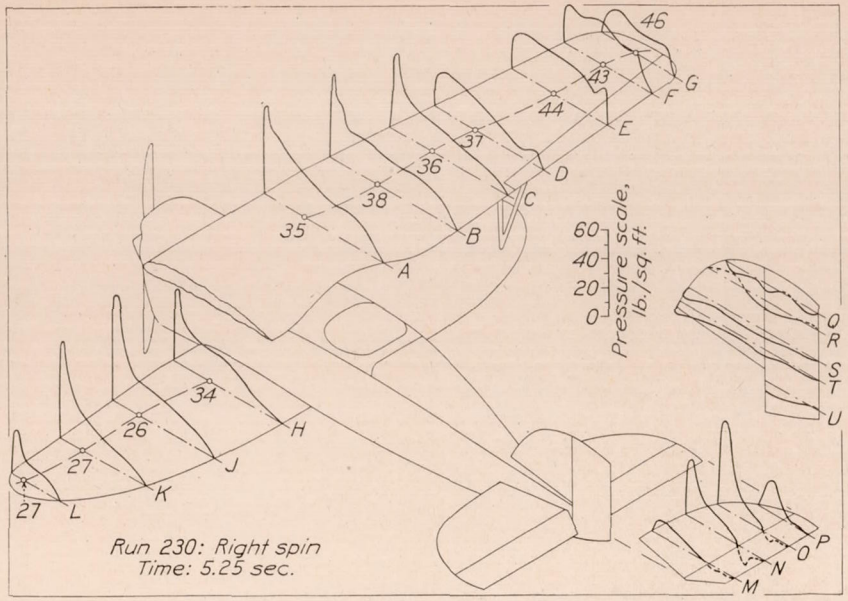

FIGURE 75m

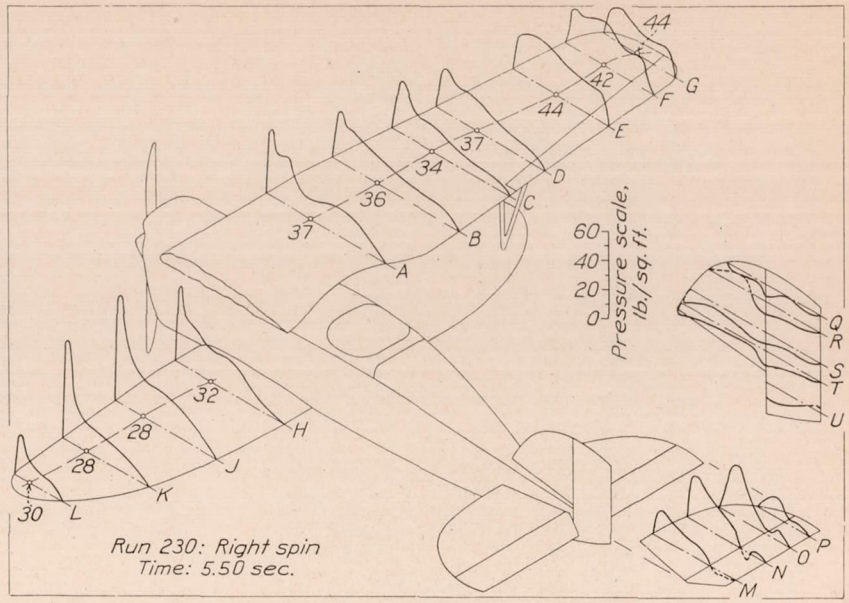

FIGURE 75n

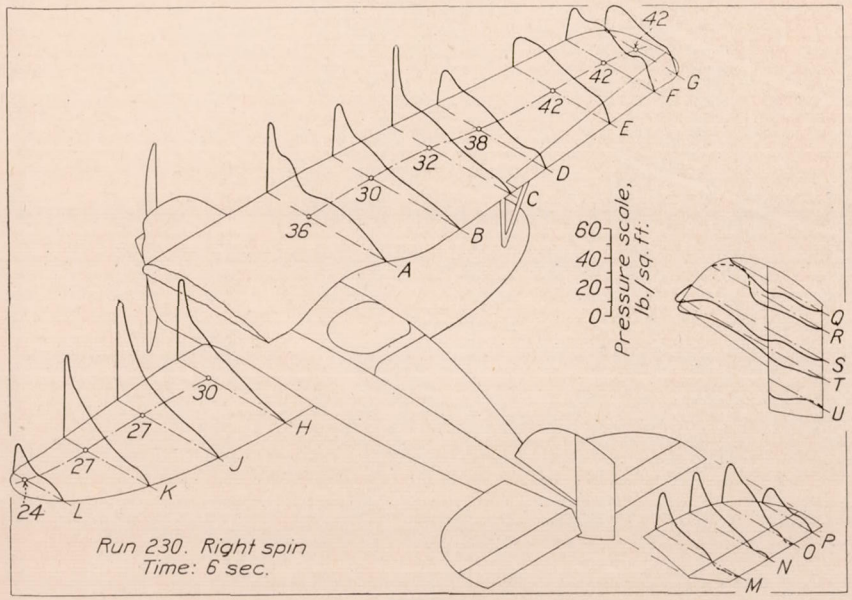

FIGURE 75o

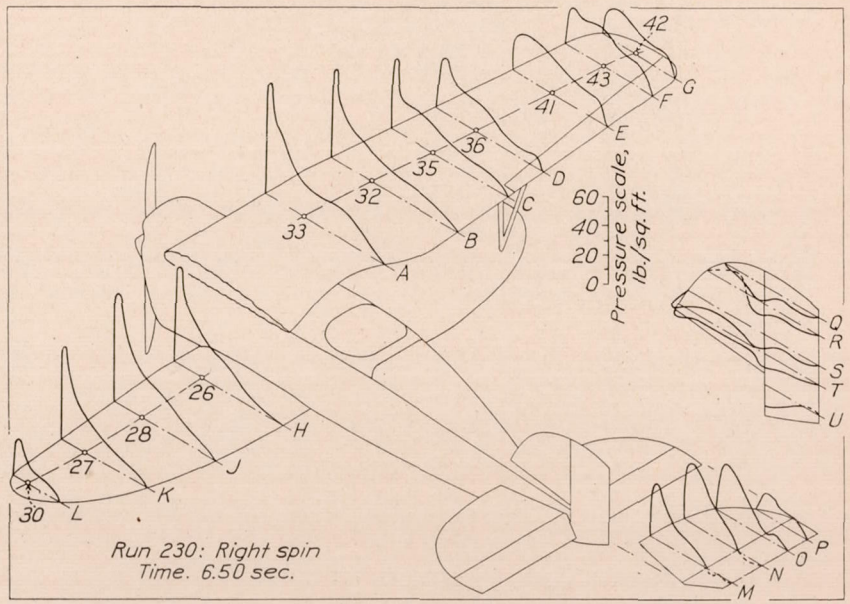

FIGURE 75p

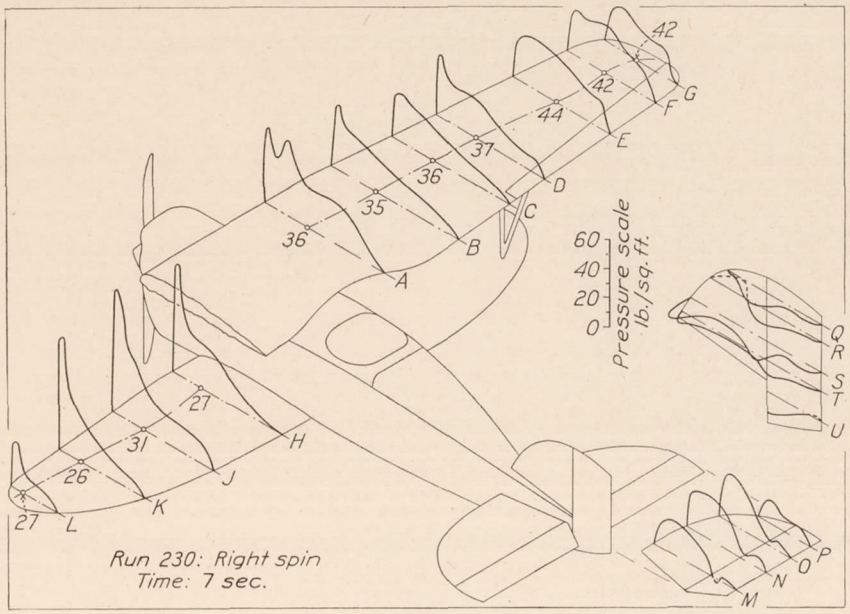

FIGURE 75q

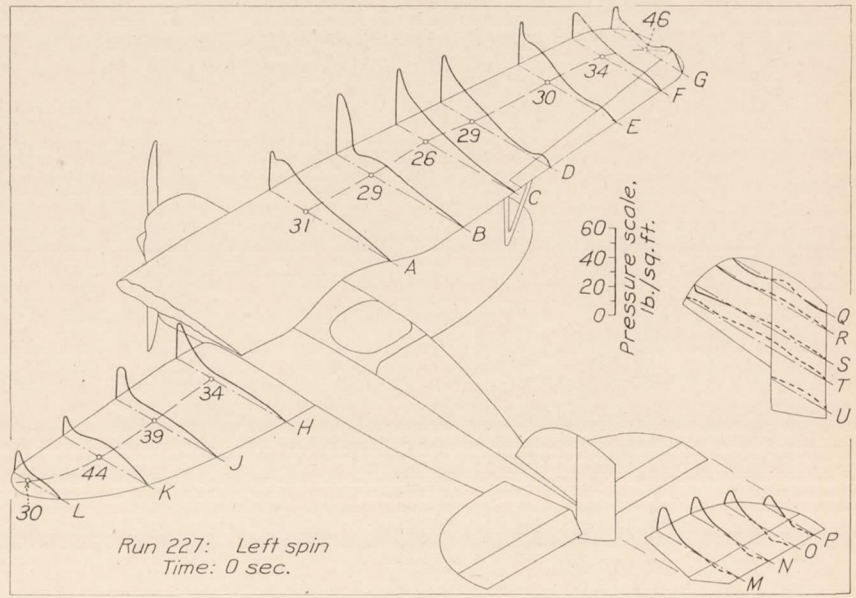

FIGURE 76a

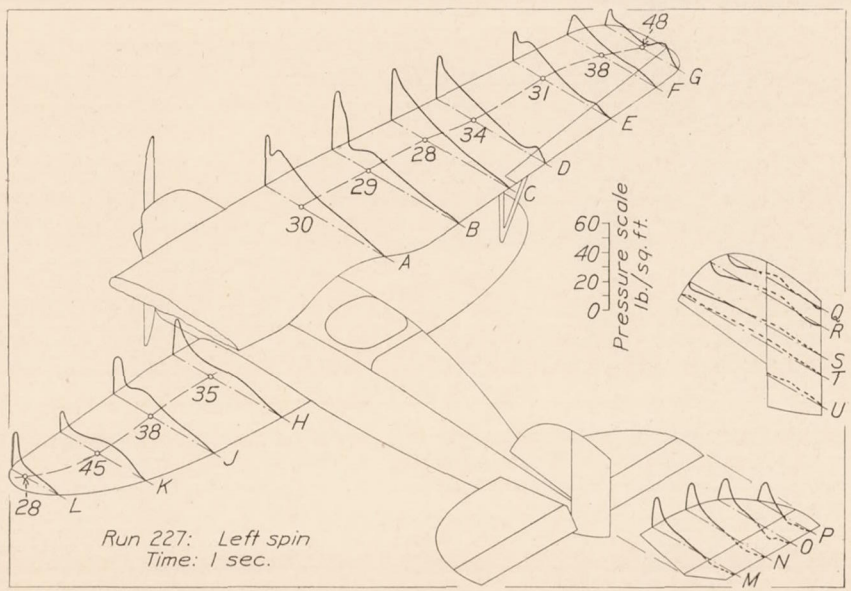

FIGURE 76b

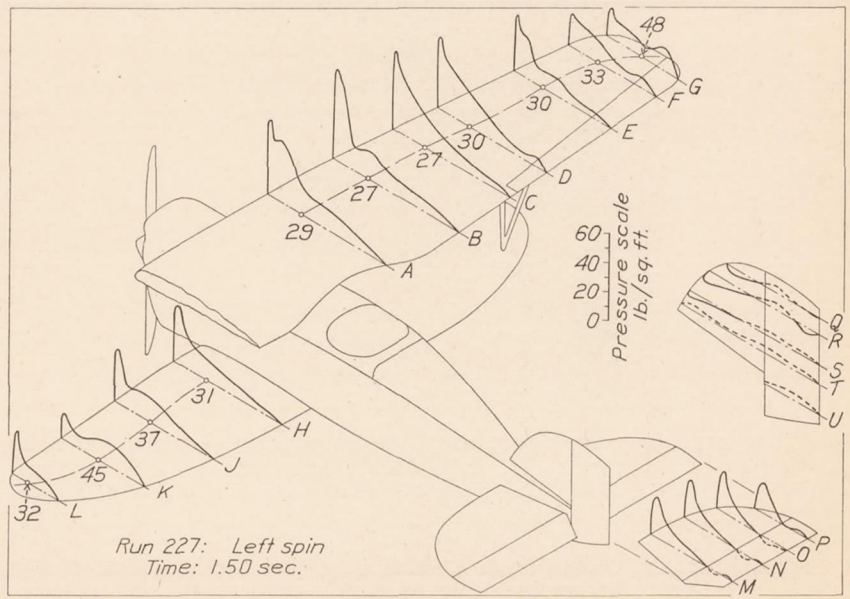

FIGURE 76c

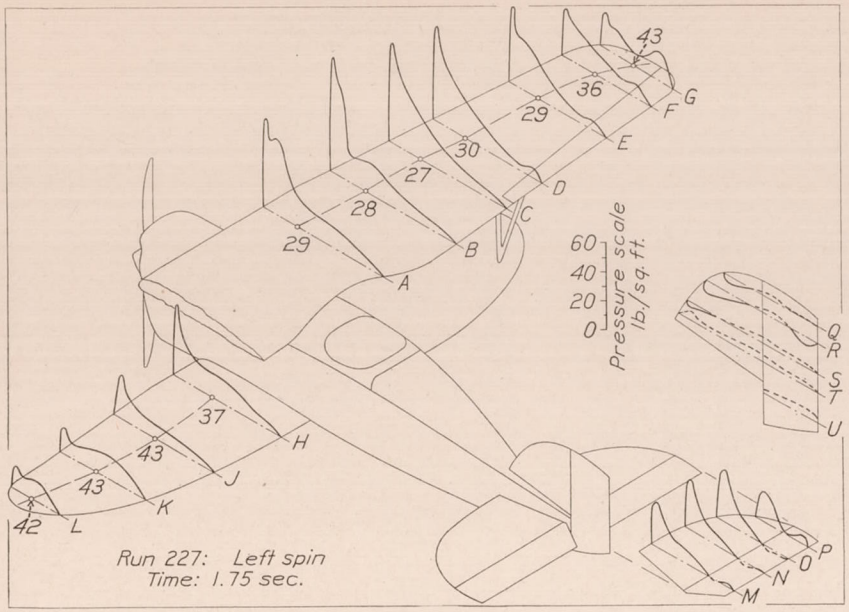

FIGURE 76d

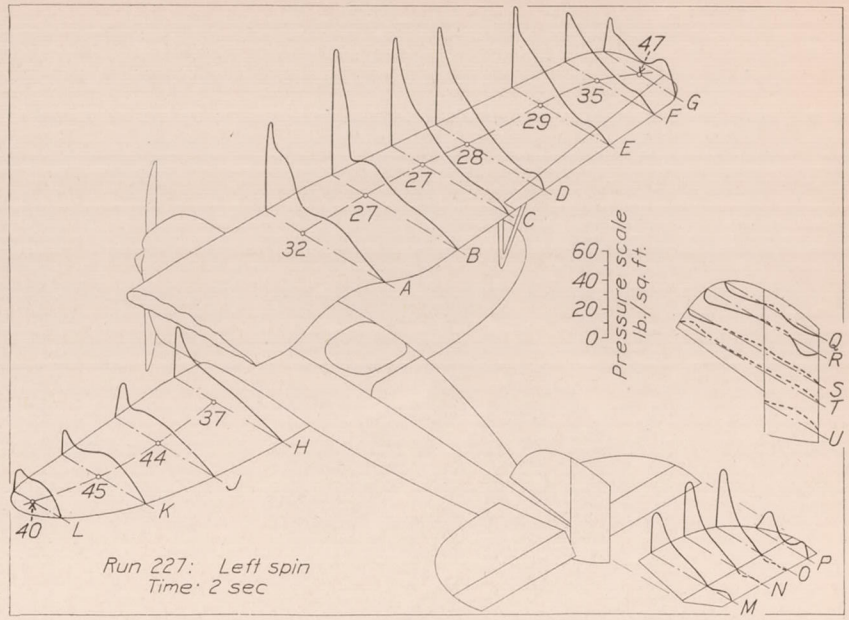

FIGURE 76e

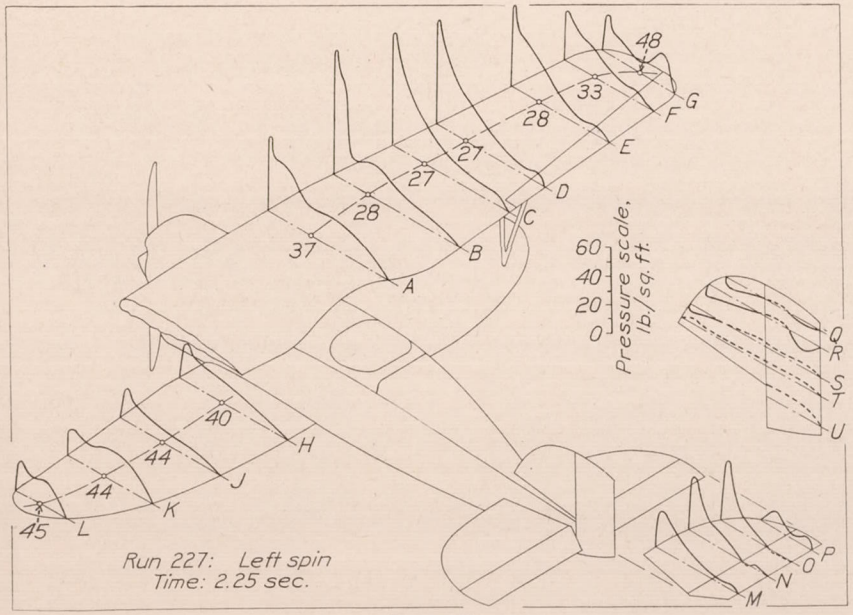

FIGURE 76f

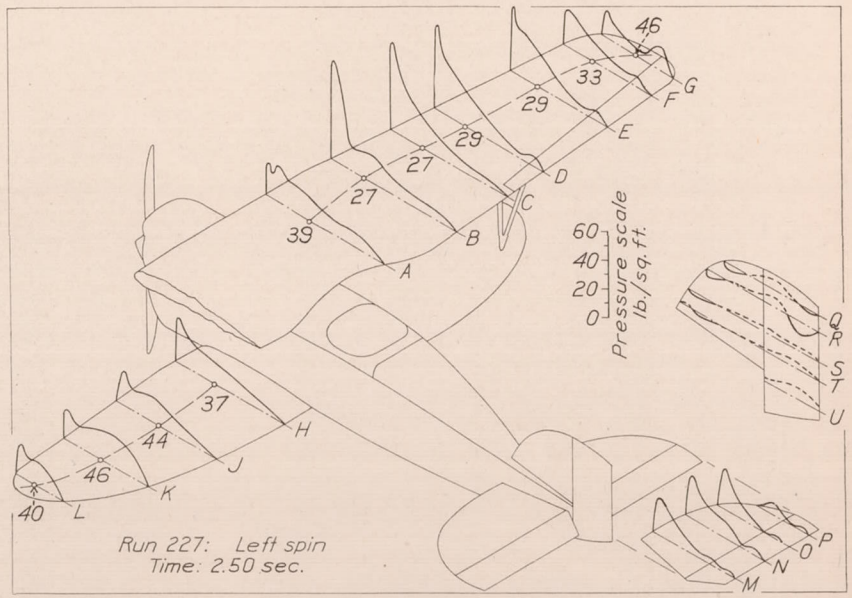

FIGURE 76g

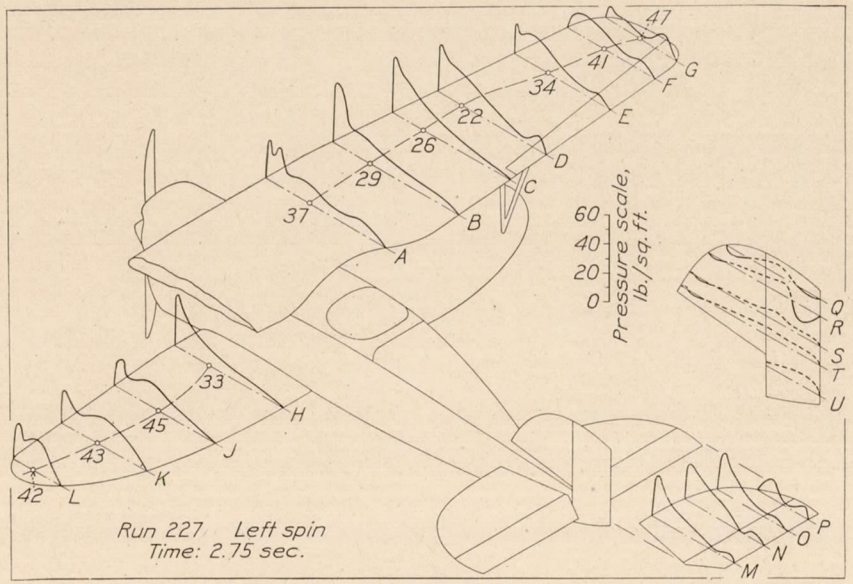

FIGURE 76h

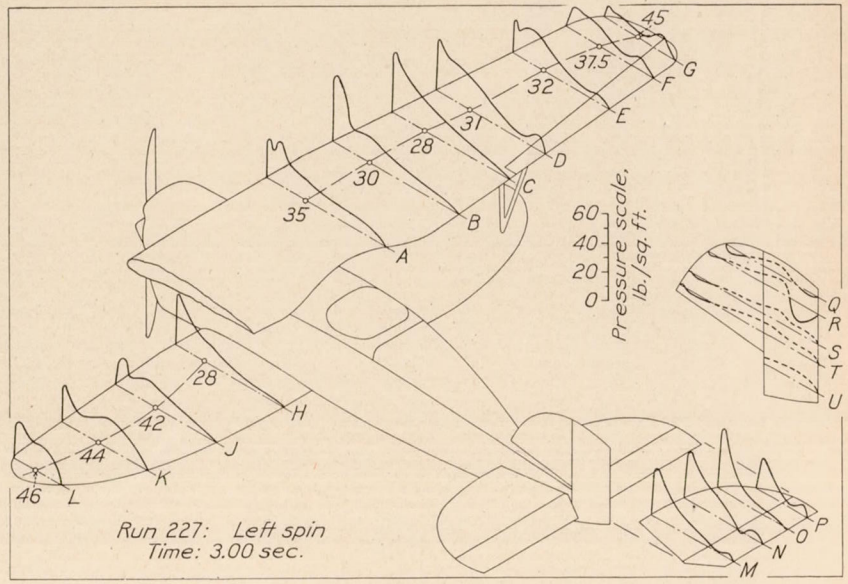

FIGURE 76i

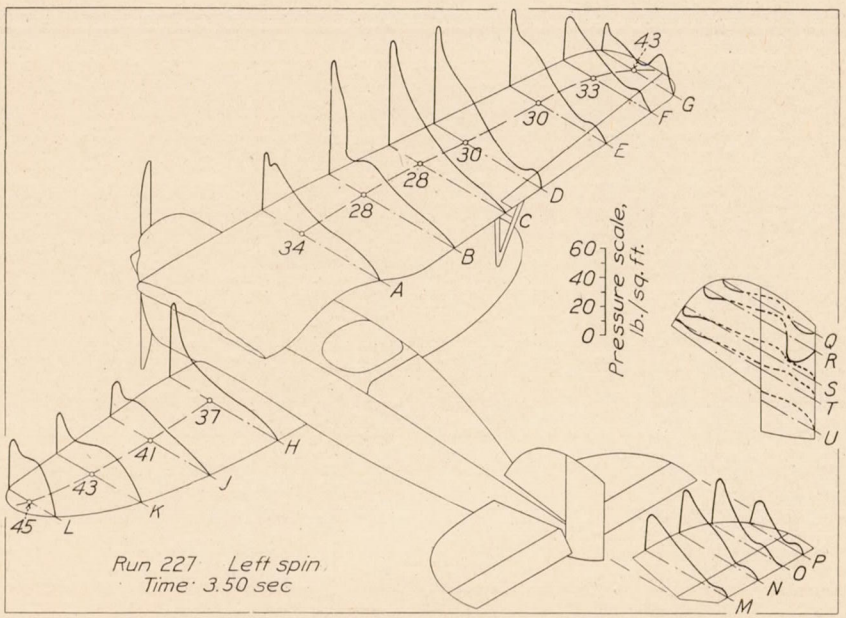

FIGURE 76j

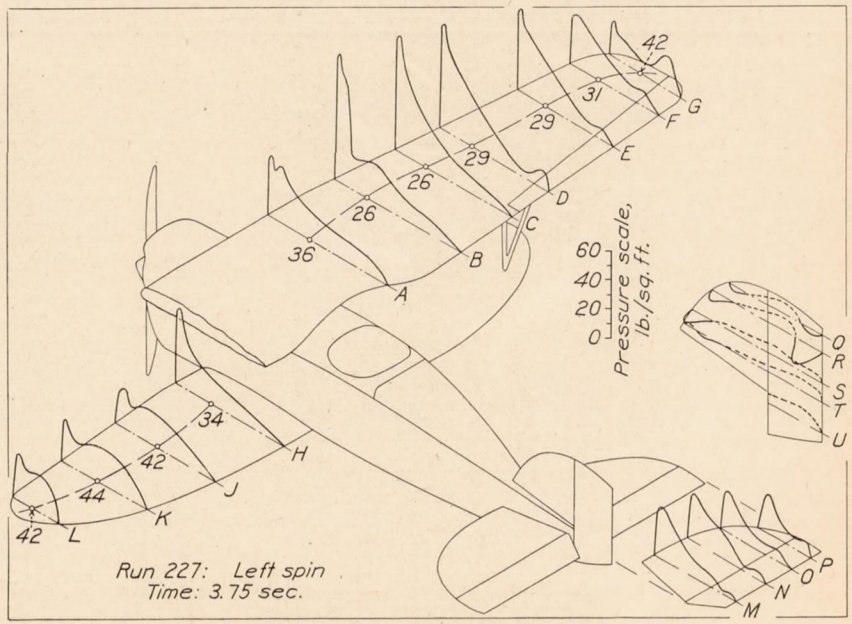

FIGURE 76k

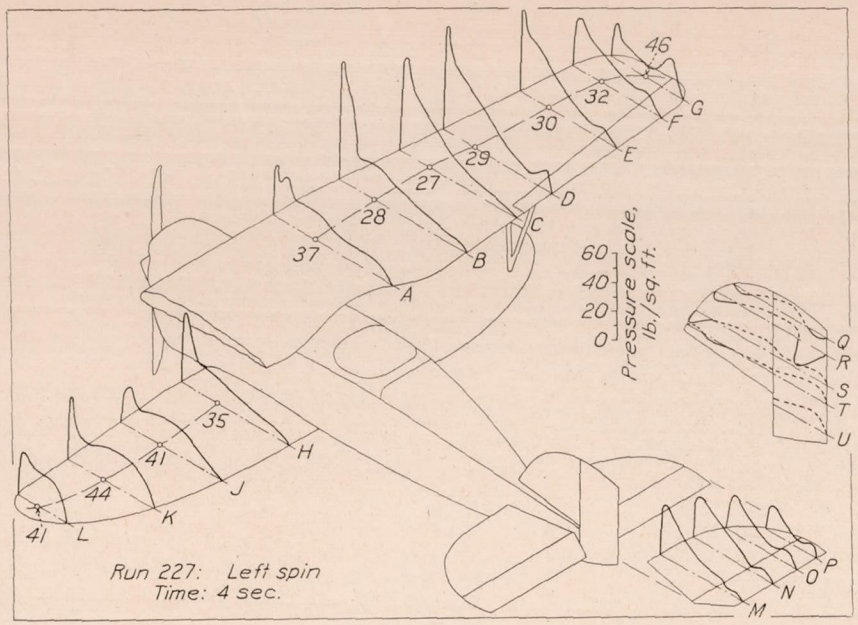

FIGURE 76l

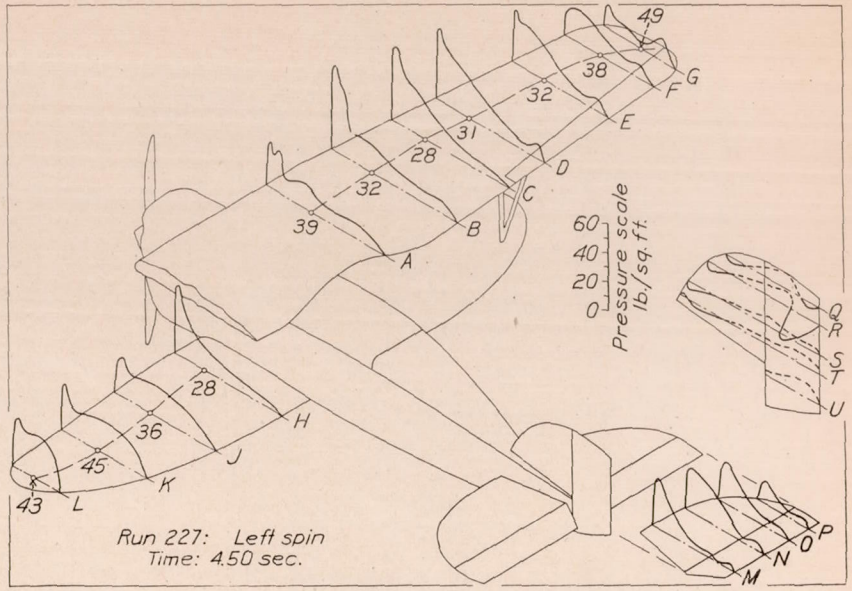

FIGURE 76m

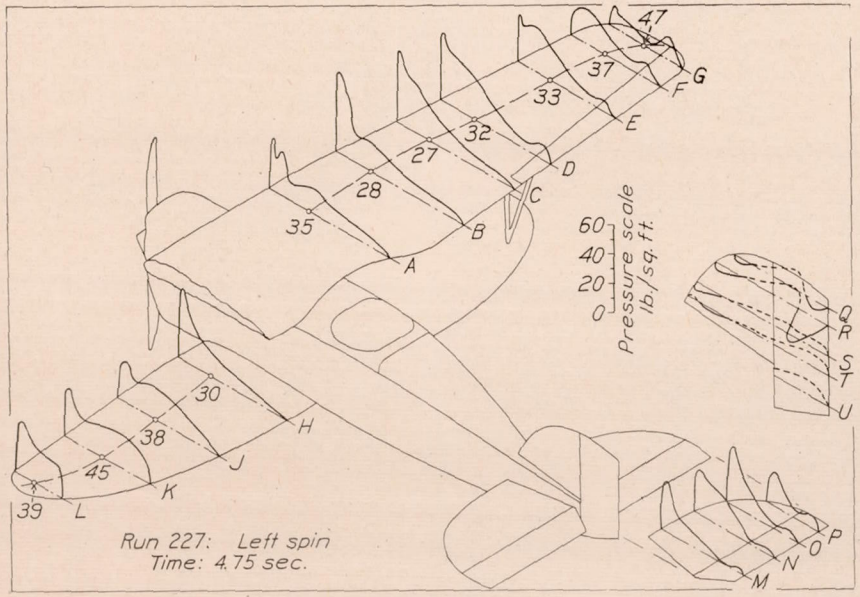

FIGURE 76n

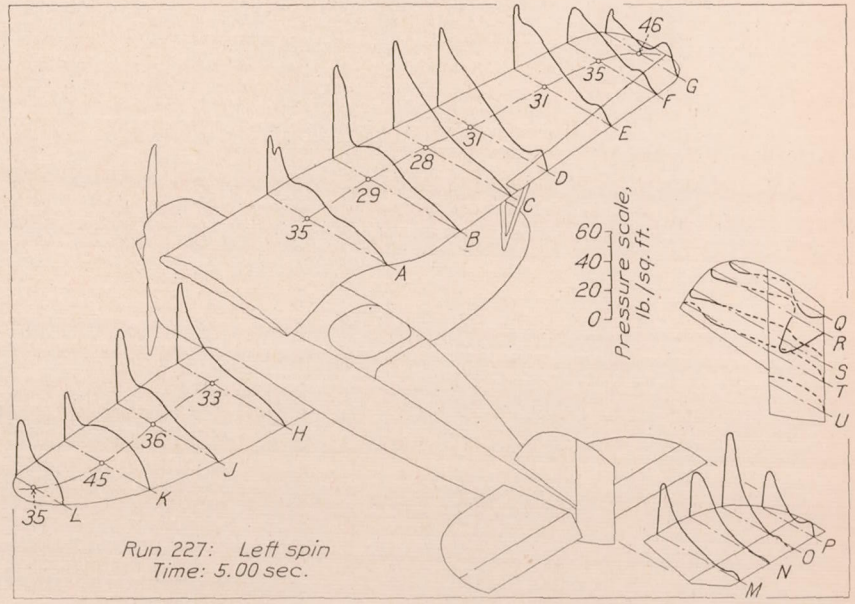

FIGURE 76o

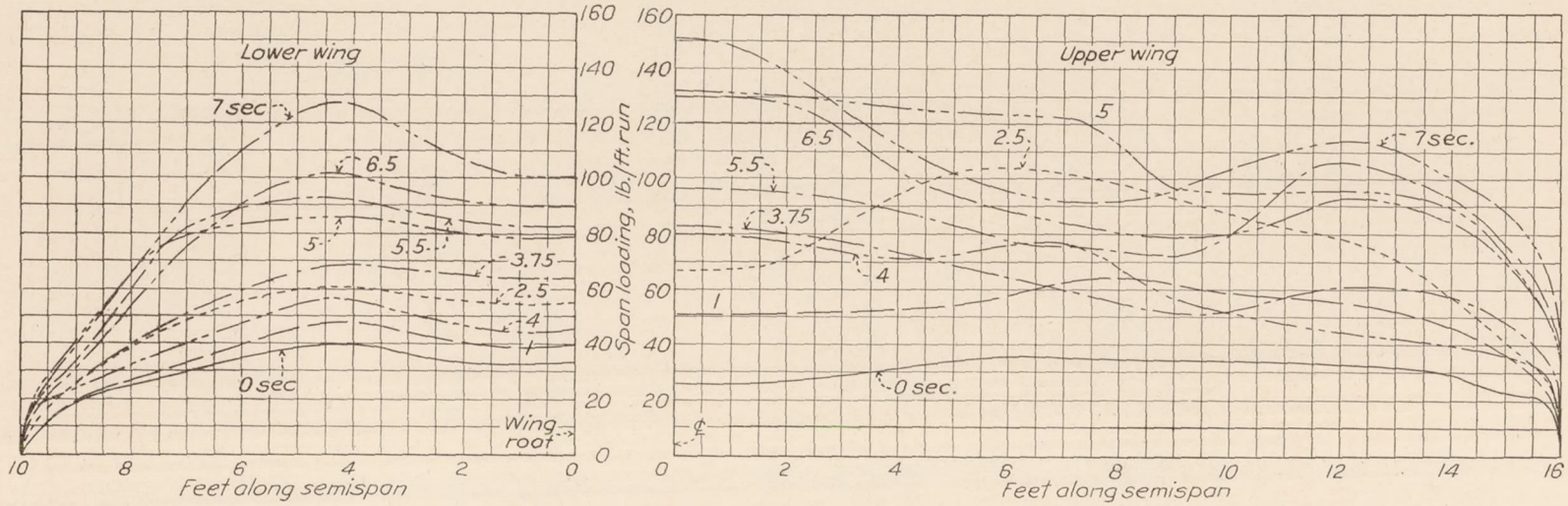

FIGURE 77.—Variation of span load distribution in a right spin. (Run No. 230)

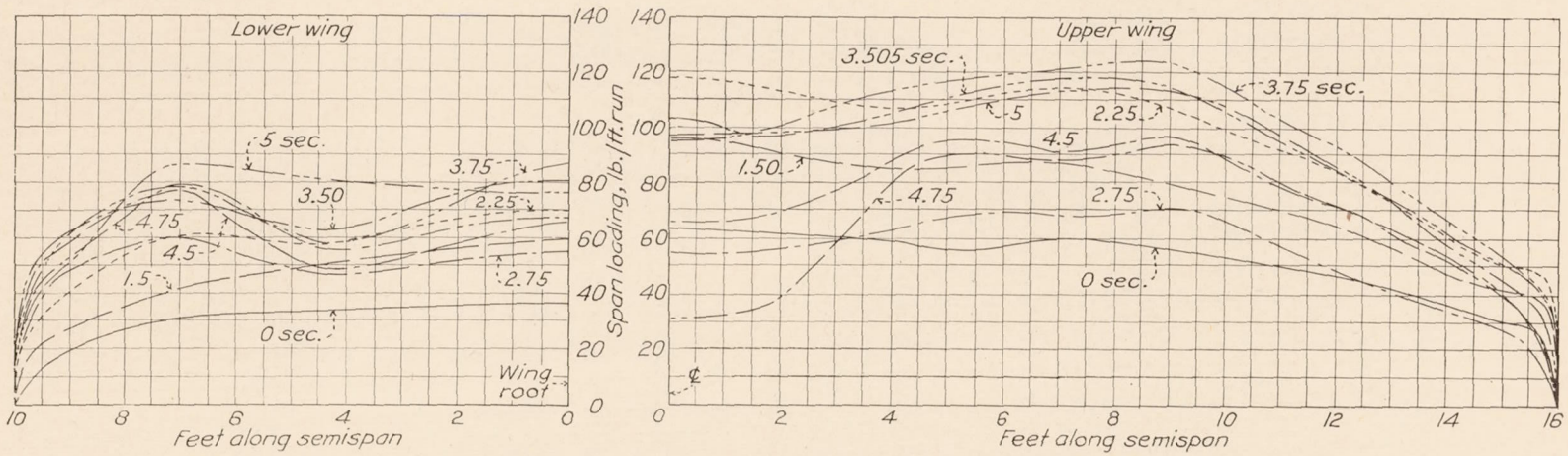

FIGURE 78.—Variation of span load distribution in a left spin. (Run No. 227)

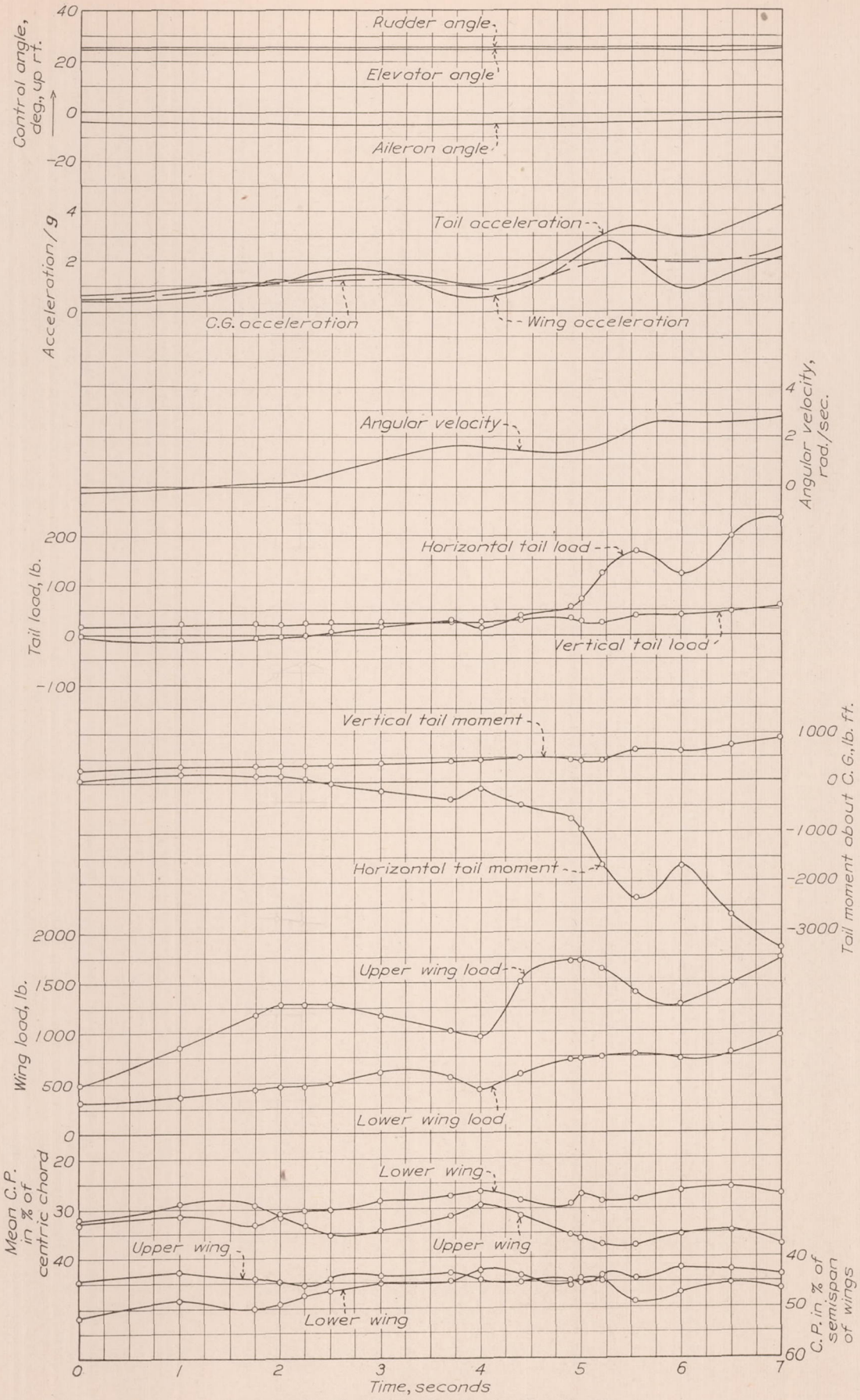

FIGURE 79.—Time history of a right spin. (Run No. 230)

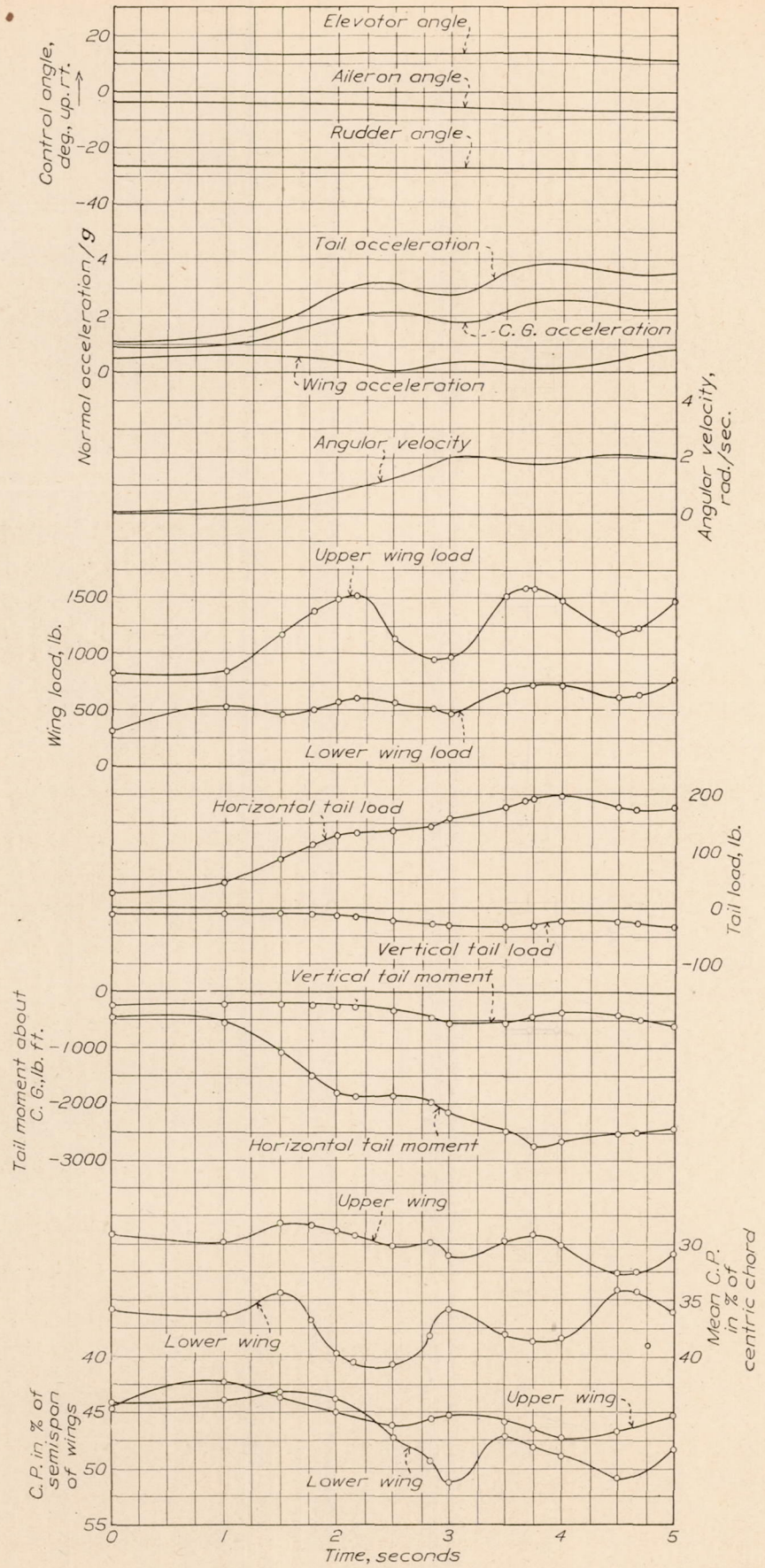

FIGURE 80.—Time history of a left spin. (Run No. 227)

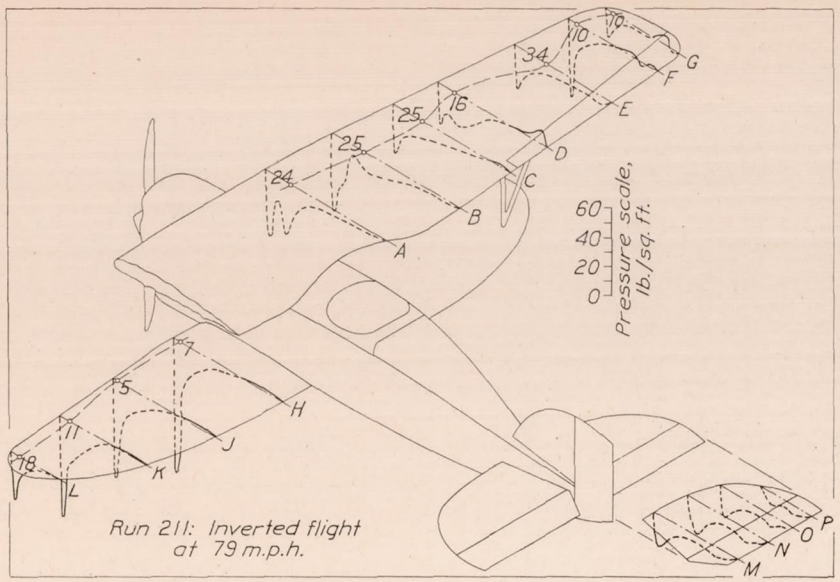

FIGURE 81

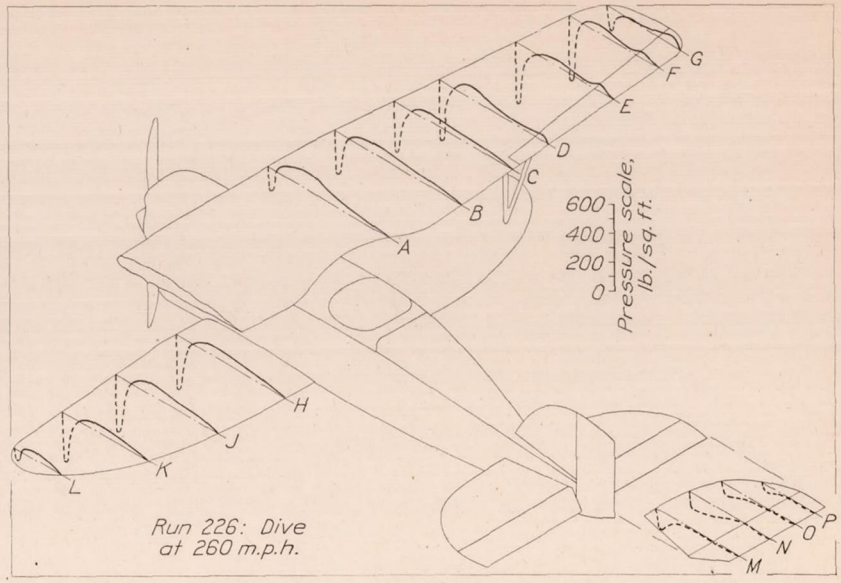

FIGURE 83

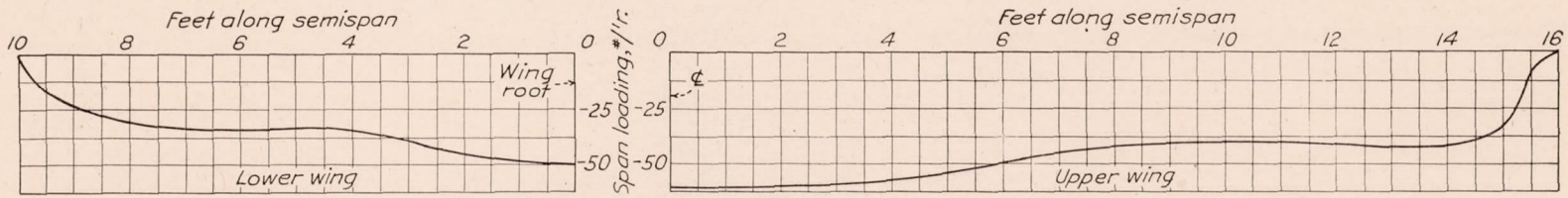

FIGURE 82.—Span load distribution in inverted flight at 79 miles per hour. (Run No. 211)

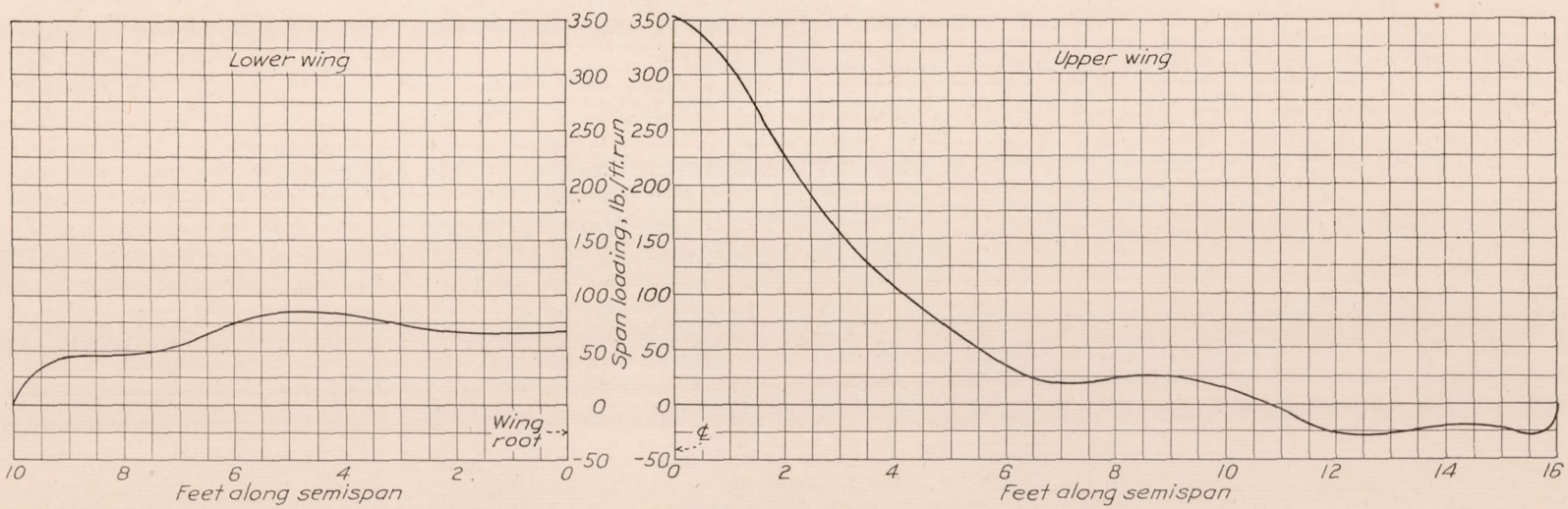

FIGURE 84.—Span load distribution in a dive at 260 miles per hour. (Run No. 226)

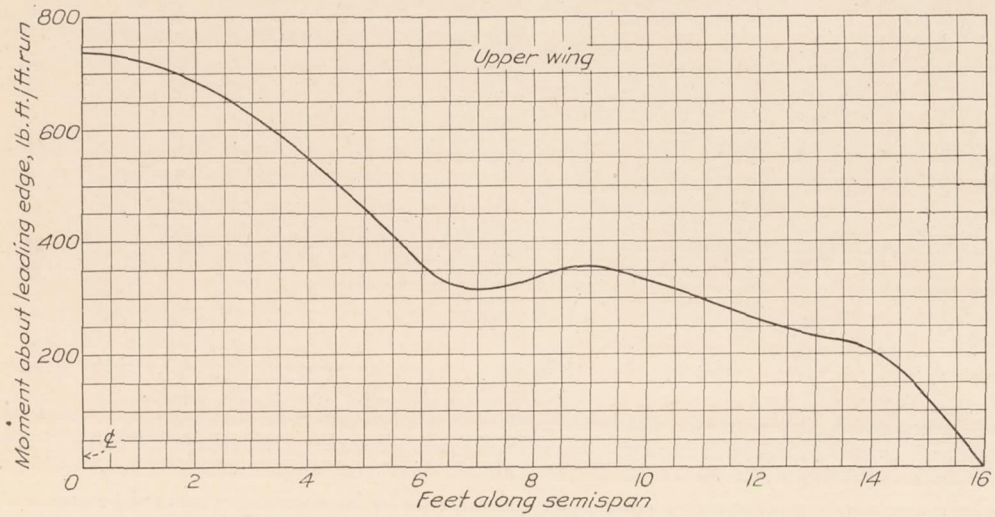

FIGURE 85.—Span moment distribution in a dive at 260 miles per hour. (Run No. 226.) (Moments referred to true leading edge at each point as datum)

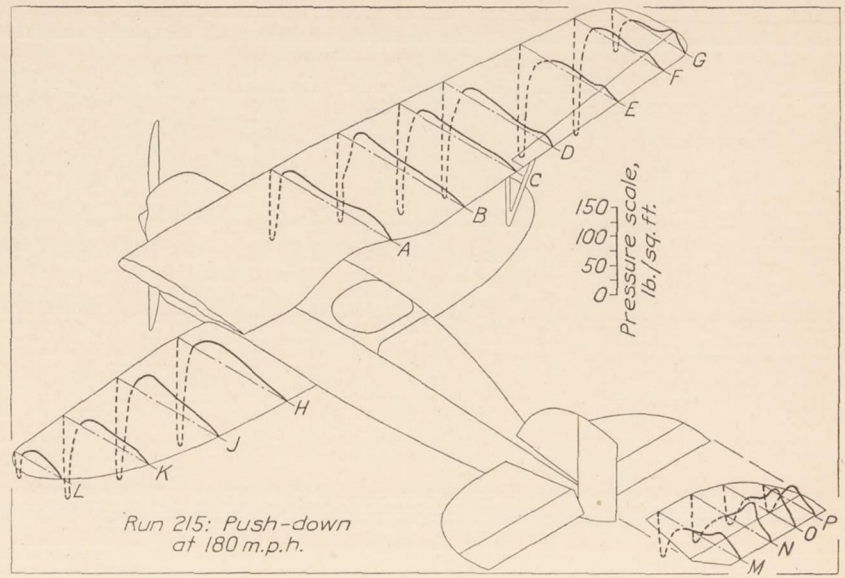

FIGURE 87

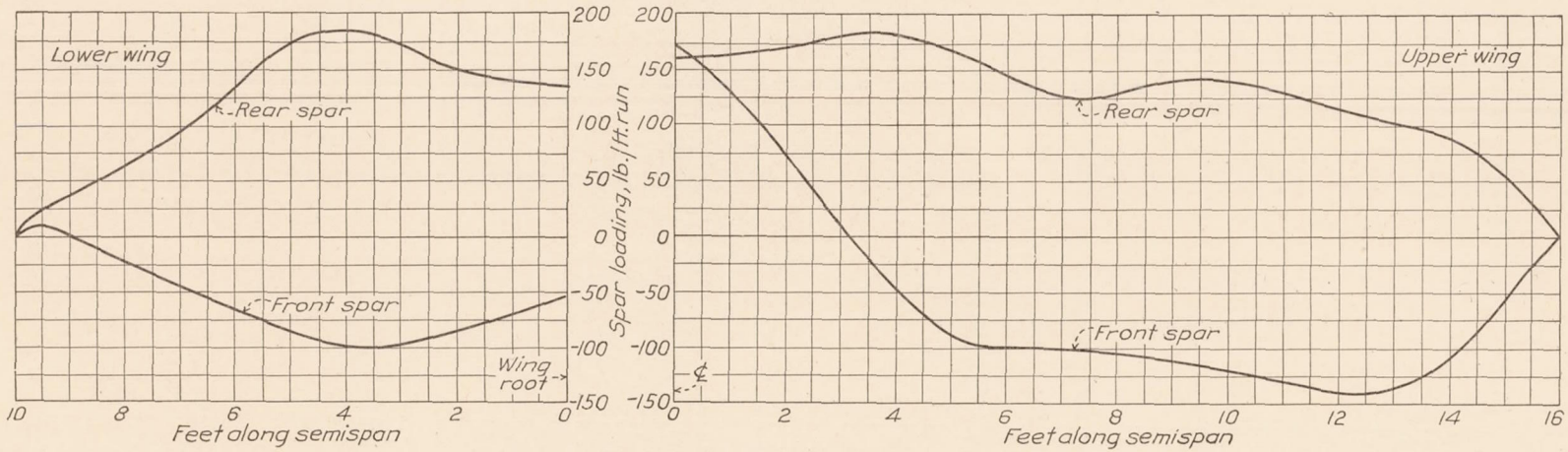

FIGURE 86.—Spar loading in a dive at 260 miles per hour. (Run No. 226)

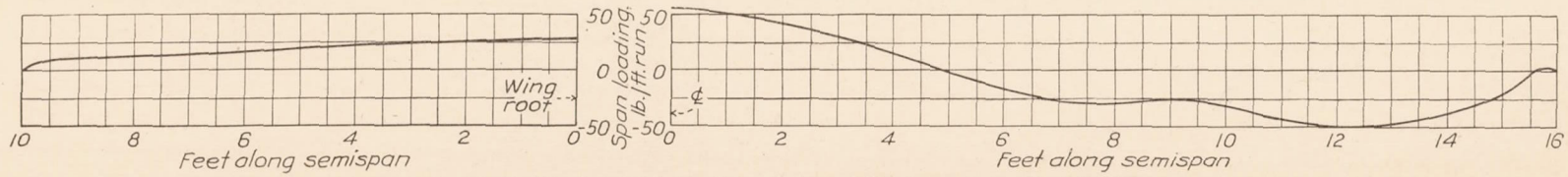

FIGURE 88.—Span load distribution in a push-down at 180 miles per hour. (Run No. 215)

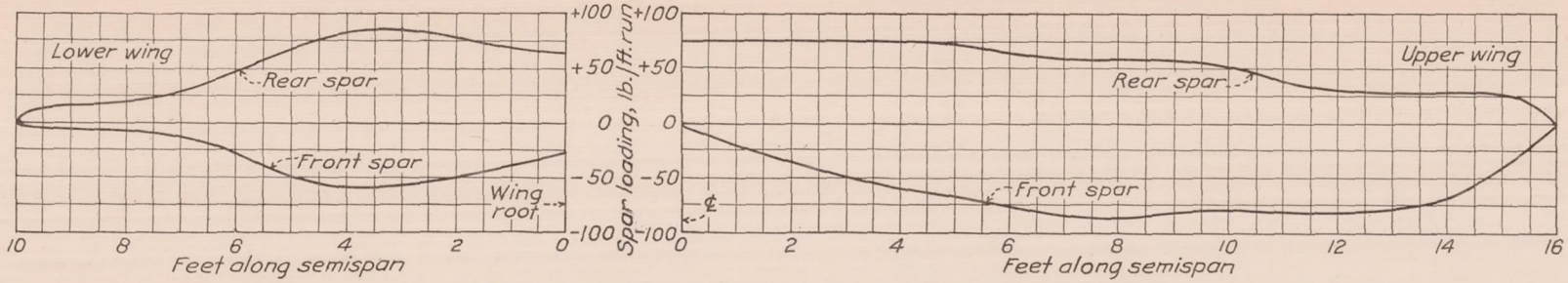

FIGURE 89.—Spar loading at zero lift (push-down at 180 miles per hour; run No. 215)

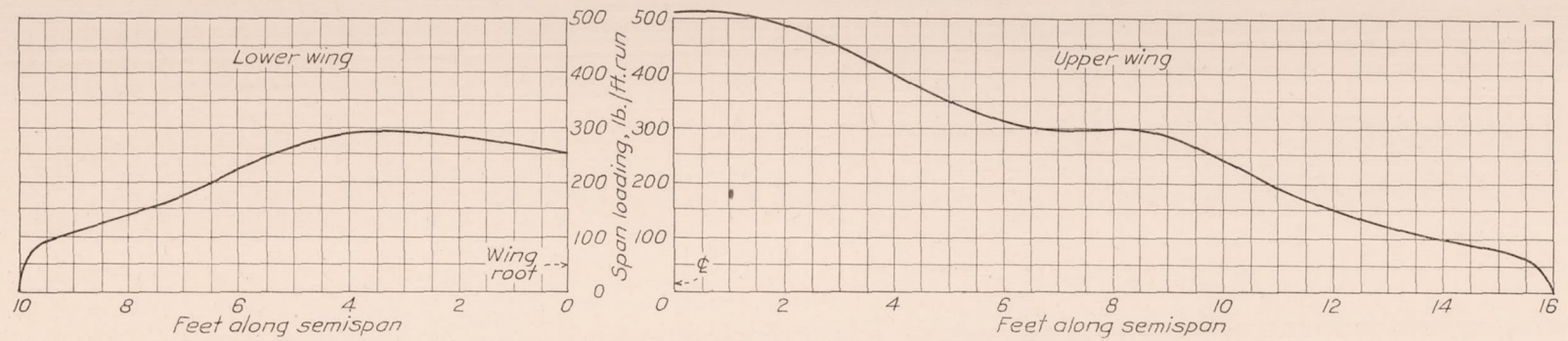

FIGURE 91.—Span load distribution in a pull-out from dive. (Run No. 226)

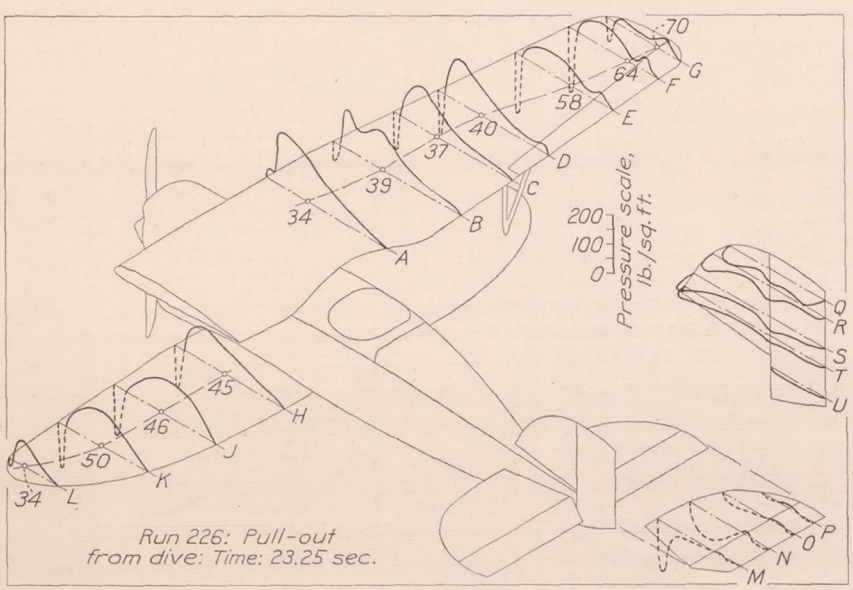

FIGURE 90

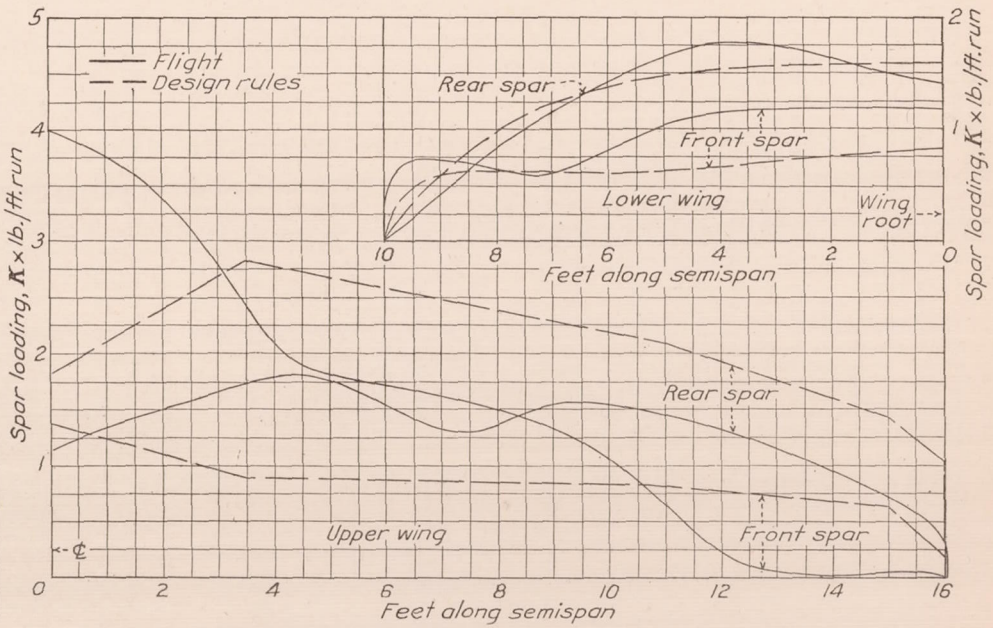

FIGURE 92.—Comparison of low angle of attack spar loads from flight tests (run No. 226) and design rules

taken care of in the high angle of attack condition. On both wings the center of pressure is somewhat farther forward than is assumed in the design, the total load is higher, and the relative efficiency of the upper wing is only 1.02 as against the design assumption of 1.29. Of these factors, the first tends to decrease the severity of the condition as compared to the specifications, while the second and third tend to increase it. It is impossible to say from one case, of course, what center of pressure position is most likely to be encountered in the critical condition for the rear spars, since the load factor changes with the pressure distribution. Definite conclusions on this point, therefore, are not warranted. The comparison is little changed if both total loads are assumed to be the same, and the effect of the discrepancy between the relative upper wing efficiencies remains as the most significant factor. The case, however, emphasizes the importance of extended research into the mutual interference of biplane wings, and also points out that the supposed factor of safety of 2 is not unlikely to be overworked, even under conditions which are not considered in any respect abnormal. From the standpoint of the operating personnel, it would seem that the airplane should be handled very gently in pull-outs from fast dives until the low angle of attack condition is more thoroughly known and provided for.

Tail loads.—The important tail loads are summarized in Table IV. For each run listed, several conditions are given in chronological order to cover the following: 1. Maximum horizontal surface down load; 2. Maximum horizontal surface up load; 3. Maximum stabilizer pressure; 4. Maximum elevator pressure; 5. Maximum vertical surface load; 6. Maximum fin pressure; 7. Maximum rudder pressure. Vertical surface pressures were not worked up for the pull-ups since they are relatively low and of little interest.

Tail surface specifications for pursuit type airplanes impose average loads of 45 and 40 pounds per square foot on the horizontal and vertical surfaces, respectively. It is interesting, as a primary comparison between observed and specified loads, to note the values given in the columns of average loads in Table V. It must be borne in mind while doing this that the specifications are supposed to incorporate a factor of safety of 2; thus, any value given in the table exceeding one-half the specified value is to be considered an overload and vice versa. It will be noted that the horizontal tail surface loads in the pull-ups are generally lower than one-half the design load, exceeding this value in Runs 134 and 137, and closely approaching it in Run 133. It is worth noting that the applied load factor (C. G. acceleration) in Run 133 is 6, making the safety factor for both wings and tail surfaces approximately 2 (on the basis of loads only) in the same maneuver. In the two dives listed, however, the tail loading is excessive, being 26.4 and 30.7 pounds per square foot for Runs 213 and 226 respectively, indicating that the specifications should be revised upward. Other high loadings on the horizontal surfaces occur in the high-speed barrel rolls, Runs 222 and 225, the values exceeding one-half the design loading, but remaining less than the dive loadings. It is interesting to note that in the rolls the maximum up load is of the same order of magnitude as the down loads, whereas in all other maneuvers the down loads only are severe.

On the vertical surfaces only two loads listed exceed the safe value, in the right barrel roll, Run 222, and in the pull out of a dive, Run 226. Since the barrel roll under discussion was quite severe and may be considered an unusual or test case, it would not be reasonable to expect that under normal conditions vertical tail surface loads would be so high. The load in the pull out must be considered a fair one, however, and the possibility of the vertical surfaces receiving high loads under normal conditions can not be denied. In this case the maximum load occurs simultaneously with the low incidence condition discussed previously in the report.

Besides the average loading likely to be encountered on tail surfaces, the specifications must anticipate the distribution of load with particular respect to the high concentrations that may occur in some places, usually the leading edges of stabilizer and fin. The present specifications dispose the load uniformly over the fixed surfaces whence it decreases until, at the trailing edge of the movable element, its value is one-third the value over the fixed surface. In addition, special leading-edge loads are applied extending from the leading edge back one-fifth the chord of the fixed surface, and having a uniform value equal to three times the specified average loading. Thus, the leading-edge load for a pursuit airplane stabilizer would be 135 pounds per square foot and for the fin 120 pounds per square foot. On the horizontal surfaces the maximum pressures on the leading edge occur in the severe pull-ups and exceed the specified leading edge value by a very appreciable margin, although fortunately they are usually quite local in character and do not extend over the specified area. The fact that they not only exceed half the specified loading but actually exceed the whole of it is well worth noting. In all of these cases (pull-ups), however, the accelerations at the C. G. were greater than 6. In the less severe power-on pull-ups, the maximum pressures recorded are under 135 pounds per square foot, but in some cases considerably greater than half that value, indicating that the specifications should be revised upward. In one dive, Run 226, the pressure was equal to that specified within the experimental error, and it would seem from this that to double the present leading edge specifications would give a much more reasonable value.

In no case does the pressure on the leading edge of the fin exceed the specified value, although in the pull out it reaches a value of 90 pounds per square foot.

A few comparisons of some of the worst rib loads with the specifications are given in Figures 93 and 94. They are self-explanatory and need no further comment.

Slip stream investigation.—A number of level flight runs and pull-ups, both power on and power off, were made with orifices located on six ribs in the central portion of the upper wing, and one rib near the root of each lower wing to determine the effect of the slip stream on the pressure distribution.

Referring to the level flight pressure plots (figs. 95a to 95c), no pronounced difference between right and left sides can be observed in the slow-speed condition on the upper wing, although an appreciable difference on the lower wing is apparent, the effect of the rotation of the slip stream being, as would be expected, to reduce the effective angle of attack on the right side. This effect on the lower wing occurs throughout the speed range. On the upper wing at the higher speeds, a similar effect is noticeable, although the differences are not greater than might be expected as a result of the deformed leading edge. The pressure plots for the peak loads in pull-ups show no appreciable differences in the character of the pressure distribution, with the exception that the leading-edge pressure on the right lower wing is lower than that of the left lower wing in the power-on pull-ups, whereas both pressures are about equal in the power-off pull-ups.

The span load curves show more clearly what differences exist. In Figures 99 and 100 it is seen that the slip stream increases the load on the central portion of the upper wing, while the shape of the load curve remains much the same. The effect of the rotation of the slip stream on the lower wing, however, is pronounced as the figures show.

Figures 101 and 102 show that no appreciable dissymmetry of load exists on either the upper or lower wings at the peak loads of the pull-ups as a result of the slip stream rotation, although in the power-on pull-ups the total load in the region affected is greater than the load in the power-off pull-ups for the same *initial* air speed. This increment of load is due to an increased air speed, which is composed of both the slip stream increment and the natural increase obtaining as a result of the power-on conditions.

From Figure 103, which represents the condition in a dive at high speed, it is apparent from the lower wing rib loads that the rotation of the slip stream is still effective. The low point at rib A′, which is also apparent in the other span load curves, is probably not due to slip stream effect nor to any interference from the fuselage. The pressure records for this rib show violent fluctuations of pressure for the points aft of about the quarter chord point. This fact, in combination with the knowledge that a rather abrupt discontinuity existed in the upper surface wing curve near the leading edge of rib A′, would lead one to believe that the streamline flow over this rib was disrupted, and hence caused a marked decrease in the lift. This is further apparent from the pressure plots for the dive. (Fig. 98.) The condition may thus be considered as purely local and having no connection with the slip stream.

Fabric pressures.—Coincident with the slip stream measurements, records were also obtained of the fabric pressures on rib C and several other points. For this purpose each pressure capsule was connected to one of the flush orifices in the wing surface and to an open tube terminating inside the wing near the flush orifice. Pressures as obtained are tabulated in Table V and need no special comment other than that minus signs indicate downward acting pressures and vice versa, regardless of whether the orifice is on the upper or lower surface of the wing.

CONCLUSIONS

It is concluded from these tests that:

1. In any condition of flight characterized by low angles of attack with the center of pressure well back of the elastic axis, the wing, unless quite rigid, may deflect torsionally to such an extent as to greatly alter the load distribution. This means that the load distribution is a function of the torsional rigidity of the wing structure and this fact should be taken into account in the design rules.

2. Regardless of the cause, the effect of wing twist on the load distribution is the same and this effect can be satisfactorily calculated.

3. The maximum forward position of the center of pressure on upper and lower wings is unaffected by the factors involved in accelerated flight.

4. The maximum forward position of the center of pressure on the upper wing of the full-scale airplane is the same as that for the model wing. This point is questionable with respect to the lower wing, since strictly comparable data are not available.

5. The maximum normal force coefficient of the upper wing of a biplane reaches an appreciably higher value during a maneuver involving positive angular velocity in pitch than it does in steady flight, while lower wing normal force coefficients corresponding to the angle of attack at which the upper wing maximums occur are essentially the same for both pitching and steady flight. This means that the relative wing-loading ratio for the true high angle of attack condition (which always involves a positive angular velocity in pitch) is greater than would be expected from steady-flight (wind tunnel) data. On the *PW–9*, this increase is about 16.3 per cent of the steady-flight value.

8493—30——6

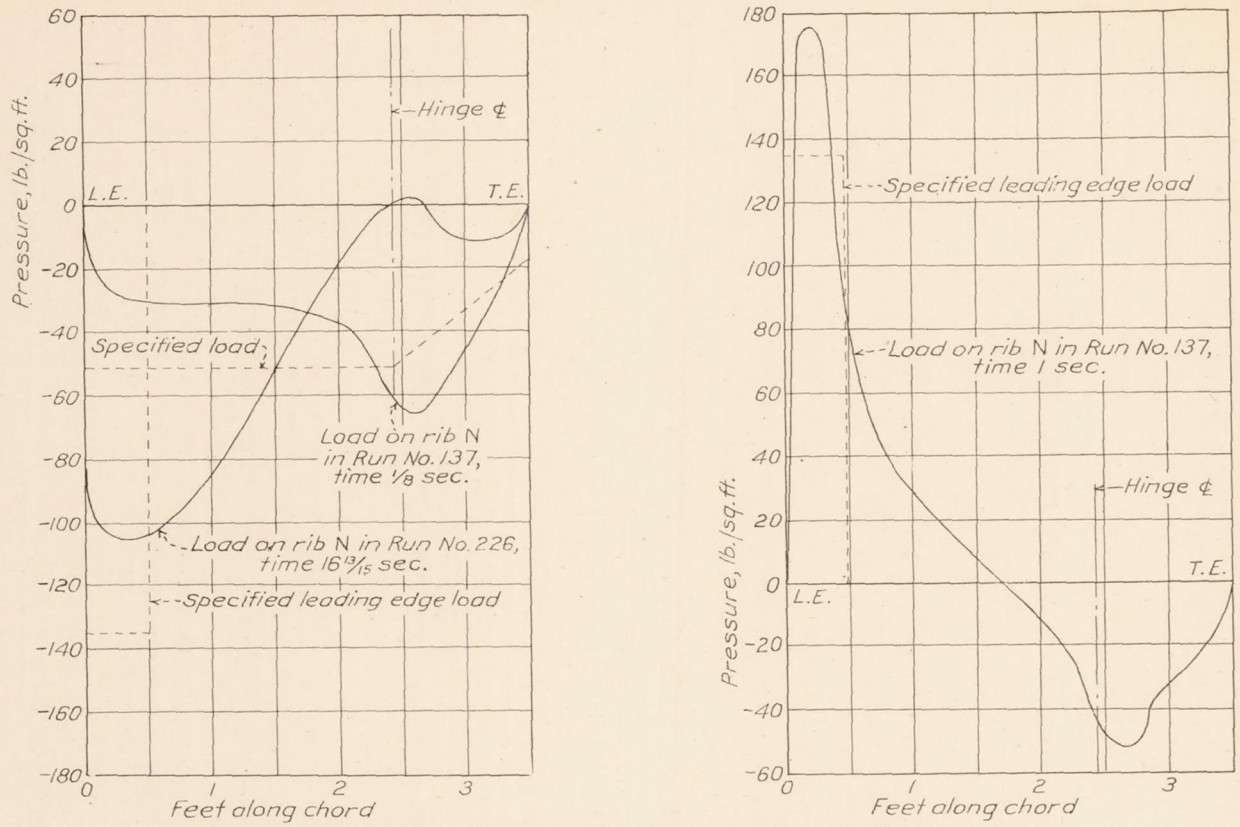

FIGURE 93.—Comparison of worst horizontal surface rib loads with specifications

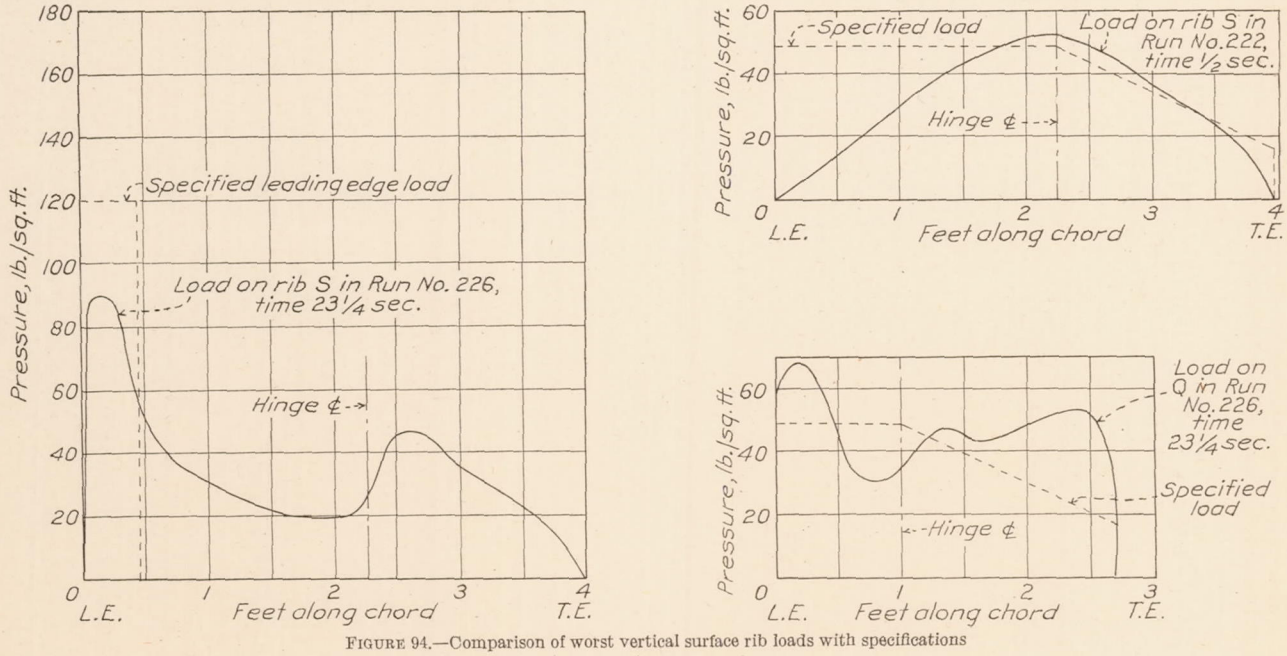

FIGURE 94.—Comparison of worst vertical surface rib loads with specifications

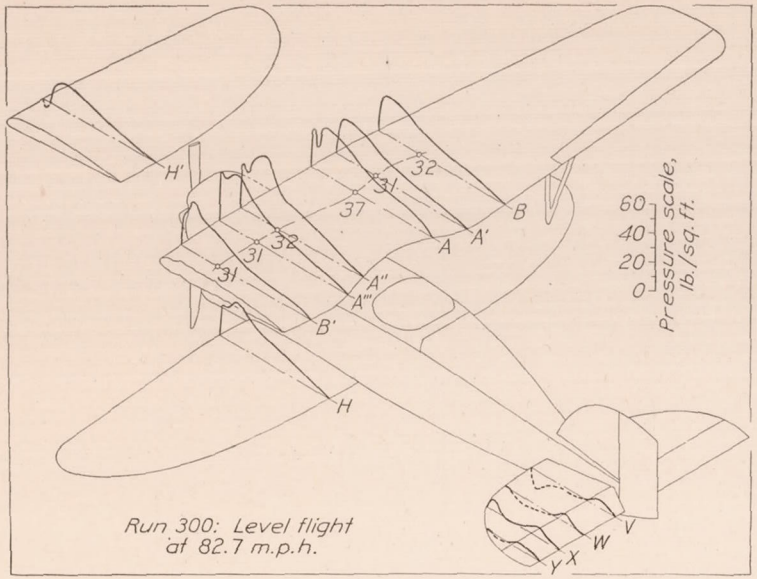

FIGURE 95a

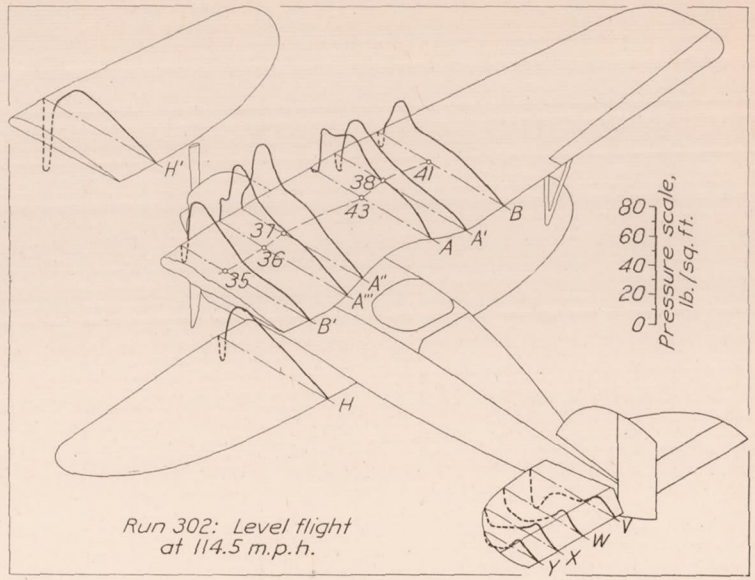

FIGURE 95b

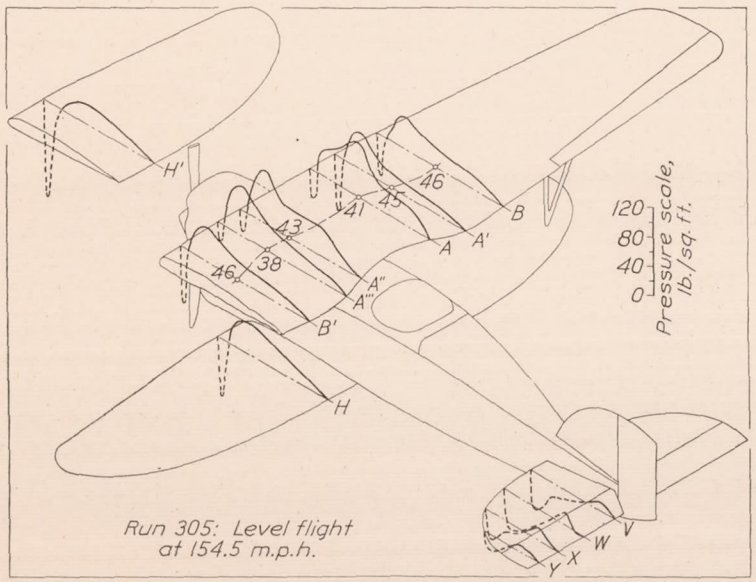

FIGURE 95c

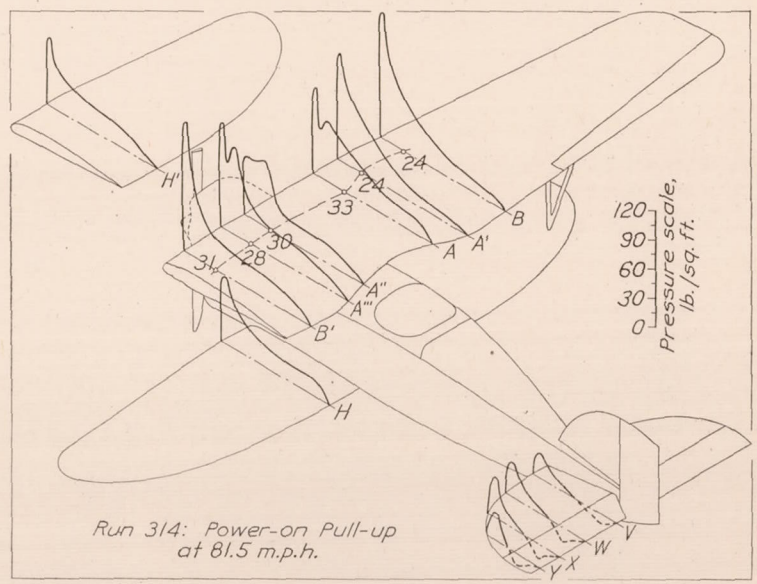

FIGURE 96a

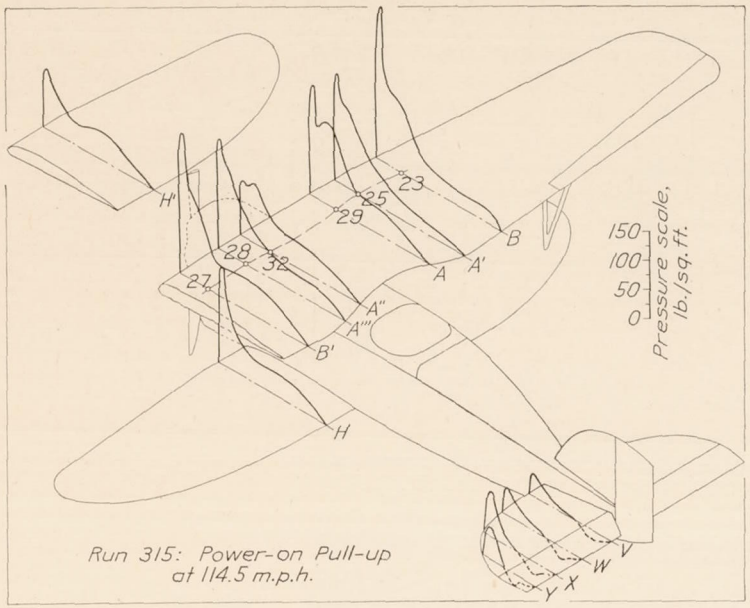

FIGURE 96b

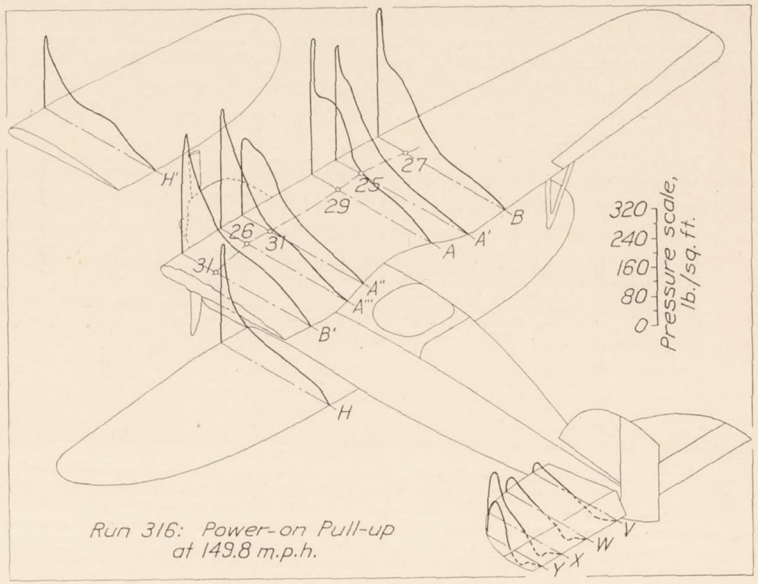

FIGURE 96c

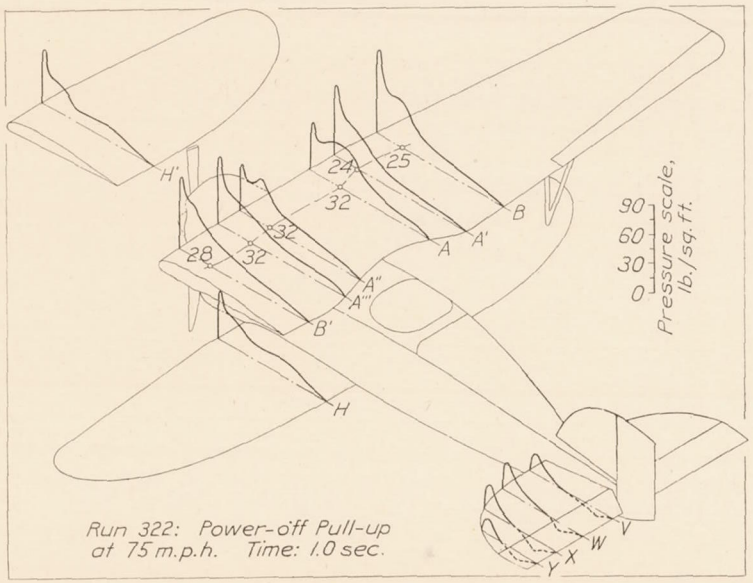

FIGURE 97a

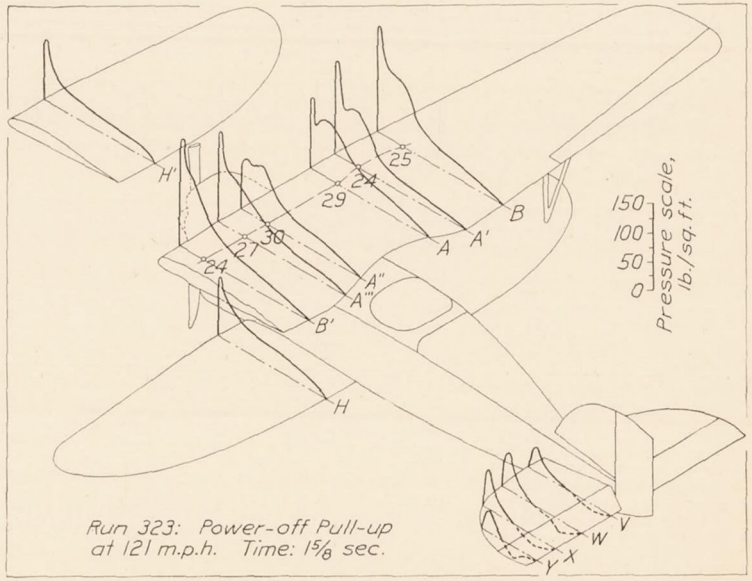

FIGURE 97b

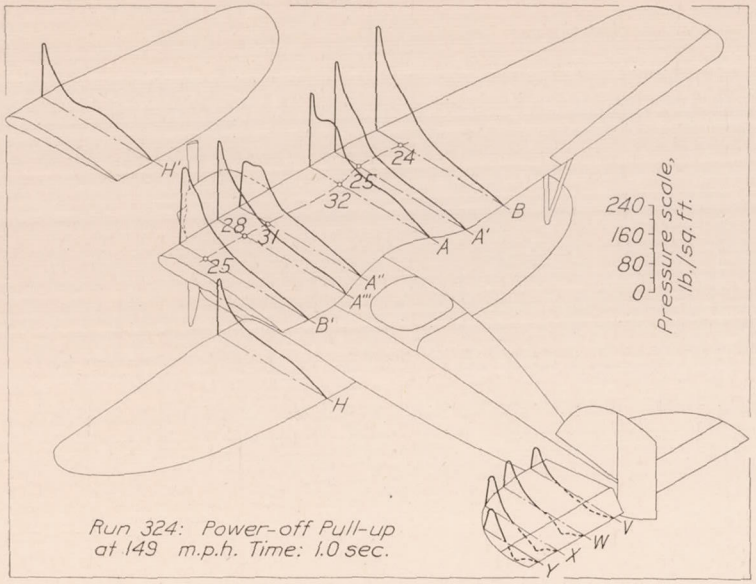

FIGURE 97c

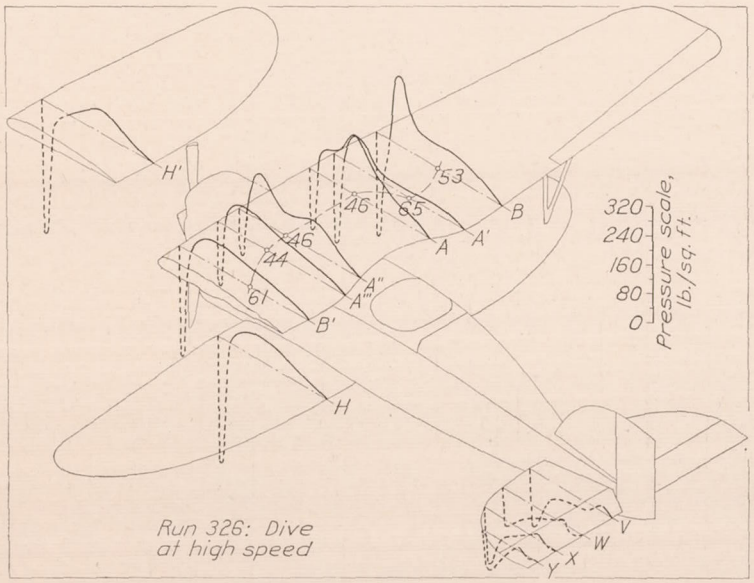

FIGURE 98

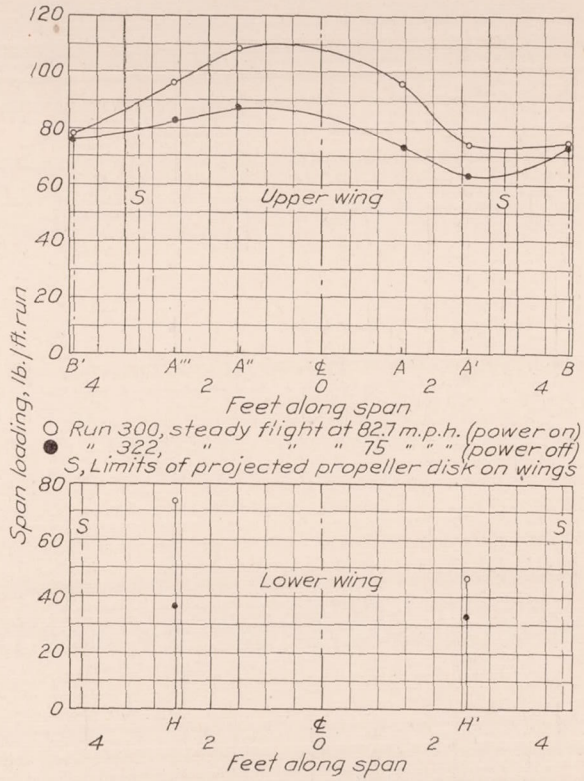

FIGURE 99.—Span load distribution in slip stream

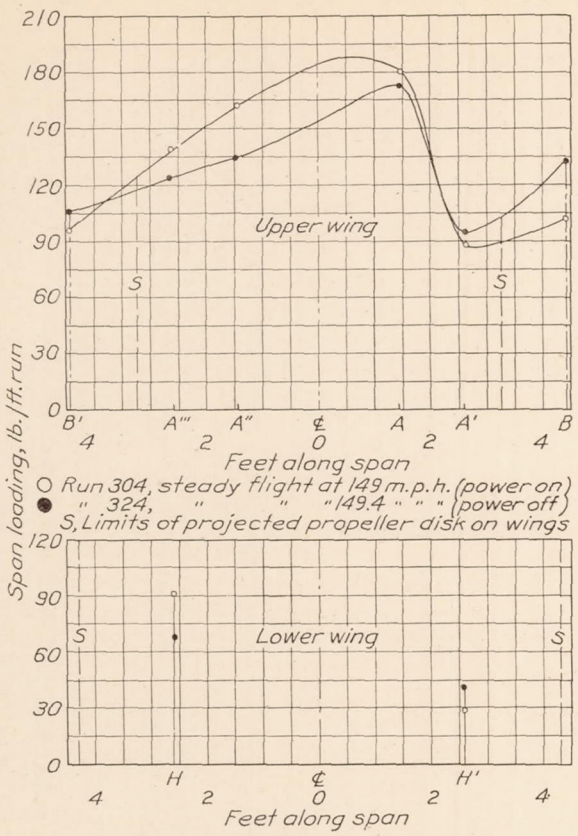

FIGURE 100.—Span load distribution in slip stream

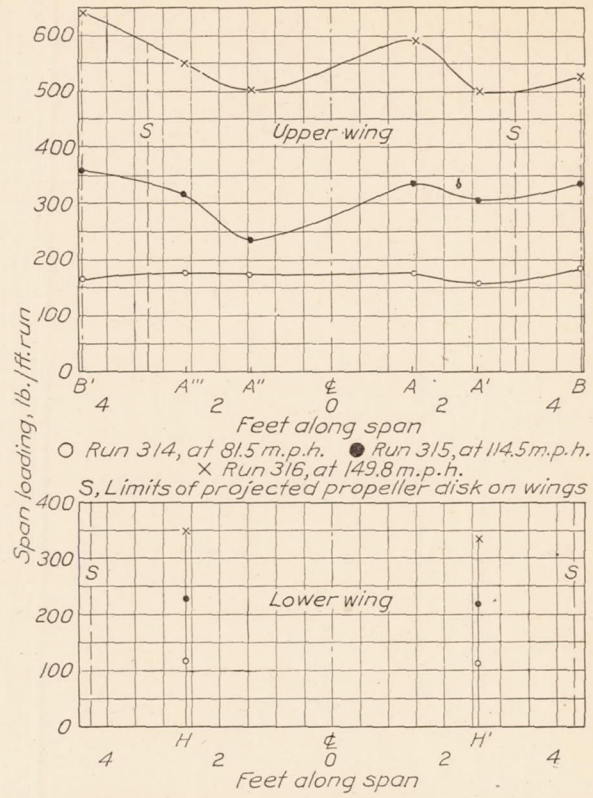

FIGURE 101.—Span load distribution in slip stream. Peak loads in power-on pull-ups.

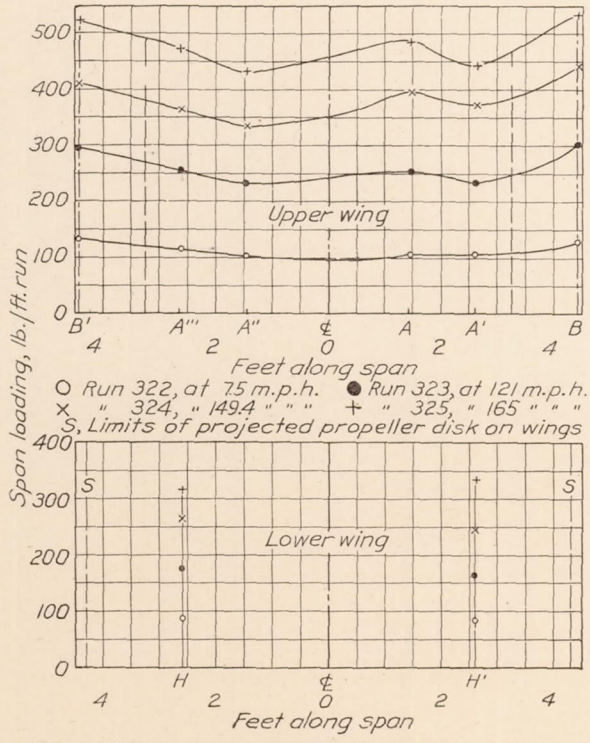

FIGURE 102.—Span load distribution in slip stream. Peak loads in power-on pull-ups

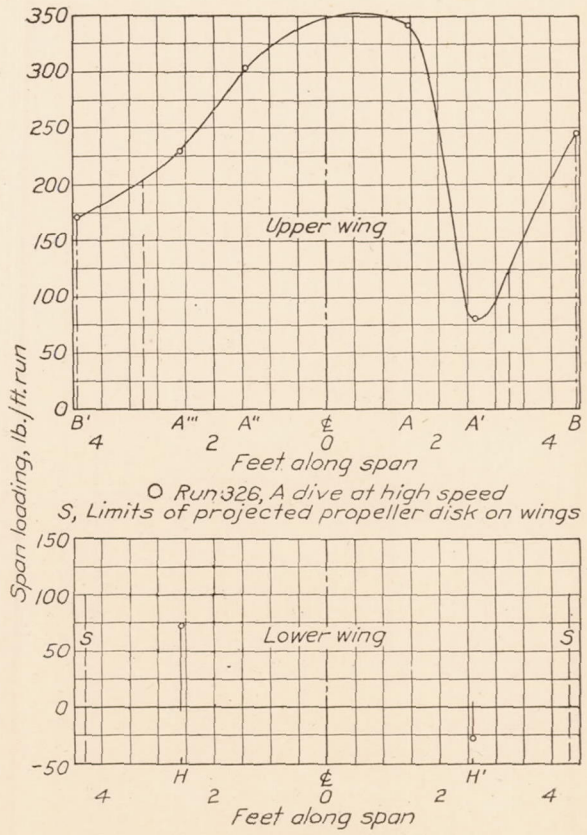

FIGURE 103.—Span load distribution in slip stream

6. In power-on maneuvers involving high angle of attack, a varying inertia load exists along the fuselage which is critical for the engine support. This inertia load should be considered in the fuselage analysis conditions.

7. The strip method of computing span-load curves for the high angle of attack condition gives results which check the measured load distribution very satisfactorily for wings tapering similarly to those of the *PW–9*.

8. The position of the center of pressure at sections near the tip is an important factor requiring further study. In the present case on the upper wing the center of pressure locus bends to the rear at the tip, thus increasing the front spar bending moment in the bay for the high angle of attack condition by an amount which is not provided for by the present rules concerning tip loss.

9. Design rules should include proper determination of the center of pressure position on biplanes.

10. In barrel rolls the maximum dissymmetry of load occurs shortly after the peak load, and the total load when this maximum value occurs is not appreciably less than the peak.

11. When the maximum dissymmetry of load occurs in a roll, the lower wing is not stalled and the asymmetrical loading on this wing is of such a nature as to oppose the rolling of the airplane.

12. In a spin the inside wings are stalled approximately to the plane of symmetry, while the outside wings remain unstalled, although at a high angle of attack.

13. Leading-edge pressures on the wings reach values of the order of 450 pounds per square foot, both in dives and in pull-ups.

14. Conditions governing the critical rear spar loads should be studied at greater length. The present report shows that in normally executed pull outs from fast dives, rear spar loads may be greater than have heretofore been considered.

15. Tail-load specifications should be revised upward. This is particularly true of leading-edge loads, which should be at least doubled.

16. The effect of the slip stream is to cause dissymmetry of load on the two root portions of the lower wing, and to increase the load on the central portion of the upper wing without giving rise to any dissymmetry thereon.

17. Abrupt changes in contour of the wing curvature near the leading edge may seriously affect the lift.

LANGLEY MEMORIAL AERONAUTICAL LABORATORY,
NATIONAL ADVISORY COMMITTEE FOR AERONAUTICS,
LANGLEY FIELD, VA., *February 3, 1930.*

BIBLIOGRAPHY

Reference 1: Handbook of Instructions for Airplane Designers. Engineering Division, Army Air Service (1925).

Reference 2: General Specifications for the Design of Airplanes for the United States Navy—SD–24–B. Bureau of Aeronautics, Navy Department.

Reference 3: Airworthiness Requirements of Air Commerce Regulations. Aeronautics Bulletin No. 7–A. Aeronautics Branch, Department of Commerce.

Reference 4: Norton, F. H.: Pressure Distribution Over the Wings of an MB–3 Airplane in Flight. N. A. C. A. Technical Report No. 193 (1924).

Reference 5: Crowley, jr., J. W.: Pressure Distribution Over a Wing and Tail Rib of a VE–7 and of a TS Airplane in Flight. N. A. C. A. Technical Report No. 257 (1927).

Reference 6: Norton, F. H.: N. A. C. A. Recording Air-Speed Meter. N. A. C. A. Technical Note No. 64 (1921).

Reference 7: Reid, H. J. E.: A Study of Airplane Maneuvers with Special Reference to Angular Velocities. N. A. C. A. Technical Report No. 155 (1922).

Reference 8: Norton, F. H.: N. A. C. A. Control Position Recorder. N. A. C. A. Technical Note No. 97 (1922).

Reference 9: Norton, F. H., and Warner, E. P.: Accelerometer Design. N. A. C. A. Technical Report No. 100 (1921).

Reference 10: Coleman, D. G.: N. A. C. A. Flight-path-angle and Air-Speed Recorder. N. A. C. A. Technical Note No. 233 (1926).

Reference 11: Rhode, R. V.: The pressure Distribution Over the Horizontal and Vertical Tail Surfaces of the F6C–4 Pursuit Airplane in Violent Maneuvers. N. A. C. A. Technical Report No. 307 (1929).

Reference 12: Howard, H. B.: Some Problems in Aeroplane Structural Design. The Journal of the Royal Aeronautical Society, April, 1926.

Reference 13: Handbook of Strength Calculations, Air Ministry. Air Publication 970 (His Majesty's Stationery Office), 1928.

Reference 14: Loeser, jr., O. E.: Pressure Distribution Tests on PW–9 Wing Models from −18° through 90° Angle of Attack. N. A. C. A. Technical Report No. 296 (1929).

TABLE I.—CHARACTERISTICS OF PW–9 AIRPLANE

Span of upper wing	32 feet 0 inch.
Span of lower wing	22 feet 5¾ inches.
Centric chord of upper wing	5 feet 3¼ inches.
Distance from center line to centric chord	7 feet 10 inches.
Centric chord of lower wing	4 feet 6 inches.
Distance from center line to centric chord	5 feet 7⅜ inches.
Gap	52 inches.
Stagger [1]	+2° 22′.
Dihedral (upper wing lower surface)	1° 6′.
Dihedral (lower wing lower surface)	1° 23′.
C. G. position:	
Aft leading edge of root section, lower wing	18¼ inches.
Above lower surface root section, lower wing	23¾ inches.
Distance from C. G. to center line of elevator hinge	14 feet 11⅝ inches.
Distance from C. G. to center line of rudder hinge	15 feet 3⅝ inches.
Area of upper wing	160.4 square feet.
Area of lower wing	80.8 square feet.
Total wing area	241.2 square feet.
Area of horizontal tail surfaces	29.84 square feet.
Area of vertical tail surfaces	10.74 square feet.
Weight of airplane during tests	2,970 pounds.
Rated horsepower at 2,000 r. p. m.	375.
Power loading	7.92 pounds per hp.
Wing loading	12.3 pounds per square foot.
I_x	1,697 slugs-feet.[2]
I_y	1,875 (approximately).
I_z	2,600 (approximately).

[1] Stagger measured at a section parallel to the plane of symmetry, and passing through the centroid of the plan form of one lower wing between a line perpendicular to the chord of the upper wing and a line drawn from a point one-third chord length from the leading edge of the lower wing to a point similarly located on the upper wing.

TABLE II.—TRUE ORDINATES OF PRESSURE RIBS

Rib	B′ Chord=68 inches		A‴ Chord=70 inches		A″ Chord=64 inches		A Chord=64 inches	
Station chord	Upper chord	Lower chord	Upper chord	Lower chord	Upper chord	Lower chord	Upper chord	Lower chord
Per cent	*Per cent*	*Per cent*	*Per cent*	*Per cent*	*Per cent*	*Per cent*	*Per cent*	*Per cent*
0	2.52	2.52	3.14	3.14	1.87	1.87	1.87	1.87
1.25	4.34	.88	4.98	1.47	4.11	.23	4.16	.30
2.50	5.35	.53	5.88	1.07	5.11	−.16	5.02	−.16
5.00	6.91	.19	7.28	.76	6.56	−.47	6.40	−.48
7.50	8.15	.00	8.39	.67	7.73	−.50	7.56	−.52
10.00	9.15	−.10	9.29	.57	8.70	−.47	8.65	−.45
15.00	10.40	−.12	10.50	.41	10.20	−.19	10.12	−.20
20.00	11.03	−.06	11.12	.26	11.10	0	11.05	−.02
30.00	11.38	0	11.24	0	11.43	0	11.32	0
40.00	11.10	0	10.63	−.03	10.88	0	10.65	0
50.00	10.13	0	9.50	0	9.77	0	9.52	0
60.00	8.70	0	8.00	0	8.41	0	8.19	−.08
70.00	7.14	0	6.28	−.13	6.72	0	6.45	−.16
80.00	5.35	0	4.22	−.46	4.95	0	4.53	−.33
90.00	3.10	0	1.83	−.70	3.68	0	2.14	−.53
95.00	1.75	0	.57	−.79	1.52	0	.78	−.69
100.00	.26	0	−.66	−.89	.22	0	.52	−.75

Rib	A′ Chord=70 inches		B Chord=68 inches		C Chord=64 inches		D Chord=60.4 inches	
Station chord	Upper chord	Lower chord	Upper chord	Lower chord	Upper chord	Lower chord	Upper chord	Lower chord
Per cent	*Per cent*	*Per cent*	*Per cent*	*Per cent*	*Per cent*	*Per cent*	*Per cent*	*Per cent*
0	2.24	2.24	2.35	2.35	2.42	2.42	2.52	2.52
1.25	4.28	.60	4.68	1.00	4.56	.91	4.47	.99
2.50	5.26	.26	5.69	.63	5.58	.58	5.46	.60
5.00	6.69	.03	7.12	.28	7.00	.27	6.80	.28
7.50	7.83	−.04	8.24	.10	8.03	.08	7.76	.17
10.00	8.75	−.07	9.15	0	8.86	0	8.51	.07
15.00	10.10	0	10.40	0	10.05	0	9.77	0
20.00	10.83	0	11.11	0	10.80	0	10.77	0
30.00	11.13	0	11.50	.03	11.17	0	11.27	0
40.00	10.57	0	10.90	.03	10.62	0	10.62	0
50.00	9.47	0	9.85	0	9.67	0	9.50	0
60.00	8.16	0	8.72	0	8.42	0	8.06	0
70.00	6.49	0	7.06	0	6.79	0	6.46	0
80.00	4.62	0	5.09	0	4.98	0	4.70	0
90.00	2.57	0	3.08	0	2.80	0	2.64	0
95.00	1.46	0	1.76	0	1.58	0	1.49	0
100.00	.23	0	.25	0	.23	0	.26	0

TABLE II.—TRUE ORDINATES OF PRESSURE RIBS—Continued

Rib	E Chord=54 inches		F Chord=49.2 inches		G Chord=42 inches		H′ Chord=58.8 inches	
Station chord	Upper chord	Lower chord	Upper chord	Lower chord	Upper chord	Lower chord	Upper chord	Lower chord
Per cent	*Per cent*	*Per cent*	*Per cent*	*Per cent*	*Per cent*	*Per cent*	*Per cent*	*Per cent*
0	2.48	2.48	2.78	2.78	2.52	2.52	2.89	2.89
1.25	4.54	.91	4.62	.96	4.14	1.14	5.09	1.36
2.50	5.52	.54	5.62	.59	4.95	.69	5.95	.87
5.00	6.95	.20	7.02	.26	5.95	.36	7.31	.31
7.50	7.96	.11	7.97	.18	6.47	.24	8.50	.15
10.00	8.75	.06	8.72	.08	6.88	.17	9.35	0
15.00	9.82	0	9.93	0	7.45	.02	10.52	0
20.00	10.61	0	10.63	−.08	7.95	0	11.13	0
30.00	11.08	0	11.00	0	8.52	0	11.34	0
40.00	10.46	0	10.40	0	8.55	0	10.88	0
50.00	9.45	0	9.42	0	8.10	0	9.84	0
60.00	8.12	0	8.17	0	7.21	0	8.56	0
70.00	6.46	0	6.71	0	5.90	0	7.07	0
80.00	4.67	0	4.68	0	4.28	0	5.07	0
90.00	2.57	0	2.50	0	2.45	0	2.72	0
95.00	1.48	0	1.40	0	1.43	0	1.53	0
100.00	.31	0	.26	0	.38	0	.29	0

Rib	H Chord=58.8 inches		J Chord=54 inches		K Chord=44.8 inches		L Chord=25.6 inches	
Station chord	Upper chord	Lower chord	Upper chord	Lower chord	Upper chord	Lower chord	Upper chord	Lower chord
Per cent	*Per cent*	*Per cent*	*Per cent*	*Per cent*	*Per cent*	*Per cent*	*Per cent*	*Per cent*
0	2.69	2.69	2.48	2.48	2.66	2.66	3.36	3.36
1.25	5.00	1.15	4.55	.98	4.73	.98	5.39	1.25
2.50	5.88	.68	5.52	.56	5.67	.45	6.25	.70
5.00	7.28	.24	7.00	.13	7.19	.02	7.62	.12
7.50	8.36	.10	8.13	−.06	8.26	−.09	8.51	−.12
10.00	9.25	0	9.05	−.13	8.93	−.09	9.26	−.20
15.00	10.41	−.12	10.37	−.19	10.00	−.07	10.50	−.23
20.00	11.02	−.14	11.01	−.17	10.71	0	11.44	−.16
30.00	11.21	−.02	11.09	−.04	11.34	0	12.23	0
40.00	10.56	0	10.51	0	10.72	0	12.20	0
50.00	9.53	0	9.56	0	9.73	0	11.72	0
60.00	8.22	0	8.28	0	8.64	0	11.10	0
70.00	6.50	0	6.52	0	7.17	0	10.05	0
80.00	4.54	0	4.58	0	5.34	0	8.25	0
90.00	2.34	−.31	2.46	−.22	3.06	0	5.55	0
95.00	1.07	−.43	1.11	−.43	1.70	0	3.71	0
100.00	.29	−.53	−.35	−.69	.33	0	1.48	0

TABLE III.—RECORDED PRESSURES

[Level flight pressures are given in per cent q except in slip stream runs; all others in pounds per square foot]

Rib		Upper wing							Lower wing				Stabilizer and elevator				Vertical tail surfaces				
		A	B	C	D	E	F	G	H	J	K	L	M	N	O	P	Q	R	S	T	U
Run No. 18. Level flight at 74 m. p. h. q=14 pounds per square foot																					
Orifice	1	152	186	138	134	127	74	93	149	111	149	74									
	2	49	130	149	149	115	134	74	111	111	93	81									
	3	182	93	119	160	186	131	67	160	167	111	44									
	4	152	186	160	89	74	78	37	134	104	67	22									
	5	167	127	93	19	19		49	74	67	15										
	6	74	56	44	114	22		49	37	19											
	7	49	15	19		26															
Run No. 90. Level flight at 112 m. p. h. q=32.1 pounds per square foot																					
Orifice	1	49	0	0	−36	−39	−49	16	−32	−32	−31	41									
	2	16	54	36	32	24	44	24	29	16	49	44									
	3	113	79	49	98	60	58	31	94	65		32									
	4	110	112	88	52	44	49	21	81	81	41	13									
	5	112	74	52	18	13	37	65	54	50	15										
	6	55	39	32	31	28			23	21											
	7	34	13	12		19	15														
Run No. 23. Level flight at 133.2 m. p. h. q=45.4 pounds per square foot																					
Orifice	1	−6	−31	−90	−102	−78	−118	−15	−61	−76	−81	15									
	2	−4	−11	−6	−13	−11	−6	11	−14	−17	0	31									
	3	68	34	11	74	90	42	13	71	56	56	31									
	4	88	79	69	41	37	44	18	69	63	40	11									
	5	113	57	40	11	10	13	19	86	44	11										
	6	39	32	25	19	25	28	14	15	14											
	7	31	13	11		13	23														

TABLE III.—RECORDED PRESSURES—Continued

Run No. 88. Level flight at 151.6 m. p. h. q=59 pounds per square foot

Rib		Upper wing							Lower wing				Stabilizer and elevator				Vertical tail surfaces				
		A	B	C	D	E	F	G	H	J	K	L	M	N	O	P	Q	R	S	T	U
Orifice	1	−49	−107	−147	−147	−137	−150	−37	−132	−117	−105	−4									
	2	−35	−44	−40	−57	−56	−35	−2	−45	−47	−26	23									
	3	57	9	4	65	16	18	12	53	32		24									
	4	57	53	57	38	36	36	15	63	65	35	10									
	5	107	56	40	13	11	9	19	47	49	12										
	6	44	29	24	22	25	22	16	18	15											
	7	37	12	9		20	11														

Run No. 65. Pull-up at 79 m. p. h. Time: 0 second

Orifice	1	29	36	23	29	21	13	17	26	25	26	16	−7	4	2	5					
	2	16	26	31	26	26	23	12	18	21	19	13	−1	−6	−2	−2					
	3	31	21	26	23	21	18	11	21	26	17	6	−4	−6	−3	−4					
	4	29	30	23	13	11	11	6	15	15	7	4	−5	−4	−7	−3					
	5	20	18	14	3	3	5	1	9	9	2		−4	−3	−3	−2					
	6	10	9	8	3	3		8	4	3			−2	−4	−4						
	7	7	3	2		3	1														

Run No. 65. Time: 0.25 second

Orifice	1	34	39	26	31	26	20	18	31	31	31	16	−5	6	3	7					
	2	16	29	36	31	29	26	13	22	23	26	14	2	−8	−4	−3					
	3	34	23	32	24	22	19	13	23	29	18	8	−6	−9	−7	−9					
	4	30	34	26	15	12	12	8	16	16	7	5	−10	−16	−15	−6					
	5	22	21	15	3	3	5	12	13	9	3		−7	−10	−9	−3					
	6	11	9	9	3	3		9	5	3			−4	−5	−5						
	7	8	3	2		4	1														

Run No. 65. Time: 0.50 second

Orifice	1	39	47	44	47	42	34	18	41	39	39	23	2	15	11	10					
	2	23	42	47	40	36	34	13	29	31	31	15	2	−4	2	−1					
	3	40	33	42	30	29	23	13	26	35	21	9	−3	−7	−5	−9					
	4	36	36	28	17	15	14	8	16	18	9	6	−7	−12	−14	−5					
	5	23	24	17	4	4	5	12	16	10	3		−5	−9	−8	−2					
	6	12	10	9	3	3		9	6	3			−3	−4	−4						
	7	8	3	2		4	1														

Run No. 65. Time: 0.75 second

Orifice	1	52	60	60	61	55	44	30	47	48	47	26	11	21	21	14					
	2	31	52	57	52	47	43	22	35	36	34	16	4	0	5	2					
	3	44	36	47	35	34	28	19	28	38	22	10	−2	−6	−4	−7					
	4	42	43	34	18	17	17	13	16	18	10	7	−4	−9	−10	−3					
	5	25	24	19	4	6	7	22	13	12	4		−3	−5	−6	−1					
	6	14	11	10	3	5		15	8	4			−2	−3	−4						
	7	8	3	3		4	1														

Run No. 65. Time: 1 second

Orifice	1	62	66	68	68	62	49	35	52	48	52	29	12	25	24	15					
	2	36	60	67	61	52	45	24	36	38	36	18	6	3	7	4					
	3	47	37	52	36	36	30	22	26	38	23	10	−1	−1	1	−1					
	4	47	47	36	19	17	18	16	15	18	11	9	−1	−3	−3	1					
	5	27	28	20	4	6	7	24	13	12	4		−1	−2	0	0					
	6	15	12	9	3	5		17	8	4			−1	−1	−2						
	7	8	3	4		5	1														

Run No. 65. Time: 1.12 seconds

Orifice	1	62	70	68	73	68	53	36	52	44	52	26	13	25	23	15					
	2	36	60	67	65	55	45	26	36	38	34	18	7	3	7	5					
	3	47	37	52	36	38	31	23	23	38	22	10	0	0	3	2					
	4	49	47	36	18	17	18	17	15	16	11	9	1	−1	3	3					
	5	27	28	19	4	6	7	24	11	12	4		1	1	3	2					
	6	15		9	3	3		18	8	4			1	−1	−1	−1					
	7	7	3	4		5	1														

Run No. 65. Time: 1.25 seconds

Orifice	1	57	70	68	73	68	53	37	51	42	52	26	12	24	21	14					
	2	36	60	67	65	55	45	26	36	38	34	18	7	3	7	4					
	3	47	37	52	36	38	31	23	21	35	21	10	1	1	3	3					
	4	47	47	36	17	17	18	17	12	15	11	9	2	3	3	3					
	5	25	28	19	5	6	7	24	11	10	3		1	2	3	3					
	6	14		9	3	3		18	7	3			1	0	−1						
	7	7	3	4		5	1														

TABLE III.—RECORDED PRESSURES—Continued

Run No. 65. Time: 1.50 seconds

Rib		Upper wing							Lower wing				Stabilizer and elevator				Vertical tail surfaces				
		A	B	C	D	E	F	G	H	J	K	L	M	N	O	P	Q	R	S	T	U
Orifice	1	54.5	62	62	65	57	49	32	47	42	47	29	------	17	17	11	------	------	------	------	------
	2	34.0	52	57	55	47	47	25	31	35	36	16	6	16	------	3	------	------	------	------	------
	3	44.0	41	47	33	34	28	20	23	36	20	9	1+	1−	2	2	------	------	------	------	------
	4	46.0	42	34	16	15	16	16	13	15	9	8	1+	−12	3	3	------	------	------	------	------
	5	26.0	23	17	4	5	7	22	12	10	3	------	1−	2	2	1−	------	------	------	------	------
	6	14.0	11	7	2	3	5	16	8	3	------	------	1+	−4	1	------	------	------	------	------	------
	7	6.0	2	3	------	3	1	------	------	------	------	------	------	------	------	------	------	------	------	------	------

Run No. 65. Time: 1.75 seconds

Orifice	1	49	57	51	57	51	44	29	41	36	44	21	------	14	10	8	------	------	------	------	------
	2	31	46	47	49	41	41	21	26	30	31	15	5	−1	------	3	------	------	------	------	------
	3	40	32	42	30	30	25	17	21	29	18	9	−1	0	−1	−1	------	------	------	------	------
	4	36	40	31	14	14	15	13	12	14	9	6	−1	−9	2	−1	------	------	------	------	------
	5	21	20	16	3	4	5	20	9	9	2	------	−1	1	2	−1	------	------	------	------	------
	6	11	7	7	2	3	7	15	8	2	------	------	1	−6	−1	------	------	------	------	------	------
	7	6	2	3	------	3	1	------	------	------	------	------	------	------	------	------	------	------	------	------	------

Run No. 130. Pull-up at 116 m. p. h. Time: −0.02 second

Orifice	1	14.0	0	−19.2	−8.3	−8.8	−3.1	0	−6.8	−7.8	−2.6	10.4	------	−3.6	5.2	−2.6	------	------	------	------	------
	2	11.4	14.5	10.9	12.5	7.8	9.9	7.3	3.6	4.7	8.3	12.0	------	−13.5	3.6	.5	------	------	------	------	------
	3	34.8	21.8	15.6	24.4	17.2	19.2	9.9	27.0	21.8	------	10.4	------	5.2	.5	------	------	------	------	------	------
	4	36.9	29.6	28.0	15.1	14.0	15.1	6.2	20.8	23.4	14.6	------	------	6.3	0	−5.7	------	------	------	------	------
	5	32.8	20.8	15.6	4.7	3.6	4.7	7.8	------	15.1	4.7	------	------	2.6	3.1	0	------	------	------	------	------
	6	18.2	11.4	8.3	7.8	8.3	5.2	7.3	4.2	4.2	------	------	------	1	−2.1	------	------	------	------	------	------
	7	12.0	4.2	2.6	------	1.5	4.2	------	------	------	------	------	------	------	------	------	------	------	------	------	------

Run No. 130. Time: 0.23 second

Orifice	1	23.9	0	−19.2	4.2	−5.2	0	0	20.3	2.6	17.7	15.6	------	−5.2	15.6	−11.4	------	------	------	------	------
	3	20.8	14.6	10.9	15.6	17.2	12.0	7.3	21.3	20.8	19.2	14.0	------	−24.9	−12.0	−10.4	------	------	------	------	------
	3	34.8	27.6	17.7	24.4	17.2	19.2	12.5	31.7	30.2	------	10.4	------	−24.4	−19.2	------	------	------	------	------	------
	4	39.5	36.4	28.1	15.1	14.0	15.6	6.2	24.4	23.4	17.7	------	−23.2	−15.6	−32.7	−8.8	------	------	------	------	------
	5	32.8	22.9	16.6	5.7	4.2	4.7	7.8	------	16.6	5.2	------	−23.9	−24.9	−24.4	−8.8	------	------	------	------	------
	6	19.3	11.4	9.9	7.8	8.3	5.2	7.3	7.3	5.7	------	------	−7.3	−11.4	−11.4	------	------	------	------	------	------
	7	13.0	5.2	4.2	------	1.6	4.2	------	------	------	------	------	------	------	------	------	------	------	------	------	------

Run No. 130. Time: 0.48 second

Orifice	1	39.0	21.3	20.8	49.4	15.6	16.1	9.9	59.3	53.1	50.5	30.7	------	29.1	21.8	13.0	------	------	------	------	------
	2	32.8	28.1	21.8	57.2	65.0	35.9	15.6	46.8	48.4	42.7	23.4	------	−10.9	−.5	−6.2	------	------	------	------	------
	3	57.2	51.5	42.2	33.8	30.2	31.2	15.6	50.4	45.8	------	14.0	------	−18.7	−16.1	−14.6	------	------	------	------	------
	4	56.1	40.6	40.0	21.9	18.7	19.8	12.0	33.8	32.8	21.3	------	------	−32.2	−33.8	−3.7	------	------	------	------	------
	5	43.2	33.8	24.4	5.7	5.2	8.8	20.3	------	20.3	6.8	------	------	−22.9	−21.8	------	------	------	------	------	------
	6	22.9	16.6	12.5	10.4	10.4	8.8	14.6	9.9	6.8	------	------	------	−10.4	−10.9	------	------	------	------	------	------
	7	14.6	5.2	5.2	------	3.6	7.3	------	------	------	------	------	------	------	------	------	------	------	------	------	------

Run No. 130. Time : 0.73 second

Orifice	1	118.0	114.0	109.0	114.0	119.0	77.5	60.8	92.5	88.4	87.4	49.4	------	53.0	44.7	26.0	------	------	------	------	------
	2	78.5	100.0	86.3	100.0	92.6	69.7	43.2	72.8	77.0	72.8	31.2	------	1	8.8	−4.2	------	------	------	------	------
	3	88.4	87.9	75.4	69.2	67.6	55.6	36.9	62.4	65.5	------	19.2	------	−18.2	−14.0	------	------	------	------	------	------
	4	86.8	78.0	71.3	32.2	32.8	32.2	23.4	37.4	41.1	25.0	------	−17.2	−32.2	−31.2	−14.0	------	------	------	------	------
	5	52.0	47.3	34.3	83.2	9.9	14.0	36.9	------	23.4	8.8	------	−14.0	−21.3	−19.8	−2.6	------	------	------	------	------
	6	31.2	21.8	18.2	12.0	13.0	18.2	32.2	12.5	7.3	------	------	−4.7	−9.4	−10.9	------	------	------	------	------	------
	7	17.7	5.7	15.6	------	6.2	9.4	------	------	------	------	------	------	------	------	------	------	------	------	------	------

Run No. 130. Time: 0.98 second

Orifice	1	165.0	171.0	168.0	170.0	176.0	124.0	97.8	125.0	114.0	112.0	59.8	------	84.7	65.5	40.0	------	------	------	------	------
	2	116.5	155.0	147.0	145.0	135.0	119.0	73.8	88.4	102.0	89.5	41.6	------	13.0	17.2	−.5	------	------	------	------	------
	3	102.0	119.0	111.0	84.7	89.0	79.0	55.2	62.4	78.5	------	23.4	------	−13.0	−8.8	------	------	------	------	------	------
	4	122.0	117.0	85.8	36.4	37.9	43.2	38.5	40.0	44.2	32.8	------	−15.1	−28.1	−27.0	−12.5	------	------	------	------	------
	5	62.4	57.2	39.0	17.1	19.2	22.3	57.2	------	25.0	12.0	------	−13.5	−18.7	−16.6	−2.6	------	------	------	------	------
	6	40.5	24.4	------	22.8	16.6	23.9	41.1	15.6	7.8	------	------	−3.1	−8.3	−8.8	------	------	------	------	------	------
	7	23.4	9.4	------	------	10.9	14.5	------	------	------	------	------	------	------	------	------	------	------	------	------	------

Run No. 130. Time: 1.23 seconds

Orifice	1	135.0	124.0	145.0	142.0	180.0	135.0	97.7	109.0	98.8	89.0	62.4	------	69.2	65.5	44.7	------	------	------	------	------
	2	88.3	107.0	123.0	139.0	130.0	125.0	63.4	85.2	89.4	63.0	43.2	------	17.7	19.8	3.1	------	------	------	------	------
	3	82.6	87.8	87.8	59.8	87.3	72.8	53.0	59.8	71.7	------	29.6	------	−8.3	−5.2	------	------	------	------	------	------
	4	96.2	100.0	68.0	42.7	40.6	42.2	50.5	35.4	44.2	38.5	------	−11.4	−22.4	−21.8	−11.4	------	------	------	------	------
	5	44.7	40.0	29.6	19.2	21.3	20.3	59.2	------	34.8	16.6	------	−9.3	−16.1	−13.5	−2.6	------	------	------	------	------
	6	46.8	19.2	22.9	28.6	19.8	23.9	41.1	20.8	9.9	------	------	−1.0	−7.3	−6.8	------	------	------	------	------	------
	7	19.8	16.6	16.1	------	10.9	14.6	------	------	------	------	------	------	------	------	------	------	------	------	------	------

TABLE III.—RECORDED PRESSURES—Continued

Run No. 130. Time: 1.48 seconds

Rib		Upper wing							Lower wing				Stabilizer and elevator				Vertical tail surfaces				
		A	B	C	D	E	F	G	H	J	K	L	M	N	O	P	Q	R	S	T	U
Orifice	1	97.7	85.8	67.6	114.0	102.0	93.6	54.6	92.5	66.6	65.0	59.2	45.2	64.0	59.8	36.4					
	2	70.7	41.6	59.8	91.0	52.0	85.8	47.8	67.6	48.4	46.8	42.1	12.0	18.2	17.2	2.1					
	3	72.3	41.1	39.0	36.9	37.4	33.8	38.0	49.4	34.8		26.0	−3.6	−7.8	−6.2						
	4	80.6	52.0	33.8	28.6	37.4	26.4	33.3	28.1	30.2	27.6		−8.8	−17.2	−19.8	−9.4					
	5	31.2	23.4	24.4		23.9	22.4	53.6		28.6	19.8		−7.3	−13.0	−13.0	−3.1					
	6	20.8	16.6	18.2	18.7	20.8	23.9	33.3	19.2	14.0			−3.1	−5.7	−6.8						
	7	14.0	9.8	11.4		13.0	16.6														

Run No. 130. Time: 1.73 seconds

Orifice	1	78.0	78.0	52.0	83.2	72.8	64.0	48.3	83.2	62.4	59.8	48.8	39.0	48.8	49.3	29.6					
	2	56.2	33.8	52.0	65.0	42.6	57.2	33.2	59.3	41.6	41.6	41.6	8.8	12.5	14.0	2.1					
	3	62.4	33.8	28.6	26.0	24.4	28.6	27.0	44.2	31.2		23.4	−4.7	−9.9	−6.2						
	4	65.0	41.6	28.6	20.3	18.7	22.3	18.2	23.4	24.4	22.4		−8.8	−15.1	−15.1	−7.8					
	5	26.0	19.2	20.8		15.1	18.2	32.2		24.9	14.6		−7.3	−10.4	−10.4	−2.6					
	6	14.6	14.0	14.5	13.5	19.7	18.2	21.3	10.9	13.0			−2.6	−5.2	−6.8						
	7	10.9	6.8	7.8		10.4	10.4														

Run No. 132. Pull-up at 137 m. p. h. Time: −0.02 second

Orifice	1	0	−18.2	−36.4	−36.4	−33.8	−44.2	−5.2	−29	−37	−25	6		−8.8		−3.6					
	2	0	0	−2.6	−3.6	−5.2	−2.6	2.6	−10	−8	0		−3.6	−19.8	−8.3	1.0					
	3	31.2	15.6	6.8	26.0	13.0	10.4	5.7	30	21			−.5	0	−1.0						
	4	36.4	31.2	26.0	16.1	12.5	15.6	5.2	26		18		−.5	5.2	4.7	1.6					
	5		26.0	17.2	2.1	2.6	5.2	5.2			6		0	2.1	3.6	−1.0					
	6	20.8	13.0	10.4	5.2	9.4	10.4	7.8	5	5			0	0							
	7	18.2	6.2	4.2		2.6	3.6														

Run No. 132. Time: 0.23 second

Orifice	1	0	−18.2	−36.4	−36.4	−33.8	−44.2	−5.2	−27	−37	−18	6		−10.4	−5.2	−6.8					
	2	0	0	−2.6	−3.6	−2.6	−2.6	2.6	−7	5	3	16	−8.3	−27.6	−8.8	−1.6					
	3	31.2	15.6	6.8	28.6	13.0	10.4	5.7	30	21		12	−2.1	−7.8	−5.2						
	4	36.4	31.2	26.0	16.1	12.5	15.6	5.2	28	27	18		−13.0	−14.0	−12.0	−10.4					
	5	59.8	26.0	18.2	2.1	2.6	5.2	5.2		17	7		−6.2	−10.9	−31.7	−2.6					
	6	21.8	13.0	10.4	5.2	10.4	13.5	7.8	7	6			−7.8	−5.2	−2.6						
	7	19.2	6.8	4.2		2.6	5.2														

Run No. 132. Time: 0.48 second

Orifice	1	36.4	57.2	7.8	26.0	26.0	14.6	7.8	46	31	47	36	0.5	6.2	−8.8	10.9					
	2	26.0	31.2	39.0	46.8	33.8	36.4	14.6	47	45	50	30	2.6	−14.0	−5.2	−8.8					
	3	62.4	36.4	57.3	46.8	33.8	28.6	13.0	59	52		16	−16.6	−26.5	−22.9						
	4	67.6	62.4	42.7	26.0	19.8	20.8	9.4	39	38	24		−29.6	−38.0	−41.6	−20.8					
	5	77.0	36.4	34.8	2.6	4.2	7.8	15.6		23	9		−21.8	−22.4	−30.2	−5.2					
	6	33.8	18.7	14.6	7.8	10.4	13.0	14.6	13	9			−6.8	−14.6	−14.6						
	7	22.8	7.8	6.2		3.6	12.0														

Run No. 132. Time: 0.73 second

Orifice	1	145	150	156	135	146	109	52	123	111	118	66	13.5	36.4	26.0	18.2					
	2	93	140	135	130	99	130	56	96	102	94	46	13.5	1.6	13.0	−5.2					
	3	114	109	108	95	88	56	40	81	87		25	−10.4	−22.4	−19.8						
	4	112	104	94	35	32	35	22	47	54	31		−27.6	−33.8	−39.0	−19.3					
	5	87	69	48	50	15	16	46		29	12		−17.7	−20.3	−27.6	−4.1					
	6	39	29	22	10	16	25	46	19	10			−5.7	−12.0	−13.5						
	7	24	8	9		5	17														

Run No. 132. Time: 0.98 second

Orifice	1	193	232	237	205	229	182	83	167	148	147	89	27.6	54.6	38.5	28.6					
	2	128	198	182	198	153	167	94	126	138	120	58	19.8	19.2	26.5	3.1					
	3	136	151	143	112	119	74	64	84	106		35	−6.2	−15.6	−10.4						
	4	135	142	110	40	37	43	41	47	58	41		−19.8	−27.6	−31.7	−16.1					
	5	94	73	51		17	26	70		31	17		−14.0	−17.2	−22.9	−4.2					
	6	55		28	21	21	36	61	29	12			−3.1	−10.4	−10.4						
	7			21		9	18														

Run No. 132. Time: 1.23 seconds

Orifice	1	125	122	128	148	198	163	79	130	134	114	76	27.6	45.8	33.8	18.7					
	2	83	83	86	140	130	148	81	101	109	94	54	18.7	14.6	22.9	3.6					
	3	92	59	60	63	96	65	45	75	66		35	−1.6	−12.0	−9.4						
	4	106	75	63	36	33	39	35	37	48	41		−17.2	−23.4	−27.7	−13.5					
	5	77	44			18	23	61		30	22		−12.0	−15.6	−19.8	−4.2					
	6	31			23	21	31	52	24				−2.6	−8.3	−9.4						
	7					8	16														

TABLE III.—RECORDED PRESSURES—Continued

Run No. 132. Time: 1.48 seconds

Rib	Upper wing							Lower wing				Stabilizer and elevator				Vertical tail surfaces				
	A	B	C	D	E	F	G	H	J	K	L	M	N	O	P	Q	R	S	T	U
Orifice 1	125.0	96.2	83.2	118.0	131.0	104.0	80.6	96.2	83.2	105.0	75.3	43.2	64.4	59.8	33.3					
2	78.0	67.6	72.8	100.0	98.8	98.8	51.4	78.0	57.7	80.6	47.8	12.0	12.5	18.2	−.5					
3	78.6	46.8	43.2	46.8	53.0	61.4	38.0	58.7	38.5		28.1	−7.3	−12.5	−10.9						
4	87.4	65.0	41.6	33.3	31.2	33.8	29.6	26.0	32.2	24.9		−14.0	−23.4	−23.9	−11.4					
5	43.2	24.9	23.4		21.3	22.4	49.4		28.0	17.1		−9.9	−16.1	−16.1	−3.1					
6	18.2	22.3	21.8	17.7	23.4	27.6	32.2	15.6	14.5			−4.7	−7.8	−10.4						
7	13.5	10.9			15.6	13.5														

Run No. 132. Time: 1.73 seconds

Orifice 1	96.7	96.0	73.0	99	108	80.6	59	89	83	96.0	66	29	44	42	26					
2	62.0	70.0	66.5	83	83	80.6	40	70	70	70.7	46	7	7	11	−3					
3	67.5	47.0	36.0	37	56	52.0	33	56	39		23	−7	−14	−11						
4	70.0	50.0	31.0	26	25	29.0	19	23	29	26.0		−11	−22	−23	−9					
5	36.5	23.0	22.0		13	14.0	39		23	14.0		−9	−15	−16	3					
6	14.0	18.0	18.0	14	17	22.0	25	15	12			−4	−7	−9						
7	9.0	9.8			8	10.0														

Run No. 137. Pull-up at 181 m. p. h. Time: 0 second

Orifice 1	−36	−78	−94	−107	−110	−122	−29	−96	−94		0		−26.0	−26.0	−13.0					
2	−25	−31	−36	−31	−44	−29	−3	−39	−39	−24	21	−9.4	−39.5	−16.6	0					
3	39	12	−5	44	8	19	8	34	22		21	0	−1.6	−1.6						
4	55	47	42	30	23	25	10	42	44	28		0	9.4	7.3	1.6					
5	65	42	26	9	7	8	13		31	11		.5	1.6	5.2	0					
6	29	21	15	13	16	17	11	10	12			0	−1.0	−4.2						
7	27	9	7		9	5														

Run No. 137. Time: 0.13 second

Orifice 1													−26.0	−39.0	−24.4					
2												−16.6	−30.2	−27.5	−19.7					
3												−23.1	−42.7	−32.2						
4												−44.7	−65.5		−27.0					
5												−35.9	−54.5	−47.8	−14.0					
6												−19.7	−19.2	−20.3						

Run No. 137. Time: 0.38 second

Orifice 1	10	104	5	−78	−31	−65	−3	75	34		63		28	42	24					
2	36	34	42	8	5	26	22	75	65	70	45	−4	−15	−11	−14					
3	88	12	16	86	45	49		94	93		28	−25	−38	−34						
4	112	83	76	41	50	36	15	71	74	44		−43	−65	−44	−28					
5	95	61	38	13	8	9	22		42	16		−29	−48	−45	−8					
6	43	34	27	18	20	19	15	21	16			−14	−20	−20						
7	33	12	10		12	6														

Run No. 137. Time: 0.75 second

Orifice 1	353	340	369	336	299	250	178	241	241		143		151	158	96					
2	216	302	308	318	265	224	128	195	229	239	93	28	26	40	1					
3	215	247	218	198	185	160		146	187		51	−18	−34	−26						
4	260	240	196	78	90	88	65	80	101	58		−36	−62	−50	−26					
5	121	137	74		24	34	115		57	23		−22	−45	−41	−6					
6	74	59	44	29	34	48	75	42	19			−8	−20	−19						
7	41	16	19		21	13														

Run No. 137. Time: 0.92 second

Orifice 1	374.0	403	426	392.0	387.0	313.0	213.0	291	286	247	166		172.0	130.0	115					
2	265.0	356	354	364.0	317.0	265.0	155.0	213	252	220	98	38.0	35.4	36.0	12					
3	249.0	314	258	208.0	208.0	178.0		148	186		69	−11.4	−28.1	−17.0						
4	271.0	255	200	82.6	91.0	98.0	84.2	93	101	74		−29.0	−54.0		−20					
5	165.0	147	91		34.3	41.6	130.0		61			−19.0	−37.0	−34.3	−6					
6	74.4			62.0	36.4	59.7	88.4					−5.0	−16.0	−14.0						
7					23.9	27.0														

Run No. 137. Time: 1 second

Orifice 1	317	263	340	355	368	317	211	268	275		164		176	147	106					
2	202	265	279	325	310	258	152	200	240	203	96	38	37	42	4					
3	199	185	172	161	201	171		147	183		66	−10	−23	−18						
4	210	193	98	85	86	93	77	80	98	76		−28	−52	−44	−21					
5	90				32	42	122		54			−16	−38	−32	−5					
6	64			52	36	55	86					−5	−16	−16						
7					25	29														

TABLE III.—RECORDED PRESSURES—Continued

Run No. 137. Time: 1.25 seconds

Rib	Upper wing							Lower wing				Stabilizer and elevator				Vertical tail surfaces				
	A	B	C	D	E	F	G	H	J	K	L	M	N	O	P	Q	R	S	T	U
Orifice 1	210	211	199	250	169	234	142	208	239		130		143	113	82					
2	139	161	169	215	229	187	106	171	205	168	76	27	15	32	−2					
3	151	143	94	101	140	109	67	116	161		54	−7	−25	−20						
4	161	117	66	62	60	67	56	68	86	65		−25	−49	−42	−21					
5	71	60			18	29	80		47			−18	−36	−31	−6					
6	39			35	29	44	62					−6	−16	−16						
7					18	25														

Run No. 222. Right barrel roll at 167 m. p. h. Time: −0.25 second

Orifice 1	−36.4		−104.0	−114.4		−137.8	−39.0	−93.6	−101.4	−94.6	−5.2	−57	−44	−35		4				4
2	−39.0		−42.6	−49.4	−52.0	−31.2	−10.4	−42.6	−41.6	−24.9	18.2	−11	−40	−16	0	4	2	4		3
3	43.7	10.4	12.0	35.4	8.3	10.4		27.0	18.7		23.4	−3	−1	0		2	4	4		3
4		26.0	40.6	26.0	22.9	22.4	9.4	39.5		23.4			12	8	2	12	13	12	4	
5	70.2	34.8	24.4		8.8	5.0	17.2			10.4		−2	4	6	0		1	9	1	
6	32.3	21.8	13.5	19.2	18.7		11.4					2	−2	−1			4	4	3	
7		8.8	6.8		4.0	6.8														

Run No. 222. Time: 0 second

Orifice 1	−36.4		−104.0	−114.3		−138.0	−39.0	−94.0	−101.4	−94.5	−5.2	−57	−21	−39		5				4
2	−39.0		−42.6	−49.4	−52.0	−31.2	−10.4	−39.0	−41.6	−25.0	18.2	−14	−42	−18	0	4	2	6		3
3	43.7	10.4	12.0	36.4	8.3	10.4		30.2	18.7		23.4	−3	−1	−9		2	4	4		3
4		26.0	40.5	26.0	22.9	22.4	9.4	39.6		25.0			0			12	14	12	5	
5	74.4	36.4	25.0		8.8	4.7	17.2			10.9		−11	−3	−4	0		2	10	1	
6	35.4	21.8	15.1	19.2	18.7		11.4					0	−2	−2			4	4	3	
7		9.4	7.3		4.2	6.8														

Run No. 222. Time: 0.25 second

Orifice 1	−57		−91	−104		−128	−36	−81	−67	−80		43	13	29		13				12
2	−21		−26	−13	0	−23	−8	−30	−31	−10	22	−17	−48	−22	−14	17	6	11		15
3	60	25	23	39	17	18		39	32		26	−21	−23	−24		25	21	29		9
4		32	45	33	25	24	10	45		28			−41		−19	29	36	30	21	
5	87	44	28		9	5	14			11		−31	−35	−32	−8		14	28	13	
6	38	25	17	17	17		10					−15	−17	−14			11	10	7	
7		11	8		4	7														

Run No. 222. Time: 0.50 second

Orifice 1	166		191	33		50.0	94	31	73	32	52	0		16		21				33
2	82			100	95	86.0	43	34	63	70	47	0	−19	−3	−8	38	21	19		27
3	146	113	134	117	109	88.0		75	99		32	−15	−27	−22		48	43	52		21
4		65	112	52	48	50.0		69		36			−49		−18	31	47	47	49	
5	113	94	55		12	8.3	55			14		−21	−30	−30	−5		32	39	36	
6	52	41	31	19	21		34					−11	−11	−13			17	15	16	
7		15	10		7	11.0														

Run No. 222. Time: 0.75 second

Orifice 1	263		338	219		196	151	218	205	192	120			69		−3				37
2	145			228	207	193	86	140	180	161	76	9	9	23	−3	30	0	20		36
3	194	213	208	159	169	137		114	143		47	−10	−17	−14		55	37	42		11
4		99	166	72	68	72		76		47			−30	−36	−17	31	47	53	39	
5	121	116	74		18	22	77			18		−14	−20	−22	−3		29	35	33	
6	49	49	35	24	28		42					−8	−8	−7			14	13	12	
7		17	12		11	17														

Run No. 222. Time: 0.88 second

Orifice 1	299		350	336		374	164	236	224	207	133			66		−3				32
2	161			302	274	244	111	171	198	178	79	12	12	30	0	22	−3	20		34
3	181	239	224	172	180	156		121	146		50	−7	−13	−10		55	32	34		10
4		124	180	74	74	75		67		51			−27	−32	−14	30	42	47	36	
5	113	118	85		27	30	75			20		−11	−18	−19	−3		27	31	28	
6	41	49	34	29	48							−6	−7	−6			13	11	10	
7		19			18	23														

Run No. 222. Time: 1 second

Orifice 1	237		330	322		291	159	224	218	193	135			69		−4				26
2	115			288	182	186	66	160	182	172	75	13	21	33	3	12	−6	19		29
3	130	213	216	159	87	131		108	138		56	−6	−10	−3		35	27	32		9
4		117	171	73	72	68		59		49			−23	−28	−13		36	43	31	
5	96	87	81		43	39	68			20		−8	−17	−16	−3		23	26	25	
6		41		36	52							−5	−6	−3			11	10	8	
7		19			27	29														

TABLE III.—RECORDED PRESSURES—Continued

Run No. 222. Time: 1.50 seconds

Rib		Upper wing							Lower wing				Stabilizer and elevator				Vertical tail surfaces				
		A	B	C	D	E	F	G	H	J	K	L	M	N	O	P	Q	R	S	T	U
Orifice	1	182		73	81	55	42	55	156	156	144	99			66		−9				17
	2	98		77	91	62	69	43	117	141	124	52	17	36	42	20	0	−21	17		19
	3	114	91	87	68	64	69		65	99		38	0	4			13	5	17		7
	4		75	81		54	54		50		35			−10	0			10		16	
	5	70	52	42		31	43	55			16		0	−3	3	7		8	11	13	
	6		33		30	40		34					0	0	3			6	6	5	
	7		17			25	29														

Run No. 222. Time: 2 seconds

Orifice	1	165		52	39	39	26	36	125	110	90	56			61		−10				16
	2	82		52	52	43	47	31	90	96	77	28	22	40	48	33	−2	−21	13		16
	3	114	56	70	39	49	43		55	72		22	5	9			8	0	10		7
	4		50	52	31	36	36		37		19			8	10			7	12	10	
	5	45	39	28		25	26	42			11		5	8	11	9		5	6	10	
	6		20	17	19	25		23					5	4	5			4	4	3	
	7		15			16	21														

Run No. 222. Time: 2.50 seconds

Orifice	1	147		36	26	21	12	31	99	88	80	52			−55		−10				7
	2	82		39	42	30	37	29	67	73	62	22	23	51	36	22	−2	−12	8		9
	3	94	41	57	34	42	39		39	44		21	12	24			−5	3	4		3
	4		43	43	20	33	35		31		16			21	22	17	0	0	0	3	
	5	45	26	20		26	28	43			7		10	17	23	10		−3	2	4	
	6		15	12	19	28		27					9	10	12			2	2	0	
	7		9	12		18	24														

Run No. 225. Left barrel roll at 163 m. p. h. Time: 0 second

Orifice	1	−36		−104	−104		−128	−36	−91	−91	−86	−8			−39				−5	0	5
	2	−30		−36	−44	−43	−29	−8	−39	−36	−18	18		−41	−16	1	2	−3	−3	2	4
	3	44	18	0	39	8	10		30	19		21	0	0			7	3	3		3
	4		22	39	26	23	23	10	40		26			13	11	3		13	8	3	
	5	62	36	24	9	8	5	14			9		2	4	7	0		2	9	4	
	6	33	22	14	16	21		9					0	−1	−2			3	2	3	
	7		9	6		7	5														

Run No. 225. Time: 0.25 second

Orifice	1	−36		−104	−75	−99	−82	−35	−81	−67	−71	8			11				−7	−3	0
	2	−20		−36	0	−10	−26	−8	−13	−23	0	24		−40	−24	−14	−9	−8	−7	−5	−7
	3	44	18	10	46	8	15		44	30	30	22	−9	−26	−26		−17	−12	−18		−3
	4		26	39	29	25	24	12	48		11			−14		−19		−18	−17	−5	
	5	70	39	26	12	9	7	14					−24	−37	−34	−10		−14	−12	−10	
	6	35	26	15	17	23		11					−9	−16	−17			−5	−2	−7	
	7		12	8		8	8														

Run No. 225. Time: 0.50 second

Orifice	1	110		41	81	69	63	39	31	73	0	70			34					−6	−19
	2	48		88	114	78	57	22	77	70	120	47		−17	−6	−8	−18	−15	−6	−9	−12
	3	88	64	73	99	80	69		89	75		32	−10	−24	−23		−31	−27	−34		−7
	4		50	86	48	41	42		74		38			−49		−18		−30	−30	−30	
	5	104	69	45	19	13	14	52			14		−22	−36	−33	−3		−18	−20	−28	
	6	52	35	27	24	31		44					−6	−15	−16			−6	−5	−10	
	7		16	12		13	16														

Run No. 225. Time: 0.75 second

Orifice	1	358		364	314	284	234	119	218	205	211	120			73						−29
	2	159			289	255	217	108	164	169	190	81		9	23	5	−18	−5	3	−9	−17
	3	220	232	234	176	169	144		125	146		43	−6	−21	−19		−33	−28	−39		−8
	4		93	182	66	69	78		83		49			−51		−18		−34	−33	−36	
	5	138	121	66	23	27	34	138			17		−19	−37	−32	−3		−20	−24	−30	
	6	72	56	39	33	40		85					−2	−16	−15			−3	−5	−13	
	7		19	17		20	25														

Run No. 225. Time: 0.88 second

Orifice	1	397		381	351	334	255	155	245	241	248	141									−24
	2	191			320	274	227	127	188	203	203	86		35	36	4	−17	−3	7	−7	−18
	3	240	273	252	187	185	156		125	161		50	3	−19	−16		−33	−30	−35		−8
	4		105	193	74	83	87		83		52			−54	−53	−17		−34	−30	−33	
	5	138	130	88	25	30	43	156			20		−17	−34	−29	−3		−20	−22	−28	
	6	77	52	40	36	40		96					−2	−15	−12			−2	−5	−13	
	7		26	20		22	28														

TABLE III.—RECORDED PRESSURES—Continued

Run No. 225. Time: 1 second

Orifice	Upper wing							Lower wing				Stabilizer and elevator				Vertical tail surfaces				
Rib	A	B	C	D	E	F	G	H	J	K	L	M	N	O	P	Q	R	S	T	U
1	358		356	338	328	218	179	272	265	236	153	47								−21
2	225			312	262	220	122	200	224	197	85		36	43	6	−16	0	10	−7	−18
3	226	270	242	182	177	152		125	166		54	0	−13	−13		−35	−28	−33		−9
4		99	182	81	84	84		74		55		−16	−49	−44	−15		−34	−29	−28	
5	121	121	88	21	33	42	150			20		−2	−29	−26	−3		−18	−20	−24	
6	72	41	37	36	40		90						−12	−11			−2	−4	−12	
7		19	19		20	27														

Run No. 225. Time: 1.50 seconds

Orifice	Upper wing							Lower wing				Stabilizer and elevator				Vertical tail surfaces				
Rib	A	B	C	D	E	F	G	H	J	K	L	M	N	O	P	Q	R	S	T	U
1	164		179	165	146	63	57	132	131	140	115	41								−16
2	92			148	112	99	43	113	96	97	66		29	30	5	−11	2	6	−7	−18
3	119	153	124	96	87	69		101	58		47	2	−10	−9		−23	−17	−21		−12
4		68	100	45	45	42	18	52		57			−30	−28	−9		−24	−20	−20	
5	70	66	45	15	20	25	75					−11	−19	−15	−2		−12	−15	−19	
6	30	30	22	26	31		39					−1	−9	−8			−9	−4	−9	
7		12	8		13	15														

Run No. 225. Time: 2 seconds

Orifice	Upper wing							Lower wing				Stabilizer and elevator				Vertical tail surfaces				
Rib	A	B	C	D	E	F	G	H	J	K	L	M	N	O	P	Q	R	S	T	U
1	110		113	94	73	42	29	122	135	137	103	41								−17
2	58		85	95	65	52	21	96	114	107	59	20	25	28	3	−9	0	6	−5	−17
3	84	109	82	69	55	42		81	68		41	2	−8	−9		−21	−14	−18		−11
4		47	76	35	32	30	14	41		44			−25	−24	−9		−22	−17	−18	
5	53	51	34	13	17	18	49					−10	−15	−15	−2		−12	−15	−19	
6	21	25	17	19	26		23					0	−7	−9			−12	−4	−9	
7		7	7		11	12														

Run No. 225. Time: 3 seconds

Orifice	Upper wing							Lower wing				Stabilizer and elevator				Vertical tail surfaces				
Rib	A	B	C	D	E	F	G	H	J	K	L	M	N	O	P	Q	R	S	T	U
1	57		93	91	93	68	39	68	94	93	66	24		61						−13
2	26		72	83	72	67	26	62	86	73	35	13	21	23	5.0	−9	−12	2	−5	−12
3	46	73	62	55	55	43		51	58		25	4	0	−2		−17	−14	−15		−9
4		36	55	25	26	26	14	28		21			−10	−12	−4.0		−18	−12	−12	
5	35	31	23	10	13	16	34			9		−15	−4	−6	−.5		−10	−13	−12	
6	19	12	13	16	19		13					−1	−2	−4			−19	−5	−8	
7		5	6		8	9														

Run No. 227. Left spin. Time: 0 second

Orifice	Upper wing							Lower wing				Stabilizer and elevator				Vertical tail surfaces				
Rib	A	B	C	D	E	F	G	H	J	K	L	M	N	O	P	Q	R	S	T	U
1	27	42	39	33	30	19	17	25	22	15	16	18	13	12	9	2		4	−3	−3
2	23	42	31	29	20	18	11	20	23	9	9	4	3	3	2	2	2	1	−2	−4
3	25	31	26	18	20	15	9	12	10		5	−1	−1	−1		−5	−3	−3		−2
4	23	8	18	9	8	8	5	5		11		−3	−4	−5	−2	−2	−4	−4	−4	
5	13	12	11	2	3	5	12			4		−2	−3	−3	−1	0	−3	−2	−3	
6	8	6	4	5	4	5	8	3				0	−1	−2			−1	−1	−2	
7	4	2	1		2	3														

Run No. 227. Time: 1 second

Orifice	Upper wing							Lower wing				Stabilizer and elevator				Vertical tail surfaces				
Rib	A	B	C	D	E	F	G	H	J	K	L	M	N	O	P	Q	R	S	T	U
1	35	39	36	30	21	9	13	25	26	15	26	22	20.0	18	15.0	4		4	−3	−3
2	23	42	30	26	15	16	8	21	27	9	8	6	5.0	4	3.0	−1	4	2	−2	−5
3	29	31	26	18	19	13	7	12	10		5	0	−.5	−1		−5	−3	−3		−2
4	26	8	21	10	9	8	5	7		11		−3	−3.0	−6	−2.0	−2	−5	−4	−4	
5	15	14	12	3	3	5	12			5		−2	−3.0	−3	−.5	0	−3	−3	−3	
6	9	7	5	8	4	5	5	3				−1	−1.0	−2			2	−1	−2	
7	4	2	2		2	3														

Run No. 227. Time: 1.50 seconds

Orifice	Upper wing							Lower wing				Stabilizer and elevator				Vertical tail surfaces				
Rib	A	B	C	D	E	F	G	H	J	K	L	M	N	O	P	Q	R	S	T	U
1	52.0	62.4	54.6	48.9	39.0	21.9	20	40	36	18	31	27	27.0	28	20.0	4		4	−5	−4
2	39.0	57.0	44.2	39.0	29.8	20.8	14	34	32	14	15	10	9.0	8	6.0	0	6	2	−3	−5
3	41.6	45.8	39.0	27.6	26.0	18.2	12	19	16		9	1	0	0		−5	−1	−3		−2
4	36.4	15.6	26.5	13.5	11.9	11.9	8	13		15		−3	−3.0	−4	.5	−2	−5	−4	−4	
5	15.6	18.7	16.1	3.6	4.2	4.7	16			7		−1	−3.0	−3	2.0	0	−3	−3	−3	
6	12.5	8.8	6.8	7.3	3.6	6.8	12	3				1	.5	−2			4	−2	−2	
7	5.7	3.1	3.1		2.1	4.2														

Run No. 227. Time: 1.75 seconds

Orifice	Upper wing							Lower wing				Stabilizer and elevator				Vertical tail surfaces				
Rib	A	B	C	D	E	F	G	H	J	K	L	M	N	O	P	Q	R	S	T	U
1	62.4	79.0	67.6	64.5	52.0	32.8	23.9	49	16	18	16	31	35	36	21	5		4	−6	−4
2	47.9	70.2	60.3	52.0	36.4	30.2	16.6	33	30	14	11	13	12	14	9	0	6.0	1	−3	−5
3	52.0	56.2	47.8	32.2	33.3	22.9	15.6	21	19		13	3	2	2		−3	−.5	−4		−4
4	41.6	18.2	33.8	14.6	13.5	14.0	9.9	16		16		−1	−3	−3	2	−1	−4.0	−3	−4	
5	17.2	20.8	18.2	4.2	5.2	6.8	19.8			9		0	−2	−2	6	0	−2.0	−3	−3	
6	14.0	10.4	7.8	7.0	5.7	8.8	15.1	52				2	0	−2			6.0	−2	−2	
7	6.8	4.2	4.2		2.1	4.2														

TABLE III.—RECORDED PRESSURES—Continued

Run No. 227. Time: 2 seconds

Rib		Upper wing							Lower wing				Stabilizer and elevator				Vertical tail surfaces				
		A	B	C	D	E	F	G	H	J	K	L	M	N	O	P	Q	R	S	T	U
Orifice	1	62	87	75	68	57	35	26	36	13	18	16	30	39.0	42.0	10	5		4	−6	−4
	2	48	75	66	57	42	32	18	29	27	16	15	15	15.0	15.0	9	1	6	1	−3	−7
	3	44	58	51	35	34	24	16	21	16		15	4	2.0	2.0		−3	0	−4		−4
	4	40	18	33	16	14	15	10	16		18		0	−3.0	−3.0	3	0	−1	−3	−4	
	5	17	23	19	5	6	7	20			9		1	−.5	−.5	9	1	−2	−3	−4	
	6	18	11	8	7	6	7	16	6				3	0	−1.0			7	−3	−2	
	7	8	5	5		4	3												−2		

Run No. 227. Time: 2.25 seconds

Orifice	1	52	87	79	73	57	35	26	20	13	18	22	27	39	44.0	6	6		4	−4	−9
	2	39	75	68	60	42	32	18	26	23	20	17	17	16	15.0	9	1	6	1	−2	−8
	3	38	56	51	35	36	24	15	19	16		17	4	4	3.0		−2	0	−4		−4
	4	36	18	34	17	15	15	9	16		21		2	−1	−2.0	3	−1	−3	−3	−4	
	5	19	23	19	5	5	7	22			11		2	2	−.5	7	2	−2	−3	−4	
	6	20	12	9	7	6	7	14	7				3	1	−1.0			8	−2	−2	
	7	12	5	6		4	2														

Run No. 227. Time: 2.50 seconds

Orifice	1	23	69	61	58	45	25	18	31	13	21	22	25	29	28	3.0	4		2	−2	−6
	2	18	61	55	44	33	25	13	26	23	20	17	17	16	13	7.0	−5	0	1	2	−8
	3	25	43	40	29	30	21	9	19	16		17	4	7	2		−7	−4	−4		−4
	4	19	16	27	14	13	11	5	15		21		4	2	0	.5	−4	−6	−3	−4	
	5	17	18	14	4	4	5	16			12		2	4	2	4.0	2	−3	−3	−5	
	6	10	8	6	7	6	7	8	5				3	3	0			9	−3	−2	
	7	9	5	3		4	2														

Run No. 227. Time: 2.75 seconds

Orifice	1	27	42	39	33	21	6	9	36	16	23	26	30.0	26	28	8	4		0	0	−6
	2	18	42	35	29	15	12	7	29	21	20	17	15.0	19	14		−5	−2	0	1	−8
	3	25	31	29	23	20	15	6	19	10		22	4.0	5			−7	−6	−5		−4
	4	11	16	22	12	11	10	3	10		20		.5	0	3	3	−4	−9	−6	−5	
	5	13	14	13	3	4	5	13			9		1.0	4	4	7	2	−5	−4	−5	
	6	6	7	6	10	6	7	5	3				4.0	3	0			11	−3	−4	
	7	8	4	2		4	3														

Run No. 227. Time: 3 seconds

Orifice	1	27	46	42	36	23	9	9	36	16	26	26	34.0	34	44		4		0	0	−7
	2	21	44	37	31	17	16	7	30	21	20	24	17.0	20	17	9	−5	−2	0	2	−8
	3	29	34	31	25	23	15	7	21	11			4.0	4			−7	−7	−6		−4
	4	19	16	24	14	12	11	4	11		20		.5	−1	3	2	−4	−9	−8	−6	
	5	13	16	15	4	4	5	12			9		.5	4	2	7	2	−5	−5	−5	
	6	8	8	7	10	6	9	5	2				3.0	3	0			12	−4	−4	
	7	8	4	2		4	3														

Run No. 227. Time: 3.50 seconds

Orifice	1	41	79	73	68	54	31	21	52	21	30	36	27	32	34		3	0	6	0	−9
	2	33	70	66	55	40	32	14	39	27	23	30	21	22	19	10	−5	−7	0	2	−10
	3	37	56	51	39	36	25	13	23	19			6	8			−8	−9	−7		−4
	4	31	18	36	19	17	16	8	15		22		3	2	6	2	−4	−5	−8	−7	
	5	19	24	21	5	6	7	22			13		2	4	3	5	3	17	−5	−9	
	6	12	12	9	10	8	10	12	8				3	3	0				−4	−5	
	7	11	4	4		4	3														

Run No. 227. Time: 3.75 seconds

Orifice	1	42	87	79	72	57	35	24	52	21	30	31	35	32	28		4		11	−2	−9
	2	33	75	72	60	46	35	17	41	27	26	28	24	23	18	11	−6	0	0	2	−10
	3	38	58	54	41	39	28	15	26	19		25	8	10			−8	−7	−7		−4
	4	29	22	39	19	18	17	9	18		24		5	3	7	7	−6	−9	−6	−7	
	5	19	26	21	5	6	9	23			14		2	5	7	9	4	−6	−4	−8	
	6	14	12	9	12	8	10	11	6				3	4	2			19	−4	−5	
	7	12	4	4		4	3														

Run No. 227. Time: 4 seconds

Orifice	1	35	82	75	72	57	31	23	49	21	44	31	36	30	25		4		11	−2	−7
	2	26	70	66	57	43	35	16	39	27	26	26	23	24	18	11	−6	0	−1	2	−10
	3	31	53	51	39	39	25	12	21	19		23	8	9			−8	−7	−6		−4
	4	19	22	36	19	17	16	8	16		24		5	3	6		−6	−7	−2	−5	
	5	19	23	20	5	6	9	22			16		2	5	9	7	4	−5	−3	−8	
	6	11	12	83	12	8	10	9	5				3	4	4			20	−4	−5	
	7	10	5	3		4	3														

TABLE III.—RECORDED PRESSURES—Continued

Run No. 227. Time: 4.50 seconds

Rib		Upper wing							Lower wing				Stabilizer and elevator				Vertical tail surfaces				
		A	B	C	D	E	F	G	H	J	K	L	M	N	O	P	Q	R	S	T	U
Orifice	1	31	58	52	49	36	19	17	47	22	33	34	34.0	30	28		4		6	0	−7
	2	23	51	49	42	30	21	10	36	27	26	28	17.0	26	20	7	−7	0	1	3	−10
	3	29	43	36	32	30	23	9	23	19		30	3.0	8			−11	−7	−6		−4
	4	11	18	29	16	15	14	5	13		22		2.0	3	5		−8	−10	−5	−5	
	5	17	18	16	5	6	7	16			15		.5	5	6	5	4	−7	−4	−8	
	6	9	9	7	10	8	10	7	3				4.0	4	3			25	−4	−5	
	7	9	7	3		4	3														

Run No. 227. Time: 4.75 seconds

Rib		Upper wing							Lower wing				Stabilizer and elevator				Vertical tail surfaces				
		A	B	C	D	E	F	G	H	J	K	L	M	N	O	P	Q	R	S	T	U
Orifice	1	35	55	49	46	33	16	15	47	22	33	36	34.0	30	41		4		6	0	−9
	2	23	51	44	39	26	21	10	36	27	26	30	13.0	24	20	10	−7	2	2	2	−10
	3	29	41	36	32	30	23	9	23	19		22	3.0	7			−14	−9	−6		−4
	4	11	18	29	16	15	14	5	13		22		.5	2	3		−8	−12	−7	−6	
	5	17	18	16	5	6	7	16			16		.5	4	5	8	6	−7	−5	−8	
	6	10	8	7	10	8	10	7	4				4.0	3	2			27	−5	−5	
	7	7	5	3		4	3														

Run No. 227. Time: 5 seconds.

Rib		Upper wing							Lower wing				Stabilizer and elevator				Vertical tail surfaces				
		A	B	C	D	E	F	G	H	J	K	L	M	N	O	P	Q	R	S	T	U
Orifice	1	42	65	61	55	45	22	19	56	52	35	41	37	32.0	54		4		6	−3	−9
	2	30	61	55	49	36	27	13	43	44	29	35	17	23.0	23	13	−5	2	1	0	−10
	3	38	51	46	37	34	24	11	29	25		18	4	3.0			−9	−6	−8		−5
	4	29	18	36	19	17	16	7	16		25		2	5	0	5	−4	−10	−9	−8	
	5	21	23	20	5	6	7	18			16		1	0	2	9	6	−7	−7	−9	
	6	12	11	9	12	8	10	9	7				4	1.0	−1			30	−5	−5	
	7	10	4	4		4	3														

Run No. 230. Right spin. Time: 0 seconds.

Rib		Upper wing							Lower wing				Stabilizer and elevator				Vertical tail surfaces				
		A	B	C	D	E	F	G	H	J	K	L	M	N	O	P	Q	R	S	T	U
Orifice	1	10	28	21	23	23	19	13	16	22	26	10	3	9	13	6.0	2		1	0	3
	2	10	21	25	18	17	20	8	15	21	20	6	0	1	2	−.5	2	−6	1	2	3
	3	10	16	18	8	12	10	7	12	10		4	−2	−2	−2		4	4	4	3	0
	4	7	4	11	5	6	7	5	5	9	7		−1	−4	−4	−3.0	−2	3	4	3	
	5	5	9	6	3	4	3	5	9		2		−2	−3	−3	−.5	5	4	2	2	
	6	3	2	3	3	4	3	4	0	2			−2	−1	−3			0	2	0	
	7	4	2	1		2	2														

Run No. 230. Time: 1 second.

Rib		Upper wing							Lower wing				Stabilizer and elevator				Vertical tail surfaces				
		A	B	C	D	E	F	G	H	J	K	L	M	N	O	P	Q	R	S	T	U
Orifice	1	16	39	36	38	39	31	19	20	26	30	13	3	2.0	9	4.0	2		−3	2	3
	2	21	31	35	31	30	30	13	16	23	22	8	0	−.5	3	−.5	4	−6	1	2	3
	3	19	22	29	20	23	17	10	16	10		5	−3	−2.0	−2		6	4	6	3	0
	4	16	8	18	11	10	12	6	7	11	8		−1	−5.0	−5	−3.0	−2	8	6	5	
	5	13	12	12	2	4	5	5	10		2		−2	−4.0	−3	−.5	5	4	4	2	
	6	6	5	5	3	4	3	4	−1	2			−2	−2.0	−3			0	2	0	
	7	4	2	1		2	2														

Run No. 230. Time: 1.75 seconds.

Rib		Upper wing							Lower wing				Stabilizer and elevator				Vertical tail surfaces				
		A	B	C	D	E	F	G	H	J	K	L	M	N	O	P	Q	R	S	T	U
Orifice	1	20	58	55	58	60	49	29	29	36	37	19	3	2	12	9.0	4		−3	3	3
	2	26	47	53	49	46	43	20	21	32	29	11	0	1	3	.5	4	−7	0	2	3
	3	25	35	40	29	33	23	16	19	19		7	−3	−2	−2		6	4	6	3	0
	4	18	11	24	14	14	16	9	9	13	9		−2	−7	−4	−2.0	−1	6	7	5	
	5	15	18	16	4	9	7	8	11		4		−2	−4	−3	−.5	5	4	2	4	
	6	7	7	7	3	6	7	4	−2	4			−2	−2	−3			0	2	1	
	7	6	4	3		4	3														

Run No. 230. Time: 2 seconds.

Rib		Upper wing							Lower wing				Stabilizer and elevator				Vertical tail surfaces				
		A	B	C	D	E	F	G	H	J	K	L	M	N	O	P	Q	R	S	T	U
Orifice	1	20	62	61	61	54	31	21	29	42	42	19	3	3	15	7.0	5		−2	3	3
	2	23	51	57	55	43	20	16	23	32	29	11	0	1	3	2.0	3	−9	0	2	3
	3	25	39	43	30	30	17	14	19	19		7	−3	−2	−2		6	5	3	3	0
	4	16	11	27	15	20	23	9	9	13	11		−3	−9	−4	−.5	−1	8	8	5	
	5	15	18	17	5	11	9	9	11		4		−3	−4	−2	−.5	3	4	4	4	
	6	7	14	7	5	10	9	5	−2	6			−2	−2	−3			0	2	1	
	7	8	5	3		6	2														

Run No. 230. Time: 2.25 seconds.

Rib		Upper wing							Lower wing				Stabilizer and elevator				Vertical tail surfaces				
		A	B	C	D	E	F	G	H	J	K	L	M	N	O	P	Q	R	S	T	U
Orifice	1	18	59	65	61	42	19	15	31	45	42	19	3	4	17	9.0	4		0	3	3
	2	23	55	60	55	30	20	10	26	35	32	13	1	1	3	2.0	2	−7	0	3	4
	3	25	41	46	23	23	15	10	19	21		9	−3	−2	−2		5	4	6	3	0
	4	18	16	27	19	15	17	9	9	13	11		−1	−10	−4	−1.0	0	6	8	5	
	5	15	18	17	6	15	16	8	11		4		−2	−4	−2	−.5	4	4	4	4	
	6	7	15	9	5	13	10	5	−2	6			−2	−2	−2			0	2	1	
	7	9	6	4		8	2														

TABLE III.—RECORDED PRESSURES—Continued

Run No. 230. Time: 2.50 seconds.

Rib		Upper wing							Lower wing				Stabilizer and elevator				Vertical tail surfaces				
		A	B	C	D	E	F	G	H	J	K	L	M	N	O	P	Q	R	S	T	U
Orifice	1	20	73	55	39	33	16	13	35	45	44	19	3	6	16	9	4	------	5	3	3
	2	26	57	44	31	30	20	10	26	35	35	13	1	3	4	3	2	−5	1	3	4
	3	25	43	26	28	23	17	11	21	21	------	9	−3	−2	−1	------	6	4	6	3	0
	4	16	16	22	20	17	17	9	10	16	11	------	−1	9	−5	−2	−1	6	8	5	------
	5	16	18	21	8	13	11	8	14	------	4	------	−2	−4	−3	−1	4	4	4	4	------
	6	10	12	16	8	13	12	7	−2	5	------	------	−2	−2	−3	------	------	0	2	1	------
	7	9	6	6	------	8	2	------	------	------	------	------	------	------	------	------	------	------	------	------	------

Run No. 230. Time: 3 seconds.

Orifice	1	27	55	42	21	17	16	13	36	48	47	19	5	13	21	13.0	4	------	5	4	4
	2	26	42	32	31	17	20	11	30	38	35	13	2	4	7	4.0	1	−6	1	3	5
	3	25	26	26	22	20	17	13	23	26	------	7	−3	−2	−1	------	5	4	6	3	0
	4	26	16	18	14	15	17	10	13	18	11	------	−2	−9	−6	−2.0	−1	6	8	5	------
	5	16	18	18	6	11	11	8	16	------	4	------	−2	−4	−4	−.5	4	------	4	4	------
	6	11	12	10	8	10	12	7	2	5	------	------	−2	−2	−3	------	------	0	2	1	------
	7	10	6	7	------	8	3	------	------	------	------	------	------	------	------	------	------	------	------	------	------

Run No. 230. Time: 3.75 seconds

Orifice	1	27	52	36	17	17	16	13	36	48	47	19	7	16	25	16.0	2	------	5	2	4
	2	39	38	27	18	17	20	13	30	38	31	13	3	7	9	7.0	1	−6	2	3	7
	3	35	26	24	15	19	17	14	21	25	------	5	−3	−1	−2	------	6	4	6	3	−1
	4	26	11	11	11	15	18	11	15	18	9	------	−3	−9	−8	−2.0	0	6	8	6	------
	5	13	14	12	5	11	11	9	------	------	4	------	−3	−6	−5	−.5	4	------	4	4	------
	6	11	9	8	5	10	10	8	3	3	------	------	−2	−1	−3	------	------	0	2	1	------
	7	8	5	5	------	6	4	------	------	------	------	------	------	------	------	------	------	------	------	------	------

Run No. 230. Time: 4 seconds

Orifice	1	42	55	42	39	21	16	13	25	34	30	9	12	26	28	19.0	5	------	−3	0	5
	2	33	48	42	29	14	17	11	19	27	22	9	3	4	7	−.5	4	−6	0	1	7
	3	31	34	31	15	14	10	11	21	19	------	4	−3	−4	−4	------	8	5	6	3	−2
	4	29	11	16	12	10	12	8	10	18	9	------	−4	−10	−10	−4.0	2	8	8	7	------
	5	13	14	14	2	8	7	8	------	------	2	------	−4	−7	−7	−1.0	4	------	4	4	------
	6	10	7	12	3	8	7	5	0	3	------	------	−2	−4	−5	------	------	0	3	1	------
	7	7	4	4	------	4	3	------	------	------	------	------	------	------	------	------	------	------	------	------	------

Run No. 230. Time: 4.5 seconds

Orifice	1	39	82	68	58	33	22	35	36	52	50	21	8	29	39	19	6	------	−3	7	7
	2	39	73	66	49	23	21	36	30	42	35	15	3	8	10	2	4	−7	0	4	7
	3	42	53	52	25	20	15	15	26	29	------	9	−2	−2	−2	------	9	5	8	3	−1
	4	42	16	27	20	15	19	14	15	21	13	------	−4	−11	−8	−5	0	8	8	7	------
	5	23	23	19	5	13	11	9	------	------	5	------	−3	−5	−5	−1	4	------	4	5	------
	6	12	10	19	5	10	12	9	5	4	------	------	−4	−1	−4	------	------	0	3	1	------
	7	10	4	7	------	8	3	------	------	------	------	------	------	------	------	------	------	------	------	------	------

Run No. 230. Time: 4.9 seconds

Orifice	1	16	100	79	64	33	25	23	50	61	62	25	8	26.0	40	19	6	------	4	9	7
	2	26	78	74	52	23	23	24	39	55	43	17	4	10.0	14	7	1	−6	1	5	7
	3	31	59	55	29	24	18	18	29	35	------	10	−2	−.5	0	------	6	5	6	3	−1
	4	42	18	29	20	19	25	17	16	22	15	------	−3	−15.0	−7	−3	−1	4	8	7	------
	5	23	23	25	5	21	18	13	------	------	6	------	−2	−5.0	−4	−1	4	------	4	5	------
	6	17	15	18	17	13	19	11	5	5	------	------	−2	−2.0	−3	------	------	0	2	2	------
	7	16	9	7	------	10	3	------	------	------	------	------	------	------	------	------	------	------	------	------	------

Run No. 230. Time: 5 seconds

Orifice	1	52	82	68	55	26	30	17	52	69	65	29	8	26	45	16.0	6	------	5	9	7
	2	33	67	74	42	23	27	18	41	57	47	19	5	11	15	10.0	1	−5	2	6	7
	3	38	48	43	25	24	21	19	29	37	------	10	−1	1	1	0	5	4	5	3	−1
	4	42	18	24	19	21	27	17	18	22	15	------	−3	−15	−6	−.5	−1	3	8	5	------
	5	27	23	24	6	22	20	13	------	------	6	------	−2	−5	−3	------	4	------	4	1	------
	6	18	17	16	12	15	18	12	5	5	------	------	−2	−2	−3	------	------	0	3	1	------
	7	18	10	6	------	10	4	------	------	------	------	------	------	------	------	------	------	------	------	------	------

Run No. 230. Time: 5.25 seconds

Orifice	1	62	58	28	23	23	26	15	50	73	68	31	9	------	61	13	4	------	8	9	7
	2	48	44	53	26	26	27	18	39	57	47	21	8	14	17	15	1	−6	4	6	7
	3	44	39	34	25	29	24	21	26	37	------	11	0	4	3	------	4	4	5	3	−1
	4	39	25	22	17	26	29	------	21	22	15	------	−3	−11	−5	1	−1	5	4	3	------
	5	27	24	19	6	22	20	16	------	------	6	------	−2	−4	−2	0	3	------	4	2	------
	6	20	20	12	10	17	20	12	5	------	------	------	−2	−1	−2	------	------	−2	2	1	------
	7	17	12	6	------	13	6	------	------	------	------	------	------	------	------	------	------	------	------	------	------

TABLE III.—RECORDED PRESSURES—Continued

Run No. 230. Time: 5.50 seconds

Rib		Upper wing							Lower wing				Stabilizer and elevator				Vertical tail surfaces				
		A	B	C	D	E	F	G	H	J	K	L	M	N	O	P	Q	R	S	T	U
Orifice	1	45	28	23	23	21	19	18	52	73	68	28	18		25	8	4		11	9	9
	2	33	34	35	29	26	27	21	34	51	49	19	15	24	36	11	1	−9	4	5	10
	3	31	26	34	22	30	25	24	29	37		10	6	10	6		8	5	8	3	−4
	4	31	25	18	16	26	29		21	24	15		−3	−5	3	5	0	8	7	10	
	5	13	19	16	6	19	18	16			6		−2	2	7	2	3		4	6	
	6	19	11	8	7	19	20	13	5				−2	3	3			3	3	2	
	7	12	8	5		16	8														

Run No. 230. Time: 6 seconds

Orifice	1	49	35	57	20	21	19	18	56	69	58	22	27		30	13	2		17	9	9
	2	39	38	35	26	23	25	20	46	57	43	17	10	14	23	8	5	−10	4	5	11
	3	31	31		20	24	21	22	31	42		7	3	5	9		8	6	8	3	−2
	4	31	22	21	15	19	24		21	24	13		−3	1	2	6	3	6	8	6	
	5	15	18	16	6	14	14	13			6		−2	0	2	3	3		4	7	
	6	18	9	8	7	13	17	11	4	5			−2	2	−2			2	4	2	
	7	10	3	5		10	9														

Run No. 230. Time: 6.50 seconds

Orifice	1	77	62	49	23	23	22	18	66	75	65	26	37.0		34	13	2		17	9	9
	2	57	44	32	36	26	27	20	51	61	50	19	18.0	32	30	11	7	−10	6	4	14
	3	48	31		22	29	23	23	38	44		9	5.0	8	9		11	6	9	3	−2
	4	36	25	22	17	22	25		23	28	15		−3.0	−3	3	9	3	9	12	9	
	5	21	19	17	7	16	16	13			6		.5	−3	6	4	3		4	7	
	6	20	12	10	7	15	15	11	3	6			−2.0	−2	2			2	4	2	
	7	13	6	6		10	9														

Run No. 230. Time: 7 seconds

Orifice	1	52	35	28	42	23	22	20	74	84	77	31	15		31	13	2		22	9	10
	2	42	44	32	34	29	30	26	56	70	56	20	23	29	30	11	12	−11	7	3	14
	3	35	34		25	33	28	28	35	51		10	12	12	9		11	7	11	3	−2
	4	51	29	27	22	27	32		28	30	16		−3	3	3	9	4	10	17	9	
	5	27	24	20	9	20	20	18			6		3	6	6	4	3		4	8	
	6	27	15	11	7	19	17	15	3	12			2	6	2			0	4	2	
	7	14	7	6		16	10														

Run No. 211. Inverted flight at 79 m. p. h.

Orifice	1	−36	−52	−32	−21	−21	−52	−17	−91	−68	−68	−31	21	18	18	5					
	2	−42	−36	−26	−21	−25	−26	−12	−52	−34	−34	−13	−9	−13	−9	−5					
	3	−16	−29	−18	−21	−14	−13	−4	−21	−21		−4	−5	−6	−5						
	4	−35	−6	−13	−5	−6	−3	−1	−7		−3		−7	−9	−8	−5					
	5	−7	−12	−9	1	−4	3	7			1		−6	−6	−5	−2					
	6	−4	−5	−4	8	−5	−3	−1	2	2			−3	−4	−4						
	7		−2	1		−5	2														

Run No. 226. Dive at 260 m. p. h.

Orifice	1	−158	−296	−348	−419	−423	−440	−149	−373	−394	−338	−70	−133	−104	−81	−46					
	2	−88		−183		−182	−117	−148	−184	−207	−149	24	−30	−93	−40	−4					
	3	41	−31	−73	55	−37	19	−6	−10	−31		46	−8	−9	−7						
	4		32	41	44	40	36	17	66	78	49			2	−7	−3					
	5	114	62	37	20	18	11	32	53		19		−8	−8	−5	−1					
	6	58	43	27	34	49		24		23			−5	−9	−11						
	7		18	25		22	13														

Run No. 226. Pull out from dive

Orifice	1	36.4		−120	−151	−203	−216	−72	−140	−176	−151	0	−70.0	−65.0	−21.0	−2.6	68		90	49	17
	2	32.2		−14	−32	−41	−52	0	−42	−62	−13	78	−23.0	−88.0	−18.0	4.2	30	40	41	31	17
	3	177.0	140.0	66	−148	52	55	25	88	82		62	−6.2	−6.2	−2.6		47	26	20		10
	4		104.0	146	78	73	67		110	124	75			7.3	3.6	0	43	50	47	21	
	5	147.0	130.0	88	20	20	11	49	78		26		−5.2	−12.5	2.6	−.5	52	25	39	16	
	6	78.4	59.2	29	26	39		26					0		−8.8			22	14	13	
	7		24.4	16		18	13														

Run No. 215. Push down at 180 m. p. h.

Orifice	1	−120		−188	−198	−193	−198	−70	−183	−172	−141	−43	−73	−78	−61	−39					
	2	−75		−94	−93	−90	−70	−24	−95	−98	−60	7	−11	−30	−7	10					
	3	5	−26	−41	10	−21	−7	−3	0	−15		21	9	18	19						
	4		18	14	15	11	14	6	26	33	16	8		46	45	20					
	5		18	12	7	6	7	22	24		8		20	26	31	6					
	6	14	12	9	13	11	13	10	9	11			8	12	10						
	7	20	7	5		4	5														

TABLE IV.—RECORDED PRESSURES IN SLIPSTREAM

[Pounds per square foot]

Rib		A	A′	B	A″	A‴	B′	H	H′	V	W	X	Y
Run No. 300. Level flight at 82.7 m. p. h.													
Orifice	1	27	16	21	31	34	21	21	−5	−12	0.5	7	0
	2	16	25	26	26	31	26	22	0	−4	−5.0	0	0
	3	31	26	26	36	35	34	29	16	0	1.0	3	4
	4	31	26	26	44		27	19	16	4	6.0	7	3
	5	23	17	17	23	20	19	13	10	5	4.0	4	1
	6	14	9	10	16	11	8	5	4	1	0	1	
	7	10	4	3	6	5	4						
Run No. 302. Level flight at 114.5 m. p. h.													
Orifice	1	0	−10	−9	13	16	−10	−16	−49	−25	−13	−10	−8
	2	0	5	5	16	16	18	0	−29	−9	−15	−6	−3
	3	31	21	16	36	35	34	26	5	−1	1	3	7
	4	31	31	29	52		36	24	19	6	9	10	5
	5	37	20	17	31	27	26	18	16	8	5	7	1
	6	20	12	15	25	18	10	7	7	3	0	1	
	7	16	7	5	11	8	6						
Run No. 305. Level flight at 156.7 m. p. h.													
Orifice	1	−39	−78	−57	−31	−26	−78	−81	−135	−52	−52.0	−39	−23
	2	−28	−26	−18	−3	10	−20	−33	−93	−22	−43.0	−18	−5
	3	34	17	11	36	44	21	29	−8	−3	.5	3	9
	4	44	46	36	70		42	40	24	7	15.0	17	9
	5	70	25	34	41	40	35	27	23	9	6.0	12	2
	6	33	15	22	39	23	18	10	11	3	−2.0	1	
	7	26	8	9	18	11	9						
Run No. 314. Power-on pull-up at 81.5 m. p. h.													
Orifice	1	88	109	130	60	107	134	68	69		34	40	28
	2	49	84	96	60	68	93	53	51		12	12	−2
	3	60	73	73	61	88	70	39	36	−4	−6	−5	−12
	4	55	59	61	67	60	44	24	26	−8	−15	−16	−8
	5	39	31	35	23	30	29	17	22	−10	−11	−9	−2
	6	20	12	15	19	24	22	15	12	−3	−5	−5	
	7	15	6	8	13	11	10						
Run No. 315. Power-on pull-up at 114.5 m. p. h.													
Orifice	1	187	184	260	93	188	240	165	99	40	44	75	54
	2	121	151	178	91	161	182	112	87	13	18	20	−2
	3	133	134	129	99	146	143	73	65	−6	−11	−9	−22
	4	133	116	117	86	97	116	40	36	−14	−23	−23	−12
	5	57	56	57	44	51	51	36	48	−15	−16	−16	−4
	6	45	26	24	38	30	51	22	22	−3	−8	−6	
	7	21	11	21	20	21	15						
Run No. 316. Power-on pull-up at 149.8 m. p. h.													
Orifice	1	370	317	359	213	328	265	270	198	34	48	117	100
	2	221	246	141	214	287	333	179	148	17	22	39	4
	3	226	234	216	202	258	250	118	116	−15	−16	−15	−33
	4	227	199	202	197	201	200	67	67	−24	−41	−40	−17
	5	106	94	117	99	99	110	55	68	−21	−26	−22	−5
	6	68	41	42	52	65	83	39	26	−6	−10	−7	
	7	39	18	21	28	15	30						
Run No. 322. Pull-up at 75 m. p. h. Time: 0 second													
Orifice	1	8	24	27	32	30	27	5	14	3	3.0	0	0
	2	20	27	27	26	35	30	10	13	0	0	0	0
	3	27	26	25	30	34	28	15	15	−3	0	2	2.0
	4	27	22	29	37	26	26	8	10	0	.5	3	0
	5	17	14	15	18	18	17	9	7	1	−1.0	0	.5
	6	11	7	9	12	12	10	1	3	0	−4.0	0	
	7	6	3	3	5	3	3						
Run No. 322. Time: 1 second													
Orifice	1	50	73	86	49	70	75	50	55	20	30	28	16
	2	37	60	70	37	52	60	35	37	6	13	7	−3
	3	35	47	50	35	40	55	28	30	−4	−1	−5	−9
	4	42	40	49	45	35	46	17	14	−5	−7	−11	−7
	5	23	20	24	21	23	26	17	14	−6	−5	−8	−1
	6	15	9	13	15	12	15	8	8	−1	−2	−4	
	7	8	4	4	8	9	6						

TABLE IV.—RECORDED PRESSURES IN SLIPSTREAM—Continued

Rib		A	A′	B	A″	A‴	B′	H	H′	V	W	X	Y
	Run No. 323. Pull-up at 121.5 m. p. h. Time: 0 second												
Orifice	1	0	−10	−15	10	0	−11	−28	−22	−21	−18	−13.0	−10.0
	2	3	9	3	18	20	12	−5	−12	−7	−15	−7.0	−3.0
	3	30	23	18	35	35	25	15	10	−6	0	2.0	4.0
	4	38	29	39	47	40	39	17	18	1	4	5.0	3.0
	5	35	17	24	28	26	26	17	15	5	2	3.0	.5
	6	17	9	18	23	17	15	4	4	2	−8	−.5	
	7	12	5	6	10	6	6						
	Run No. 323. Time: 1⅝ seconds												
Orifice	1	122	161	183	82	155	185	102	103			68	44
	2	77	120	158	91	127	150	75	81	13	17	19	−3
	3	92	85	120	86	94	130	58	50	−7	−6	−9	−22
	4	97	96	113	95	90	103	36	33	−11	−21	−21	−13
	5	52	42	56	46	50	54	32	25	−11	−15	−16	−2
	6	31	20	28	30	23	29	17	18	−3	−6	−6	
	7	15	8	7	14	13	8						
	Run No. 324. Pull-up at 148.5 m. p. h. Time: 0 second												
Orifice	1	0	−23	−31	−21	−25	−62	−60	−67		−30	−26	−17
	2	3	6	−3	0	5	−5	−25	−40	−7	−26	−14	−5
	3	43	31	22	35	35	40	22	3	−7	−1	−.5	2
	4	57	44	52	50	50	46	28	18	.5	2	4	2
	5	52	22	37	35	33	30	23	19	5	−1	2	0
	6	31	13	26	29	20	18	7	7	3	−3	−2	
	7	18	8	8	13	9	9						
	Run No. 324. Time: 1 second												
Orifice	1	205	255	290	104	220	272	155	150			93	67
	2	145	224	244	134	195	220	120	112	14	22	26	−4
	3	147	177	195	135	157	195	88	75	−12	−13	−16	−32
	4	160	148	162	145	127	160	55	38	−19	−32	−36	−19
	5	71	55	90	62	65	79	46	50	−15	−23	−23	−5
	6	54	32	38	44	37	37	28	26	−4	−9	−9	
	7	31	16	13	24	24	11						
	Run No. 326. Dive at high speed												
Orifice	1	−170	−245	−285	−130	−176	−304	−345	−366	−147	−100	−149	−103
	2	−104	−130	−136	−60	−75	−120	−200	−255	−55		−55	−28
	3	62	10	−32	64	40	−5	16	−36	−30	−10	−4	5
	4	78	78	182	128			63	18	−9	6	12	4
	5	158	23	75	64	72	65	58	53	5	−5	5	−3
	6	74	16	62	80	43	46	17	19	1	−10	−3	
	7	33	18	17	38	23	23						

TABLE V.—FABRIC PRESSURES

[Pounds per square foot]

Rib	Orifice											
	1 U	2 U	3 U	4 U	5 U	6 U	1 L	2 L	3 L	4 L	5 L	6 L
Run No. 300. Level flight at 82.7 m. p. h.												
C	10	16	23	17	10	4	10		0.5	3	3	3
F						3						5
J	5	10					10	8				
Run No. 301. Level flight at 91.7 m. p. h.												
C	5	15	23	21	13	4	6		0.5	3	3	3
F						3						6
J	0	9					7	8				
Run No. 302. Level flight at 114.5 m. p. h.												
C	−10	9	16	26	14	4	−10		0	3	3	4
F						3						9
J	−8	6					−3	0				
Run No. 303. Level flight at 134 m. p. h.												
C	−23	0	14	26	14	4	−29		−1	3	5	7
F						3						14
J	−18	0					−15	−5				
Run No. 304. Level flight at 149.4 m. p. h.												
C	−32	−5	13	29	14	2	−42		−3	5	8	11
F						4						16
J	−31	−2					−29	−15				
Run No. 305. Level flight at 156.7 m. p. h.												
C	−39	−10	10	31	16	1	−49		−5	5	8	12
F						5						17
J	−38	−5					−34	−16				
Run No. 316. Pull-up, power-on, at 149.8 m. p. h.												
C	244	195	177	130	62	28	31		55	31	14	6
F						16						26
J	166	109					42	85				
Run No. 326. Dive at high speed												
C	−167	−88	−18	61	25	−13	−179		−18	11	29	39
F						20						50
J	−143	−56					−196	2 6				

TABLE VI.—TAIL SUMMARY

Run No.	Maneuver	Initial air speed, miles per hour	Time (seconds)	Horizontal surfaces					Vertical surfaces				
				Total normal force, pounds	Average load *N. F.* 14.92	Total moment about hinge center line	Maximum pressure, pounds per square foot	Location of maximum pressure	Total normal force, pounds	Average load *N. F.* 10.74	Total moment about hinge center line	Maximum pressure, pounds per square foot	Location of maximum pressure
130	Pull up	116	¼	−220.0	−14.7	−58	−32.7	0–4					
			½	−124.0	−8.3	150	−33.8	0–4					
			1	98.0	6.6	285	84.7	N–1					
			1½	108.0	7.2	295	64.0	N–1					
131	do	126	¼	−199.0	−13.3	−89	−30.2	O–4					
			½	−119.0	−8.0	86	−38.5	N–4					
			1	57.0	3.8	309	83.3	N–1					
132	do	137	½	−206.0	−13.8	24	−41.6	O–4					
			1½	48.0	3.2	186	64.4	N–1					
133	do	149	¼	−319.0	−21.3	9	−43.0	N–4					
			½	−155.0	−10.4	120	−46.0	O–4					
			1	56.0	3.7	158	60.0	N–1					
134	do	154	⅛	−343.0	−22.9	−133	−54.0	N–4					
			¼	−211.0	−14.1	−52	−56.0	O–4					
			⅝	162.0	10.8	486	137.0	N–1					
135	do	163	⅜	−290.0	−19.4	84	−60.0	O–4					
			⅞	177.0	11.8	525	134.0	N–1					
136	do	172	¼	−275.0	−18.4	−97	−45.7	N–2					
			⅝	2.4	.2	224	−62.0	N–4					
			⅞	200.0	13.4	540	156.0	N–1					
137	do	181	⅛	−453.0	−30.1	−164	−65.5	N–4					
			⅜	−258.0	−17.3	270	−65.0	N–4					
			1	224.0	14.9	600	176.0	N–1					
200	Pull up, power off	108	¼	−165.0	−11.0	−46	−24.0	N–1					
			1¼	70.0	4.7	206	56.0	O–1					
209	do	139	¼	−192.0	−12.9	−53	−34.0	O–4					
			1	42.0	2.8	190	75.0	O–1					
213	Dive		12	−395.0	−26.4	−450	−97.0	N–1					
215	Push down	[1] 186.1	3½	−50.4	−3.4	−520	−78.0	N–1					
222	Right roll	[3] 167	¼	−359.0	−24.1	−230	−48.0	N–2					
			½	−197.5	−13.2	−22	−49.0	N–4	268.0	25.0	123.2	52	S–3
			¾						228.0	21.1	52.5	55	Q–3
			1	97.5	6.5	305	69.0	O–1					
			2½	364.0	24.4	300	55.0	O–1					
225	Left roll	[3] 163	0						22.6	2.1	15.0	13	R–4
			¼	−349.6	−23.4	390	−40.0	N–2					
			½						174.4	16.2	55.0	−34	S–3
			¾	−28.0	−1.9	−160	73.0	O–1	−168.0	−15.6	−10.0	−39	S–3
			⅞	98.0	6.6	450	−54.0	N–4					
			1	111.6	7.5	435	−49.0	N–4	−138.0	−12.8	−40.0	−35	Q–3
226	Dive	[1] 260.0	16 13/16	−458.0	−30.7	324	−133.0	M–1					
226	Pull-out from dive	[1] 230.0	23¼	−324.0	−21.7	−550	−88.0	N–2	294	27.4	−43	90	S–1
[2] 315	Pull up	114.5	½	−321.6	−21.5	−80	−44.2	X–4					
			1⅛	81.8	5.5	276	75.0	X–1					
			1¼	146.8	9.8	359	75.0	X–1					
			1½	186.8	12.5	207	52.0	X–1					
[2] 316	do	149.8	15/16	−451.0	−30.2	−46	−53.6	V–1					
			1	−400.0	−26.8	60	−62.4	X–4					
			1⅝	217.6	14.6	480	121.0	X–1					
			1¾	219.6	14.7	410	117.0	X–1					
[2] 323	do	121.5	0	−72.0	−4.8	−104	−21.0	V–1					
			1⅝	98.4	6.6	287	68.0	X–1					
[2] 324	do	148.5	0	−130.8	−8.8	−245	−30.2	W–1					
			1	147.2	9.9	341	93.0	X–1					
[2] 326	High-speed dive		4	−498.0	−33.4	−705	−149.0	X–1					

[1] Air speed at given timing line.

[2] Pressures recorded on left horizontal tail surfaces.

[3] Approximate airspeed.

U. S. GOVERNMENT PRINTING OFFICE: 1931

For sale by the Superintendent of Documents, Washington, D. C. - - - Price 60 cents

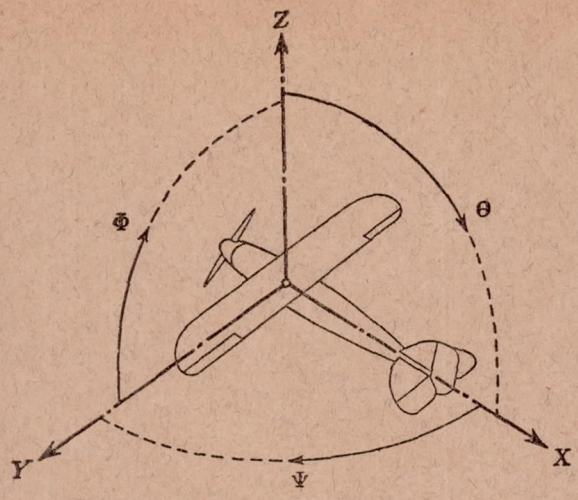

Positive directions of axes and angles (forces and moments) are shown by arrows

Axis		Force (parallel to axis) symbol	Moment about axis			Angle		Velocities	
Designation	Symbol		Designation	Symbol	Positive direction	Designation	Symbol	Linear (component along axis)	Angular
Longitudinal	X	X	rolling	L	$Y \longrightarrow Z$	roll	Φ	u	p
Lateral	Y	Y	pitching	M	$Z \longrightarrow X$	pitch	Θ	v	q
Normal	Z	Z	yawing	N	$X \longrightarrow Y$	yaw	Ψ	w	r

Absolute coefficients of moment

$$C_L = \frac{L}{qbS} \qquad C_M = \frac{M}{qcS} \qquad C_N = \frac{N}{qfS}$$

Angle of set of control surface (relative to neutral position), δ. (Indicate surface by proper subscript.)

4. PROPELLER SYMBOLS

D, Diameter.
p_e, Effective pitch.
p_g, Mean geometric pitch.
p_s, Standard pitch.
p_v, Zero thrust.
p_a, Zero torque.
p/D, Pitch ratio.
V', Inflow velocity.
V_s, Slip stream velocity.

T, Thrust.
Q, Torque.
P, Power.
(If "coefficients" are introduced all units used must be consistent.)
η, Efficiency $= T\ V/P$.
n, Revolutions per sec., r. p. s.
N, Revolutions per minute, r. p. m.
Φ, Effective helix angle $= \tan^{-1}\left(\frac{V}{2\pi rn}\right)$

5. NUMERICAL RELATIONS

1 hp = 76.04 kg/m/s = 550 lb./ft./sec.
1 kg/m/s = 0.01315 hp
1 mi./hr. = 0.44704 m/s
1 m/s = 2.23693 mi./hr.

1 lb. = 0.4535924277 kg
1 kg = 2.2046224 lb.
1 mi. = 1609.35 m = 5280 ft
1 m = 3.2808333 ft.